frontiers | Research Topics

Interactions between pathogens and host immune system in patients with immunodeficiency: Estimation from high-throughput sequencing

Edited by
Jinmin Ma, Eda Altan and Gilberto Sabino-Santos

Published in
Frontiers in Cellular and Infection Microbiology

ISSN 1664-8714
ISBN 978-2-8325-2590-6
DOI 10.3389/978-2-8325-2590-6

About Frontiers

Frontiers is more than just an open access publisher of scholarly articles: it is a pioneering approach to the world of academia, radically improving the way scholarly research is managed. The grand vision of Frontiers is a world where all people have an equal opportunity to seek, share and generate knowledge. Frontiers provides immediate and permanent online open access to all its publications, but this alone is not enough to realize our grand goals.

Frontiers journal series

The Frontiers journal series is a multi-tier and interdisciplinary set of open-access, online journals, promising a paradigm shift from the current review, selection and dissemination processes in academic publishing. All Frontiers journals are driven by researchers for researchers; therefore, they constitute a service to the scholarly community. At the same time, the *Frontiers journal series* operates on a revolutionary invention, the tiered publishing system, initially addressing specific communities of scholars, and gradually climbing up to broader public understanding, thus serving the interests of the lay society, too.

Dedication to quality

Each Frontiers article is a landmark of the highest quality, thanks to genuinely collaborative interactions between authors and review editors, who include some of the world's best academicians. Research must be certified by peers before entering a stream of knowledge that may eventually reach the public - and shape society; therefore, Frontiers only applies the most rigorous and unbiased reviews. Frontiers revolutionizes research publishing by freely delivering the most outstanding research, evaluated with no bias from both the academic and social point of view. By applying the most advanced information technologies, Frontiers is catapulting scholarly publishing into a new generation.

What are Frontiers Research Topics?

Frontiers Research Topics are very popular trademarks of the *Frontiers journals series*: they are collections of at least ten articles, all centered on a particular subject. With their unique mix of varied contributions from Original Research to Review Articles, Frontiers Research Topics unify the most influential researchers, the latest key findings and historical advances in a hot research area.

Find out more on how to host your own Frontiers Research Topic or contribute to one as an author by contacting the Frontiers editorial office: frontiersin.org/about/contact

Interactions between pathogens and host immune system in patients with immunodeficiency: Estimation from high-throughput sequencing

Topic editors

Jinmin Ma — Beijing Genomics Institute (BGI), China

Eda Altan — University of Turku, Finland

Gilberto Sabino-Santos — Tulane University, United States

Citation

Ma, J., Altan, E., Sabino-Santos, G., eds. (2023). *Interactions between pathogens and host immune system in patients with immunodeficiency: Estimation from high-throughput sequencing*. Lausanne: Frontiers Media SA. doi: 10.3389/978-2-8325-2590-6

Table of contents

frontiers | Frontiers in Cellular and Infection Microbiology

TYPE Editorial
PUBLISHED 16 May 2023
DOI 10.3389/fcimb.2023.1200638

OPEN ACCESS

EDITED AND REVIEWED BY
Nahed Ismail,
University of Illinois Chicago, United States

*CORRESPONDENCE
Jinmin Ma
majinmin@genomics.cn

RECEIVED 05 April 2023
ACCEPTED 10 May 2023
PUBLISHED 16 May 2023

CITATION
Ma J and Sabino-Santos G (2023) Editorial: Interactions between pathogens and host immune system in patients with immunodeficiency: estimation from high-throughput sequencing.
Front. Cell. Infect. Microbiol. 13:1200638.
doi: 10.3389/fcimb.2023.1200638

Editorial: Interactions between pathogens and host immune system in patients with immunodeficiency: estimation from high-throughput sequencing

Jinmin Ma[1]* and Gilberto Sabino-Santos[2,3]

[1]BGI-Shenzhen, Shenzhen, China, [2]Department of Microbiology and Immunology, School of Medicine, Tulane University, New Orleans, LA, United States, [3]Center for Virology Research, Ribeirao Preto Medical School, University of Sao Paulo, Ribeirao Preto, Sao Paulo, Brazil

KEYWORDS

immunodeficiency, high-throughput sequencing (deep sequencing), mNGS (metagenomic next-generation sequencing), pathogen diagnosis, COVID-19

Editorial on the Research Topic
Interactions between pathogens and host immune system in patients with immunodeficiency: estimation from high-throughput sequencing

In recent years, meta-genomics sequencing (mNGS) has enabled the unbiased simultaneous detection of thousands of pathogens without *a priori* knowledge of a hypothesis to diagnose potential pathogens. This technology has been widely applied for clinical purposes and is particularly effective in detecting pathogens in critical infectious cases, making it a powerful tool for complex contagious diseases. In the past, discovering new pathogens usually took months to years, such as HIV from 1979 to 1986 and the SARS virus in 2003 (Peiris et al., 2004). However, with mNGS technology, the discovery process can now be completed in just a few days, as demonstrated by SARS-CoV-2 in 2019 (Lu et al., 2020), which benefited from large-scale mNGS applications. Moreover, new disease-causing pathogens have been discovered, such as Pseudorabies Virus (Ai et al., 2018) and the arenaviruses (Li et al., 2015). These viruses were known to infect a broad range of species across the globe and were previously thought to be non-pathogenic to humans.

Immunodeficient populations are susceptible to opportunistic pathogens that can cause severe disease, even though they may be harmless to immunocompetent individuals. The application of mNGS for diagnosing pathogens in clinical samples has been ongoing for years, starting with the case report of infectious *Leptospira santarosai* in 2014 (Wilson et al., 2014). Patients with immunodeficiency pose significant challenges for infectious disease diagnosis since pathogen detection is a prerequisite for precision therapy. Therefore, this Research Topic focuses on (i) performing simultaneous pathogen detection and immune evaluation on clinical samples, (ii) exploring differences in response to different pathogens

in distinct immunodeficiency types, and (iii) providing guidance for clinical targeting of drugs and precision therapy strategies. Immunodeficiency can arise from various factors such as genetics, transplantation, and HIV/AIDS. Infectious diseases require complex immune responses, which may lead to opportunistic infections with different symptoms in immunodeficient individuals. The 13 studies included in this Research Topic can be categorized into five groups: 1) Rare pathogen infection; 2) transplantation patients; 3) genetic susceptibility; 4) fungal infection, and 5) other opportunistic infections (as shown in Figure 1A).

In the category of rare pathogen infections, Zhou et al. reported the first instance of direct detection through mNGS of *Treponema pallidum* in patients with ocular involvement and typical MRI results. They suggest using mNGS as a potential supplementary tool for the diagnosis and differential diagnosis of neurosyphilis.

Transplant patients are at high risk of infection with long-term use of immunosuppressive drugs. This Research Topic includes studies on organ transplantation Liver transplantation (Huang et al.) and stem cell transplantation (Zhang et al.) patients. For the liver transplantation patient's infection research, the author demonstrated that mNGS was superior (pathogen-positive rate: 64.3%) over traditional laboratory methods (pathogen-positive rate: 28.6%) for early identification and assisted in clinical decision-making for donor-derived infections. In addition, mNGS is a powerful technology to help the diagnosis of fever after stem cell transplantation, with the sensitivity of mNGS versus conventional microbiological at 91.2% vs. 41.2%, respectively, in peripheral blood samples.

Three studies observed individuals with autoimmune and genetically-related diseases to be susceptible to infections. One of the research papers identified the microbial agent responsible for causing pneumonia in patients with myasthenia gravis, an autoimmune neuromuscular disorder that affects neuromuscular junctions and leads to fluctuations in muscle weakness. Early infection discovery can lead to accurate antibiotic options and interventions when risk factors are present (Su et al.). Another study focused on the role of rheumatic diseases in complex infections, with the lungs being a common target for autoimmune-mediated injury. Metagenomic next-generation sequencing was a powerful complement to conventional methods in identifying pathogens in patients with rheumatic diseases (Jiang et al.). Finally, a study focused on the influence of rare genetic defects arising from inborn errors of immunity on COVID-19 severity. The study found that, in severe COVID-19-related patients, mutations were enriched in pathways related to tuberculosis, primary immunodeficiency, influenza, and HC-pLoF. This discovery identified candidate genes and pathways that can potentially be used as COVID-19 diagnostic markers to help distinguish patients at higher risk (Liu et al.).

Fungal infections are typically not found in individuals with standard immune systems but are more likely to occur in older individuals with compromised immune systems. One of the challenges in diagnosing fungal infections is the significant variation in fungi and their appearance in different samples. In this regard, mNGS-specific indicators can accurately and rapidly identify pathogens in patients with invasive fungal infections (IFIs) more effectively than conventional microbiological tests (CMTs), which has important clinical implications (Wang et al.). Other authors have shown that mNGS is a valuable and effective method for diagnosing pulmonary aspergillosis through bronchoalveolar lavage fluid (BALF) and blood samples (Bao et al.) but not for detecting Cryptococcus. For immunocompromised patients, these authors recommend using BALF detection when compared to tissue and cerebrospinal fluid (CSF) methods (Su et al.). Additionally,

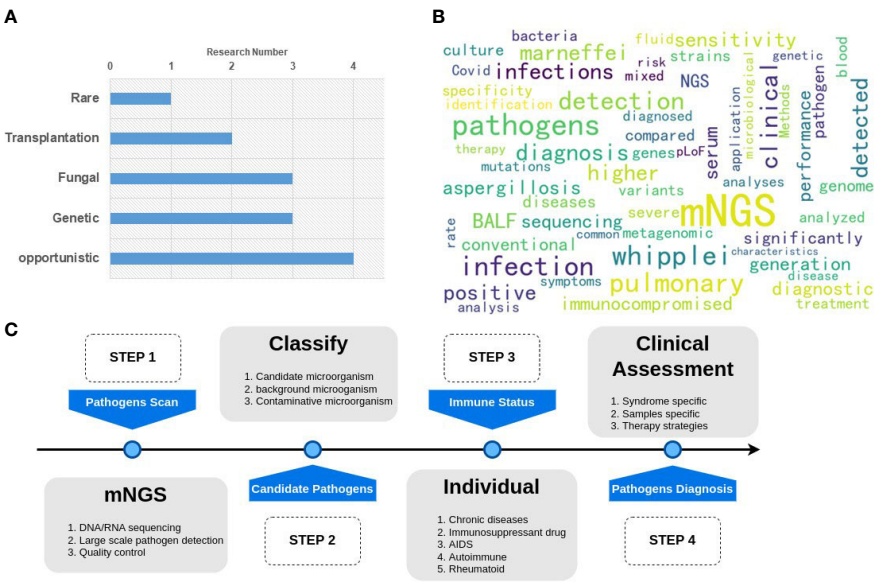

FIGURE 1
Graphical summary of the Research Topic. **(A)** the classification and number of the papers; **(B)** the hot keywords of the research. **(C)** A general pipeline of mNGS application for clinical pathogen detection.

positive mNGS results for diagnosing cryptococcosis were found to be correlated with lower lymphocyte counts, higher IL-2, and higher serum antigen assays in immunocompromised patients.

Opportunistic pathogens can become pathogenic when the immune system weakens, or due to inborn errors of immunity, although they may be harmless to healthy individuals. For people living with HIV (PLHIV), *Talaromyces marneffei* can cause talaromycosis, and due to weak immunity, lead to significant morbidity and mortality if not diagnosed promptly. mNGS has been shown to be a powerful technique with high specificity and sensitivity for the rapid diagnosis of talaromycosis (Mao et al.). BALF samples analyzed by mNGS are a good option for early identification of *T. marneffei* in PLHIV with excellent performance in identifying mixed infections, enabling timely treatment, and potential mortality reduction. However, *T. marneffei* infection was first reported in patients with inborn errors of immunity with IL12RB1 gene mutation (Liu et al.), even in children who were not infected with HIV, which shows that susceptibility to *T. marneffei* appears to be related to genetics. *Tropheryma whipplei* is another opportunistic pathogenic bacterium associated with Whipple's disease (WD). Using mNGS in a previous study (Lin et al.), the overall prevalence of *T. whipplei* was found to be 4.0 (70/1725). According to this largest *T. whipplei* cohort research, *T. whipplei* should be considered a potential contributing factor in some lung diseases, even in immunocompetent patients. Besides its high performance in pathogen identification, mNGS technology can also obtain genome information of the pathogen, enabling the analysis of mutations related to the severity of the disease. In this topic, two genomes of *Tropheryma whipplei* were assembled and characterized after mNGS pathogen identification (Lv et al.).

Regarding these 13 studies, all relevant keywords were analyzed in Figure 1B. It was found that the primary sample type used was BALF, and the diagnosis results in terms of sensitivity, specificity, and significance were the primary points of comparison between mNGS and culture or other traditional methods.

Although mNGS can detect a wide range of pathogens, clinical diagnosis requires additional individual information to make a final decision. Therefore, the entire pipeline for mNGS pathogen diagnosis should follow four steps, as shown in Figure 1C. Step 1 involves the pathogen scan, which includes sample sequencing and data analysis. Step 2 consists of the classification of microorganisms to identify candidate pathogens. Step 3 involves the estimation of individual immunity to assess the patient's susceptibility to specific pathogens. Step 4 involves clinical assessment. A final diagnosis report is then generated based on the results of these four steps.

Despite this, generating a final diagnosis remains a challenging task due to the complexity of the interaction between pathogens and the human immune system. Therefore, further studies should address clinical issues such as pathogen colonization and infection. Additionally, in the future, using artificial intelligence methods to generate clinical pathogen reports automatically could promote more effectively the widespread application of mNGS.

Author contributions

JM draft and final write the manuscript, GS-S reviewed and edited the manuscript. All authors contributed to the article and approved the submitted version.

Acknowledgments

We thank Senior Researcher Eda Altan from the University of Turku in Turku, Finland, for organizing and editing the manuscripts on this Research Topic with professional knowledge in pathogen and human immunology. We also thank Emily Hannon, a native English speaker, for proofreading this manuscript.

Conflict of interest

The authors declare that the research was conducted in the absence of any commercial or financial relationships that could be construed as a potential conflict of interest.

Publisher's note

References

Ai, J. W., Weng, S. S., Cheng, Q., Cui, P., Li, Y. J., Wu, H. L., et al. (2018). Human endophthalmitis caused by pseudorabies virus infection, chin. *Emerg. Infect. Dis* 24, 1087–1090. doi: 10.3201/eid2406.171612

Li, K., Lin, X. D., Wang, W., Shi, M., Guo, W. P., Zhang, X. H., et al. (2015). Isolation and characterization of a novel arenavirus harbored by rodents and shrews in zhejiang province, China. *Virology* 476, 37–42. doi: 10.1016/j.virol.2014.11.026

Lu, R., Zhao, X., Li, J., Niu, P., Yang, B., Wu, H., et al. (2020). Genomic characterisation and epidemiology of 2019 novel coronavirus: implications for virus origins and receptor binding. *Lancet* 395, 565–574. doi: 10.1016/S0140-6736(20)30251-8

Peiris, J. S. M., Guan, Y., and Yuen, K. Y. (2004). Severe acute respiratory syndrome. *Nat. Med.* 10, 317–319. doi: 10.1038/nm1143

Wilson, M. R., Naccache, S. N., Samayoa, E., Biagtan, M., Bashir, H., Yu, G., et al. (2014). Actionable diagnosis of neuroleptospirosis by next-generation sequencing. *N. Engl. J. Med.* 370, 2408–2417. doi: 10.1056/NEJMoa1401268

frontiers | Frontiers in Cellular and Infection Microbiology

ORIGINAL RESEARCH
published: 27 May 2022
doi: 10.3389/fcimb.2022.888582

Rare Variants in Inborn Errors of Immunity Genes Associated With Covid-19 Severity

Panhong Liu[1,2], Mingyan Fang[2,3], Yuxue Luo[2], Fang Zheng[4], Yan Jin[4], Fanjun Cheng[5], Huanhuan Zhu[2] and Xin Jin[2,3,6]**

[1] College of Life Sciences, University of Chinese Academy of Sciences, Beijing, China, [2] Beijing Genomeics Institute At Shenzhen, BGI-Shenzhen, Shenzhen, China, [3] Beijing Genomeics Institute In Singapore, BGI-Singapore ,Singapore, Singapore, [4] Department of Pediatrics, Union Hospital, Tongji Medical College, Huazhong University of Science and Technology, Wuhan, China, [5] Department of Hematology, Union Hospital, Tongji Medical College, Huazhong University of Science and Technology, Wuhan, China, [6] School of Medicine, South China University of Technology, Guangzhou, China

OPEN ACCESS

Edited by:
Eda Altan,
Bahçeşehir University, Turkey

Reviewed by:
Saad Ahmed Sami,
University of Chittagong, Bangladesh
Hao Liu,
University of Massachusetts Medical School, United States
Aurélie Cobat,
Institut National de la Santé et de la Recherche Médicale (INSERM), France

***Correspondence:**
Xin Jin
jinxin@genomics.cn
Huanhuan Zhu
zhuhuanhuan1@genomics.cn

Specialty section:
This article was submitted to Clinical Microbiology, a section of the journal Frontiers in Cellular and Infection Microbiology

Received: 03 March 2022
Accepted: 21 April 2022
Published: 27 May 2022

Citation:
Liu P, Fang M, Luo Y, Zheng F, Jin Y, Cheng F, Zhu H and Jin X (2022) Rare Variants in Inborn Errors of Immunity Genes Associated With Covid-19 Severity. Front. Cell. Infect. Microbiol. 12:888582. doi: 10.3389/fcimb.2022.888582

Host genetic factors have been shown to play an important role in SARS-CoV-2 infection and the course of Covid-19 disease. The genetic contributions of common variants influencing Covid-19 susceptibility and severity have been extensively studied in diverse populations. However, the studies of rare genetic defects arising from inborn errors of immunity (IEI) are relatively few, especially in the Chinese population. To fill this gap, we used a deeply sequenced dataset of nearly 500 patients, all of Chinese descent, to investigate putative functional rare variants. Specifically, we annotated rare variants in our call set and selected likely deleterious missense (LDM) and high-confidence predicted loss-of-function (HC-pLoF) variants. Further, we analyzed LDM and HC-pLoF variants between *non-severe* and *severe* Covid-19 patients by (a) performing gene- and pathway-level association analyses, (b) testing the number of mutations in previously reported genes mapped from LDM and HC-pLoF variants, and (c) uncovering candidate genes *via* protein-protein interaction (PPI) network analysis of Covid-19-related genes and genes defined from LDM and HC-pLoF variants. From our analyses, we found that (a) pathways Tuberculosis (hsa:05152), Primary Immunodeficiency (hsa:05340), and Influenza A (hsa:05164) showed significant enrichment in *severe* patients compared to the *non-severe* ones, (b) HC-pLoF mutations were enriched in Covid-19-related genes in *severe* patients, and (c) several candidate genes, such as *IL12RB1*, *TBK1*, *TLR3*, and *IFNGR2*, are uncovered by PPI network analysis and worth further investigation. These regions generally play an essential role in regulating antiviral innate immunity responses to foreign pathogens and in responding to many inflammatory diseases. We believe that our identified candidate genes/pathways can be potentially used as Covid-19 diagnostic markers and help distinguish patients at higher risk.

Keywords: Covid-19, inborn errors of immunity, gene-level tests, pathway-based analysis, PPI network analysis

INTRODUCTION

Since December 2019, the coronavirus diseases 2019 (Covid-19) (Gorbalenya et al., 2020) caused by the SARS-CoV-2 virus (Severe Acute Respiratory Syndrome Coronavirus 2) (Zhu et al., 2020) has spread rapidly across the world. By January 2022, the ongoing SARS-CoV-2 pandemic has caused more than 360 million confirmed cases and more than 5 million deaths. Host genetic factors have been shown to play critical roles in the disease susceptibility and severity (Ellinghaus et al., 2020; COVID-19 Host Genetics Initiative, 2021; Pairo-Castineira et al., 2021; Shelton et al., 2021; Kousathanas et al., 2022). The Covid-19 Host Genetics Initiative (Covid-19 HGI, https://www.covid19hg.org/) is an international initiative to share the results of host genome-wide associations study (GWAS) meta-analysis of Covid-19 disease. The most recent Covid-19 HGI release 6 has reported 24 lead SNPs (P < 5e-8) mapped to nearly 136 genes, such as *LZTFL1*, *ABO*, *OAS1*, *DPP9*, and *IFNAR2* (COVID-19 Host Genetics Initiative, 2021). The estimated heritability of Covid-19 symptoms explained by these common variants was 6.5% (Pairo-Castineira et al., 2021). A twin study with participants from the TwinsUK cohort reported that 31% of phenotypic variance of predicted Covid-19 is due to host genetic factors (Williams et al., 2020). This leads to a large proportion of unexplained heritability (nearly 25%), commonly referred to as "missing heritability". There is increasing evidence that rare variants also make a major contribution to missing heritability of many complex diseases and traits (Hunt et al., 2013; Zuk et al., 2014; Misawa et al., 2020).

Recently, the rare variants attracted researchers' attention in explaining the missing heritability of Covid-19 disease. For example, Zhang et al. found that the rare predicted loss-of-function (pLoF) variants in the IRF7- and TLR3-dependent type I interferon (IFN) pathway were enriched in patients who developed risky Covid-19 (Zhang Q. et al., 2020). Smieszek et al. reported that pLoF variant in gene *IFNAR2* (c.966C>A/p.Y322X) might play a role not only in clinical manifestation of Covid-19 but also in the response to vaccination (Smieszek et al., 2021). In addition, multiple studies found that the pLoF variants in *TLR7* gene enriched in severely affected male patients, and the deficiency of TLR7 would impair innate immunity and increase severity of COVID-19 (van der Made et al., 2020; Asano et al., 2021; Fallerini et al., 2021; Mantovani et al., 2021). As previously reported, the rare variants were more likely to be functional and tended to have stronger effects on complex diseases (Gorlov et al., 2011). The study of genetic effects of rare variants is necessary to elucidate the severity of Covid-19.

To explore the genetic contributions of rare variants in Covid-19 patients with inborn errors of immunity (IEI) genes, we recruited and investigated nearly 500 hospitalized patients from Union Hospital of Tongji Medical College of Huazhong University of Science and Technology (abbr. Union Hospital) (Zhu et al., 2021). Based on patients' genomic data and clinical information, we carried out three major analyses to investigate the effects of putative functional rare variants (LDM and HC-pLoF): (a) gene- and pathway-level tests of these rare variants between *severe* and *non-severe* patients; (b) examination of the significance of previously reported rare variants and genes in our dataset; and c) rare mutation accumulation analysis and PPI network analysis in only *severe* patients. From these analyses, we (a) identified candidate functional pathways that are responsible for innate immune disorders and respiratory diseases, such as Tuberculosis (hsa:05152), Primary Immunodeficiency (hsa:05340), and Influenza A (hsa:05164); (b) successfully replicated two Covid-19 associated SNPs (rs780744847 and rs541048548) mapped on genes *TLR3* and *ICAM3*, respectively; and (c) suggested several candidate genes, including *IL12RB1, TBK1, TLR3*, and *IFNGR2*, which might be involved in SARS-CoV-2 cell entry, host immune responses, and Covid-19 disease severity.

Until now, literature based on the Chinese population has replicated and discovered some Covid-19-associated common variants (Wang et al., 2020; Wu et al., 2021a; Wu et al., 2021b; Zhu et al., 2021), but genetic background of rare variants is currently insufficiently understood in the Chinese population. Our work is an effort to fill this gap. We hope that it will serve as a useful scientific reference to assess the genetic mechanism of rare variants in Covid-19 and advance our understanding of disease etiology.

MATERIALS AND METHODS

Patient Recruitment and Quality Control

All subjects in this study were collected from the Union Hospital. We used PLINK 2.0 (Chang et al., 2015) to infer sex of individuals from SNP genotypes and VerifyBamID (Zhang F. et al., 2020) to assess DNA contamination level. Individuals were excluded if their inferred sex was inconsistent with that of clinically recorded. We also removed individuals with estimated contamination rates greater than 0.05. After sample quality control, there were 451 unrelated individuals with 159 mild and moderate patients, and 292 severe and critical patients. The severity classification criteria were made by the National Health Commission of P.R. China (Wu and McGoogan, 2020). We reclassified the mild/moderate patients as *non-severe* patients and the severe/critical patients as *severe* patients.

Whole Genome Sequencing

Cell-free DNA (cf-DNA) was extracted from 200 ul plasma using MagPure Circulating DNA Kit following the manufacturer's instructions. The 40 ul cf-DNA was extracted from each sample and used to create a library using MGIEasy Cell-free DNA Library Prep Kit according to the library preparation pipeline. Sequencing was conducted by the DNBSEQ platform (MGI, Shenzhen, China) to generate 100 bp paired-end reads. The mean sequencing depth was 17.8× for all samples.

Genotype Calling

The blood samples of some patients were collected at different time points during hospitalization. To increase the average depth of study, sequence fastq files of each patient were merged together to generate one GVCF file by BWA (Li and Durbin, 2009) and Sentieon Genomics software (Freed et al., 2017).

Joint variant calling was then performed on GVCF files of all participants using the Sentieon GVCFtyper algorithm. The resulting VCF file was used for subsequent genomic analyses.

After the application of excessHet (<54.69) filter, Variant Quality Score Recalibration (VQSR) was completed by using the Genome Analysis Toolkit (GATK version 4.1.2) (DePristo et al., 2011). Known variant files were downloaded from the GATK bundle. For SNP sets, we used SNPs of HapMap, 1000G_omin and 1000G_phase1 database as training sets, the SNPs of HapMap as true sets, and the SNPs of dbSNP as known sets. For indel sets, we used indel of Mills_and_1000G_gold_standard database as training and true sets. We used the annotations "DP", "QD", "MQRankSum", "ReadPosRankSum", "FS", and "SOR" to train VQSR. Finally, we used a sensitivity threshold of 99.7% and 99% for the SNPs and INDELs, respectively, to define genotyped sites that passed VQSR filtration.

To improve the genotyping accuracy, we used the Beagle 4.0 software (Browning and Browning, 2016) to perform LD-based genotype refinement and imputation by taking genotype likelihoods as inputs. Low-quality variants with dosage imputation score DR2 < 0.3 were filtered out.

Principal Component Analysis

Principal component analysis (PCA) (Pearson, 1901) was performed using a subset of autosomal bi-allelic SNPs by applying PLINK 2.0 (Chang et al., 2015). Several restrictions were applied to select SNPs for PCA analysis, including keeping SNPs with minor allele frequency (MAF) ≥ 5%, Hardy–Weinberg Equilibrium P ≥ 1e-6, and removing one of a pair of SNPs if the LD was greater than 0.5 (in a window of 50 SNPs with a step of 5 SNPs). To select an adequate number of significant PCs in the association analysis, we performed hypothesis testing for each eigenvalue by using software Eigenstrat (Price et al., 2006).

Functional Annotation

We annotated rare variants (MAF < 0.5%) in our final call set by using the Ensembl Variant Effect Predictor (VEP, build 103, GRCh38) (McLaren et al., 2016) with default parameters. The databases for annotation included dbSNP (Sherry et al., 2001), gnomAD (Karczewski et al., 2020), and 1000 Genomes Project (Clarke et al., 2012). In addition, we used Combined Annotation Dependent Depletion (CADD) score to predict missense variants that had potential effects on protein function. The CADD score was annotated by CADD plug-in (Kircher et al., 2014). Missense variants with CADD score > MSC (Mutation Significance Cut-off) score (95% confidence interval) (Itan et al., 2016) were predicted as likely deleterious missense (LDM) variants. We also used LOFTEE (Karczewski et al., 2020) plug-in to identify high-confidence pLoF (HC-pLoF) for stop-gained, frameshift, and splice site disrupting variants. Finally, we focused on the LDM and HC-pLoF variants in the subsequent analyses.

Rare Variants Analyses

To investigate the cumulative effects of multiple rare variants, we performed gene-based association analysis using KGGSeq 1.0 (Li et al., 2017) with the sequence kernel association test (SKAT) (Wu et al., 2010), the Optimized SKAT (SKAT-O) (Lee et al., 2012), and Burden test. We used the binary collapsing method (burden test) implemented in KGGseq. We further carried out pathway-based analysis by testing the Kyoto Encyclopedia of Genes and Genomes (KEGG) gene sets (Kanehisa and Goto, 2000). The adjusted covariates included age, sex, and the top six principal components. We defined the suggestive significance threshold for gene-based association test as 1e–6 and for pathway-based association test as 0.05.

We also focused on 24 type I IFN genes (denoted as IFN-genes) that were found as an enrichment in a life-threatening Covid-19 study (Zhang Q. et al., 2020; Kosmicki et al., 2021) and 136 genes located in 50 kb of lead SNPs reported by the Covid-19 Host Genetics Initiative (release 6, denoted as HGI-genes) (COVID-19 Host Genetics Initiative, 2021) (**Supplementary Table S1**).The mutation accuracy of variants in these 159 known candidate genes (one overlap between 24 IFN-genes and 136 HGI-genes) was manually checked by using Samtools 1.10 (Danecek et al., 2021).

Finally, we performed an analysis of rare variant accumulation in genes identified by two approaches. The first approach detected genes if one variant met the following two conditions: (a) the mutations occurred in only *severe* patients, and (b) the variant harbored no less than three effect allele counts. We denoted these genes as "individual variant-driven" genes. The second approach determined genes if (a) all mutations in the gene occurred in only *severe* patients, and (b) the total number of mutations in the gene is at least three. We denoted these genes as "all variant-driven" genes. We note that genes identified by the two methods may have some overlap. Each of the two gene sets was then used for PPI network analysis with the above 159 known candidate genes. We used the STRING version 10.5 (Search Tool for the Retrieval of Interacting Genes/Proteins) (Szklarczyk et al., 2019) to build the PPI network. The minimum required interaction score to the highest confidence was set to 0.900.

RESULTS

Participant Characteristics

In this study, participants included 451 Covid-19 patients aged 23 to 97 years old and all declared Han Chinese population. In **Table 1**, we provide participant characteristics for *non-severe* and *severe* patients, respectively. A total of 159 (35.25%) and 292 (64.75%) patients were grouped as *non-severe* and *severe*, respectively. The same as previously reported (Cummings et al., 2020; Yang et al., 2020), patients with older age (*severe*: an average of 64 years old vs. *non-severe*: an average of 58 years old, t-test p = 4.6e-05) and men (*severe* 52.74% vs. *non-severe* 42.14%, Fisher's exact test p = 0.04) were at a higher risk of developing severe symptoms.

Data Quality

After quality control, the dataset consisted of 22,107,585 and 680,522 variants from autosomes and X chromosome,

TABLE 1 | Participant characteristics.

	Number, n (%)	Men, n (%)	Age, average (sd)	Depth, average (sd)
All patients	451			21.67
Non-severe	159 (35.25%)	67 (42.14%)	58.33 (14.62)	19.04 (8.94)
Severe	292 (64.75%)	154 (52.74%)	64.11 (13.31)	23.1 (10.43)

respectively (**Figure 1**). Then we compared chip array sequencing results with genotype after LD-based refinement by Beagle 4.0 on 218 individuals. The heterozygote concordance rate increased from an average of 94.4% to 97.4%, and the improvement is more dramatic for samples with lower sequencing depth (**Figure 2A**). After filtering in variants by imputation score DR2 > 0.3, the final dataset for further analyses had a total of 22,532,360 variants, and the PCA on 575,888 autosome SNPs detected no outlier samples (**Figure 2B**).

Rare Variants Statistics

After filtering by MAF, we obtained a total of 13,934,341 rare variants for VEP annotation. Among the resulting annotations, there were 88,790 missense variants and 4881 pLoF variation (including stop-gained, frameshift, and splice site disrupting variants). Damaging effects of these missense and pLoF variants were then predicted by CADD and LOFTEE plug-in, respectively. About 43.41% missense variants were predicted as LDM variants (38,548) and 85.68% pLoF variants were predicted as HC-pLoF variants (4182). Thus, in total, 42,730 predicted

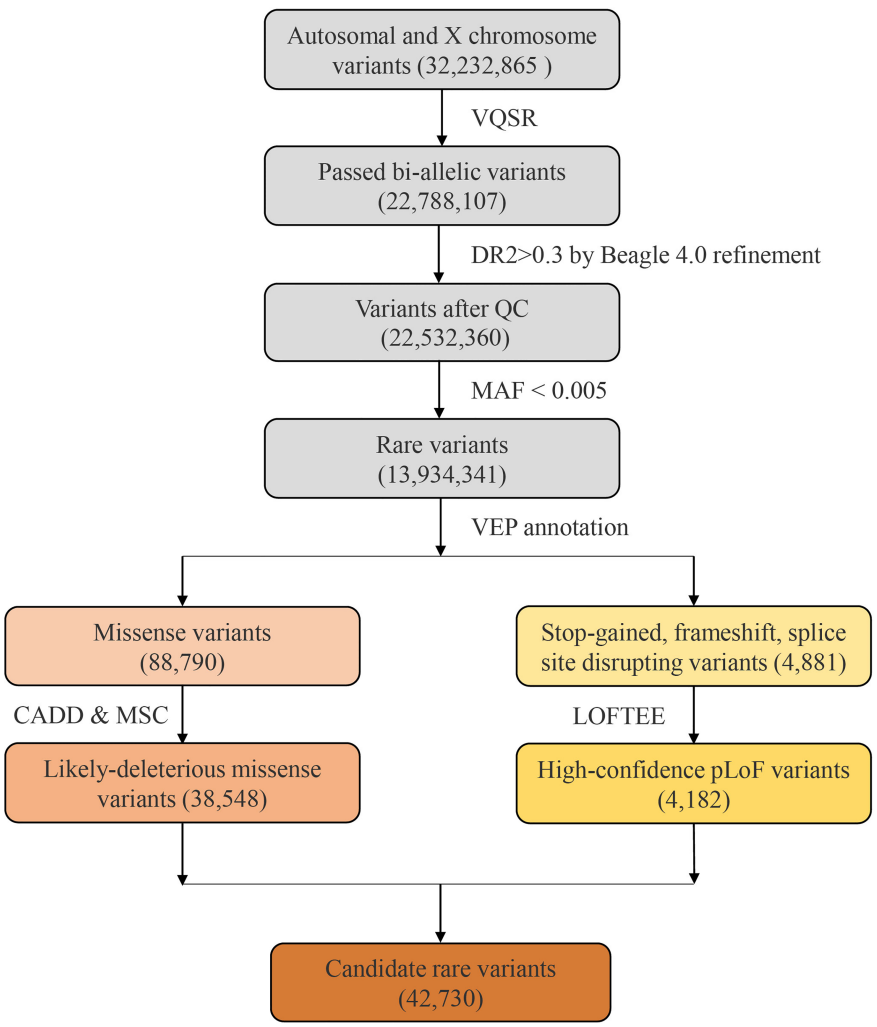

FIGURE 1 | The flow diagram of rare variants analysis. A total of 32,232,865 variants were identified from the 451 Covid-19 patients with whole genome sequencing. After filtering by VQSR and MAF, 13,934,341 rare variants were annotated by VEP, and 42,730 candidate variants were included.

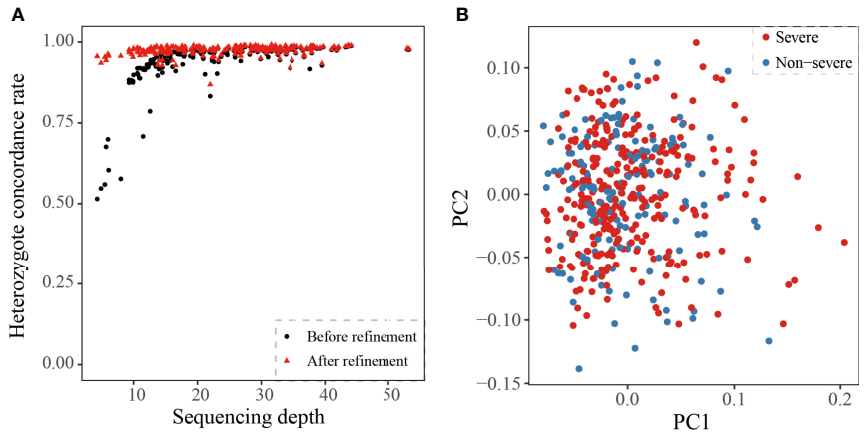

FIGURE 2 | Quality estimate of the cohort. **(A)** Heterozygote concordance rate vs. sequencing depth for 218 array-genotyped individuals. The black point and red triangle represent one sample before and after refinement. **(B)** PCA of 159 non-severe and 292 severe Covid-19 patients. The red and blue represent the severe or non-severe patients.

likely damaging variants were applied for further analysis. For both LDM variants and HC-pLoF variants, we first tested the difference of their numbers between *non-severe* and *severe* patients and found no significant difference (**Supplementary Table S2**).

Gene- and Pathway-Level Analysis of Rare Variants

The gene-level analysis of rare variants was performed between *severe* and *non-severe* patients *via* KGGSeq. We performed the gene-based tests for genes mapped by all 42,730 rare variants, 38,548 LDM variants, and 4182 HC-pLoF variants, respectively. The gene-based analyses did not identify genes that passed the significance threshold of 1e-6 (**Supplementary Figures S1A–C**).

Furthermore, we leveraged the biological knowledge that sets of genes acting together in pathways. In total, we tested 307 KEGG pathways and detected Tuberculosis (hsa:05152, P-burden = 0.036) between *severe* and *non-severe* patients on LDM and HC-pLoF variants (**Supplementary Table S3**). Tuberculosis (TB) is an airborne infectious disease caused by Mycobacterium tuberculosis (Mtb). It first attacks the lungs, then other parts of the body through the circulatory system. This transmission characteristic is remarkably similar to that of Covid-19. As previously reported, Tuberculosis pathway was significant with acute respiratory distress syndrome and lung injury in mice and humans (Sweeney et al., 2017). The TB/Covid-19 Global Study Group observed a phenomenon that TB and SARS-CoV-2 might be co-infected, that is, TB was often diagnosed concurrently or after Covid-19 infection and the co-infection might account for increased case fatality rate (The TB/COVID-19 Global Study Group, 2021). Our finding brought up a possible explanation that patients with rare mutations enriched in Tuberculosis pathway were more likely to develop severe Covid-19 symptoms. More details about this candidate pathway, including the contributed genes, the corresponding gene-based results, and the number of carriers in cases and controls, were provided in **Supplementary Table S4**. When focusing on only pLOF variants enriched on KEGG, two significant pathways highlighted: Primary immunodeficiency (hsa:05340, P-burden = 0.014) and Influenza A (hsa:05164, P-burden = 0.021) (**Supplementary Table S2**). Primary immunodeficiencies (PID) are a group of potentially serious disorders that can cause increased susceptibility to severe infections, autoimmune diseases, and malignancy. Several studies revealed that patients with PID displayed higher morbidity and mortality from Covid-19 (Hunt et al., 2013; Zuk et al., 2014; Trinder et al., 2020; Kousathanas et al., 2022). Influenza is an infectious respiratory disease caused by influenza virus. Bibert et al. observed that gene pathways involved in the detection of Influenza A overlapped with those involved in the detection of SARS-CoV-2 virus (Bibert et al., 2021). In these two biological pathways, three functional genes, *IKBKG*, *IRF7*, and *IFNAR1*, were previously identified to have an effect on Covid-19 severity (Zhang Q. et al., 2020). More details about these two potentially functional pathways are provided in **Supplementary Tables S5 and S6**.

Tested on 159 Candidate Genes

In addition to uncovering unknown possibly associated genes or pathways, we also tested 159 previously reported candidate genes, with 24 in the IFN pathway (Zhang Q. et al., 2020; Kosmicki et al., 2021) and 136 located within 50 kb of significant common variants in the Covid-19 HGI (COVID-19 Host Genetics Initiative, 2021). Specifically, we focused on LDM and HC-pLOF variants to aggregate potential effects of rare variants. For missense variants in both IFN- and HGI-genes, we did not detect significant difference between *severe* and *non-severe* patients.

In the 24 IFN-genes, we found one HC-pLoF variant rs780744847 (c.1180C>T/p.R394*) on *TLR3* mutated in only *severe* patients but no mutations in *non-severe* patients. It was reported that the *TLR3* deficiency may lead to increased incidences of viral infections and impair the production of type

I IFN throughout SARS-CoV-2 infection (Zhang Q. et al., 2020). Moreover, mutations of inborn errors of TLR3-dependent type I IFN immunity more often occurred in highly critical patients than in mild patients and healthy controls.

For the 136 HGI-genes, we found that the number of HC-pLoF mutations occurred in the *severe* group was more than that of the *non-severe* groups (16 in *severe* and 2 in *non-severe* patients, Fisher's exact test p = 0.043) (**Table 2**). We also detected a HC-pLoF variant rs541048548 (c.1053del/p.A352fs) on *ICAM3* only mutated in *severe* patients. The gene *ICAM3* played an important role in the immunopathogenesis of SARS virus (Chan et al., 2007) and had been reported that its expression was downregulated in asymptomatic Covid-19 cases compared with symptomatic patients (Masood et al., 2021).

Mutation Accumulation Analyses

In the mutation accumulation analysis, we first investigated whether there were potentially functional mutations unique to *severe* patients. We filtered in rare variants mutated in only *severe* patients and with minor allele count (MAC) greater than or equal to three. This resulted in 756 rare variants mapped to 700 genes. Among these variants, we observed a very rare mutation rs777044791 in gene *CCR3* at locus 3p21.31 (**Table 3**). The physical distance between rs777044791 and rs11385942 is 0.43 MB (GRCh38), a distance typically flanked into the same genomic region (Casto and Feldman, 2011). The variant rs11385942 is a common variant located at locus 3p21.31 in European populations and was first identified to be associated with respiratory failure due to Covid-19 from GWAS analysis in Italian and Spanish populations (Ellinghaus et al., 2020). This finding was repeated in other studies based on European populations (COVID-19 Host Genetics Initiative, 2021; Pairo-Castineira et al., 2021; Shelton et al., 2021), verifying its effects on Covid-19 disease. In the Chinese population, common variant studies at this locus did not replicate significance (Wang et al., 2020; Wu et al., 2021b;

TABLE 2 | The pLoF variants identified in Covid-19 patients in 159 candidate genes.

Gene	SNP	Variant annotation	HGVSc/HGVSp	Genotype	Sample ID	Sex	Age range	Phenotype	Category
TLR3	rs780744847	Stop gained	c.1180C>T/p.Arg394Ter	Het	U312	F	70-79	Severe	IFN-genes
THBS3	rs748584696	Stop gained	c.853C>T/p.Arg285Ter	Het	U088	F	80-89	Severe	HGI-genes
THBS3	chr1_155206198_A_C	Splice donor variant	c.286+2T>G	Het	U359	F	70-79	Severe	HGI-genes
TAC4	rs372635644	Splice acceptor variant	c.124-1G>A	Het	U429	F	60-69	Severe	HGI-genes
TYK2	rs770927552	Frameshift variant	c.209_212del/p.Cys70SerfsTer21	Het	U422	F	80-89	Severe	HGI-genes
C6orf15	chr6_31112292_C_T	Splice acceptor variant	c.68-1G>A	Het	U107	M	60-69	Severe	HGI-genes
CAT	rs777641795	Splice donor variant	c.1195+1G>A	Het	U012	M	40-49	Non-severe	HGI-genes
CDH15	chr16_89179469_C_G	Stop gained	c.96C>G/p.Tyr32Ter	Het	U174	F	50-59	Severe	HGI-genes
CDSN	chr6_31116133_G_GA	Frameshift variant	c.1481dup/p.Cys496LeufsTer20	Het	U021	F	50-59	Non-severe	HGI-genes
ICAM3	rs541048548	Frameshift variant	c.1053delC/p.Ala352ArgfsTer11	Het	U225	M	70-79	Severe	HGI-genes
ICAM3	rs541048548	Frameshift variant	c.1053delC/p.Ala352ArgfsTer11	Het	U047	F	70-79	Severe	HGI-genes
MYDGF	rs745851558	Splice donor variant	c.174+1G>T	Het	U071	M	70-79	Severe	HGI-genes
PLEKHA4	chr19_48853718_CA_C	Frameshift variant	c.1289delT/p.Leu430ArgfsTer4	Het	U261	F	60-69	Severe	HGI-genes
PLEKHA4	chr19_48853720_GCCGGT_G	Frameshift variant	c.1283_1287delACCGG/ p.Asp428AlafsTer76	Het	U261	F	60-69	Severe	HGI-genes
PPP1R15A	rs768756506	Frameshift variant	c.1535_1536delAT/ p.Tyr512CysfsTer14	Het	U309	M	60-69	Severe	HGI-genes
PSORS1C2	rs79153019	Frameshift variant	c.281delC/p.Pro94LeufsTer35	Het	U075	M	60-69	Severe	HGI-genes
PSORS1C2	rs79153019	Frameshift variant	c.281delC/p.Pro94LeufsTer35	Het	U150	M	60-69	Severe	HGI-genes
PSORS1C2	rs79153019	Frameshift variant	c.281delC/p.Pro94LeufsTer35	Het	U144	M	60-69	Severe	HGI-genes
TULP2	chr19_48881045_T_TC	Frameshift variant	c.1528_1529insG/ p.Gln510ArgfsTer17	Het	U176	F	70-79	Severe	HGI-genes

TABLE 3 | The comparison of allele frequency for two loci.

	rs777044791	rs11385942
CHROM	chr3	chr3
POS (hg38)	46,266,186	45,834,967
ALT	T	GA
REF	C	G
Variant annotation	Missense variant	Intron variant
Allele frequency		
Severe (N = 292)	0.005	0
Non-severe (N = 159)	0	0
ChinaMAP	0.002	0.004
1000G_EAS	0	0.005
1000G_EUR	0	0.0805
1000G_SAS	0	0.296
1000G_AFR	0	0.053
gnomAD_EAS	0.0005	0.0006

Zhu et al., 2021), and no rare variant studies had been conducted. Our work raised a possibility that SNPs in locus 3p21.31 might also play an important role in Covid-19 severity in the Chinese population.

Then, we performed PPI network analysis for the 700 "individual variant-driven" genes with the 159 known genes (**Figure 3A**). From the results, we found two candidate genes *IL12RB1* and *TRAF3IP3* that had extensive interactions with IFN- and HGI-genes. Gene *IL12RB1* (Interleukin 12 Receptor Subunit Beta 1) encodes a type I transmembrane protein that binds to interleukin-12 (IL12) and is involved in IL12 transduction. Mutations in *IL12RB1* damage the development of IL17-producing T lymphocytes and increase the susceptibility to Salmonella and mycobacterial infections (van de Vosse et al., 2013). Our PPI network analysis indicated that *IL12RB1* and *TYK2* had experimentally determined interactions, which were compiled from a set of public databases and were more likely to be credible (Zhang et al., 2013). Gene *TYK2* had been previously identified to be associated with Covid-19 critical illness (Pairo-Castineira et al., 2021), implying the potential effects of *IL12RB1* to the aggravation of Covid-19. The gene *TRAF3IP3* (TRAF3 Interacting Protein 3) encodes a protein that plays essential roles in both innate and adaptive immunity. Knockout mouse experiments of this gene observed a decrease in white blood cell count in males and an increased susceptibility to bacterial infection (Gardin and White, 2011). In our results, TRAF3IP3 was experimentally determined with protein TRAF3 encoded by gene *TRAF3*, which was included in a newly created pathway "Activation of NLRP3 inflammasome by SARS-CoV-2" (WP4876) (Siu et al., 2019). In response to viral infection, *TRAF3IP3* bridges *TRAF3* and *MAVS* leading to interferon production, indicating it's probably strong relationship with Covid-19 disease.

We also performed PPI network analysis for the 778 "all variant-driven" genes with the 159 known genes (**Figure 3B**), from which three genes, *TBK1*, *TLR3*, and *IFNGR2* were highlighted. Specifically, *TBK1* (TANK Binding Kinase 1) encodes a protein that plays important roles in antiviral innate immune response and in regulating inflammatory response to foreign agents (Fitzgerald et al., 2003; Mori et al., 2004). A previous study observed colocalization of *TBK1* with the M protein of SARS-CoV-2, which might hinder the dsRNA-induced IFN production at the step or upstream of *TBK1* (Zheng et al., 2020). The gene *TLR3* (Toll Like Receptor 3) encodes a member of the TLR family that plays a primary role in recognition of pathogen and innate immunity activation. It recognizes dsRNA participated in multiple viral infections and induces type I IFNs production (Kawai and Akira, 2007). The gene *IFNGR2* (Interferon Gamma Receptor 2) encodes the non-ligand-binding beta chain of the gamma interferon receptor. A recent study revealed a new set of genes that upregulated in severe Covid-19 patients compared to mild ones, probably triggered by *IFNGR1* and *IFNGR2* (Henriques-Pons et al., 2021).

In summary, our mutation accumulation analyses and PPI network analyses suggested that *IL12RB1*, *TRAF3IP3*, *TBK1*, and *TLR3* and *IFNGR2* are key regions in *severe* Covid-19 patients compared with *non-severe*, implying their functions and associations with Covid-19 severity.

CONCLUSION

In our study, we have uncovered several functional pathways associated with Covid-19 severity, for example, Tuberculosis (hsa:05152), Primary Immunodeficiency (hsa:05340), and Influenza A (hsa:05164). These pathways are all responsible for innate immune disorders and respiratory diseases, highlighting the importance of host innate immune system against Covid-19. Our mutation accumulation analysis and PPI network analysis suggested several novel candidate genes in the Chinese population, including *IL12RB1*, *TBK1*, *TLR3*, and *IFNGR2*. These genes are potentially involved in SARS-CoV-2 cell entry, host immune responses, and finally influencing Covid-19 severity.

On one hand, our work filled the gap of IEI analysis in Covid-19 patients in the Chinese population; on the other hand, we replicated several Covid-19-associated genes first identified from a European population and also discovered some candidate genes specific to the Chinese population.

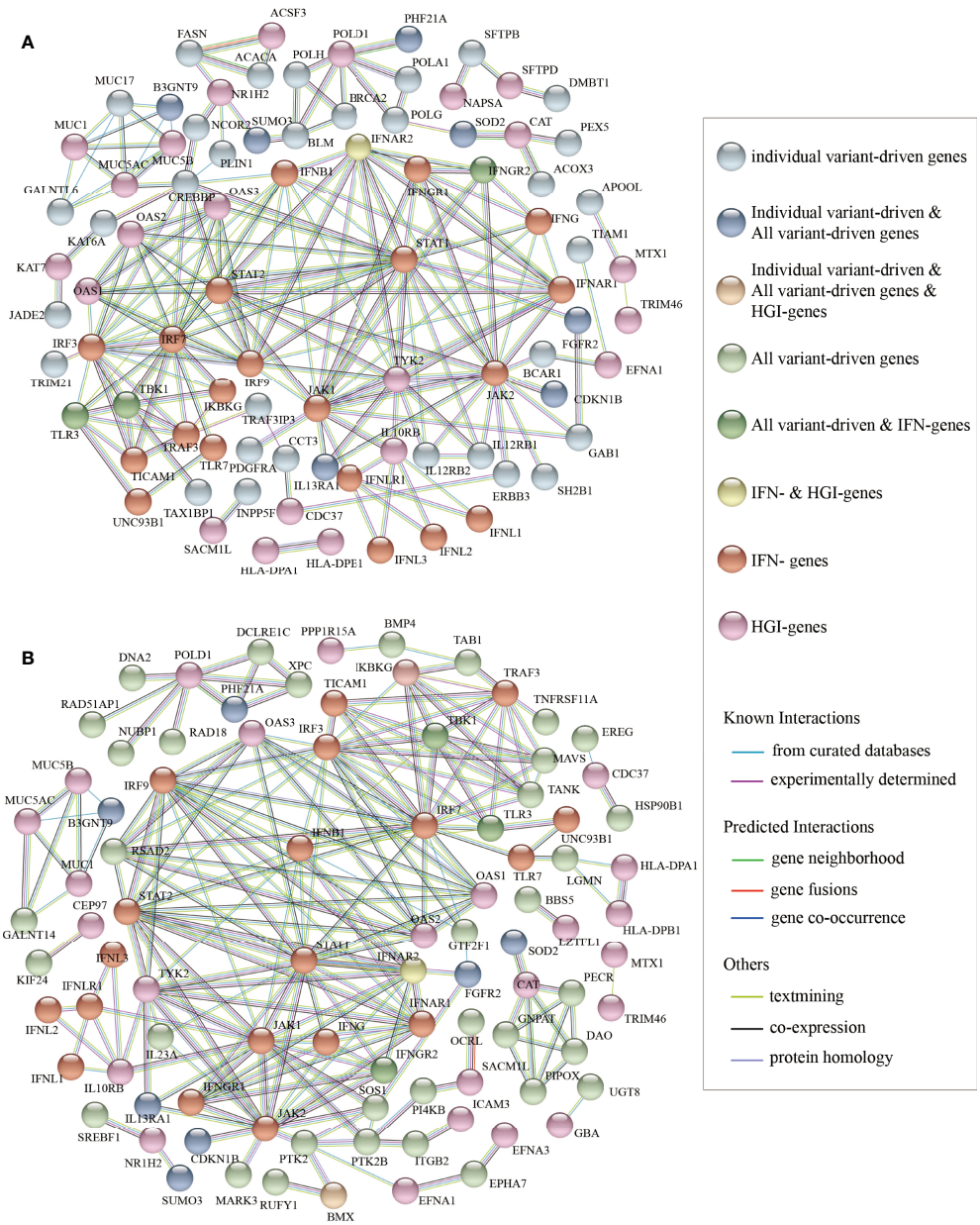

FIGURE 3 | The results of protein-protein interaction network analysis. The plot of the PPI network **(A)** between the "individual variant-driven" genes with the candidate genes, and **(B)** between the "all variant-driven" genes with the candidate genes.

DISCUSSION

SARS-CoV-2 is a strain of coronavirus and is highly pathogenic and transmissible. After exposure to the virus, ordinary people may not develop noticeable symptoms or develop mild to moderate symptoms, while people with IEI tend to suffer severe and critical symptoms, or even death (Zhang S.-Y. et al., 2020). There is increasing evidence that the host genetic variants in genes related to immunodeficiency or inflammasomes might attribute to Covid-19 clinical manifestations (Elhabyan et al., 2020). Many clinical drug treatments for Covid-19 were cultivated from this finding, including type I IFNs (e.g., IFN-α1b), TNF inhibitors, anti-IFN-γ antibodies, JAK1 inhibitors, and STAT1 inhibitors (Ku et al., 2021).

In this work, we carried out the first study of rare variants in IEI genes associated with Covid-19 severity in the Chinese population. The identified functional candidate pathways Tuberculosis, Primary Immunodeficiency, and Influenza A were previously known to be part of antiviral immune responses and viral eradication, and we discovered their potential influences in Covid-19. We also suggested several putative genetic regions probably involved in susceptibility and severity of Covid-19, including genes *IL12RB1*, *TRAF3IP3*,

TBK1, *TLR3*, and *IFNGR2*. Our work highlighted the importance of rare IEI in Covid-19 patients and people with IEI defects are more likely to be infected with SARS-CoV-2 and to develop severe symptoms. Thus, we appeal more studies on IEI in both the Chinese population and other populations to pinpoint causal genes of Covid-19 severity and finally help identify those patients at higher risk.

Despite the many compelling and significant findings of our work, there are still a few limitations to be noted. First, the sample size we used is relatively small, and the limited sample size limits the statistical power for identifying rare variants. More studies with large sample sizes are demanded to validate our results and uncover more candidate variants. Second, our work has suggested several candidate genes and pathways potentially related to Covid-19 severity, yet unfortunately, due to resources limitations, we are unable to perform web-lab experiments and verify gene functions at this stage. More persuasive experimental designs are needed to investigate how these candidate genes/pathways affect disease progression.

Covid-19 is assessed as a complex infectious disease and affected many risk factors. Symptoms of Covid-19 are highly variable, ranging from unnoticeable to severe and even death. The host genetic background is only partly responsible for the phenotypic heterogeneity. In recent years, multi-omics studies have proven a powerful and successful strategy to provide a broader perspective in understanding disease development and biological phenomena. Several multi-omics analyses of Covid-19 have been proposed to integrate multiple "omes" data to unravel disease mechanisms at multiple omics levels (Su et al., 2020; Montaldo et al., 2021; Overmyer et al., 2021; Stephenson et al., 2021; Wu et al., 2021a). The integrative analyses of rare genome and other "omes" data (e.g., proteome, transcriptome, epigenome, metabolome, and microbiome) may inspire us to discover new risk factors for severe Covid-19 disease.

DATA AVAILABILITY STATEMENT

The data that support the findings of this study have been deposited into CNGB Sequence Archive (CNSA) (Guo et al., 2020) of China National GeneBank DataBase (CNGBdb) (Guo et al., 2020) with accession number CNP0002853.

ETHICS STATEMENT

The studies involving human participants were reviewed and approved by Medical Ethics Committee of Union Hospital, Tongji Medical College, Huazhong University of Science and Technology. The patients/participants provided their written informed consent to participate in this study.

AUTHOR CONTRIBUTIONS

XJ and HZ conceived the study, designed the research program, and managed the project. PL and HZ performed the statistical analyses. MF advised on statistical methods. PL and HZ wrote the manuscript. FC, FZ, and YJ collected the samples. YL finished the laboratory processing and data acquisition. All authors participated in revising the manuscript. All authors read and approved the final manuscript.

FUNDING

This study was supported by National Natural Science Foundation of China (No. 31800765, 32171441, 32000398), Natural Science Foundation of Guangdong Province, China (2017A030306026), and Guangdong-Hong Kong Joint Laboratory on Immunological and Genetic Kidney Diseases (2019B121205005).

ACKNOWLEDGMENTS

We thank the families who participated in the study and made this research study possible. We would like to acknowledge Mingya Wang's, Chang Bian's, and Linxi Wang's contributions on correcting grammatical errors in this study.

SUPPLEMENTARY MATERIAL

The Supplementary Material for this article can be found online at: https://www.frontiersin.org/articles/10.3389/fcimb.2022.888582/full#supplementary-material

Supplementary Figure 1 | Results of gene-based association tests of rare variants. **(A)**. The QQ plots of gene-based association analyses between severe and non-severe patients for **(A)** 42,730 candidate rare variants; **(B)** 38,548 rare likely-deleterious missense variants, and **(C)** 4182 high-confidence pLoF variants. The color represents different association methods integrated in KGGseq, including SKAT test (in blue), SKAT-O (in red), and burden test (in orange).

REFERENCES

Asano, T., Boisson, B., Onodi, F., Matuozzo, D., Moncada-Velez, M., Luxman Maglorius Renkilaraj, M. R, et al. (2021). "X-Linked Recessive TLR7 Deficiency in ~1% of Men Under 60 Years Old With Life-Threatening COVID-19". *Sci. Immunol.* 6 (62), eabl4348. doi: 10.1126/sciimmunol.abl4348

Bibert, S., Guex, N., Lourenco, J., Brahier, T., Papadimitriou-Olivgeris, M., Damonti, L., et al. (2021). Transcriptomic Signature Differences Between SARS-CoV-2 and Influenza Virus Infected Patients. *Front. Immunol.* 12, 1990. doi: 10.3389/fimmu.2021.666163

Browning, B. L., and Browning, S. R. (2016). Genotype Imputation With Millions of Reference Samples. *Am. J. Hum. Genet.* 98 (1), 116–126. doi: 10.1016/j.ajhg.2015.11.020

Casto, A. M., and Feldman, M. W. (2011). Genome-Wide Association Study SNPs in the Human Genome Diversity Project Populations: Does Selection Affect Unlinked SNPs With Shared Trait Associations? *PLoS Genet.* 7 (1), e1001266. doi: 10.1371/journal.pgen.1001266

Chan, K. Y. K., Ching, J. C. Y., Xu, M. S., Cheung, A. N. Y., Yip, S.-P., Yam, L. Y. C., et al. (2007). Association of ICAM3 Genetic Variant With Severe Acute Respiratory Syndrome. *J. Infect. Dis.* 196 (2), 271–280. doi: 10.1086/518892

Chang, ,. C. C., Chow, C. C., Tellier, L. C., Vattikuti, S., . Purcell, S. M, and Lee, J. J (2015). Second-Generation PLINK: Rising to the Challenge of Larger and Richer Datasets. *GigaScience* 4, 7. doi: 10.1186/s13742-015-0047-8

Clarke, L., Zheng-Bradley, X., Smith, R., Kulesha, E., Xiao, C., Toneva, I., et al. (2012). The 1000 Genomes Project: Data Management and Community Access. *Nat. Methods* 9 (5), 459–462. doi: 10.1038/nmeth.1974

COVID-19 Host Genetics Initiative. (2021). Mapping the Human Genetic Architecture of COVID-19. *Nature* 600 (7889), 472–477. doi: 10.1101/2021.11.08.21265944

Cummings, M. J., Baldwin, M. R., Abrams, D., Jacobson, S. D., Meyer, B. J., Balough, E. M., et al. (2020). Epidemiology, Clinical Course, and Outcomes of Critically Ill Adults With COVID-19 In New York City: A Prospective Cohort Study. *Lancet (Lond. Engl.)* 395 (10239), 1763–1770. doi: 10.1016/S0140-6736(20)31189-2

Danecek, P., Bonfield, J. K., Liddle, J., Marshall, J., Ohan, V., Pollard, M. O., et al. (2021). Twelve Years of SAMtools and BCFtools. *GigaScience* 10 (2), giab008. doi: 10.1093/gigascience/giab008

DePristo, M. A., Banks, E., Poplin, R., Garimella, K. V., Maguire, J. R., Hartl, C., et al. (2011). A Framework for Variation Discovery and Genotyping Using Next-Generation DNA Sequencing Data. *Nat. Genet.* 43 (5), 491–498. doi: 10.1038/ng.806

Elhabyan, A., Elyaacoub, S., Sanad, E., Abukhadra, A., Elhabyan, A., and Dinu, V. (2020). The Role of Host Genetics in Susceptibility to Severe Viral Infections in Humans and Insights Into Host Genetics of Severe COVID-19: A Systematic Review. *Virus Res.* 289, 198163. doi: 10.1016/j.virusres.2020.198163

Ellinghaus, D., Degenhardt, F., Bujanda, L., Buti, M., Albillos, A., Invernizzi, P., et al. (2020). Genomewide Association Study of Severe Covid-19 With Respiratory Failure. *N. Engl. J. Med* 383 (16), 1522–1534. doi: 10.1056/NEJMoa2020283

Fallerini, C., Daga, S., Mantovani, S., Benetti, E., Picchiotti, N., Francisci, D., et al. (2021). Association of Toll-Like Receptor 7 Variants With Life-Threatening COVID-19 Disease in Males: Findings From a Nested Case-Control Study. *ELife* 10, 1–2. doi: 10.7554/eLife.67569

Fitzgerald, K. A., McWhirter, S. M., Faia, K. L., Rowe, D. C., Latz, E., Golenbock, D. T., et al. (2003). IKKepsilon and TBK1 Are Essential Components of the IRF3 Signaling Pathway. *Nat. Immunol.* 4 (5), 491–496. doi: 10.1038/ni921

Freed, D.N., Aldana, R., Weber, J.A., and Edwards, J. (2017). The Sentieon Genomics Tools - A Fast and Accurate Solution to Variant Calling From Next-Generation Sequence Data. *bioRxiv*. Available at: http://biorxiv.org/content/early/2017/05/12/115717.abstract.

Gardin, A., and White, J. (2011). "The Sanger Mouse Genetics Programme: High Throughput Characterisation of Knockout Mice". *Acta Ophthalmolog.* 89 (s248). doi: 10.1111/j.1755-3768.2011.4451.x

Gorbalenya, A. E., Baker, S. C., Baric, R. S., de Groot, R. J., Drosten, C., Gulyaeva, A. A., et al. (2020). The Species Severe Acute Respiratory Syndrome-Related Coronavirus: Classifying 2019-NCoV and Naming It SARS-CoV-2. *Nat. Microbiol.* 5 (4), 536–544. doi: 10.1038/s41564-020-0695-z

Gorlov, I. P., Gorlova, O. Y., Frazier, M. L., Spitz, M. R., and Amos, C. I. (2011). Evolutionary Evidence of the Effect of Rare Variants on Disease Etiology. *Clin. Genet.* 79 (3), 199–206. doi: 10.1111/j.1399-0004.2010.01535.x

Guo, X., Chen, F., Gao, F., Li, L., Liu, K., You, L., et al. (2020). CNSA: A Data Repository for Archiving Omics Data. *Database*, 2020 1–6. doi: 10.1093/database/baaa055

Henriques-Pons, A., Beghini, D. G., Santos Silva, V. D., Horita, S. I., and da Silva, F. A. B. (2021). Pulmonary Mesenchymal Stem Cells in Mild Cases of COVID-19 Are Dedicated to Proliferation; In Severe Cases, They Control Inflammation, Make Cell Dispersion, and Tissue Regeneration. *Front. Immunol.* 12. doi: 10.3389/fimmu.2021.780900

Hunt, K. A., Mistry, V., Bockett, N. A., Ahmad, T., Ban, M., Barker, J. N., et al. (2013). Negligible Impact of Rare Autoimmune-Locus Coding-Region Variants on Missing Heritability. *Nature* 498 (7453), 232–235. doi: 10.1038/nature12170

Itan, Y., Shang, L., Boisson, B., Ciancanelli, M. J., Markle, J. G., Martinez-Barricarte, R., et al. (2016). The Mutation Significance Cutoff: Gene-Level Thresholds for Variant Predictions. *Nat. Methods* 13 (2), 109–110. doi: 10.1038/nmeth.3739

Kanehisa, M., and Goto, S. (2000). KEGG: Kyoto Encyclopedia of Genes and Genomes. *Nucleic Acids Res.* 28 (1), 27–30. doi: 10.1093/nar/28.1.27

Karczewski, K. J., Francioli, L. C., Tiao, G., Cummings, B. B., Alföldi, J., Wang, Q., et al. (2020). The Mutational Constraint Spectrum Quantified From Variation in 141,456 Humans. *Nature* 581 (7809), 434–443. doi: 10.1038/s41586-020-2308-7

Kawai, T., and Akira, S. (2007). Signaling to NF-KappaB by Toll-Like Receptors. *Trends Mol. Med.* 13 (11), 460–469. doi: 10.1016/j.molmed.2007.09.002

Kircher, M., Witten, D. M., Jain, P., O'Roak, B. J., Cooper, G. M., and Shendure, J. (2014). A General Framework for Estimating the Relative Pathogenicity of Human Genetic Variants. *Nat. Genet.* 46 (3), 310–315. doi: 10.1038/ng.2892

Kosmicki, J. A., Horowitz, J. E., Banerjee, N., Lanche, R., Marcketta, A., Maxwell, E., et al. (2021). Pan-Ancestry Exome-Wide Association Analyses of COVID-19 Outcomes in 586,157 Individuals. *Am. J. Hum. Genet.* 108 (7), 1350–1355. doi: 10.1016/j.ajhg.2021.05.017

Kousathanas, A., Pairo-Castineira, E., Rawlik, K., Stuckey, A., Odhams, C. A., Walker, S., et al. (2022). Whole Genome Sequencing Reveals Host Factors Underlying Critical Covid-19. *Nature*. doi: 10.1038/s41586-022-04576-6

Ku, C.-L., Chen, I. T., and Lai, M.-Z. (2021). Infection-Induced Inflammation From Specific Inborn Errors of Immunity to COVID-19. *FEBS J.* 288 (17), 5021–5041. doi: 10.1111/febs.15961

Lee, S., Wu, M. C., and Lin, X. (2012). Optimal Tests for Rare Variant Effects in Sequencing Association Studies. *Biostat (Oxf. Engl.)* 13 (4), 762–775. doi: 10.1093/biostatistics/kxs014

Li, H., and Durbin, R. (2009). Fast and Accurate Short Read Alignment With Burrows-Wheeler Transform. *Bioinf. (Oxf. Engl.)* 25 (14), 1754–1760. doi: 10.1093/bioinformatics/btp324

Li, M., Li, J., Li, M. J., Pan, Z., Hsu, J. S., Liu, D. J., et al. (2017). Robust and Rapid Algorithms Facilitate Large-Scale Whole Genome Sequencing Downstream Analysis in an Integrative Framework. *Nucleic Acids Res.* 45 (9), e75. doi: 10.1093/nar/gkx019

Mantovani, S., Daga, S., Fallerini, C., Baldassarri, M., Benetti, E., Picchiotti, N., et al. (2022). Rare Variants in Toll-Like Receptor 7 Results in Functional Impairment and Downregulation of Cytokine-Mediated Signaling in COVID-19 Patients. *Genes Immun.* 23, 51–56. doi: 10.1038/s41435-021-00157-1

Masood, K. I., Yameen, M., Ashraf, J., Shahid, S., Mahmood, S. F., Nasir, A., et al. (2021). Upregulated Type I Interferon Responses in Asymptomatic COVID-19 Infection Are Associated With Improved Clinical Outcome. *Sci. Rep.* 11 (1), 22958. doi: 10.1038/s41598-021-02489-4

McLaren, W., Gil, L., Hunt, S. E., Riat, H. S., Ritchie, G. R. S., Thormann, A., et al. (2016). The Ensembl Variant Effect Predictor. *Genome Biol.* 17 (1), 122. doi: 10.1186/s13059-016-0974-4

Misawa, K., Hasegawa, T., Mishima, E., Jutabha, P., Ouchi, M., and Kojima, K. (2020). Contribution of Rare Variants of the SLC22A12 Gene to the Missing Heritability of Serum Urate Levels. *Genetics* 214 (4), 1079–1090. doi: 10.1534/genetics.119.303006

Montaldo, C., Messina, F., Abbate, I., Antonioli, M., Bordoni, V., Aiello, A., et al. (2021). Multi-Omics Approach to COVID-19: A Domain-Based Literature Review. *J. Trans. Med.* 19 (1), 501. doi: 10.1186/s12967-021-03168-8

Mori, M., Yoneyama, M., Ito, T., Takahashi, K., Inagaki, F., and Fujita, T. (2004). Identification of Ser-386 of Interferon Regulatory Factor 3 as Critical Target for Inducible Phosphorylation That Determines Activation. *J. Biol. Chem.* 279 (11), 9698–9702. doi: 10.1074/jbc.M310616200

Overmyer, K. A., Shishkova, E., Miller, I. J., Balnis, J., Bernstein, M. N., Peters-Clarke, T. M., et al. (2021). Large-Scale Multi-Omic Analysis of COVID-19 Severity. *Cell Syst.* 12 (1), 23–40.e7. doi: 10.1016/j.cels.2020.10.003

Pairo-Castineira, E., Clohisey, S., Klaric, L., Bretherick, A. D., Rawlik, K., Pasko, D., et al. (2021). Genetic Mechanisms of Critical Illness in COVID-19. *Nature* 591 (7848), 92–98. doi: 10.1038/s41586-020-03065-y

Pearson, K. (1901). "LIII. On Lines and Planes of Closest Fit to Systems of Points in Space". *London Edinburgh Dublin Philos. Magazine J. Sci.* 2 (11), 559–572. doi: 10.1080/14786440109462720

Price, A. L., Patterson, N. J., Plenge, R. M., Weinblatt, M. E., Shadick, N. A., and Reich, D. (2006). Principal Components Analysis Corrects for Stratification in Genome-Wide Association Studies. *Nat. Genet.* 38 (8), 904–909. doi: 10.1038/ng1847

Shelton, J. F., Shastri, A. J., Ye, C., Weldon, C. H., Filshtein-Sonmez, T., Coker, D., et al. (2021). Trans-Ancestry Analysis Reveals Genetic and Nongenetic

Associations With COVID-19 Susceptibility and Severity. *Nat. Genet.* 53 (6), 801–808. doi: 10.1038/s41588-021-00854-7

Sherry, S. T., Ward, M. H., Kholodov, M., Baker, J., Phan, L., Smigielski, E. M, et al. (2001). "DbSNP: The NCBI Database of Genetic Variation". *Nucleic Acids Res.* 29 (1), 308–311. doi: 10.1093/nar/29.1.308

Siu, K.-L., Yuen, K.-S., Castaño-Rodriguez, C., Ye, Z.-W., Yeung, M.-L., Fung, S.-Y., et al. (2019). Severe Acute Respiratory Syndrome Coronavirus ORF3a Protein Activates the NLRP3 Inflammasome by Promoting TRAF3-Dependent Ubiquitination of ASC. *FASEB J.* 33 (8), 8865–8877. doi: 10.1096/fj.201802418R

Smieszek, S. P., Polymeropoulos, V. M., Xiao, C., Polymeropoulos, C. M., and Polymeropoulos, M. H. (2021). Loss-Of-Function Mutations in IFNAR2 in COVID-19 Severe Infection Susceptibility. *J. Global Antimicrob. Resist.* 26, 239–240. doi: 10.1016/j.jgar.2021.06.005

Stephenson, E., Reynolds, G., Botting, R. A., Calero-Nieto, F. J., Morgan, M. D., Tuong, Z. K., et al. (2021). Single-Cell Multi-Omics Analysis of the Immune Response in COVID-19. *Nat. Med.* 27 (5), 904–916. doi: 10.1038/s41591-021-01329-2

Su, Y., Chen, D., Yuan, D., Lausted, C., Choi, J., Dai, C. L., et al. (2020). Multi-Omics Resolves a Sharp Disease-State Shift Between Mild and Moderate COVID-19. *Cell* 183 (6), 1479–1495.e20. doi: 10.1016/j.cell.2020.10.037

Sweeney, T. E., Lofgren, S., Khatri, P., and Rogers, A. J. (2017). Gene Expression Analysis to Assess the Relevance of Rodent Models to Human Lung Injury. *Am. J. Respir. Cell Mol. Biol.* 57 (2), 184–192. doi: 10.1165/rcmb.2016-0395OC

Szklarczyk, D., Gable, A. L., Lyon, D., Junge, A., Wyder, S., Huerta-Cepas, J., et al. (2019). STRING V11: Protein–Protein Association Networks With Increased Coverage, Supporting Functional Discovery in Genome-Wide Experimental Datasets. *Nucleic Acids Res.* 47 (D1), D607–D613. doi: 10.1093/nar/gky1131

The TB/COVID-19 Global Study Group. (2021). Tuberculosis and COVID-19 Co-Infection: Description of the Global Cohort. *Eur. Respir. J.* 59, 2102538. doi: 10.1183/13993003.02538-2021

Trinder, M., Walley, K. R., Boyd, J. H., and Brunham, L. R. (2020). Causal Inference for Genetically Determined Levels of High-Density Lipoprotein Cholesterol and Risk of Infectious Disease. *Arteriosclerosis Thrombosis Vasc. Biol.* 40 (1), 267–278. doi: 10.1161/ATVBAHA.119.313381

van der Made, C. I., Simons, A., Schuurs-Hoeijmakers, J., van den Heuvel, G., Mantere, T., Kersten, S., et al. (2020). Presence of Genetic Variants Among Young Men With Severe COVID-19. *JAMA* 324 (7), 663–673. doi: 10.1001/jama.2020.13719

van de Vosse, E., Haverkamp, M. H., Ramirez-Alejo, N., Martinez-Gallo, M., Blancas-Galicia, L., Metin, A., et al. (2013). IL-12rβ1 Deficiency: Mutation Update and Description of the IL12RB1 Variation Database. *Hum. Mutat.* 34 (10), 1329–1339. doi: 10.1002/humu.22380

Wang, F., Huang, S., Gao, H., Zhou, Y., Lai, C., Li, Z., et al. (2020). Initial Whole Genome Sequencing and Analysis of the Host Genetic Contribution to COVID-19 Severity and Susceptibility. *Cell Discov.* 6 (1), 83. doi: 10.1101/2020.06.09.20126607

Williams, F. M. K., Freydin, M., Mangino, M., Couvreur, S., Visconti, A., Bowyer, R. C. E., et al. (2020). Self-Reported Symptoms of COVID-19, including Symptoms Most Predictive of SARS-CoV-2 Infection, Are Heritable. *Twin Res. Hum. Genet.* 23, 316–321. doi: 10.1017/thg.2020.85

Wu, P., Chen, D., Ding, W., Wu, P., Hou, H., Bai, Y., et al. (2021a). The Trans-Omics Landscape of COVID-19. *Nat. Commun.* 12 (1), 4543. doi: 10.1038/s41467-021-24482-1

Wu, P., Ding, L., Li, X., Liu, S., Cheng, F., He, Q., et al. (2021b). Trans-Ethnic Genome-Wide Association Study of Severe COVID-19. *Commun. Biol.* 4 (1), 1034. doi: 10.1038/s42003-021-02549-5

Wu, M. C., Kraft, P., Epstein, M. P., Taylor, D. M., Chanock, S. J., Hunter, D. J., et al. (2010). Powerful SNP-Set Analysis for Case-Control Genome-Wide Association Studies. *Am. J. Hum. Genet.* 86 (6), 929–942. doi: 10.1016/j.ajhg.2010.05.002

Wu, Z., and McGoogan, J. M. (2020). Characteristics of and Important Lessons From the Coronavirus Disease 2019 (COVID-19) Outbreak in China: Summary of a Report of 72 314 Cases From the Chinese Center for Disease Control and Prevention. *JAMA* 323 (13), 1239–1242. doi: 10.1001/jama.2020.2648

Yang, X., Yu, Y., Xu, J., Shu, H., Xia, J., Liu, H., et al. (2020). Clinical Course and Outcomes of Critically Ill Patients With SARS-CoV-2 Pneumonia in Wuhan, China: A Single-Centered, Retrospective, Observational Study. *Lancet Respir. Med.* 8 (5), 475–481. doi: 10.1016/S2213-2600(20)30079-5

Zhang, F., Flickinger, M., Gagliano Taliun, S. A., Abecasis, G. R., Scott, L. J., McCaroll, S. A., et al. (2020). Ancestry-Agnostic Estimation of DNA Sample Contamination From Sequence Reads. *Genome Res.* 30 (2), 185–194. doi: 10.1101/gr.246934.118

Zhang, Q., Liu, Z., Moncada-Velez, M., Chen, J., Ogishi, M., Bigio, B., et al. (2020). Inborn Errors of Type I IFN Immunity in Patients With Life-Threatening COVID-19. *Science* 370 (6515), eabd4570. doi: 10.1126/science.abd4570

Zhang, Q. C., Petrey, D., Garzón, J. I., Deng, L., and Honig, B. (2013). PrePPI: A Structure-Informed Database of Protein-Protein Interactions. *Nucleic Acids Res.* 41 (Database issue), D828–D833. doi: 10.1093/nar/gks1231

Zhang, S.-Y., Zhang, Q., Casanova, J.-L., Su, H. C.COVID Team (2020). Severe COVID-19 in the Young and Healthy: Monogenic Inborn Errors of Immunity? *Nat. Rev. Immunol.* 20 (8), 455–456. doi: 10.1038/s41577-020-0373-7

Zheng, Y., Zhuang, M.-W., Han, L., Zhang, J., Nan, M.-L., Zhan, P., et al. (2020). Severe Acute Respiratory Syndrome Coronavirus 2 (SARS-CoV-2) Membrane (M) Protein Inhibits Type I and III Interferon Production by Targeting RIG-I/MDA-5 Signaling. *Signal Transduct. Target. Ther.* 5 (1), 299. doi: 10.1038/s41392-020-00438-7

Zhu, N., Zhang, D., Wang, W., Li, X., Yang, B., Song, J., et al. (2020). A Novel Coronavirus From Patients With Pneumonia in China 2019. *N. Engl. J. Med.* 382 (8), 727–733. doi: 10.1056/NEJMoa2001017

Zhu, H., Zheng, F., Li, L., Jin, Y., Luo, Y., Li, Z., et al. (2021). A Chinese Host Genetic Study Discovered Type I Interferons and Causality of Cholesterol Levels and WBC Counts on COVID-19 Severity. *iScience* 24, 103186. doi: 10.1016/j.isci.2021.103186

Zuk, O., Schaffner, S. F., Samocha, K., Do, R., Hechter, E., Kathiresan, S., et al. (2014). Searching for Missing Heritability: Designing Rare Variant Association Studies. *Proc. Natl. Acad. Sci.* 111 (4), E455 LP–E464. doi: 10.1073/pnas.1322563111

Conflict of Interest: Authors PL, MF, YL, HZ, and XJ were employed by BGI-Shenzhen.

The remaining authors declare that the research was conducted in the absence of any commercial or financial relationships that could be construed as a potential conflict of interest.

Publisher's Note: All claims expressed in this article are solely those of the authors and do not necessarily represent those of their affiliated organizations, or those of the publisher, the editors and the reviewers. Any product that may be evaluated in this article, or claim that may be made by its manufacturer, is not guaranteed or endorsed by the publisher.

frontiers | Frontiers in Cellular and Infection Microbiology

ORIGINAL RESEARCH
published: 14 June 2022
doi: 10.3389/fcimb.2022.888398

Application of Next-Generation Sequencing in Infections After Allogeneic Haematopoietic Stem Cell Transplantation: A Retrospective Study

Xiaoying Zhang[1], Yun Li[1], Jin Yin[1], Bixin Xi[2], Na Wang[1] and Yicheng Zhang[1,3]**

[1] Department of Hematology, Tongji Hospital, Tongji Medical College, Huazhong University of Science and Technology, Wuhan, China, [2] Department of Pediatrics, Tongji Hospital, Tongji Medical College, Huazhong University of Science and Technology, Wuhan, China, [3] Institute of Organ Transplantation, Tongji Hospital, Tongji Medical College, Huazhong University of Science and Technology, Wuhan, China

OPEN ACCESS

Edited by:
Jinmin Ma,
Beijing Genomics Institute (BGI), China

Reviewed by:
Xin Lu,
Chinese Center For Disease Control and Prevention, China
Jingkai Ji,
Shandong First Medical University, China

***Correspondence:**
Yicheng Zhang
yczhang@tjh.tjmu.edu.cn
Na Wang
Wangna.2001@163.com

Specialty section:
This article was submitted to Clinical Microbiology, a section of the journal Frontiers in Cellular and Infection Microbiology

Received: *02 March 2022*
Accepted: *21 April 2022*
Published: *14 June 2022*

Citation:
Zhang X, Li Y, Yin J, Xi B, Wang N and Zhang Y (2022) Application of Next-Generation Sequencing in Infections After Allogeneic Haematopoietic Stem Cell Transplantation: A Retrospective Study. Front. Cell. Infect. Microbiol. 12:888398. doi: 10.3389/fcimb.2022.888398

This retrospective study aimed to determine the characteristics of infection and diagnostic efficacy of next-generation sequencing (NGS) in patients with fever after allogeneic hematopoietic stem cell transplantation (allo-HSCT). A total of 71 patients with fever after HSCT were enrolled in this study. Compared with conventional microbiological test (CMT), we found that the sensitivity of NGS versus CMT in peripheral blood samples was 91.2% vs. 41.2%, and that NGS required significantly less time to identify the pathogens in both monomicrobial infections (P=0.0185) and polymicrobial infections (P= 0.0027). The diagnostic performance of NGS was not affected by immunosuppressant use. Viruses are the most common pathogens associated with infections. These results indicated that the sensitivity, timeliness, and clinical significance of NGS are superior for the detection of infections. Although NGS has the advantage of identifying a wide range of potential pathogens, the positive rate is related closely to the sample type. Therefore, we recommend that, in the clinical application of NGS to detect pathogens in patients after allo-HSCT, an appropriate sample type and time should be selected and submitted to improve the positive rate and accuracy of NGS. NGS holds promise as a powerful technology for the diagnosis of fever after HSCT.

Keywords: next-generation sequencing, allogeneic haematopoietic stem cell transplantation, diagnosis, infection, immunosuppression

INTRODUCTION

Allogeneic hematopoietic stem cell transplantation (allo-HSCT) is a curative option for a wide range of disorders such as hematological malignancies and some nonmalignant diseases (Blazar et al., 2020). Infections are one of the most frequent and important causes of mortality and morbidity after allo-HSCT (Styczyński et al., 2020). Allo-HSCT is a complicated and multifactorial process, in which the standard

risks are associated mainly with neutropenia, mucositis, and catheter use. In addition, myeloablative conditioning regimens, reconstitution of the immune system, use of immunosuppressive drugs, and graft-versus-host disease (GVHD) are independent risk factors for infections (Kao and Holtan, 2019). Infectious pathogens have also varied among the studies that have used different testing methods. Conventional microbiological tests remain the main methods used to identify pathogens in the clinic, such as smear microscopic examination and culture; however, these are relatively insensitive and are used mainly to detect bacteria, fungi, and parasites (Goldberg et al., 2015; Grumaz et al., 2016; Gu et al., 2019). Recently, nucleic acid amplification techniques, such as real-time quantitative polymerase chain reaction (RQ-PCR) and multiplex PCR, have been used widely for the diagnosis of infectious diseases, especially viral infections (Watzinger et al., 2006; Schlaberg et al., 2017b). Multiplex PCR has been recognized as the "gold standard" to identify viruses in central nervous system (CNS) infections (Schmidt-Hieber et al., 2016). Nevertheless, there are still some limitations to the use of RQ-PCR, such as the genetic diversity of some pathogens and the need for knowledge of the target pathogen (Schlaberg et al., 2017b). Therefore, there is an urgent need to develop novel diagnostic methods to detect potential pathogens in undetermined infections successfully.

Next-generation sequencing (NGS) has showed a constant improvement in recent decades with its continuous improvements and use in clinical settings, providing a powerful tool for success in medical practice (Goldberg et al., 2015; Wilson et al., 2019; Tang et al., 2021). NGS is capable of detecting multiple pathogens on the same day at the same time rapidly (Barreda-García et al., 2018), includingthe identification of nonculturable microbes (Íñigo et al., 2016). Recent studies have identified pathogens using NGS in the diagnosis of several diseases, including diseases of the respiratory tract (Huang et al., 2020; Li et al., 2020), urinary tract (Gasiorek et al., 2019), central nervous system (CNS) (Schmidt-Hieber et al., 2016; Liu et al., 2021), bloodstream (Grumaz et al., 2016; Eichenberger et al., 2021; Nie et al., 2022), and periprosthetic joint infections (Tarabichi et al., 2018). However, there have been relatively few studies on the use of NGS for infections after allo-HSCT. Clinical experience with the application of NGS is relatively limited. Due to the severity and uniqueness of infections in patients after allo-HSCT, the rapid and accurate diagnosis and assessment are important for rational treatment and prognosis evaluation (Sahin et al., 2016). This study aimed to compare the efficacy of NGS with that of conventional microbiological test (CMT) and to determine whether NGS technology can meet this need by evaluating its ability to detect pathogens in febrile patients after allo-HSCT. At the same time, the infection status of the patients after HSCT was evaluated.

MATERIAL AND METHOD

Patients and Study Design

We retrospectively analyzed the basic situation, pathogenic infections, clinical treatment, and prognosis of 71 patients who underwent allo-HSCT at the Hematopoietic Stem Cell Transplantation Center of Tongji Hospital, affiliated with the Huazhong University of Science and Technology between March 2019 and October 2020. These patients developed fever with or without other symptoms after transfusion and who underwent CMT and NGS tests. Different specimen types were collected for detection, according to the type of suspected infection. The clinicians prescribed CMT according to their clinical judgment of necessity. The CMT included smear microscopy, culture, RQ-PCR, T-SPOT TB test, serological tests, and the detection of antigens (**Supplementary Methods**). The samples were collected and transported to Huada Laboratories (Shenzhen, China) for NGS. The treatment choice was individualized for each patient.

Infection Prophylaxis and Virus Monitoring

All the patients were treated in a transplantation cabin. Antimicrobial prophylaxis was used routinely: voriconazole 0.4 g once every 12 h, acyclovir 400 mg once every 12 h, and trimethoprim-sulfamethoxazole 960 mg twice a day for two days each week. When an infection was suspected, the attending physician adjusted the antimicrobial protocols according to the patients' conditions and the institutional guidelines. Ciclosporin A (CsA) and tacrolimus (FK-506) were generally used to treat GVHD. RQ-PCR was used to measure the DNA of the Epstein–Barr virus (EBV) and cytomegalovirus (CMV) in the peripheral blood (PB) weekly for the first three months, then once every two weeks from the 4th to the 9th month and then once per month from the 10th to the 12th month after transplantation.

Diagnosis of Infection

Fever was defined as an axillary temperature ≥37.3°C. The diagnosis was based on clinical symptoms, laboratory tests, radiographic, microbiologic, histopathologic findings, and treatment outcome information. The final diagnosis of infections was performed by two independent experienced clinicians according to published consensus criteria (Ascioglu et al., 2002; De Pauw et al., 2008; Haidar and Singh, 2022). The appropriate clinical specimens were collected for testing (i.e., blood samples, sputum, urine, nasopharyngeal swabs, puncture fluids, tissue samples, aspirates, and bronchoalveolar lavage fluid) according to the type of suspected infection. The site of infection included mainly the bloodstream, respiratory tract, CNS, and skin. The day of infection onset was defined as the day on which the diagnostic test was performed. Multiple positive results for different organisms on the same day were considered as separate events, and one microorganism in two non-adjacent organs was counted as two infectious events. In addition, if the detected microorganism was a possible contaminant (for example, Candida in a fecal culture or coagulase-negative Staphylococcus species in a blood culture) and was isolated in only one culture, it was excluded from the analysis.

NGS Procedure

Qualified sample from patient was collected and stored according to standard procedures. After DNA extraction, the DNA libraries were constructed and sequenced by MGISEQ-

2000 platform. Next, High-quality sequencing data were generated by removing low-quality and short (length <35 bp) reads, followed by computational substraction of human host sequences mapped to the human reference genome (hg19) using Burrows-Wheeler Alignment. The remaining data by removal of low-complexity reads were classified by simultaneously aligning to Pathogens metagenomics Database (PMDB), which were downloaded from the NCBI (ftp://ftp.ncbi.nlm.nih.gov/genomes/) (Schoch et al., 2020), consisting of bacteria, fungi, viruses and parasites.

To eliminate false positive, periodic environmental assessments was conducted, and standard operation Procedures (SOP) was established to monitor contamination for periodic disinfection of reagents, instruments, and laboratory surfaces. Possible contaminants in non-template references or positive controls were continuously tracked, and conservative criteria was used to minimize false positive results. As for the cut-off value of NGS for pathogen detection, the criteria were shown as below: 1) Bacteria (mycobacteria excluded), viruses, and parasites: NGS identified a microbe (species level) whose coverage rate scored 10-fold greater than that of any other microbes according to Langelier's study. 2) Fungi: NGS identified a microbe (species level) whose coverage rate scored 5-fold higher than that of any other fungus because of its low biomass in DNA extraction. 3) Mycobacteria: Mycobacterium tuberculosis (MTB) was considered positive when at least 1 read was mapped to either the species or genus level due to the difficulty of DNA extraction and low possibility for contamination.

Statistical Analysis

All the clinical and laboratory data were collected during the onset of the infection. The sensitivity, specificity, positive predictive value (PPVs), and negative predictive value (NPVs) were calculated according to the definitions. The Chi-square or Fisher's exact tests were used for categorical variable comparisons, as appropriate. The kappa (κ) statistic was used to assess the test concordance. The student's t-test or Kruskal–Wallis test was used for the continuous variables, as appropriate. Statistical analyses were conducted using SPSS version 26.0 (IBM Corp., Armonk, NY, USA), and figures were rendered using GraphPad Software (version 8.02; Mariakerke, Belgium) and R Software (version 3.6.3). The statistical significance set at P <0.05 (two-tailed) was considered to be statistically significant.

RESULTS

Patients' Characteristics and Infection Among All Patients

Thirty-seven patients were male and 34 were female, and the patients had a median age of 23 years (range, 14–33). The primary diseases included acute myeloid leukemia (AML, n = 29), acute lymphoblastic leukemia (ALL, n = 15), myelodysplastic syndrome (MDS, n = 3), aplastic anemia (AA, n = 22), and T lymphoblastic lymphoma (T-LBL, n = 2). Thirteen patients were HLA-matched, and 58 underwent HLA-mismatched donor transplantation. All the patients received myeloablative conditioning regimens. At the onset of the symptoms, 23 patients (32.2%) had agranulocytosis and 58 (81.7%) received immunosuppressive therapy. The patient samples comprised mainly peripheral blood (57.7%). The median values of CRP, PCT, and IL-6 in all of the patients were 70.4 (IQR, 20.7–148.6), 0.445 (IQR, 0.263–1.378), and 50.22 (IQR, 7.20–124.00), respectively. The baseline clinical and biochemical data of the 71 patients are described in **Table 1**.

According to the consensus criteria, the diagnosis was confirmed in 54 patients. Only one patient's NGS and CMT results were negative, but based on the subsequent pathological biopsy results, the patient was diagnosed with an invasive fungal infection. Most of the patients' infections were viral, followed by polymicrobial infections. The infections were present mainly in the bloodstream, followed by pulmonary, digestive, and urinary tract infections. Five patients were diagnosed with central infections (diagnosed using intracranial biopsy or cerebrospinal fluid analysis), and two patients were diagnosed with skin and soft tissue infections (**Figure 1B**).

TABLE 1 | Patient characteristics.

	All patients (n = 71)
Age, years (median, IQR)	23 (14-33)
Female	37 (52.1%)
Protopathy	
AA	22 (30.1%)
ALL	15 (21.1%)
AML	29 (40.8%)
MDS	3 (4.2%)
T-LBL	2 (2.8%)
Transplantation way	
Haplo	58 (81.7%)
MSD	6 (8.5%)
MUD	7 (9.9%)
N engraftment, days (median, IQR)	13 (11-15)
PLT engraftment, days(median, IQR)*	13 (12-16)
Main Symptoms	
fever	50 (70.4%)
diarrhea	8 (11.3%)
cough	3 (4.2%)
rash	3 (4.2%)
blurred version	1 (1.4%)
headaches	3 (4.2%)
ascites	1 (1.4%)
tic	1 (1.4%)
Sample collection time	
Peri-planting period	12 (16.9%)
<100D	25 (35.2%)
>100D	34 (47.9%)
Agranulocytic	23 (32.4%)
Immunosuppressive drugs	58 (81.7%)

PLT engraftment, days (median, IQR): excluded 3 cases without PLT engraftment. AA, aplastic anemia; ALL, Acute lymphoblastic leukemia; AML, Acute myeloid leukemia; MDS, Myelodysplastic syndromes; T-LBL, T lymphoblastic lymphoma; Haplo, Haploidentical stem cell transplantation; MSD, Matched sibling donor; MUD, Matched unrelated donor.*

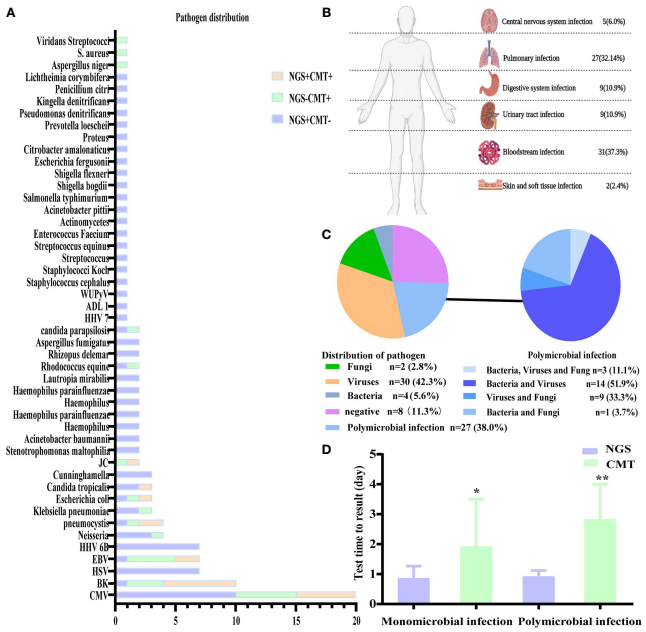

FIGURE 1 | Distribution of pathogens identified in patients with fever after allo-HSCT using CMT versus NGS. **(A)** The figure showed the number of subjects in whom each causative microbe was detected. Orange bars indicate microbes detected by CMT and also predicted as pathogens by NGS (CMT+NGS+). Purple bars indicate microbes detected by NGS only (CMT–NGS+). Green bars indicate the number of cases with microbes detected only by CMT (CMT+NGS–); **(B)** distribution of types of infection was shown from patients with clinical diagnosis; **(C)** distribution of pathogens was shown from patients. Polymicrobial infection accounted for 38.0% among all the subjects and different kinds of polymicrobial infection were also shown in the right; **(D)** the diagnostic time required for NGS and CMT were compared in subjects with monomicrobial infection or polymicrobial infection. *P<0.05; **P<0.001 by Wilcoxon rank-sum test.

Diagnostic Performance of NGS and CMT

The comparison of the sensitivity, specificity, PPVs, and NPVs of the peripheral blood samples by NGS and the CMT method for all 41 patients is shown in **Table 2**. The diagnostic value of NGS was significantly higher than that of CMT (P < 0.001). The results of NGS and CMT were concordant in 15 of the 41 (36.6%) patients. Our results showed that the sensitivity of NGS and CMT were respectively 91.2% and 41.2% for pathogen identification in the PB samples of 41 patients.

In the present study, the pathogens of NGS and CMT detected in the patients are shown in **Figure 1A**. Viruses, especially CMV, which was the highest percent, accounted for the majority of the pathogens, and NGS was better for the detection of rare bacteria and fungi. According to the NGS results, viruses (n=30, 42.3%) were the most common pathogens identified, followed by polymicrobial (**Figure 1C**). The top two causative pathogens identified were CMV (n=20), BK (n=10). We further analyzed the test time required to determine the pathogenic diagnosis. For monomicrobial infections and polymicrobial infections, the detection cycles required for NGS and CMT were significantly different. CMT required significantly more time to identify the pathogens than NGS (P = 0.0185, P=0.0027) (**Figure 1D**). Meanwhile, we analyzed the detection performance of NGS and CMT in monomicrobial and polymicrobial infections. The sensitivity of NGS and CMT were 81.58% vs 57.89% (P = 0.0445) for monomicrobial infections, respectively, and 68.75% vs 37.50% (P=0.1556) for polymicrobial infections, respectively. This indicated that NGS was more sensitive than CMT for monomicrobial infections and a suggestive, but not significant benefit in polymicrobial infections.

TABLE 2 | Comparison of positive results among next-generation sequencing and conventional microbiological tests.

		Positive	Negative	*P <0.001*
NGS	Positive	31	5	
	Negative	3	2	
CMT	Positive	14	2	
	Negative	20	5	
	Sensitivity%	Specificity%	PPV	*NPV*
NGS	91.2	28.6	0.861	0.4
CMT	41.2	71.4	0.875	0.8

Positive, patients with a positive clinical diagnosis; NGS, next-generation sequencing; CMT, conventional microbiological tests.

Distribution of the Infections in the Different Periods After Transplantation

Based on the occurrence of symptoms in the different periods after transplantation, the 71 patients were divided into three groups (**Figure 2**). The male-to-female ratio, primary disease, mode of transplantation, and complications of GVHD in the three groups are shown in **Supplementary Table 1**. Among them, seven and nine patients in Groups 2 and 3, respectively, were complicated with GVHD at the time of infection. The positive pathogens are

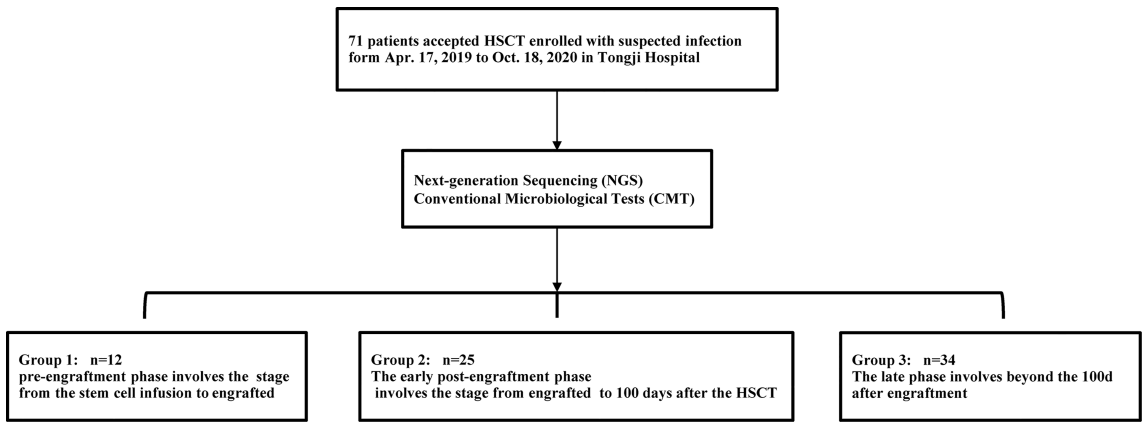

FIGURE 2 | Trial process. Between Apr.17, 2019 to Oct.18, 2020, 71 patients who developed fever with/without other symptoms after the transfusion and underwent CMT and NGS tests were screened for eligibility in this study. In terms of the time of clinical symptoms appeared, the patients were divided into three groups.

shown in **Figures 3A–C** with CMV being the most common infection. Patients with Aspergillus fumigatus in Group 1 had a history of fungal infection before transplantation. In Group 2, there was a high detection rate of cystitis with the detection of BK and JC viruses in the urine. Group 3 had more complex pathogenic pathogens, fungal species, and rare bacterial species. The detection results for fever and other infectious symptoms in Group 1 were mainly negative. The main reason for this is that the disease was diagnosed as an ALG-related serum sickness and implantation syndrome, and the results of NGS and CMT were used as exclusion tests. Second, it may have been an immune disorder in patients with peri-implantation and a low pathogen detection rate. In Group 2, the pathogens that were detected were mainly viruses ($P = 0.0203$), especially CMV; an HHV6 infection also needed special attention. In Group 3, fungal, viral, mixed, and rare pathogens accounted for a relatively high proportion of the pathogens, which may have been related to late post-transplantation patients with GVHD and other transplantation-related complications, patients taking immunosuppressants, and other reasons (**Figure 3**).

No Significant Influence of Immunosuppression on the Diagnostic Accuracy of NGS and CMT

To determine whether the diagnostic performance of NGS was affected by immunosuppression, we evaluated the relationship between immunosuppression and the positive rate of CMT and NGS. Our results showed that there was no significant difference in the positivity rate between NGS and CMT, regardless of the use of immunosuppressants. That is, the positivity rate was not affected by the use of immunosuppressants (**Figure 4A**). In addition to the routine use of immunosuppressants according to the anti-GVHD regimen, patients after HSCT will need to have their dosage and usage of immunosuppressive mediations adjusted individually when GVHD occurs. Therefore, we investigated the distribution of pathogens in GVHD patients. CMV infection was also the most common, of which six cases were intestinal GVHD coinfected with gastrointestinal CMV infections, and NGS had excellent performance in diagnosing HHV 6 B and Cunninghamella (**Figure 4B**). At the same time, we analyzed the positive results of NGS and CMT in patients with agranulocytosis, but also found no significant effect (**Figure 4C**).

Effect of the Different Specimen Types on the NGS and CMT Results

The distribution of pathogens in different tissues, organs, and systems is different; therefore, the type of samples submitted for examination will be related closely to the test results. Six patients had different NGS and CMT samples and different detection results, which helped obtain a clearer diagnosis and identify the pathogen of potential infection (**Table 3**). The treatment details for the two representative cases are shown in **Figures 5C, D**. We can draw conclusions from these cases because of the distribution of pathogens in the blood, tissue, or cross, and the appropriate timing is also of great significance in improving the positive rate of detection. In addition, we found that, except for the timing of the examination, the selection of samples was crucial for the detection of a positive rate. The detection rates of NGS and CMT in the different inspection specimens are shown in **Figures 5A, B**, respectively. The CMT of peripheral blood samples, especially the positive rate of the blood cultures, was not as high as that of NGS, but for common pathogens in diseased tissues, such as in the gastrointestinal mucosa of patients with diarrhea and sputum/bronchoalveolar lavage fluid samples of patients with cough, the positive rates of NGS and CMT are similar.

DISCUSSION

Fever after allo-HSCT is complicated. Infection after transplantation is one of the leading causes of fever and other symptoms, and is the most common and important cause of death. Early diagnosis and timely treatment are considered to be

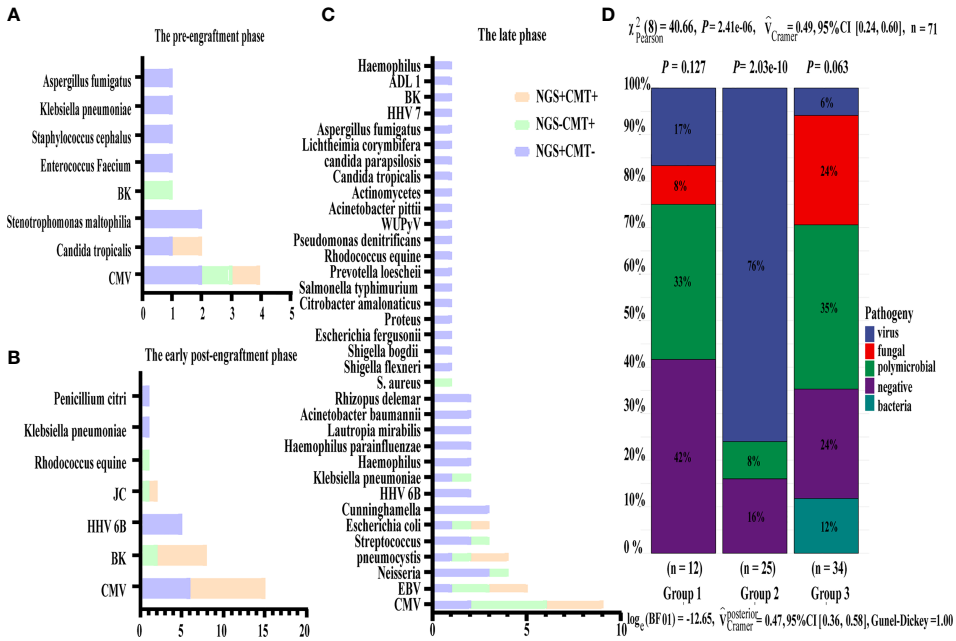

FIGURE 3 | Distribution of pathogens identified in three group using CMT versus NGS. **(A–C)** Respectively showed the number of subjects in whom each causative microbe was detected in three group. Orange bars indicate microbes detected by CMT and also predicted as pathogens by NGS (CMT+NGS+). Purple bars indicate microbes detected by NGS only (CMT–NGS+). Green bars indicate the number of cases with microbes detected only by CMT (CMT+NGS–). **(D)** Distribution of pathogens was shown from patients in three group. Virus infection accounted for 76% among group 2 and there were significant differences in pathogen species.

the most critical factors in determining the outcomes. Conventional microbiological test (CMT) are obtained when clinicians make a series of differential diagnoses according to the clinical manifestations of cases; however, usually, a test can only correspond to one pathogen, the coverage rate is low, and difficult to cultivate (Duan et al., 2021). Different pathogens have different culture times (Miao et al., 2018). Recently, NGS has become a sensitive technology for the detection of pathogens in human biopsy samples and body fluids, including blood, urine, cerebrospinal fluid, and bronchoalveolar lavage fluids (Huang et al., 2021), demonstrating the potential of NGS to accelerate and improve the diagnosis and management of diseases.

Pendleton et al.demonstrated that, in principle, real-time metagenomics methods using currently available tools can identify pathogens faster than traditional culture-based techniques and have the potential to identify pathogens that cannot grow in cultures (Pendleton et al., 2017). A study on the application of NGS in 108 patients with suspected infections treated with immunosuppressive corticosteroids showed that the sensitivity of NGS was 80.6%, which also played an important role in optimizing the antibiotic treatment of CMT-negative patients (Wang et al., 2020). Moreover, NGS results were not affected by immunosuppression. The combination of NGS and conventional methods increased the CSF detection rate in patients with tuberculous meningitis to 95.65%. They believed that NGS was an alternative method for detecting the presence of mycobacterial DNA in CSF samples of TBM patients and may be used as a first-line CSF test (Wang et al., 2019).

However, there have been few studies on the detection of NGS infections after HSCT. Therefore, we conducted a retrospective study in patients from our center who developed fever after HSCT between March 2019 and October 2020, and 71 patients were tested using NGS. Most of the patients' infections were viral, followed by polymicrobial infections. For both monomicrobial and polymicrobial infections, the detection time of NGS is significantly shorter than that of CMT, and NGS showed a higher sensitivity, especially for monomicrobial infections. Probably, just because of the small sample size, this has not yet become noticeable in the polymicrobial infections Accelerated pathogen identification is expected to improve customized antimicrobial therapy, avoid increased antibiotic resistance, improve patient prognosis, and promote antimicrobial management by minimizing the need for extensive empirical antimicrobial coverage (Dumford and Skalweit, 2016; Cazzola et al., 2017; Pendleton et al., 2017; Robilotti et al., 2017). CMT may not be comprehensive for some rare pathogens (Grumaz et al., 2020), which may lead to a detection delay, whereas NGS can sequence the whole DNA/RNA of the sample without any primers or probes. It has a commitment to identifying the most pathogens. Among the 41 patients with peripheral blood samples, 34 were diagnosed clinically with an infection. The sensitivity of NGS versus CMT in peripheral blood after transplantation was 91.2% and 41.2%, respectively, which was higher than that of CMT. However, the specificity of NGS is not as specific as that of CMT, which may be attributed to the differences in specimen types and cut-off values.

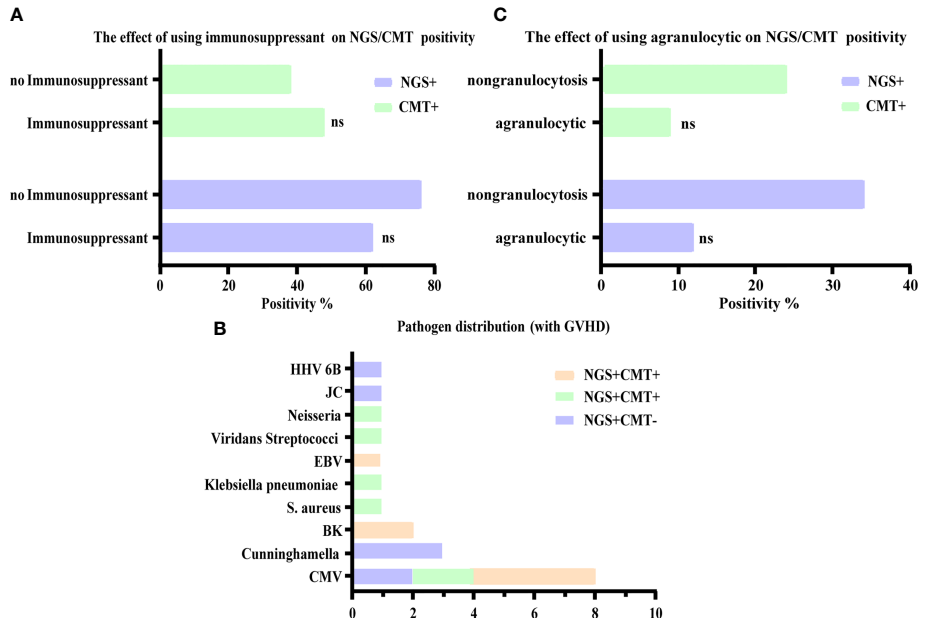

FIGURE 4 | Influence of other factors on the diagnostic accuracy of NGS and CMT. **(A, C)** Respectively shown that the positive microbiological detection rate of NGS and CMT was no significant correlation with immunosuppression and agranulocytic. **(B)** The number of detected microbes in patients with GVHD were presented, of which mainly were CMV. ns, non-significant statistical difference.

This suggests that caution should be exercised when interpreting NGS results alone, for clinical use. False-positive results may be due to the DNA contamination of background pathogens included in library preparation, low-quality readings from samples, misannotated species, or contaminants from database entries (Miller et al., 2019; Zhang et al., 2019; Zhang et al., 2020). In addition to establishing standardized operating rules, it is necessary to interpret the results further and reasonably.

In the groups studied, although the patients who were post-HSCT were most likely to develop viral infections, the distribution of pathogens was different in different periods. We found that the main causes of fever in the peri-implantation period were non-infectious diseases, such as ALG serum disease and implantation syndrome. After engraftment, the patients who had early infections had mainly viral infections, including CMV infections and cystitis caused by BK and JC. In the late stage after transplantation, the causes of fever and infection varied, and viral and mixed infections occurred first and second, respectively. Regardless of the period, the primary pathogenic viral infection was CMV, which showed that more attention should be paid to the detection and prevention of CMV in clinical practice. More often, NGS plays a major role in ruling out infection in the early post-transplantation period, while in the late post-transplantation period, the role of NGS is more accessible to identify the causative pathogen, especially after 100 days of transplantation. In addition, our results showed that the use of immunosuppressants or agranulocytosis does not affect the NGS detection results. Patients with GVHD may have compromised immune systems. NGS is also an excellent method for detecting pathogens in patients during this period. Intestinal GVHD patients co-infected with gastrointestinal CMV infections were also more common in our study. For patients with normal immune function and stable vital signs, CMT may be used to detect and retain samples simultaneously; if no positive result is found or if the patient's symptoms have not been alleviated within three days, NGS should be submitted immediately. However, patients with unstable signs or those in an immunosuppressive state should undergo simultaneous CMT and NGS tests. Standardizing the examination process using these diagnostic methods is important to identify pathogens and carry out effective targeted treatment (**Supplementary Figure 1**).

NGS can be used to detect a wide range of pathogens. There is no limitation to the use of one CMT to detect a single pathogen. This also reduces the mixed-packed testing methods of multiple laboratory methods. Packaged laboratory testing methods often require patients to undergo multiple tests, regardless of the cost or number of tests, which will not reduce the burden on patients and may even increase the burden on the patients (Miao et al., 2018). It is more sensitive to rare bacteria and fungi, and its detection period is short. However, because of false positives (Schlaberg et al., 2017a; Blauwkamp et al., 2019), the use of NSG requires strict standardization of detection techniques and an accurate interpretation of the results by clinicians to avoid overtreatment while treating the patient's diseases (Fan et al., 2018).

This study had several limitations. First, due to its high cost of detection, NGS is usually performed only once per patient, which limits its widespread use and repeated testing. In addition, since this was a retrospective study, the time and tissue samples used for NGS were not precisely the same as those used for CMT, and the

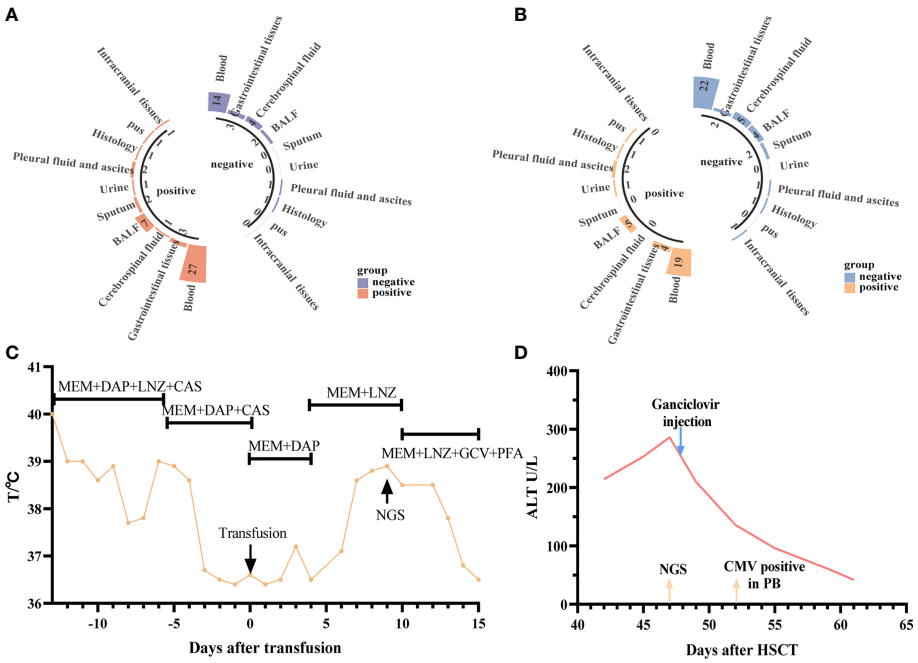

FIGURE 5 | Diagnostic value of NGS and CMT in different specimens. **(A, B)** Respectively shown that the positive microbiological detection rate of NGS and CMT using different specimens **(C)** representative case 1. A 5-year-old male patient with SAA developed a fever after hematopoietic stem cell (HSC) infusion. Meropenem and Daptomycin was given based on previous treatments but the symptom was not improved after 7 days of treatment. The CMT had negative results both blood and urine. Then the anti-infective regimen was adjusted according to NGS results (HHV-6B), which was obtained at +9d. After 7-day' s therapy the patient' s symptoms were improved; **(D)** representative case 2. A 22-year-old female patient with SAA developed low fever and persistent ALT elevation, and had no positive results in various laboratory tests. The liver puncture was performed, she was diagnosed with CMV infection (liver) based on the results from NGS at +47d. And then modified as soon as the NGS results were obtained (Ganciclovir). After only 5 days, CMV copy number was detected in peripheral blood. The patients' symptoms were finally improved.

TABLE 3 | Details of patients with different types of samples.

ID	Symptoms	Clinical diagnosis	NGS (pathogen, the sequence)	Specimen types	CMT Restult	Specimen types
P1	fevers, rash and cutaneous ulcer	cGVHD(Skin), skin soft tissue infection, EBV syndrome	HSV1 156;EBV 26; CMV 10	Peripheral blood	S. aureus, Klebsiella pneumoniae	secretions
P2	fever and cough	Pulmonary infection, human herpesvirus 6B infection	HHV-6B 517;	Peripheral blood	Klebsiella pneumoniae	sputum
P3	fever with cough, sputum and diarrhea	aGVHD (Gastrointestinal),CMV gastroenteritis, pulmonary infection.	HSV1 3738; HHV-6B 20; HHVB 7type 568; CMV 7; Torque teno virus 25;	Intestinal tissue	Viridans Streptococci, Neisseria	Fiber bronchoscope rinse solution
P4	Low fever and abdominal pain	CMV gastroenteritis, CMV hyperemia, cystitis	CMV 137; BK 10; EBV 3	Peripheral blood	BKV;CMV	Urine;Gastric mucosa
P5	Intermittent low fever	Pneumocystis carinii pneumonia	EBV 6	pleural effusion	Pneumocystis carinii	Fiber bronchoscope rinse solution
P6	fever with cough, sputum	pulmonary infection	Neisseria 3155; Haemophilus parainfluenzae 2579; Haemophilus 21; Prevotella loescheii 680; Rhodococcus equine 278; Pseudomonas denitrificans 10; Kingella denitrificans 114; WUPyV 9009; CMV 1485; HSV1 1326; HHV 7 73; EBV 53680; Rhodococcus equine 278; Pseudomonas denitrificans 10; Kingella denitrificans 114; WUPyV 9009; CMV 1485; HSV1 1326; HHV 7 73; EBV 53	sputum	negative	Peripheral blood

GVHD, graft versus host disease.

time of NGS specimen collection may have been later than that of CMT. As the collection time of NGS may have been different from the time that had the highest number of pathogens in the samples, repeated NGS tests may increase the sensitivity. Second, the sample size in our study was relatively small. To verify our conclusions, we have conducted a prospective study with a larger sample size. Finally, NGS could not perform a drug susceptibility test and, therefore, could not be substituted for conventional testing.

In summary, NGS has the potential to detect pathogens in patients undergoing febrile allogeneic hematopoietic stem cell transplantation. NGS is expected to become a valuable tool in the first-line diagnosis of infection and to provide valuable information for optimizing antibiotic treatment in cases.

DATA AVAILABILITY STATEMENT

The datasets presented in this study can be found in online repositories. The name of the repository and accession number can be found below: NCBI: PRJNA820385.

ETHICS STATEMENT

Ethical review and approval was not required for the study on human participants in accordance with the local legislation and institutional requirements. Written informed consent from the participants' legal guardian/next of kin was not required to participate in this study in accordance with the national legislation and the institutional requirements.

AUTHOR CONTRIBUTIONS

YZ and NW designed and supervised the clinical study, who have contributed equally to this work and share corresponding authorship. XZ and performed statistical analyses and wrote the manuscript. YL collected clinical data. JY and BX were responsible for diagnosis and patient management. YZ and NW revised the manuscript; All authors contributed to the article and approved the submitted version.

FUNDING

This study was supported by the National High Technology Research and Development Program of China (2021YFA1101504) and the National Natural Science Foundation of China (Grant No. 81873446, 82070217, 81600120 and 81873427).

SUPPLEMENTARY MATERIAL

The Supplementary Material for this article can be found online at: https://www.frontiersin.org/articles/10.3389/fcimb.2022.888398/full#supplementary-material

REFERENCES

Ascioglu, S., Rex, J. H., De Pauw, B., Bennett, J. E., Bille, J., Crokeart, F., et al. (2002). Defining Opportunistic Invasive Fungal Infections In Immunocompromised Patients With Cancer And Hematopoietic Stem Cell Transplants: An International Consensus. *Clin. Infect. Dis.* 34, 7–14. doi: 10.1086/323335

Barreda-García, S., Miranda-Castro, R., De-Los-Santos-Álvarez, N., Miranda-Ordieres, A. J., and Lobo-Castañón, M. J. (2018). Helicase-Dependent Isothermal Amplification: A Novel Tool In The Development Of Molecular-Based Analytical Systems For Rapid Pathogen Detection. *Anal. Bioanal. Chem.* 410, 679–693. doi: 10.1007/S00216-017-0620-3

Blauwkamp, T. A., Thair, S., Rosen, M. J., Blair, L., Lindner, M. S., Vilfan, I. D., et al. (2019). Analytical And Clinical Validation Of A Microbial Cell-Free Dna Sequencing Test For Infectious Disease. *Nat. Microbiol.* 4, 663–674. doi: 10.1038/S41564-018-0349-6

Blazar, B. R., Hill, G. R., and Murphy, W. J. (2020). Dissecting The Biology Of Allogeneic Hsct To Enhance The Gvt Effect Whilst Minimizing Gvhd. *Nat. Rev. Clin. Oncol.* 17, 475–492. doi: 10.1038/S41571-020-0356-4

Cazzola, M., Rogliani, P., Aliberti, S., Blasi, F., and Matera, M. G. (2017). An Update On The Pharmacotherapeutic Management Of Lower Respiratory Tract Infections. *Expert Opin. Pharmacother.* 18, 973–988. doi: 10.1080/14656566.2017.1328497

De Pauw, B., Walsh, T. J., Donnelly, J. P., Stevens, D. A., Edwards, J. E., Calandra, T, et al. (2008). Revised Definitions Of Invasive Fungal Disease From The European Organization For Research And Treatment Of Cancer/Invasive Fungal Infections Cooperative Group And The National Institute Of Allergy And Infectious Diseases Mycoses Study Group (Eortc/Msg) Consensus Group. *Clin. Infect. Dis.* 46, 1813–1821. doi: 10.1086/588660

Duan, H., Li, X., Mei, A., Li, P., Liu, Y., Li, X., et al. (2021). The Diagnostic Value Of Metagenomic Next-Generation Sequencing In Infectious Diseases. *BMC Infect. Dis.* 21, 62. doi: 10.1186/S12879-020-05746-5

Dumford, D., and Skalweit, M. (2016). Antibiotic-Resistant Infections And Treatment Challenges In The Immunocompromised Host. *Infect. Dis. Clin. North Am.* 30, 465–489. doi: 10.1016/J.Idc.2016.02.008

Eichenberger, E. M., De Vries, C. R., Ruffin, F., Sharma-Kuinkel, B., Park, L., Hong, D., et al. (2021). Microbial Cell-Free Dna Identifies Etiology Of Bloodstream Infections, Persists Longer Than Conventional Blood Cultures, And Its Duration Of Detection Is Associated With Metastatic Infection In Patients With Staphylococcus Aureus And Gram-Negative Bacteremia. *Clin. Infect. Dis.* ciab742. doi: 10.1093/Cid/Ciab742

Fan, S., Ren, H., Wei, Y., Mao, C., Ma, Z., Zhang, L., et al. (2018). Next-Generation Sequencing Of The Cerebrospinal Fluid In The Diagnosis Of Neurobrucellosis. *Int. J. Infect. Dis.* 67, 20–24. doi: 10.1016/J.Ijid.2017.11.028

Gasiorek, M., Hsieh, M. H., and Forster, C. S. (2019). Utility Of Dna Next-Generation Sequencing And Expanded Quantitative Urine Culture In Diagnosis And Management Of Chronic Or Persistent Lower Urinary Tract Symptoms. *J. Clin. Microbiol.* 58, e00204–19. doi: 10.1128/Jcm.00204-19

Goldberg, B., Sichtig, H., Geyer, C., Ledeboer, N., and Weinstock, G. M. (2015). Making The Leap From Research Laboratory To Clinic: Challenges And Opportunities For Next-Generation Sequencing In Infectious Disease Diagnostics. *Mbio* 6, E01888–E01815. doi: 10.1128/Mbio.01888-15

Grumaz, C., Hoffmann, A., Vainshtein, Y., Kopp, M., Grumaz, S., Stevens, P., et al. (2020). Rapid Next-Generation Sequencing-Based Diagnostics Of Bacteremia In Septic Patients. *J. Mol. Diagn.* 22, 405–418. doi: 10.1016/J.Jmoldx.2019.12.006

Grumaz, S., Stevens, P., Grumaz, C., Decker, S. O., Weigand, M. A., Hofer, S., et al. (2016). Next-Generation Sequencing Diagnostics Of Bacteremia In Septic Patients. *Genome Med.* 8, 73. doi: 10.1186/S13073-016-0326-8

Gu, W., Miller, S., and Chiu, C. Y. (2019). Clinical Metagenomic Next-Generation Sequencing For Pathogen Detection. *Annu. Rev. Pathol.* 14, 319–338. doi: 10.1146/Annurev-Pathmechdis-012418-012751

Haidar, G., and Singh, N. (2022). Fever Of Unknown Origin. *N. Engl. J. Med.* 386, 463–477. doi: 10.1056/Nejmra2111003

Huang, C., Chen, H., Ding, Y., Ma, X., Zhu, H., Zhang, S., et al. (2021). A Microbial World: Could Metagenomic Next-Generation Sequencing Be Involved In Acute Respiratory Failure? *Front. Cell Infect. Microbiol.* 11. doi: 10.3389/Fcimb.2021.738074

Huang, J., Jiang, E., Yang, D., Wei, J., Zhao, M., Feng, J., et al. (2020). Metagenomic Next-Generation Sequencing Versus Traditional Pathogen Detection In The Diagnosis Of Peripheral Pulmonary Infectious Lesions. *Infect. Drug Resist.* 13, 567–576. doi: 10.2147/Idr.S235182

Íñigo, M., Coello, A., Fernández-Rivas, G., Rivaya, B., Hidalgo, J., Quesada, M. D., et al. (2016). Direct Identification Of Urinary Tract Pathogens From Urine Samples, Combining Urine Screening Methods And Matrix-Assisted Laser Desorption Ionization-Time Of Flight Mass Spectrometry. *J. Clin. Microbiol.* 54, 988–993. doi: 10.1128/Jcm.02832-15

Kao, R. L., and Holtan, S. G. (2019). Host And Graft Factors Impacting Infection Risk In Hematopoietic Cell Transplantation. *Infect. Dis. Clin. North Am.* 33, 311–329. doi: 10.1016/J.Idc.2019.02.001

Li, Y., Sun, B., Tang, X., Liu, Y. L., He, H. Y., Li, X. Y., et al. (2020). Application Of Metagenomic Next-Generation Sequencing For Bronchoalveolar Lavage Diagnostics In Critically Ill Patients. *Eur. J. Clin. Microbiol. Infect. Dis.* 39, 369–374. doi: 10.1007/S10096-019-03734-5

Liu, W., Fan, Z., Zhang, Y., Huang, F., Xu, N., Xuan, L., et al. (2021). Metagenomic Next-Generation Sequencing For Identifying Pathogens In Central Nervous System Complications After Allogeneic Hematopoietic Stem Cell Transplantation. *Bone Marrow Transplant.* 56, 1978–1983. doi: 10.1038/S41409-021-01243-8

Miao, Q., Ma, Y., Wang, Q., Pan, J., Zhang, Y., Jin, W., et al. (2018). Microbiological Diagnostic Performance Of Metagenomic Next-Generation Sequencing When Applied To Clinical Practice. *Clin. Infect. Dis.* 67, S231–S240. doi: 10.1093/Cid/Ciy693

Miller, S., Naccache, S. N., Samayoa, E., Messacar, K., Arevalo, S., Federman, S., et al. (2019). Laboratory Validation Of A Clinical Metagenomic Sequencing Assay For Pathogen Detection In Cerebrospinal Fluid. *Genome Res.* 29, 831–842. doi: 10.1101/Gr.238170.118

Nie, J., Yang, L., Huang, L., Gao, L., Young, K. H., Le Grange, J. M., et al. (2022). Infection Complications In Febrile Chimeric Antigen Receptor (Car)-T Recipients During The Peri-Car-T Cell Treatment Period Examined Using Metagenomic Next-Generation Sequencing (Mngs). *Cancer Commun*. 10.1002/cac2.12260. doi: 10.1002/Cac2.12260

Pendleton, K. M., Erb-Downward, J. R., Bao, Y., Branton, W. R., Falkowski, N. R., Newton, D. W., et al. (2017). Rapid Pathogen Identification In Bacterial Pneumonia Using Real-Time Metagenomics. *Am. J. Respir. Crit. Care Med.* 196, 1610–1612. doi: 10.1164/Rccm.201703-0537le

Robilotti, E., Holubar, M., Seo, S. K., and Deresinski, S. (2017). Feasibility And Applicability Of Antimicrobial Stewardship In Immunocompromised Patients. *Curr. Opin. Infect. Dis.* 30, 346–353. doi: 10.1097/Qco.0000000000000380

Sahin, U., Toprak, S. K., Atilla, P. A., Atilla, E., and Demirer, T. (2016). An Overview Of Infectious Complications After Allogeneic Hematopoietic Stem Cell Transplantation. *J. Infect. Chemother.* 22, 505–514. doi: 10.1016/J.Jiac.2016.05.006

Schlaberg, R., Chiu, C. Y., Miller, S., Procop, G. W., and Weinstock, G. (2017a). Validation Of Metagenomic Next-Generation Sequencing Tests For Universal Pathogen Detection. *Arch. Pathol. Lab. Med.* 141, 776–786. doi: 10.5858/Arpa.2016-0539-Ra

Schlaberg, R., Queen, K., Simmon, K., Tardif, K., Stockmann, C., Flygare, S., et al. (2017b). Viral Pathogen Detection By Metagenomics And Pan-Viral Group Polymerase Chain Reaction In Children With Pneumonia Lacking Identifiable Etiology. *J. Infect. Dis.* 215, 1407–1415. doi: 10.1093/Infdis/Jix148

Schmidt-Hieber, M., Silling, G., Schalk, E., Heinz, W., Panse, J., Penack, O., et al. (2016). Cns Infections In Patients With Hematological Disorders (Including Allogeneic Stem-Cell Transplantation)-Guidelines Of The Infectious Diseases Working Party (Agiho) Of The German Society Of Hematology And Medical Oncology (Dgho). *Ann. Oncol.* 27, 1207–1225. doi: 10.1093/Annonc/Mdw155

Schoch, C. L., Ciufo, S., Domrachev, M., Hotton, C. L., Kannan, S., Khovanskaya, R., et al. (2020). NCBI Taxonomy: A Comprehensive Update on Curation, Resources and Tools. *Database* 2020, baaa062. doi: 10.1093/database/baaa062

Styczyński, J., Tridello, G., Koster, L., Iacobelli, S., Van Biezen, A., Van Der Werf, S., et al. (2020). Death After Hematopoietic Stem Cell Transplantation: Changes Over Calendar Year Time, Infections And Associated Factors. *Bone Marrow Transplant.* 55, 126–136. doi: 10.1038/S41409-019-0624-Z

Tang, W., Zhang, Y., Luo, C., Zhou, L., Zhang, Z., Tang, X., et al. (2021). Clinical Application Of Metagenomic Next-Generation Sequencing For Suspected Infections In Patients With Primary Immunodeficiency Disease. *Front. Immunol.* 12. doi: 10.3389/Fimmu.2021.696403

Tarabichi, M., Shohat, N., Goswami, K., and Parvizi, J. (2018). Can Next Generation Sequencing Play A Role In Detecting Pathogens In Synovial Fluid? *Bone Joint J.* 100-B, 127–133. doi: 10.1302/0301-620x.100b2.Bjj-2017-0531.R2

Wang, S., Ai, J., Cui, P., Zhu, Y., Wu, H., and Zhang, W. (2020). Diagnostic Value And Clinical Application Of Next-Generation Sequencing For Infections In Immunosuppressed Patients With Corticosteroid Therapy. *Ann. Transl. Med.* 8, 227. doi: 10.21037/Atm.2020.01.30

Wang, S., Chen, Y., Wang, D., Wu, Y., Zhao, D., Zhang, J., et al. (2019). The Feasibility Of Metagenomic Next-Generation Sequencing To Identify Pathogens Causing Tuberculous Meningitis In Cerebrospinal Fluid. *Front. Microbiol.* 10. doi: 10.3389/Fmicb.2019.01993

Watzinger, F., Ebner, K., and Lion, T. (2006). Detection And Monitoring Of Virus Infections By Real-Time Pcr. *Mol. Aspects Med.* 27, 254–298. doi: 10.1016/J.Mam.2005.12.001

Wilson, M. R., Sample, H. A., Zorn, K. C., Arevalo, S., Yu, G., Neuhaus, J., et al. (2019). Clinical Metagenomic Sequencing For Diagnosis Of Meningitis And Encephalitis. *N Engl. J. Med.* 380, 2327–2340. doi: 10.1056/Nejmoa1803396

Zhang, H. C., Ai, J. W., Cui, P., Zhu, Y. M., Hong-Long, W., Li, Y. J., et al. (2019). Incremental Value Of Metagenomic Next Generation Sequencing For The Diagnosis Of Suspected Focal Infection In Adults. *J. Infect.* 79, 419–425. doi: 10.1016/J.Jinf.2019.08.012

Zhang, Y., Cui, P., Zhang, H. C., Wu, H. L., Ye, M. Z., Zhu, Y. M., et al. (2020). Clinical Application And Evaluation Of Metagenomic Next-Generation Sequencing In Suspected Adult Central Nervous System Infection. *J. Transl. Med.* 18, 199. doi: 10.1186/S12967-020-02360-6

Conflict of Interest: The authors declare that the research was conducted in the absence of any commercial or financial relationships that could be construed as a potential conflict of interest.

Publisher's Note: All claims expressed in this article are solely those of the authors and do not necessarily represent those of their affiliated organizations, or those of the publisher, the editors and the reviewers. Any product that may be evaluated in this article, or claim that may be made by its manufacturer, is not guaranteed or endorsed by the publisher.

frontiers | Frontiers in Cellular and Infection Microbiology

ORIGINAL RESEARCH
published: 16 June 2022
doi: 10.3389/fcimb.2022.886359

Metagenomic Next-Generation Sequencing Versus Traditional Laboratory Methods for the Diagnosis and Treatment of Infection in Liver Transplantation

Jun-Feng Huang[1,2,3†], Qing Miao[4†], Jian-Wen Cheng[2,3†], Ao Huang[2,3], De-Zhen Guo[2,3], Ting Wang[1], Liu-Xiao Yang[1], Du-Ming Zhu[1], Ya Cao[5], Xiao-Wu Huang[2,3], Jia Fan[2,3,6], Jian Zhou[2,3,6] and Xin-Rong Yang[2,3*]*

[1] Liver Surgery Intensive Care Unit, Department of Intensive Care Medicine, Zhongshan Hospital, Fudan University, Shanghai, China, [2] Department of Liver Surgery and Transplantation, Liver Cancer Institute, Zhongshan Hospital, Fudan University; Key Laboratory of Carcinogenesis and Cancer Invasion (Fudan University), Ministry of Education, Shanghai, China, [3] Shanghai Key Laboratory of Organ Transplantation, Zhongshan Hospital, Fudan University, Shanghai, China, [4] Department of Infectious Diseases, Zhongshan Hospital, Fudan University, Shanghai, China, [5] Cancer Research Institute, Central South University; Key Laboratory of Carcinogenesis and Cancer Invasion, Ministry of Education, Changsha, China, [6] Institute of Biomedical Sciences, Fudan University, Shanghai, China

Background: Metagenomic next-generation sequencing (mNGS) has emerged as an effective method for the noninvasive and precise detection of infectious pathogens. However, data are lacking on whether mNGS analyses could be used for the diagnosis and treatment of infection during the perioperative period in patients undergoing liver transplantation (LT).

Methods: From February 2018 to October 2018, we conducted an exploratory study using mNGS and traditional laboratory methods (TMs), including culture, serologic assays, and nucleic acid testing, for pathogen detection in 42 pairs of cadaveric liver donors and their corresponding recipients. Method performance in determining the presence of perioperative infection and guiding subsequent clinical decisions was compared between mNGS and TMs.

Results: The percentage of liver donors with mNGS-positive pathogen results (64.3%, 27/42) was significantly higher than that using TMs (28.6%, 12/42; P<0.05). The percentage of co-infection detected by mNGS in liver donors was 23.8% (10/42) significantly higher than 0.0% (0/42) by TMs (P<0.01). Forty-three pathogens were detected using mNGS, while only 12 pathogens were identified using TMs. The results of the mNGS analyses were consistent with results of the TM analyses in 91.7% (11/12) of donor samples at the species level, while mNGS could be used to detect pathogens in 66.7% (20/30) of donors deemed pathogen-negative using TMs. Identical pathogens were detected in 6 cases of donors and recipients by mNGS, among which 4 cases were finally confirmed as donor-derived infections (DDIs). For TMs, identical pathogens were

OPEN ACCESS

Edited by:
Jinmin Ma,
Beijing Genomics Institute (BGI), China

Reviewed by:
Chiyu Zhang,
Fudan University, China
Jianwei Chen,
Beijing Genomics Institute (BGI), China
Akira Shishido,
University of Maryland Medical Center, United States

***Correspondence:**
Xin-Rong Yang
yang.xinrong@zs-hospital.sh.cn
Jian Zhou
zhou.jian@zs-hospital.sh.cn

†These authors have contributed equally to this work

Specialty section:
This article was submitted to Clinical Microbiology, a section of the journal Frontiers in Cellular and Infection Microbiology

Received: *28 February 2022*
Accepted: *17 May 2022*
Published: *16 June 2022*

Citation:
Huang J-F, Miao Q, Cheng J-W, Huang A, Guo D-Z, Wang T, Yang L-X, Zhu D-M, Cao Y, Huang X-W, Fan J, Zhou J and Yang X-R (2022) Metagenomic Next-Generation Sequencing Versus Traditional Laboratory Methods for the Diagnosis and Treatment of Infection in Liver Transplantation. Front. Cell. Infect. Microbiol. 12:886359. doi: 10.3389/fcimb.2022.886359

detected in only 2 cases. Furthermore, 8 recipients developed early symptoms of infection (<7 days) after LT; we adjusted the type of antibiotics and/or discontinued immunosuppressants according to the mNGS results. Of the 8 patients with infections, 7 recipients recovered, and 1 patient died of severe sepsis.

Conclusions: Our preliminary results show that mNGS analyses can provide rapid and precise pathogen detection compared with TMs in a variety of clinical samples from patients undergoing LT. Combined with symptoms of clinical infection, mNGS showed superior advantages over TMs for the early identification and assistance in clinical decision-making for DDIs. mNGS results were critical for the management of perioperative infection in patients undergoing LT.

Keywords: liver transplantation, metagenomic next-generation sequencing, donor-derived infection, perioperative infection, immunocompromised patient

INTRODUCTION

Liver transplantation (LT) is the most effective treatment for end-stage liver cirrhosis and liver cancer (Dogan and Kutluturk, 2020). The civilian organ donation program has been the sole source of organs for transplant in China since January 2015, and the number of voluntary donations has increased every year (Huang et al., 2015). Infection-related complications have become the leading cause of morbidity and mortality for patients undergoing LT due to the use of immunosuppressive agents (Nam et al., 2018). Perioperative infections are particularly serious and can lead to liver graft failure and even death (Heldman et al., 2019). Such infections in liver recipients can arise from reactivation of latent pathogens, donor-derived infections (DDIs), or primary infections (Pettengill et al., 2019). The early and precise detection of infectious pathogens can be used to optimize the administration of antibiotics and immunosuppressants to improve clinical outcomes for patients undergoing LT (Huang et al., 2020). Therefore, development of a more rapid, sensitive, and specific method for the identification of potential pathogens for these patients is urgently needed.

Traditional laboratory methods (TMs) for the screening of potential pathogens usually include cell culture, serologic assays, and nucleic acid testing. However, testing all potential pathogens in liver donors and corresponding recipients using TMs is extremely time-consuming. Metagenomic next-generation sequencing (mNGS) is a promising approach to determine the presence and abundance of transplant-related infections and identify co-infection in an unbiased manner (Simner et al., 2018). The use of mNGS can overcome the limitations of current diagnostic tests, allowing for hypothesis-free, culture-independent, pathogen detection directly from clinical specimens regardless of the type of microbe; mNGS can even be used for novel organism discovery (Simner et al., 2018). To date, there are few reports on the use of mNGS to identify potential pathogens in liver donors and their corresponding recipients.

In this study, the diagnostic performance of mNGS was evaluated and compared with the use of TMs in patients undergoing LT. Furthermore, the feasibility of using mNGS for the diagnosis and treatment of perioperative infections in LT recipients was evaluated. We found that the use of mNGS provided rapid and precise detection of pathogens compared with TMs in a variety of clinical samples from patients undergoing LT. Combined with symptoms of clinical infection, the use of mNGS could offer an advantage over the use of TMs for the diagnosis of DDIs and the precise treatment of these perioperative infections.

Abbreviations: AB, acinetobacter baumannii; ACC, accuracy; CA, candida albicans; CMV, Cytomegalovirus; CRP, C-reactive protein; CS, clonorchis sinensis; D, donor; DDI, donor-derived infection; DNBs, DNA nanoballs; EBV, Epstein-Barr virus; HBV, Hepatitis B virus; HCV, Hepatitis C virus; HIV, Human immunodeficiency virus; KP, klebsiella pneumoniae; LT, liver transplantation; mNGS, metagenomic next-generation sequencing; NPV, negative predictive value; PCT, procalcitonin; POD, postoperative days; PPV, positive predictive value; R, recipient; RPR, Rapid plasma reagin; SDSMRN, the number of unique reads of standardized species; TMs, traditional laboratory methods; TTV, Torque Teno Virus; VZV, varicella zoster virus.

MATERIALS AND METHODS

Ethics Statement

An application for ethical review was approved by the Ethical Review Committee of Zhongshan Hospital affiliated with Fudan University.

Patients, Perioperative Management, and Sample Collection

This study was a single-center, prospective cohort study from February 1, 2018 to October 30, 2018. A total of 42 cadaveric liver donors and their corresponding recipients were enrolled. All donors' clinical data were obtained prior to procurement. All recipients received orthotropic LT and induction of immunosuppression intraoperatively with basiliximab and methylprednisolone. The regimen for antibiotic prophylaxis for LT consisted of cefepime and micafungin for 7 days postoperatively. Immunosuppressant therapy after LT consisted of a triple-drug regimen of cyclosporine or tacrolimus, mycophenolate mofetil, and methylprednisolone; the doses of

these drugs were decreased over 7 days. Recipient outcomes were examined for the entire length of the hospital stay.

The donor's samples, including blood, preservation fluid, liver and perihepatic tissue (diaphragm or omentum), were obtained preoperatively. Microbiological monitoring of the liver recipients involved the routine sampling of blood and abdominal drainage fluid on postoperative days (POD) 1, 4, and 7. When the recipient was diagnosed with a postoperative infection, additional samples from the sputum, bronchoalveolar lavage fluid, and urine were collected for pathogen analysis according to the clinical situation. All samples were subjected to TMs as well as mNGS testing in a pairwise manner. TMs for pathogen detection included culture of bacterial and fungal; PCR-based assay of *Epstein-Barr virus* (EBV), *Cytomegalovirus* (CMV), *Hepatitis B virus* (HBV), *Hepatitis C virus* (HCV); serological assay including 1,3-Beta-D-glucan, Galactomannan antigen, Interferon-gamma release assays for *Tuberculosis*, *Cryptococcus* antigen, HBV, HCV and *Human immunodeficiency virus* (HIV) serological test, EBV early antigen and viral capsid antigen, CMV immunoglobulin G/M (IgG/M), *Toxoplasma gondii* IgG/M, Rapid plasma reagin (RPR) test for *Syphilis* and stool microscopy for parasitic ova. The diagnostic assessment performances of the TMs and mNGS were compared.

Sample Processing

All samples were promptly stored in sterile containers and placed at 4°C prior to analysis. For blood samples, 3–4 mL of blood was centrifuged at 4,000 rpm for 10 min at 4°C within 8 h of collection, and plasma samples were transferred to new sterile tubes. An aliquot of 3–5 mL preservation fluid or drainage fluid was collected, according to standard sterile procedures (Cornaglia et al., 2012). Tissue homogenates, including those of liver and perihepatic tissues, were processed similarly to preservation fluid (Cornaglia et al., 2012); 1.5-mL microcentrifuge tubes containing 0.5 mL sample and 1 g of 0.5-mm glass beads were attached to a horizontal platform on a vortex mixer and agitated vigorously at 2,800-3,200 rpm for 30 min.

mNGS

DNA was extracted from 300 μL samples using the TIANamp Micro DNA Kit (DP316, TIANGEN BIOTECH, Beijing, China), following the manufacturer's instructions. DNA libraries were constructed through DNA fragmentation, end-repair, adapter-ligation, and PCR amplification (Long et al., 2016). The reagents were taken out from the kit, and the enzymatic reagents were briefly centrifuged and placed on ice for use; The other reagents were melted on ice, mixed with oscillation, and briefly centrifuged for use. Magnetic beads should be balanced at room temperature for 30min before use, and thoroughly mixed before adding. Anhydrous ethanol and molecular water are used to prepare 75% ethanol. internal standard (200×) was diluted 200 times in nuclease-free water. Then, the terminal repair reaction mixture was prepared for end-repair. The extracted nucleic acid was added, and then the terminal repair reaction mixture 7.0μL was added. The mixture was placed on PCR and incubated. At the end of the reaction, the PCR tube was removed for instantaneous centrifugation. 30.0μL connecting reaction mixture was added to the PCR tube, and the mixture was fully mixed and centrifuged immediately. The mixture was placed on the PCR instrument and incubated for 23 minutes, ligase was used for adapter-ligation. After PCR amplification, Agilent 2100 instrument (Agilent Technologies, Santa Clara, CA) was used for quality control of the DNA libraries and the Qubit 2.0 fluorometer (Invitrogen, Foster City, CA, USA). A qualified double-stranded DNA library was transformed into a single-stranded circular DNA library by DNA denaturation and circularization. DNA nanoballs (DNBs) were generated from single-stranded circular DNA using rolling circle amplification (da Silva et al., 2016). The DNBs were qualified by fluorometry (Fang et al., 2018). Qualified DNBs were loaded in the flow cell and sequenced on the BGISEQ-50 platform (Jeon et al., 2014). High-quality sequencing data were generated by removing low-quality and short reads (length <35 bp), followed by computational subtraction of human host sequences mapped to the human reference genome (hg19) using Burrows-Wheeler alignment (Li and Durbin, 2010). After removal of low-complexity reads, the remaining sequencing data were classified by simultaneous alignment to sequences in the bacterial, viral, fungal, and parasite microbial genome databases.

The reference database RefSeq, downloaded from the National Center Biotechnology Information website (https://ftp.ncbi.nlm.nih.gov/genomes/), contains 4,945 whole-genome sequences of viral taxa, 6,350 bacterial genomes or scaffolds, 1,064 fungal sequences related to human infections, and 234 parasite sequences associated with human diseases.

Analyses of mNGS Results

The criteria for a positive mNGS result have been described previously (Miao et al., 2018). Briefly, bacteria, viruses, and parasites (species level) were identified with a coverage rate 10-fold greater than that of any other bacteria, virus, or parasite. Fungi (species level) were identified with a coverage rate 5-fold higher than that of any other fungi because of their low biomass after DNA extraction. *Mycobacterium tuberculosis* was considered positive when at least one read was mapped (genus or species level). *Nontuberculous mycobacteria* were considered positive when the mapped read number at either the species or genus level was in the top 10 of the list of bacteria.

The number of unique reads of standardized species (SDSMRN) was defined as the number of reads that were strictly aligned to the genome of a species after normalizing the total number of sequencing reads to 20 million (Li et al., 2020). Probable DDI was defined as the transmission of the identical pathogen detected from donor to recipient by mNGS and/or TMs (Kaul et al., 2021) and the recipient developed early infection symptoms (<7 days) as fever and/or purulent drainage observed with increased markers of laboratory infection after LT (Bandali et al., 2020).

Statistical Analysis

Sensitivity, specificity, positive predictive value (PPV), negative predictive value (NPV), and accuracy (ACC) were calculated, and the performance of mNGS and TMs for diagnostic assessments was compared using the $\chi 2$ test. A two-tailed P

value of 0.05 was considered statistically significant. Data were analyzed using SPSS, version 24.0 (SPSS, Chicago, IL, USA).

RESULTS

Recipient Characteristics

Demographic features of the recipients in the study are provided in **Table 1**. All 42 recipients underwent orthotopic cadaveric LT. The median patient age was 49 years (range, 21-72 years). Most recipients were male (36/42, 85.7%) and had been diagnosed with primary malignant liver cancer (29/42, 69.1%), followed by decompensated liver cirrhosis (9/42, 21.5%). Ascites was present in 81.0% of recipients (34/42), and antibiotics were used in 33.3% of recipients (14/42) one month before LT for either the treatment of infection or prevention of spontaneous peritonitis due to cirrhosis with ascites or upper gastrointestinal bleeding. Of the 42 patients, 8 recipients were diagnosed with postoperative infection, with pneumonia (6/8, 75.0%) being the most common infection.

The Spectrum of Pathogens in Liver Donors Detected by mNGS and TMs

The percentage of liver donors with mNGS-positive pathogen results (64.3%, 27/42) was significantly higher than when using TMs (28.6%, 12/42; P<0.05), and the percentage of co-infection of several common pathogens, detected by mNGS in liver donors was 23.8% (10/42) compared with 0.0% as detected by TMs (0/42; P<0.001; **Figure 1**).

mNGS detected 43 pathogens (bacteria: 55.8%, 24/43; viruses: 25.6%, 11/43; fungi: 14.0%, 6/43; parasites: 4.7%, 2/43), whereas only 12 pathogens were identified using TMs (bacteria: 75.0%, 9/12; viruses: 25.0%, 3/12; **Figures 2A, B**). No fungi or parasites were identified using TMs. Among 30 donors who tested negative for pathogens using TMs, mNGS identified new pathogens in 20 cases (20/30, 66.7%), including fastidious bacteria, fungi [e.g., *Pneumocystis jirovecii* and *Candida albicans* (CA)], virus [e.g., *Torque Teno Virus* (TTV), *Human parvovirus B19*, CMV and EBV] and parasite [e.g., *Echinococcus multilocularis* and *Clonorchis sinensis*]. This result reflected the low sensitivity of TMs in screening donor-derived pathogens (**Figure 2C**).

Among 12 donors who tested positive for pathogens using TMs, the results of the mNGS analysis were consistent in 11 out of 12 (91.7%) donor samples at the species level. However, at least one unique pathogen read was detected by mNGS when co-infection was observed. For the detected pathogen spectrum, common bacteria such as *Klebsiella pneumoniae* (KP), *Acinetobacter baumannii* (AB), *Escherichia coli*, and *Staphylococcus* could be detected by both TMs and mNGS, whereas fungi and unexpected viruses were only able to be identified by mNGS. Inconsistent results were only found for

TABLE 1 | Recipient characteristics (N = 42).

Characteristics	No.	%
Age (years)*		
Median (Range)	49 (21-72)	
Sex		
Male	36	85.7
Outcome		
Survival	40	95.2
Hospital stay (days)		
Median (Range)	21.5 (5-73)	
Past history		
Surgery history	19	45.2
Hypertension	7	16.7
Diabetes	6	14.3
Diagnosis		
Malignant tumor of liver		
Hepatocarcinoma	28	66.7
Intrahepatic cholangiocarcinoma	1	2.4
Hepatocirrhosis		
Hepatitis B cirrhosis	7	16.7
Primary biliary cirrhosis	1	2.4
Idiopathic cirrhosis	1	2.4
Acute liver failure	1	2.4
Secondary transplantation	3	7.1
Ascites	34	81.0
Antibiotic treatment within 1 months before surgery	14	33.3
Postoperative infection	8	19.0
Postoperative infection site		
Pneumonia	6	75.0
Sepsis	2	25.0
Urinary tract	3	37.5
Intra-abdominal	4	50.0

**Age at start of liver transplantation surgery.*

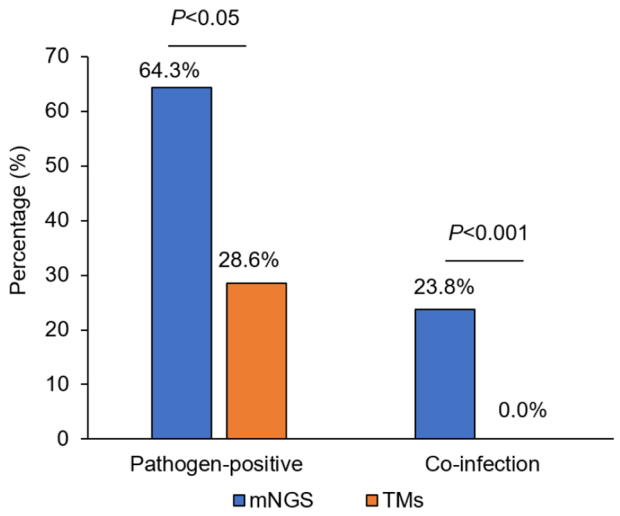

FIGURE 1 | The comparison of pathogen-positive percentage and co-infection rate detected separately by mNGS and TMs in liver donors. mNGS for metagenomic next-generation sequencing and TMs for traditional laboratory methods.

Donor 1 (D1) between mNGS and TMs: *Staphylococcus lentus* was identified by culture in both preservation fluid and perihepatic tissues, but was not detected by mNGS in any D1-related samples (**Table 2**).

The Performance of TMs and mNGS for the Detection of Donor-Recipient Transmitted Pathogens

The performance of TMs and mNGS for the detection of donor-transmitted pathogens was further evaluated. The transmission of pathogens was detected in 6 cases (6/42) from donor to recipient by mNGS, among which 4 cases were confirmed as DDIs with a 100% sensitivity and a 94.7% specificity. By TMs, the transmission was only detected in 2 cases (2/42) confirmed as DDI with sensitivity of 50.0% and a specificity of 100%. The PPV and NPV of mNGS were 66.7% and 100% for DDI diagnoses, respectively, compared with 100.0% and 95.0% for TMs, respectively. The ACC of both mNGS and TMs was 95.2% (**Table 3**). The new emerging pathogens transmitted *via* liver graft were identified by mNGS in six cases (**Table 4**). We found that KP (3/6, 50.0%), AB (2/6, 33.3%), *Varicella zoster virus* (VZV) (1/6, 16.7%), *Candida glabrata* (CG) (1/6, 16.7%), and *Clonorchis sinensis* (CS) (1/6, 16.7%) were detected by mNGS in both donor and corresponding recipient. There were 2 cases (2/6, 33.3%) with co-infection detected by mNGS in samples from D24 and D41, which could not be identified by TMs, especially the fungi and viruses.

Guided Treatment for Perioperative Infection by mNGS in Patients When TMs Results Appear Invalid

The postoperative treatment regimen of antibiotics and immunosuppressants are first routinely adjusted according to the pathogens detected in donor and corresponding recipient by TMs. Under this situation, a total of 8/42 (19.0%) recipients developed early infection symptoms (<7 days) (**Table 5**). The mean time was 2.0 days to symptom onset (range, 1–6 days) after LT, and clinical manifestations included fever, purulent drainage fluid, increased procalcitonin (PCT) or C-reactive protein (CRP) levels, and positive imaging results. Sequentially, we modified the therapeutic regimen according to the results of mNGS in all eight infected recipients, and finally seven recipients recovered and one (R24) died of severe sepsis.

Types of antibiotics were adjusted and/or immunosuppressants were withdrawed for R3, R7, R24, R28, R40, R41, and R42 (7/8, 87.5%), according to the additional pathogens identified by mNGS; the mNGS-negative results in R39 led to discontinue unnecessary broad-spectrum antibiotics (such as meropenem, which was replaced by cefoperazone sulbactam and then discontinued) (**Table 5**). The dynamic changes in SDSMRN by continuous mNGS surveillance in R28 guided the complete course of antibiotics for 30 days, as result of blood culture had been negative from POD 11 (**Table 6**). One recipient (R24) died after treatment adjustment and had received LT for drug-related acute liver failure (Model for End-stage Liver Disease score 41). In this case, VZV was only detected by mNGS in the donor liver and subsequently found in the abdominal drainage fluid of the recipient, suggesting a latent VZV infection in the donor. Despite the prompt use of antiviral therapy guided by mNGS, the recipient still succumbed to severe sepsis, which resulted in fatal liver failure on POD 6.

DISCUSSION

Infection-related complications have become the leading cause of morbidity and mortality for patients in the first months after LT (Nam et al., 2018). The early and precise detection of infectious pathogens can optimize the use of targeted antibiotics and immunosuppressants to improve clinical outcomes for patients after LT. It is great challenge to test all potential pathogens existing in liver donors and their corresponding recipients using TMs. mNGS can overcome the limitations of the current diagnostic testing (Zhou et al., 2019). In this study, we prospectively evaluated the clinical value of mNGS for the identification of pathogens in different types of samples during LT. We found that mNGS could provide rapid and precise detection of pathogens and was an ideal tool for the diagnosis of DDIs. Furthermore, mNGS was able to guide the precise treatment of perioperative infections in patients undergoing LT.

Our data revealed that positive results using mNGS analyses were consistent with those from TMs 91.7% of the time. These results suggest that mNGS can effectively detect the same pathogens as TMs and identify more latent pathogens carried by donors. As mNGS analyses often detected more than one pathogen in a single test, clinicians need to have a comprehensive understanding of results indicating the presence of co-infection (Tarabichi et al., 2018). Thus, we used our own criteria (Miao et al., 2018) to uncover co-infections and/or distinguish the

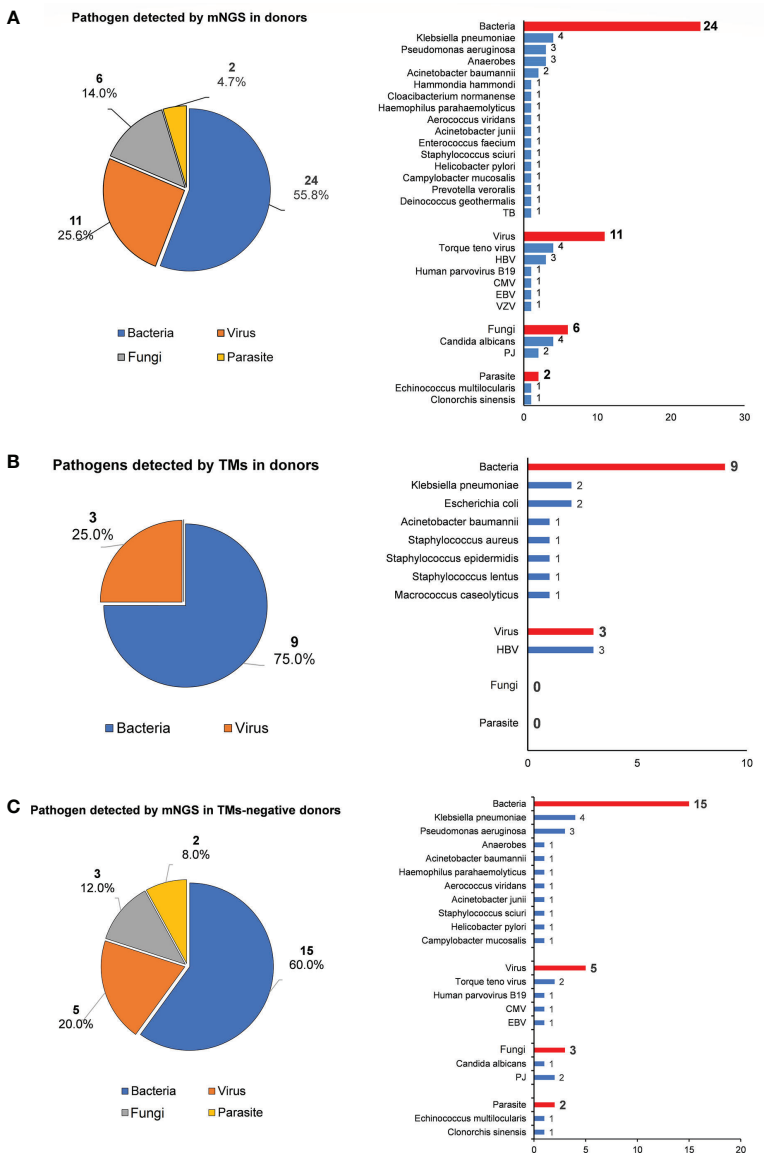

FIGURE 2 | The pathogen spectrum in liver donor detected by mNGS and TMs. **(A)** Pie chart demonstrating the distribution of different types of pathogens detected by NGS in liver donors, and a total of 43 species of pathogens were detected in donor samples with their corresponding frequencies plotted in histograms. **(B)** Pie chare demonstrating the distribution of different types of pathogens detected by TMs in donors, and a total of 12 species of pathogens were detected in donor samples with their corresponding frequencies plotted in histograms. **(C)** Pie chart shows the distribution of different types of pathogens detected in TMs-negative donor samples by mNGS, and species of pathogens were detected with their corresponding frequencies plotted in histograms.

causative pathogens. We found that CA (4/43, 9.3%) was the most common fungi within the co-infection detected by mNGS. Donor-derived fungal infections have been associated with life-threatening complications in transplant recipients (Mishkin, 2021), so mNGS analyses would allow the precise and timely detection of fungi to enable prompt treatment. It is worth noting that the average turnaround time for culture results is more than 72 hours for commonly encountered bacteria and up to weeks for more insidious pathogens such as *Aspergillus fumigates* (Simner et al., 2018). Thus, the turnaround time of mNGS (average of 48 hours) (Pendleton et al., 2017; Afshinnekoo et al., 2017) will hasten clinical decision-making, which is critical for immunocompromised recipients after LT (Simner et al., 2018).

Metagenomic sequencing combined with phylogenetic analysis could effectively identify the frequent transmission of *JC polyomavirus* from kidney transplant donor to recipient (Schreiber et al., 2019). Our study demonstrated the transmission of identical pathogens from donors to corresponding recipients in 6 of 42 cases (14.3%) by mNGS, which can promptly assist in the diagnosis of DDIs with clinical infection symptoms. As compared with TMs, mNGS was more sensitive (100% vs. 50%) with a similar specificity (94.7% vs.

TABLE 2 | mNGS results of 12 TMs-positive sample of donors.

D	Sample	TMs results	mNGS results				Correlation
			Species	NO. of unique reads	Coverage %	Depth	
1	preservation fluid	Staphylococcus lentus	/	/	/	/	no
	perihepatic tissue	Staphylococcus lentus	/	/	/	/	
5	preservation fluid	Escherichia coli	Bacteroides vulgatus	50	0.0978	1	yes
			Corynebacterium urealyticum	32	0.1191	1	
			Escherichia coli	1	0.0009	1	
14	perihepatic tissue	Staphylococcus aureus	Staphylococcus aureus	10	0.0889	1	yes
17#	blood/liver tissue	HBV	HBV	13	39.25	1.33	yes
19	preservation fluid	Macrococcus caseolyticus	Macrococcus caseolyticus	122	0.6779	1.02	yes
			Torque teno mini virus 7	1	3.46	1	
			Torque teno virus 15	1	7.84	1	
24*	preservation fluid	Klebsiella pneumoniae	Klebsiella pneumoniae	63	0.0565	1	yes
			Candida albicans	7	0.0031	1	
			Human herpesvirus 3	4	0.3195	1	
28*	preservation fluid	Klebsiella pneumoniae	Klebsiella pneumoniae	898	1.98	1.02	yes
			Prevotella veroralis	882	2.03	1.02	
			Candida albicans	15	0.0067	1	
	perihepatic tissue	Klebsiella pneumoniae	Klebsiella pneumoniae	1657	3.57	1.03	
			Prevotella veroralis	1307	3.05	1.03	
			Candida albicans	15	0.0056	1	
29#	blood/liver tissue	HBV	HBV	6	21.74	1.17	yes
32#	blood/liver tissue	HBV	HBV	2	4.67	1	yes
36	preservation fluid	Staphylococcus epidermidis	Staphylococcus epidermidis	14	0.0381	1	yes
	perihepatic tissue	Staphylococcus epidermidis	Staphylococcus epidermidis	1	0.0019	1	
39	preservation fluid	Escherichia coli	Escherichia coli	1	0.0101	1	yes
41*	perihepatic tissue	Acinetobacter baumannii	Acinetobacter baumannii	32	0.0448	1	yes
			Klebsiella pneumoniae	21	0.035	1	
			Candida albicans	4	0.0014	1	

*D, Donor; TMs, Traditional laboratory methods; mNGS, Metagenomic next-generation sequencing; HBV, Hepatitis B Virus; #donor was HBV positive; *Donor derived infection.*

100.0%) in terms of diagnoses of DDIs, respectively. As immunocompromised recipients are generally critical ill, the timely identification of the pathogens causing DDI is crucial for a precise diagnosis, which is necessary for proper treatment (Nam et al., 2018). More importantly, the mNGS-negative results of donor and corresponding recipient can assist to exclude DDI in clinical work.

With antimicrobial treatment guided by the TMs results, 8 of 42 (19.0%) recipients developed an early infection (<7 days) after LT. Targeted antibiotics were adjusted and/or immunosuppressants were discontinued according to the additional pathogens identified by mNGS. Finally, 7 recipients recovered. These examples demonstrate that mNGS can effectively guide the treatment of perioperative infection after LT, especially when routine TMs results appear inefficacy. The decrease or disappear of pathogen unique reads monitored by mNGS are correlated with improvement of clinical infection symptoms and indirectly guide the course of antibiotics (Zhang et al., 2019), especially in DDI cases. Blood culture of one recipient (R28) with DDI had been negative since POD 11, the course of antibiotics was guided by dynamic changes of unique pathogen reads detected by mNGS with clinical index of PCT for 30 days. Therefore, mNGS results might be a reliable indicator to help understand how the pathogens progress and guide the adjustment of antibiotics in DDI cases (Ai et al., 2018).

TTV load is modulated by the immune, viral, and inflammatory status, and often considered as potential marker associated with immunity status as well as infectious diseases in LT (Mrzljak and Vilibic-Cavlek, 2020). As reported, TTV viremia was significantly higher during CMV infections (Ruiz

TABLE 3 | Comparison of sensitivity and specificity between NGS and TMs in diagnosis of DDI.

		DDI	Non-DDI	Sensitivity	Specificity	PPV	NPV	ACC
NGS	**positive**	4	2	100.0%	94.7%	66.7%	100.0%	95.2%
	negative	0	36					
TMs	**positive**	2	0	50.0%	100.0%	100.0%	95.0%	95.2%
	negative	2	38					

DDI, Donor derived infection; PPV, Positive predictive value; NPV, Negative predictive value; ACC, Accuracy.

TABLE 4 | Transmission of pathogens detected by mNGS and TMs from liver donor to corresponding recipient.

	mNGS									TMs				
	Donor				Recipient					Donor			RecipientPOD 1	
					Pre-LT	POD 1								
ID	blood	pre- servation fluid	peri- hepatic tissue	liver tissue	blood	blood	drainage			blood	pre- servation fluid	peri- hepatic tissue	blood	drainage fluid
							right	middle	left					
3		CS	CS	CS	BKPyV		AB CS		CS					
24*		VZV KP	VZV			KP	VZV	VZV	VZV		KP		KP	
28*	KP	KP	KP	KP	HBV TTV	KP	KP				KP	KP	KP	
35		KP	KP	KP	AF		KP	KP	KP					
41*	AB KP CG		AB KP CG	AB KP CG	TTV	AB KP CG	AB KP CG TTV	AB KP CG	AB TTV		AB			
42*		AB				AB	AB	AB	AB					

AB, Acinetobacter baumannii; AF, Aspergillus flavus; BKPyV, BK polyomavirus; CG, Candida glabrata; CS, Clonorchis sinensis; HBV, Hepatitis B virus; KP, Klebsiella pneumoniae; LT, Liver transplantation; POD, Post operation day; TTV, Torque teno virus; VZV, Varicella zoster virus.
**Donor derived infection.*

et al., 2019). In our cohort, CMV and TTV were detected in blood and drainage in one recipient (R7) with early infection (<7 days) (**Table 5**), but we did not find TTV in the other infection recipients. The reason might be TTV loads progressively increased and peaks around 3 months post-transplant, positively correlating with the intensity of immunosuppression (Schreiber et al., 2019; Mrzljak and Vilibic-Cavlek, 2020), and then virus specific PCR monitoring will have higher sensitivity for detection of TTV loads after LT.

There was a discordant result between TMs and mNGS in one donor (D1). *S. lentus* was positively identified by TMs in preservation fluid and perihepatic tissue, but was not detected

TABLE 5 | The precise treatment of perioperative infection guided by mNGS infailure cases of TMs in LT.

R	The time of symptoms onset	TMs based diagnosis	mNGS based diagnosis	Changes in treatment strategies by mNGS results	Follow-up results
3	POD1	Negative	AB intra-abdominal infection	Cefepime changed to tigecycline	Recovery
7	POD1	AB and Candida glabrata pneumonia	CMV and TTV detected in blood and drainage	Added ganciclovir	Recovery
24	POD1	Sepsis and pneumonia (donor derived CRKP infection)	Probable DDI. KP bloodstream infection and pneumonia; VZV detected in donor and subsequently in abdominal drainage of recipient	Added ganciclovir and withdraw immunosuppressant	Death on POD 6
28	POD1	Sepsis, abdominal infection and pneumonia (donor derived CRKP infection)	Probable DDI. KP bloodstream infection, intra-abdominal infection and pneumonia	Withdraw immunosuppressant; dynamic changes in reads guided the course of antibiotics use, while blood culture result had been negative	Recovery
39	POD6	Urinary tract Enterococcus faecium and SM infection	Both blood and abdominal drainage detected negative	Meropenem changed to cefoperazone sulbactam, and then was discontinued	Recovery
40	POD1	Candida tropicalis pneunomia	Aspergillus fumigatus and candida tropicalis detected in BALF	Added voriconazole	Recovery
41	POD1	AB abdominal infection; (AB was positive in culture of preservation fluid)	Probable DDI; AB, KP and CA simultaneously detected in donor as well as in blood and abdominal drainage of recipient	Added polymyxin B for bloodstream infection and withdraw immunosuppressant	Recovery
42	POD4	Candida tropicalis and SM cultured positively in sputum	Probable DDI; AB simultaneously detected in donor and subsequently in abdominal drainage and blood of recipient	Added tigecycline and withdraw immunosuppressant	Recovery

R, recipient; TMs, Traditional laboratory methods; LT, liver transplant; POD, Post operation day; AB, Acinetobacter baumannii; CMV, Cytomegalovirus; TTV, Torque teno virus; CRKP, Carbapenem resistant klebsiella pneumoniae; DDI, Donor derived infection; KP, Klebsiella pneumoniae; CA, Candida albicans; VZV, Varicella zoster virus; SM, Stenotrophomonas maltophilia; BALF, Bronchoalveolar lavage fluid.

TABLE 6 | Dynamic changes in standardized unique read of CRKP by mNGS.

	POD 1	4	7	11	14	21	30
SDSMRN	121	324	537	390	246	177	9
Blood culture	CRKP	CRKP	CRKP	N	N	N	/

POD, Post operation day; SDSMRN, The number of unique reads of standardized species; CRKP, Carbapenem resistant klebsiella pneumoniae; N, Negative.

by mNGS. A possible reason may be that pathogen reads make up a minute fraction of the sequencing results and are of low sequencing depth, which means mNGS results could be further improved by increasing sequencing depth. One recipient (R24) died of fulminant liver failure and severe sepsis even with treatment guided by mNGS results. It is worth noting that this outcome might be associated with the poor condition of the recipient prior to LT and acute liver graft dysfunction caused by the recurrence of VZV infection after LT. Disseminated visceral VZV infection has been described as a rare but severe disease with a high mortality rate, especially in immunocompromised hosts (Kikuchi et al., 2019). More early diagnosis and timely intervention for those patients, such as the discontinuation of immunosuppressants, might be crucial to improve their clinical outcome (Mehta et al., 2021).

There were some limitations of our study. First, the results of the mNGS were not reconfirmed by PCR-based assays, and a phylogenetic analysis of the pathogens from both the donor and corresponding recipient will be very helpful to confirm diagnosis of DDI. Second, there lacks a unified standardized protocol for mNGS currently in clinical diagnosis. Due to potential breadth of detection and nucleic acid contamination in the process, interpretation of mNGS results directly from clinical specimens can be difficult and requires careful consideration. Additionally, unbiased mNGS was not routinely performed alongside RNA sequencing.

untargeted mNGS was not routinely performed alongside RNA sequencing.

Our study showed that, as compared with TMs, mNGS could yield higher sensitivity for the early identification of fastidious pathogens in patients undergoing LT, especially for DDI diagnoses. Importantly, mNGS does not replace current TMs. Alternatively, it may be considered for immunocompromised patients where achieving a timely diagnosis and treatment is imperative for improved outcomes. The large-scale multicenter randomized controlled studies are needed to further confirm the value of mNGS in routine clinical care of patients undergoing LT.

DATA AVAILABILITY STATEMENT

The data presented in the study are deposited in the CNGB Sequence Archive (CNSA) of China National GeneBank DataBase (CNGBdb), accession number CNP0003068. (http://db.cngb.org/cnsa/project/CNP0003068_275abe06/reviewlink/).

ETHICS STATEMENT

The studies involving human participants were reviewed and approved by the Ethical Review Committee of Zhongshan Hospital affiliated with Fudan University. The patients/participants provided their written informed consent to participate in this study.

AUTHOR CONTRIBUTIONS

Research design was conceived by X-RY, JZ and J-FH. J-FH, QM and J-WC performed the research and analyzed the results. First draft manuscript was prepared by J-FH and QM. AH, D-ZG, TW, L-XY, D-MZ, YC, X-WH and JF contributed to manuscript revisions. All authors contributed to the article and approved the submitted version.

FUNDING

This study was jointly supported by the National Key R&D Program of China (2019YFC1315800, 2019YFC1315802), the State Key Program of National Natural Science of China (81830102), the National Natural Science Foundation of China (82150004, 81772578, 81772551, 81872355 and 82072715), the Shanghai Municipal Health Commission Collaborative Innovation Cluster Project (2019CXJQ02), Shanghai "Rising Stars of Medical Talent" Youth Development Program (Outstanding Youth Medical Talents), the Projects from the Shanghai Science and Technology Commission (19441905000 and 21140900300), Shanghai Municipal Key Clinical Specialty.

ACKNOWLEDGMENTS

The authors thank all the patients included in our study.

REFERENCES

Afshinnekoo, E., Chou, C., Alexander, N., Ahsanuddin, S., Schuetz, A. N., and Mason, C. E. (2017). Precision Metagenomics: Rapid Metagenomic Analyses for Infectious Disease Diagnostics and Public Health Surveillance. *J. Biomol. Tech.* 28, 40–45. doi: 10.7171/jbt.17-2801-007

Ai, J. W., Zhang, H. C., Cui, P., Xu, B., Gao, Y., Cheng, Q., et al. (2018). Dynamic and Direct Pathogen Load Surveillance to Monitor Disease Progression and Therapeutic Efficacy in Central Nervous System Infection Using a Novel Semi-Quantitive Sequencing Platform. *J. Infect.* 76, 307–310. doi: 10.1016/j.jinf.2017.11.002

Bandali, A., Bias, T. E., Lee, D. H., and Malat, G. (2020). Duration of Perioperative Antimicrobial Prophylaxis in Orthotopic Liver

Transplantation Patients. *Prog. Transplant.* 30, 265–270. doi: 10.1177/1526924820933824

Cornaglia, G., Courcol, R., and Hermann, J. L. (2012). *European Manual of Clinical Microbiology* (Société franaise de microbiologie).

da Silva, F. R., Cibulski, S. P., Daudt, C., Weber, M. N., Guimaraes, L. L., Streck, A. F., et al. (2016). Novel Bovine Papillomavirus Type Discovered by Rolling-Circle Amplification Coupled With Next-Generation Sequencing. *PLoS One* 11, e0162345. doi: 10.1371/journal.pone.0162345

Dogan, S. M., and Kutluturk, K. (2020). Living Donor Versus Deceased Donor Liver Transplantation for HCC. *J. Gastrointest Cancer* 51, 1104–1106. doi: 10.1007/s12029-020-00481-1

Fang, C., Zhong, H., Lin, Y., Chen, B., Han, M., Ren, H., et al. (2018). Assessment of the cPAS-Based BGISEQ-500 Platform for Metagenomic Sequencing. *Gigascience* 7, 1–8. doi: 10.1093/gigascience/gix133

Heldman, M. R., Ngo, S., Dorschner, P. B., Helfrich, M., and Ison, M. G. (2019). Pre- and Post-Transplant Bacterial Infections in Liver Transplant Recipients. *Transpl Infect. Dis.* 21, e13152. doi: 10.1111/tid.13152

Huang, J., Jiang, E., Yang, D., Wei, J., Zhao, M., Feng, J., et al. (2020). Metagenomic Next-Generation Sequencing Versus Traditional Pathogen Detection in the Diagnosis of Peripheral Pulmonary Infectious Lesions. *Infect. Drug Resist.* 13, 567–576. doi: 10.2147/IDR.S235182

Huang, J., Millis, J. M., Mao, Y., Millis, M. A., Sang, X., and Zhong, S. (2015). Voluntary Organ Donation System Adapted to Chinese Cultural Values and Social Reality. *Liver Transpl.* 21, 419–422. doi: 10.1002/lt.24069

Jeon, Y. J., Zhou, Y., Li, Y., Guo, Q., Chen, J., Quan, S., et al. (2014). The Feasibility Study of non-Invasive Fetal Trisomy 18 and 21 Detection With Semiconductor Sequencing Platform. *PLoS One* 9, e110240. doi: 10.1371/journal.pone.0110240

Kaul, D. R., Vece, G., Blumberg, E., La Hoz, R. M., Ison, M. G., Green, M., et al. (2021). Ten Years of Donor-Derived Disease: A Report of the Disease Transmission Advisory Committee. *Am. J. Transplant.* 21, 689–702. doi: 10.1111/ajt.16178

Kikuchi, T., Arai, M., Koda, Y., Kato, J., Shimizu, T., Katano, H., et al. (2019). Late-Onset Visceral Varicella-Zoster Virus Infection Presented as Acute Liver Failure After Allogeneic Hematopoietic Stem Cell Transplantation. *Transpl Infect. Dis.* 21, e13121. doi: 10.1111/tid.13121

Li, H., and Durbin, R. (2010). Fast and Accurate Long-Read Alignment With Burrows-Wheeler Transform. *Bioinformatics* 26, 589–595. doi: 10.1093/bioinformatics/btp698

Li, Y., Sun, B., Tang, X., Liu, Y. L., He, H. Y., Li, X. Y., et al. (2020). Application of Metagenomic Next-Generation Sequencing for Bronchoalveolar Lavage Diagnostics in Critically Ill Patients. *Eur. J. Clin. Microbiol. Infect. Dis.* 39, 369–374. doi: 10.1007/s10096-019-03734-5

Long, Y., Zhang, Y., Gong, Y., Sun, R., Su, L., Lin, X., et al. (2016). Diagnosis of Sepsis With Cell-Free DNA by Next-Generation Sequencing Technology in ICU Patients. *Arch. Med. Res.* 47, 365–371. doi: 10.1016/j.arcmed.2016.08.004

Mehta, V., Ramachandran, K., Agarwal, R., Alam, S., Pamecha, V., and Gupta, E. (2021). Varicella Infection in an Immunized Pediatric Living Donor Liver-Transplant Recipient. *J. Glob Infect. Dis.* 13, 142–144. doi: 10.4103/jgid.jgid_233_20

Miao, Q., Ma, Y., Wang, Q., Pan, J., Zhang, Y., Jin, W., et al. (2018). Microbiological Diagnostic Performance of Metagenomic Next-Generation Sequencing When Applied to Clinical Practice. *Clin. Infect. Dis.* 67, S231–S240. doi: 10.1093/cid/ciy693

Mishkin, A. (2021). Emerging Fungal Pathogens in Solid Organ Transplantation. *Curr. Opin. Organ Transplant.* 26, 440–444. doi: 10.1097/MOT.0000000000000889

Mrzljak, A., and Vilibic-Cavlek, T. (2020). Torque Teno Virus in Liver Diseases and After Liver Transplantation. *World J. Transplant.* 10, 291–296. doi: 10.5500/wjt.v10.i11.291

Nam, H., Nilles, K. M., Levitsky, J., and Ison, M. G. (2018). Donor-Derived Viral Infections in Liver Transplantation. *Transplantation* 102, 1824–1836. doi: 10.1097/TP.0000000000002326

Pendleton, K. M., Erb-Downward, J. R., Bao, Y., Branton, W. R., Falkowski, N. R., Newton, D. W., et al. (2017). Rapid Pathogen Identification in Bacterial Pneumonia Using Real-Time Metagenomics. *Am. J. Respir. Crit. Care Med.* 196, 1610–1612. doi: 10.1164/rccm.201703-0537LE

Pettengill, M. A., Babu, T. M., Prasad, P., Chuang, S., Drage, M. G., Menegus, M., et al. (2019). Probable Donor-Derived Human Adenovirus Type 34 Infection in 2 Kidney Transplant Recipients From the Same Donor. *Open Forum Infect. Dis.* 6, ofy354. doi: 10.1093/ofid/ofy354

Ruiz, P., Martinez-Picola, M., Santana, M., Munoz, J., Perez-Del-Pulgar, S., Koutsoudakis, G., et al. (2019). Torque Teno Virus Is Associated With the State of Immune Suppression Early After Liver Transplantation. *Liver Transpl* 25, 302–310. doi: 10.1002/lt.25374

Schreiber, P. W., Kufner, V., Hubel, K., Schmutz, S., Zagordi, O., Kaur, A., et al. (2019). Metagenomic Virome Sequencing in Living Donor and Recipient Kidney Transplant Pairs Revealed JC Polyomavirus Transmission. *Clin. Infect. Dis.* 69, 987–994. doi: 10.1093/cid/ciy1018

Simner, P. J., Miller, S., and Carroll, K. C. (2018). Understanding the Promises and Hurdles of Metagenomic Next-Generation Sequencing as a Diagnostic Tool for Infectious Diseases. *Clin. Infect. Dis.* 66, 778–788. doi: 10.1093/cid/cix881

Tarabichi, M., Shohat, N., Goswami, K., Alvand, A., Silibovsky, R., Belden, K., et al. (2018). Diagnosis of Periprosthetic Joint Infection: The Potential of Next-Generation Sequencing. *J. Bone Joint Surg. Am.* 100, 147–154. doi: 10.2106/JBJS.17.00434

Zhang, X. X., Guo, L. Y., Liu, L. L., Shen, A., Feng, W. Y., Huang, W. H., et al. (2019). The Diagnostic Value of Metagenomic Next-Generation Sequencing for Identifying Streptococcus Pneumoniae in Paediatric Bacterial Meningitis. *BMC Infect. Dis.* 19, 495. doi: 10.1186/s12879-019-4132-y

Zhou, X., Wu, H., Ruan, Q., Jiang, N., Chen, X., Shen, Y., et al. (2019). Clinical Evaluation of Diagnosis Efficacy of Active Mycobacterium Tuberculosis Complex Infection *via* Metagenomic Next-Generation Sequencing of Direct Clinical Samples. *Front. Cell Infect. Microbiol.* 9, 351. doi: 10.3389/fcimb.2019.00351

Conflict of Interest: The authors declare that the research was conducted in the absence of any commercial or financial relationships that could be construed as a potential conflict of interest.

The reviewer CZ declared a shared parent affiliation with the authors J-FH, QM, J-WC, AH, D-ZG, TW, L-XY, D-MZ, X-WH, JF, JZ, X-RY to the handling editor at the time of review.

Publisher's Note: All claims expressed in this article are solely those of the authors and do not necessarily represent those of their affiliated organizations, or those of the publisher, the editors and the reviewers. Any product that may be evaluated in this article, or claim that may be made by its manufacturer, is not guaranteed or endorsed by the publisher.

frontiers | Frontiers in Cellular and Infection Microbiology

TYPE Original Research
PUBLISHED 01 August 2022
DOI 10.3389/fcimb.2022.925982

OPEN ACCESS

EDITED BY
Jinmin Ma,
Beijing Genomics Institute (BGI), China

REVIEWED BY
Jiazheng Xie,
Chongqing University of Posts and Telecommunications, China
Chenguang Shen,
Southern Medical University, China

*CORRESPONDENCE
Hao Tang
tanghao_0921@126.com

†These authors have contributed equally to this work and share first authorship

SPECIALTY SECTION
This article was submitted to Clinical Microbiology, a section of the journal Frontiers in Cellular and Infection Microbiology

RECEIVED 22 April 2022
ACCEPTED 05 July 2022
PUBLISHED 01 August 2022

CITATION
Bao S, Song H, Chen Y, Zhong C and Tang H (2022) Metagenomic next-generation sequencing for the diagnosis of : A retrospective study. *Front. Cell. Infect. Microbiol.* 12:925982. doi: 10.3389/fcimb.2022.925982

Metagenomic next-generation sequencing for the diagnosis of pulmonary aspergillosis in non-neutropenic patients: a retrospective study

Shujun Bao†, Huihui Song†, Yang Chen†, Caiming Zhong† and Hao Tang*

Department of Respiratory and Critical Care Medicine, Second Affiliated Hospital of Naval Medical University, Shanghai, China

This study aimed to obtain further in-depth information on the value of metagenomic next-generation sequencing (mNGS) for diagnosing pulmonary aspergillosis in non-neutropenic patients. We did a retrospective study, in which 33 non-neutropenic patients were included, of which 12 were patients with pulmonary aspergillosis and 21 were diagnosed with non-pulmonary aspergillosis. Fungi and all other co-pathogens in bronchoalveolar lavage fluid (BALF) (27 cases), blood (6 cases), and/or pleural fluid (1 case) samples were analyzed using mNGS. One of the patients submitted both BALF and blood samples. We analyzed the clinical characteristics, laboratory tests, and radiologic features of pulmonary aspergillosis patients and compared the diagnostic accuracy, including sensitivity, specificity, positive predictive value, and negative predictive value of mNGS with conventional etiological methods and serum (1,3)-β-D-glucan. We also explored the efficacy of mNGS in detecting mixed infections and co-pathogens. We further reviewed modifications of antimicrobial therapy for patients with pulmonary aspergillosis according to the mNGS results. Finally, we compared the detection of *Aspergillus* in BALF and blood samples from three patients using mNGS. In non-neutropenic patients, immunocompromised conditions of non-pulmonary aspergillosis were far less prevalent than in patients with pulmonary aspergillosis. More patients with pulmonary aspergillosis received long-term systemic corticosteroids (50% vs. 14.3%, $p < 0.05$). Additionally, mNGS managed to reach a sensitivity of 91.7% for diagnosing pulmonary aspergillosis, which was significantly higher than that of conventional etiological methods (33.3%) and serum (1,3)-β-D-glucan (33.3%). In addition, mNGS showed superior performance in discovering co-pathogens (84.6%) of pulmonary aspergillosis; bacteria, bacteria-fungi, and bacteria-PJP-virus were most commonly observed in non-neutropenic patients. Moreover, mNGS results can help guide effective treatments. According to the mNGS results, antimicrobial therapy was altered in 91.7% of patients with pulmonary aspergillosis. The diagnosis of *Aspergillus* detected in blood samples, which can be used as a supplement to BALF samples, seemed to show a higher

specificity than that in BALF samples. mNGS is a useful and effective method for the diagnosis of pulmonary aspergillosis in non-neutropenic patients, detection of co-pathogens, and adjustment of antimicrobial treatment.

KEYWORDS

metagenomic next-generation sequencing, aspergillus, pulmonary aspergillosis, non-neutropenic patients, diagnosis

Introduction

Aspergillus is one of the most ubiquitous and important pathogens in the environment, including *Aspergillus fumigatus*, *A. flavus*, *A. niger*, *A. terreus*, *A. nidulans*, and others (Sugui et al., 2014). *Aspergillus*-related lung diseases are traditionally classified into four types: pulmonary aspergilloma, allergic broncho-pulmonary aspergillosis (ABPA), chronic pulmonary aspergillosis (CPA), and invasive aspergillosis (IPA) (Chabi et al., 2015). Aspergillus occurrence and clinical manifestations depend on the host's immunological status and the existence of underlying lung disease. Recently, researchers have discovered that aspergillosis can arise in other diseases, such as long-term corticosteroid use in chronic obstructive pulmonary disease (COPD) (Patterson and Strek, 2014), diabetes mellitus, pulmonary tuberculosis, and bronchiectasis, rather than in immunocompromised hosts. Even without disease, potential hosts can be attacked when they are in contact with a large mass of *Aspergillus*.

The clinical manifestations of pulmonary aspergillosis in non-neutropenic patients are non-specific, even similar to tuberculosis (TB), which makes diagnosis difficult. Non-neutropenic patients who are immunocompromised owing to other factors have a more progressive course and a worse prognosis than the neutropenic patients. Thus, recognizing the diversity and subtle representation of the disease, assessing vulnerable groups, and using effective therapy sooner in the disease stage are very valuable.

To date, the definitive diagnostic method of pulmonary aspergillosis is a pathological investigation that takes too much time (Li, 2022). Conventional etiological methods, namely fungal smear and culture, are time-consuming and show a low detection rate. Recently, non-invasive biomarkers have made it easier to suspect and diagnose pulmonary aspergillosis (El-Baba et al., 2020). However, serum (1,3)-β-D-glucan (G) or galactomannan (GM) test results should be considered in combination with clinical manifestations in pediatric pulmonary aspergillosis cases, as the tests are not sufficiently sensitive (Tong et al., 2018). The introduction of several high-performing diagnostic tests helps redefine patient management. Researchers have suggested that *Aspergillus* antigen and *Aspergillus* immunoglobulin G (precipitins) are promising markers for the diagnosis of *Aspergillus* (Denning, 2021). However, there is an urgent need to explore new and efficient (quicker and more accurate) diagnostic tools for pulmonary aspergillosis to acquire early identification, improve patient outcomes, and reduce mortality.

Based on high-throughput sequencing, metagenomic next-generation sequencing (mNGS) is thought to be a promising microbial identification technology because of its rapid cycles and high sensitivity. mNGS identifies and classifies a wide range of pathogens (including respiratory tract (Xie et al., 2021), blood stream (Jing et al., 2021), central nervous system (Wilson et al., 2019), and prosthetic joints pathogens (Thoendel et al., 2018)), and is a widely used microbial test for infectious diseases, particularly for special and rare pathogens. It can also be used to analyze drug resistance genes and virulence factors in pathogens.

Many previous studies on the detection of pulmonary infections using mNGS have focused on pathogens. Yang et al. (Yang et al., 2021) observed that mNGS (lung biopsy, bronchoalveolar lavage fluid [BALF]) had a significantly higher sensitivity than conventional tests for diagnosing pulmonary fungal infections. Liu et al. (Liu et al., 2021) evaluated the performance of BALF-mNGS in differentiating colonization and infection with *Pneumocystis jirovecii* and suggested that the fungal load differed significantly between the two groups (*P. jirovecii* pneumonia and *P. jirovecii* colonization). However, there is still a scarcity of clinical experience in the diagnosis of fungal infections, particularly aspergillosis.

Therefore, our retrospective study aimed to contribute to this growing area of research by exploring the diagnostic performance of mNGS in non-neutropenic patients with pulmonary aspergillosis.

Materials and methods

Study design and subjects

In this retrospective study, we successively enrolled 33 non-neutropenic patients whose mNGS results (BALF and/or blood and/or pleural fluid samples) identified fungi (e.g., *Aspergillus*, *P.*

jirovecii, *Candida*, and *Cryptococcus*) and were admitted to the Department of Respiratory and Critical Care Medicine of Second Affiliated Hospital, Naval Medical University (Shanghai, China), from June 1, 2018, to January 31, 2022. The combined clinical diagnosis of pulmonary aspergillosis or non-pulmonary aspergillosis was made by two medical doctors based on host risk factors, clinical symptoms, chest computed tomography images, laboratory findings, and response to treatment. Finally, 12 patients were diagnosed with pulmonary aspergillosis, and 21 were diagnosed with non-pulmonary aspergillosis. Patients were excluded from the study based on the following criteria: (1) age <18 years; (2) neutropenia (absolute neutrophil count $<1.5\times10^9$/L); (3) mNGS not performed; and (4) incomplete medical records.

The collection of biological samples

Collection of BALF was performed by experienced bronchoscopists at Naval Medical University's Second Affiliated Hospital after treatment with atropine for spasmolysis, diazepam for sedation, and lidocaine for local anesthesia. The sampling site was chosen based on chest computed tomography (CT) images. Three 20 ml sterile saline fractions were instilled into the target subsegmental bronchi. BALF was extracted using gentle syringe suction and was placed in sterile containers. To avoid contamination, the first 20 ml of each sample was discharged, while the rest samples were kept for analysis. Furthermore, 3–5 ml of blood samples and at least 10 ml pleural fluid samples were collected.

Testing process of mNGS

DNA extraction and sequencing were conducted by the Beijing Genomics Institute (BGI). First, BALF was mixed with lysozyme and glass beads to reduce viscosity. Blood was centrifuged to separate the plasma, and pleural fluid was centrifuged to collect the sediment. The inactivated specimens were further subjected to wall breaking. Following this, DNA was extracted. The concentration and volume of the extracted samples were measured to determine the quality control results of the nucleic acids. Construction of DNA library and sequencing the DNA library was done by DNA fragmentation, end-repair, and polymerase chain reaction (PCR) amplification. This was then used for library concentration detection and quality control. Qualified DNA nanoballs were loaded onto the chip, and single-end sequencing was performed on the MGISEQ-2000 sequencing platform. Bioinformatic analysis was conducted on samples with raw data >20 million and read length >50bp (Long et al., 2016). Low-quality human host sequences were removed (Marotz et al., 2018) to improve detection sensitivity (Hasan et al., 2016). The high-quality data were classified by simultaneously aligning to microbial genome databases (Salter et al., 2014), including viruses, bacteria, fungi, and parasites. The database reference sequences were used to calculate the microbial parameters *via* multiple comparisons with de-exclusion. Eventually, clinically significant microbes were categorized as putative co-pathogens if the patients had suggestive symptoms, laboratory findings, and radiologic abnormalities.

Statistical analysis

Statistical analysis was performed using the SPSS software (version 26, IBM Corp, Armonk, NY, USA). Continuous variables were presented as mean ± standard deviation, whereas categorical variables were presented as counts and percentages. The t-test for two independent samples was used to compare the normal distribution of continuous variables between pulmonary aspergillosis and non-pulmonary aspergillosis patients, the Mann–Whitney U test was used to compare the abnormal distribution of continuous variables, and the chi-square test was used for categorical variables. The sensitivity, specificity, positive predictive value (PPV), and negative predictive value (NPV) of mNGS, conventional etiological methods, and serum (1,3)-β-D-glucan in the diagnosis of pulmonary aspergillosis were calculated using the combined clinical diagnosis as the reference standard; Wilson's method was used to calculate 95% confidence intervals for these proportions. Statistical significance was set at $P < 0.05$.

Ethics statement

Ethical approval was obtained from the Ethics Committee of Shanghai Changzheng Hospital. The patients provided their written informed consent to participate in this study.

Results

Clinical characteristics, laboratory tests, and radiologic features of pulmonary aspergillosis in non-neutropenic patients

Table 1 summarizes the patient characteristics on admission. The cohort was divided into two groups according to clinical composite diagnosis. A total of 12 pulmonary aspergillosis patients and 21 non-pulmonary aspergillosis patients were included in this study. The median age (60 vs. 68 years) and sex composition of these two groups were similar. The most prevalent symptoms of pulmonary aspergillosis in non-neutropenic patients were cough (91.7%), expectoration (75.0%), fever (75.0%), and abnormal breath sounds (90.0%). Comparing the two results, chest tightness and dyspnea were less

TABLE 1 Clinical characteristics, laboratory tests, and radiologic features of pulmonary aspergillosis and non-pulmonary aspergillosis in non-neutropenic patients on admission.

Characteristic (mean± [standard deviation] or count [percentage])	Pulmonary aspergillosis patients(n = 12)	Non-pulmonary aspergillosis patients(n = 21)	P-value
Male	7 (58.3%)	17 (81%)	0.230
Age (years)	60.3 ± 14.9	67.8 ± 17.4	0.399
Smoking history	4 (33.3%)	9 (42.9%)	0.719
At least two hospitalization times per year	6 (50.0%)	7 (33.3%)	0.465
Abnormal environmental exposure history	0 (0%)	1 (4.8%)	1.000
Less than 2 weeks after onset	7 (58.3%)	15 (71.4%)	0.471
Mechanical ventilation	3 (25%)	5 (23.8%)	1.000
Hemodynamic instability	0 (0%)	4 (19%)	0.271
Clinical symptoms			
Fever	9 (75%)	14 (66.7%)	0.710
Cough	11 (91.7%)	17 (81%)	0.630
Expectoration	9 (75%)	14 (66.7%)	0.710
Hemoptysis	3 (25%)	3 (14.3%)	0.643
Chest tightness/dyspnea	7 (58.3%)	13 (61.9%)	1.000
Abnormal breath sound	9 (90% [n=10])	18 (90% [n=20])	1.000
Underlying diseases			
Bronchiectasis	1 (8.3%)	6 (28.6%)	0.223
Interstitial lung disease	2 (16.7%)	2 (9.5%)	0.610
Emphysema/COPD	3 (25%)	2 (9.5%)	0.328
Tuberculosis	0 (0%)	3 (14.3%)	0.284
Malnutrition	5 (41.7%)	6 (28.6%)	0.471
Diabetes	6 (50%)	4 (19%)	0.114
Solid tumors	3 (25%)	6 (28.6%)	1.000
Immunocompromised conditions			
With HIV-infected	0 (0%)	2 (9.5%)	0.523
Systemic use of corticosteroids	6 (50%)	3 (14.3%)	0.044***
Use of immunosuppressive agents	3 (25%)	2 (9.5%)	0.328
Use of cytotoxic drugs	5 (41.7%)	2 (9.5%)	0.071
Use of prior broad-spectrum antibiotics	4 (33.3%)	3 (14.3%)	0.377
Chest computed tomography images			
Double lung infiltration	11 (91.7%)	17 (81%)	0.630
Multiple lesions	11 (91.7%)	18 (85.7%)	1.000
Aspergilloma	1 (8.3%)	0 (0%)	0.364
Nodular shadowing	4 (33.3%)	6 (28.6%)	1.000
Wedge or patchy shadowing	8 (66.7%)	19 (90.5%)	0.159
Cavitation sign	2 (16.7%)	0 (0%)	0.125
Crescent sign	0 (0%)	0 (0%)	NaN
Halo sign	0 (0%)	0 (0%)	NaN
Pleural effusion	7 (58.3%)	14 (58.3%)	0.716
Mediastinal lymphadenopathy	3 (25%)	6 (28.6%)	1.000
Thickening of the bronchial lumen	1 (8.3%)	6 (28.6%)	0.223
Abnormal changes under endoscopy	5 (71.4% [n=7])	11 (73.3%[n=15])	1.000
Laboratory findings			
WBC (×10^9/L)	13.2 ± 11.3	9.7 ± 3.1	0.837
Neu (%)	82.1 ± 10.6	81.3 ± 9.2	0.837
CRP (mg/L)	62.6 ± 53.5	70.5 ± 67.6	0.940
PCT (>0.5 ng/ml)	4 (36.4% [n=11])	5 (23.8% [n=21])	0.681

(Continued)

TABLE 1 Continued

Characteristic (mean± [standard deviation] or count [percentage])	Pulmonary aspergillosis patients(n = 12)	Non-pulmonary aspergillosis patients(n = 21)	P-value
ESR (>15 mm/h)	8 (80% [n=10])	13 (92.9% [n=14])	0.550
ALB (g/L)	29.4 ± 4.9	33.3 ± 4.8	0.447
Glucose control (HbA1c>6.5%)	4 (57.1% [n=7])	3 (50% [n=6])	1.000
D-dimers (>0.55 ug/ml)	11 (100% [n=11])	13 (72.2% [n=18])	0.126
Type I respiratory failure (<60 mmHg)	3 (42.9% [n=7])	5 (45.5% [n=11])	1.000
Immunosuppression (CD4/CD8 ratio<1.4)	5 (62.5% [n=8])	7 (50% [n=14])	0.675
Serum (1,3)-β-D-Glucan (>100 pg/ml)	4 (36.4% [n=11])	3 (15.8% [n=19])	0.372

HIV, human immunodeficiency virus; WBC, white blood cell; Neu, neutrophils; CRP, C-reactive protein; PCT, procalcitonin; ESR, erythrocyte sedimentation rate; ALB, albumin.
***P<0.05.

frequently observed in patients with pulmonary aspergillosis. Among the underlying diseases of pulmonary aspergillosis, diabetes (50.0%) ranked first, followed by malnutrition (41.7%), COPD (25.0%), and solid tumors (25.0%). In addition, the data showed that patients with pulmonary aspergillosis had various immunocompromised conditions: 50.0% received long-term systemic corticosteroids (used for at least 3 weeks with a daily dose of ≥0.3mg/kg/day of prednisone or the equivalent dose of prednisone) (p = 0.044), 41.7% received cytotoxic drugs (within 90 days), 33.3% received prior broad-spectrum antibiotics, and 25.0% received immunosuppressive agents (within 90 days). In contrast, immunocompromised conditions were far less prevalent in the non-pulmonary aspergillosis patients.

Among non-neutropenic patients with pulmonary aspergillosis, the most common radiologic features on chest CT were double lung infiltration (91.7%), multiple lesions (91.7%), wedge or patchy shadowing (66.7%), and nodular shadowing (33.3%). Some showed typical features such as aspergilloma (8.3%) and cavitation signs (16.7%) (Figure 1A), which may be accompanied by pleural effusion, mediastinal lymphadenopathy, and abnormal changes during endoscopy (Figure 1B). The next section of the study was concerned with the laboratory findings. Serum (1,3)-β-D-glucan levels, d-dimer levels, immunosuppression, and poor glucose control in pulmonary aspergillosis patients appeared to be higher than those in non-pulmonary aspergillosis patients, but there were no significant differences.

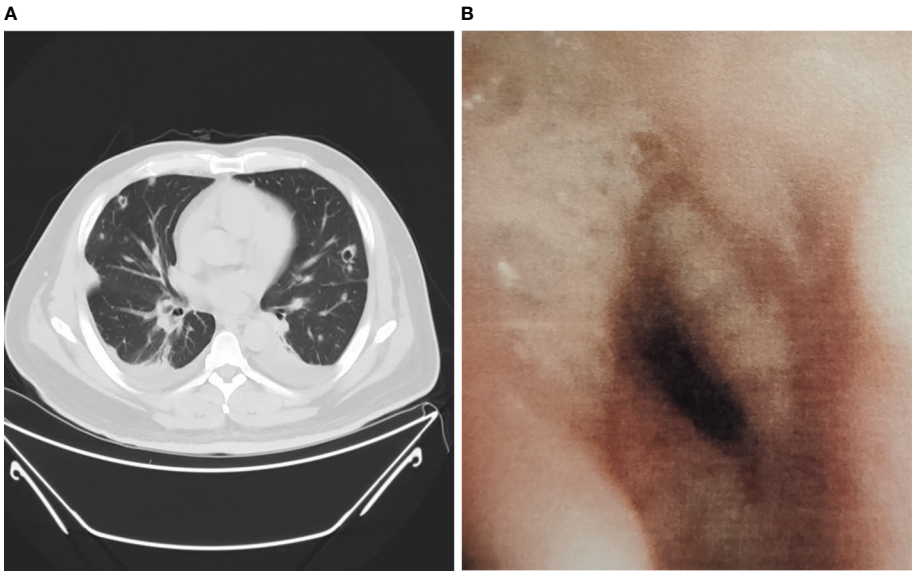

FIGURE 1
Chest CT scan and bronchoscopy of pulmonary aspergillosis in non-neutropenic patient. **(A)** Chest CT showed cavitation signs; **(B)** Bronchoscopy showed purulent secretions, mucosal hyperemia, and edema.

Comparison of diagnostic performance among mNGS, conventional etiological methods, and serum (1,3)-β-D-glucan in non-neutropenic pulmonary aspergillosis patients

One of the most well-known tools for assessing *Aspergillus* infection is the conventional etiological method; serum (1,3)-β-D-glucan and galactomannan are widely used serologic biomarkers of pulmonary aspergillosis. Recently, molecular biological techniques such as mNGS have been widely applied in clinical settings. Therefore, we compared the diagnostic accuracy of mNGS with that of conventional etiological methods and serum (1,3)-β-D-glucan. Table 2 shows it that mNGS of BALF, blood, and/or pleural fluid samples was performed in all 34 cases, conventional etiological methods in 31 cases (12 with pulmonary aspergillosis and 19 with non-pulmonary aspergillosis) and serum (1,3)-β-D-glucan in 31 cases (12 with pulmonary aspergillosis and 19 with non-pulmonary aspergillosis). The combined clinical diagnosis was used as reference to calculate the diagnostic sensitivity and specificity of mNGS. The sensitivities of mNGS, conventional etiological methods, and serum (1,3)-β-D-glucan were 91.7% (95% CI, 59.8–99.6%), 33.3% (95% CI, 11.3–64.6%), and 33.3% (95% CI, 11.3–64.6%), respectively. However, mNGS showed a low specificity of 71.4% (95% CI, 47.7–87.8%), compared with conventional etiological methods (100% [95% CI, 79.1–100%]) and serum (1,3)-β-D-glucan (84.2% [95% CI, 59.5–95.8%]). With the highest Youden index of 0.63, mNGS appears to have the most effective screening ability and the best authenticity.

Mixed infections and co-pathogens detected by mNGS

Mixed infections are common in non-neutropenic patients with pulmonary aspergillosis. Thirteen cases of putative mixed infections tested by mNGS are described in Figure 2. This method showed satisfactory performance in identifying co-pathogens (84.6%), among which *Aspergillus*-bacteria, *Aspergillus*-bacteria-fungi, and *Aspergillus*-bacteria-*P. jirovecii* (PJP)-virus were most common. *Aspergillus*-bacteria co-infections were identified by mNGS in 5 (38.5%) of 13 cases (Figure 2A). Closer inspection of the table shows that the most common bacteria were *Klebsiella pneumoniae* and *Acinetobacter baumannii*, the most common fungus was *P. jirovecii*, and the most common viruses were *Epstein–Barr virus*, *human herpesvirus 1*, and *Torque teno virus* (Figure 2B). This indicates that the prevention and treatment of mixed infections in pulmonary aspergillosis patients should be strengthened.

Impact of mNGS on antimicrobial therapy of pulmonary aspergillosis in non-neutropenic patients

Table 3 shows records of antimicrobial treatment for *Aspergillus* and other pathogens from 12 non-neutropenic patients with pulmonary aspergillosis during hospitalization. The most evident finding that emerged from the analysis is that based on the mNGS results, antimicrobial therapy was altered in 91.7% of patients, 58.4% had the antimicrobial agents or spectrum adjusted, 50% were started with anti-*Aspergillus* drugs, 16.7% were started with trimethoprim-sulfamethoxazole (TMP-SMZ), and 25% were started with anti-viral drugs.

Detection of aspergillus in BALF and blood samples by mNGS

In this study, simultaneous mNGS of BALF and blood samples was performed in three patients who were suspected to have pulmonary aspergillosis. In two of the three patients, the stringent mapped read number (SMRN) of *Aspergillus* was

TABLE 2 Diagnostic performance of mNGS, conventional etiological methods, and serum (1,3)-β-D-glucan in non-neutropenic pulmonary aspergillosis patients.

Number of cases	Methods	Pulmonary aspergillosis cohort	Non-pulmonary aspergillosis cohort	Sensitivity (95% CI)	Specificity (95% CI)	PPV (95% CI)	NPV (95% CI)	Youden index
n = 34	mNGS+	11	6	91.7% (0.598–0.996)	71.4% (0.477–0.878)	64.7% (0.386–0.847)	93.8% (0.677–0.997)	0.63
	–	1	15					
n = 31	Conventional etiological methods+	4	0	33.3% (0.113–0.646)	100% (0.791–1)	100% (0.396–1)	70.4% (0.497–0.855)	0.33
	–	8	19					
n = 31	G test+	4	3	33.3% (0.113–0.646)	84.2% (0.595–0.958)	57.1% (0.202–0.882)	66.7% (0.447–0.836)	0.18
	–	8	16					

Aspergillus detected by mNGS, Aspergillus detected by conventional etiological methods, and serum (1,3)-β-D-glucan level > 100 pg/ml were defined as positive.
PPV, positive predictive value; NPV, negative predictive value; CI, confidence interval; G, serum (1,3)-β- D-glucan.

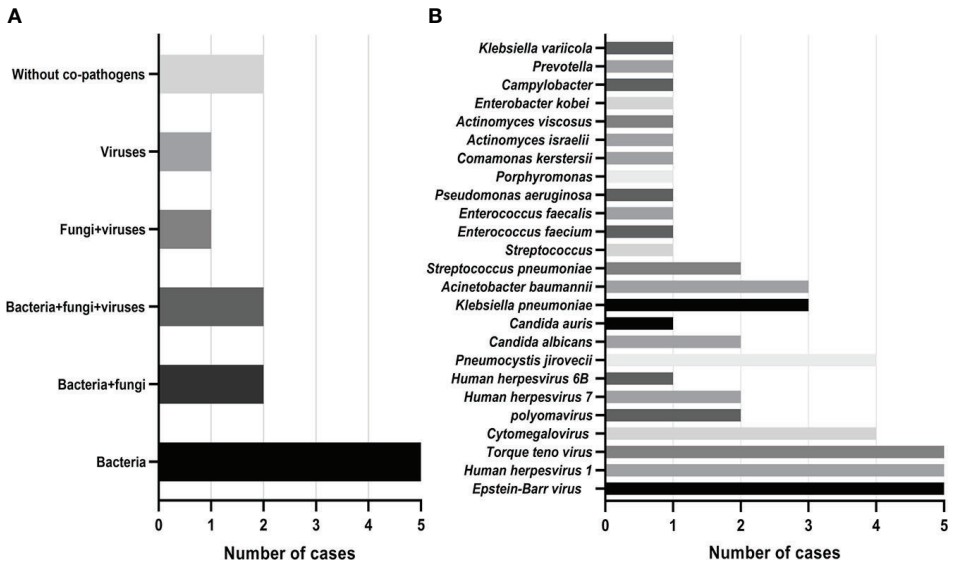

FIGURE 2
Mixed infections and co-pathogens in 13 non-neutropenic pulmonary aspergillosis cases identified using mNGS. **(A)** Number of pulmonary aspergillosis patients with mixed infections; **(B)** Number of pulmonary aspergillosis patients infected with various co-pathogens.

detected in BALF but not in blood, and the clinical composite diagnosis was non-pulmonary aspergillosis. In summary, the diagnosis of *Aspergillus* detected in blood samples, which can be used as a supplement to BALF samples, showed higher specificity than that in BALF samples.

Discussion

We performed a retrospective study to evaluate the diagnostic ability of mNGS in non-neutropenic patients with pulmonary aspergillosis. We showed that mNGS had satisfactory sensitivity in diagnosing and was useful in identifying co-pathogens in pulmonary mixed infections and directing modifications of antimicrobial treatment.

Aspergillus is a common opportunistic pathogen that can be fatal in certain conditions (such as organ transplantation, granulocytic, HIV-infected, and tumors). Currently, there is an increase in the occurrence of pulmonary aspergillosis in the non-neutropenic population owing to the increasing occurrence of non-specific factors such as COPD, diabetes, and immunosuppressive therapy.

Microbiological diagnosis of pulmonary aspergillosis is the "rate-limiting" step in achieving prompt treatment initiation and improving the prognosis of patients. Thus far, fungal smear and culture, serum (1,3)-β-D-glucan (G) or galactomannan (GM) tests, PCR, and *Aspergillus*-specific lateral flow device tests (LFD) (Jenks et al., 2019) are used in the microbiological analysis of pulmonary aspergillosis. Recent studies have shown that the polymorphism of PTX3 (which is a soluble pattern recognition receptor) is associated with increased susceptibility to invasive aspergillosis (Kang et al., 2020). However, these methods have certain limitations. Although traditional etiological culture methods help provide fungal drug sensitivity information, the clinical positivity rate is still low and fails to differentiate between contamination and colonization. Meanwhile, the sensitivity of the serum GM test in non-neutropenic patients is low and is affected by the use of antibiotics and intravenous immunoglobulins.

To date, mNGS has been clinically used. There are only few studies that have investigated the association between mNGS

TABLE 3 Impact of mNGS on antimicrobial therapy of pulmonary aspergillosis in non-neutropenic patients.

Modifications	Pulmonary aspergillosis patients (n = 12)
No change	1 (8.3%)
Remove 1 antimicrobial agent type	3 (25%)
Increase antimicrobial spectrum	2 (16.7%)
Reduce antimicrobial spectrum	2 (16.7%)
Add anti-*Aspergillus* drugs	6 (50%)
Add TMP-SMZ	2 (16.7%)
Add anti-viral drugs	3 (25%)

TMP-SMZ, trimethoprim-sulfamethoxazole.

and the diagnosis of pulmonary aspergillosis (He et al., 2019; Zhang et al., 2020; Chen et al., 2021; Ma et al., 2022). In these studies, Chen et al. (Chen et al., 2021) and Zhang et al. (Zhang et al., 2020) reported the application of NGS in diagnosing co-infection of *Aspergillus* and *P. jirovecii*, which supports the results of this study. Additionally, Zhang et al. (Zhang et al., 2020) and He et al. (He et al., 2019) reported that patients with pulmonary aspergillosis have complications such as corticosteroid-treated dermatomyositis, COPD, and asthma, which is consistent with our results.

mNGS, as a new microbial diagnostic method, can accurately distinguish species and has high value for the diagnosis of *Aspergillus*. Therefore, our research concentrated on its diagnostic value, and we revealed that the sensitivity of mNGS is significantly higher than that of conventional etiological methods and serum (1,3)-β-D-glucan, but with relatively low specificity. Another notable benefit of mNGS over other microbiological tests is the wide spectrum of pathogen identification, which enables the detection of mixed infections with a single run of non-neutropenic pulmonary aspergillosis patient samples. Therefore, patients with mixed infections might benefit from this technique.

The unbiased broad-spectrum detection of mNGS could further guide effective antimicrobial treatment. In the present study, 50% of pulmonary aspergillosis patients did not receive anti-*Aspergillus* drugs until the report of mNGS results, demonstrating that mNGS is useful for the diagnosis and proper treatment of pulmonary aspergillosis. Triazoles are the only oral drugs with anti-*Aspergillus* activity, while itraconazole and voriconazole are considered first-line drugs (Alastruey-Izquierdo et al., 2018). These findings imply that an earlier application of mNGS can guide a rapid and accurate diagnosis of pulmonary aspergillosis. This new method is expected to become a new gold standard with high therapeutic efficiency after diagnosis.

Notably, the mNGS of *Aspergillus* in BALF samples sometimes gives a false-positive result. This could be due to several factors, which include: (a) contamination of the microbial genome from the environment or body flora and (b) high host genome background and low microbial biomass of the true pathogens (Chen et al., 2020). mNGS of *Aspergillus* in blood samples has a higher specificity. A possible explanation is that healthy human blood is sterile. Meanwhile, the consistency of mNGS detection of *Aspergillus* in BALF and blood samples suggests that *Aspergillus* may be transmitted from the lungs to the bloodstream in patients with pulmonary aspergillosis (Jiang et al., 2021). In contrast, one study showed that the diagnostic value of BALF GM detection in non-neutropenic patients is superior to that of serum GM detection (Zhou et al., 2017).

The present study had several limitations. Firstly, it was a single-center retrospective study. Thereby, intrinsic bias is inevitable. In addition, the diagnostic performance of mNGS was not compared with that of the GM test, which our hospital does not routinely perform. Therefore, further studies that consider these variables are needed. Moreover, owing to the lack of general agreement on interpreting mNGS results, it is difficult to determine whether microbes reported by mNGS are significant clinical pathogens or colonized microbes, which must be categorized based on a thorough examination of clinical characteristics, laboratory tests, and parameters. Consequently, our study further analyzed the correlation between SMRN of *Aspergillus* detected by mNGS and the results of other clinical tests in 12 diagnoses of pulmonary aspergillosis cases. No significant differences between the SMRN of *Aspergillus* in BALF or blood samples and clinical data were observed.

Finally, there are certain drawbacks associated with the use of mNGS. While it takes 24–48 h to complete all processes, a single run of mNGS costs more than traditional detection methods. The high costs and requirements of mNGS are a barrier to the widespread use (such as blood routine examination). However, mNGS is a powerful tool for the unexplained and severe pneumonia, such as pulmonary aspergillosis. In addition, the generalizability of mNGS is subject to certain limitations. For instance, the cell wall of *Aspergillus* is thick and nucleic acids are difficult to release, which causes a false-negative result. Furthermore, many *Aspergillus* genome databases are incomplete, and the public database is contaminated with human *Aspergillus* sequences. Consequently, mNGS can only be used as an auxiliary diagnostic index and not as a basis for etiological diagnosis. In addition to the study of its diagnostic value, greater efforts are needed for further dynamic testing of pulmonary aspergillosis in non-neutropenic patients using mNGS during the entire disease course. It is thus worthwhile to explore its value in predicting anti-*Aspergillus* treatment efficacy (Hagiwara et al., 2014).

All the studies reviewed thus far, however, suffer from the fact that the value of mNGS for the diagnosis of pulmonary aspergillosis in non-neutropenic patients remains poorly studied; further multicenter prospective studies with large sample sizes are needed.

Conclusions

The following conclusions were drawn from this study: mNGS is a useful and unbiased diagnostic method for pulmonary aspergillosis in non-neutropenic patients and should be adopted as soon as possible. It has high sensitivity in identifying pulmonary aspergillosis and outperforms other ways in detecting mixed infections and adjusting antimicrobial treatment. This new method has high potential to be adopted as a gold standard.

Data availability statement

The data analyzed in this study is subject to the following licenses/restrictions: All data supporting this study are reasonably available from the corresponding author. Requests

to access these datasets should be directed to Hao Tang, tanghao_0921@126.com.

Ethics statement

The studies involving human participants were reviewed and approved by Medical Ethics Committee, Shanghai Changzheng Hospital. The patients/participants provided their written informed consent to participate in this study. Written informed consent was obtained from the individual(s) for the publication of any potentially identifiable images or data included in this article.

Author contributions

SB and HT conceived the project. SB, HS, YC, and CZ collected cases. HS and YC analyzed and interpreted patient data. SB and CZ wrote the manuscript. All authors have read and approved the final manuscript. SB, HS, YC, and CZ contributed equally to this work and share first authorship.

Funding

The research was sponsored by "Shuguang Program" supported by Shanghai Education Development Foundation and Shanghai Municipal Education Commission (20SG38), Shanghai Municipal Science and Technology Committee of Shanghai Outstanding Academic Leaders Plan (20XD1423300), and General Program of National Nature Science Foundation of China (No. 82070036).

Acknowledgments

The authors would like to thank all patients for participating in this study. The authors also thank the BGI (Shanghai, China) for their helpful technical support.

Conflict of interest

The authors declare that the research was conducted in the absence of any commercial or financial relationships that could be construed as a potential conflict of interest.

Publisher's note

All claims expressed in this article are solely those of the authors and do not necessarily represent those of their affiliated organizations, or those of the publisher, the editors and the reviewers. Any product that may be evaluated in this article, or claim that may be made by its manufacturer, is not guaranteed or endorsed by the publisher.

References

Alastruey-Izquierdo, A., Cadranel, J., Flick, H., Godet, C., Hennequin, C., Hoenigl, M., et al. (2018). Treatment of chronic pulmonary aspergillosis: Current standards and future perspectives. *Respiration* 96 (2), 159–170. doi: 10.1159/000489474

Chabi, M. L., Goracci, A., Roche, N., Paugam, A., Lupo, A., and Revel, M. P. (2015). Pulmonary aspergillosis. *Diagn. Interv Imaging* 96 (5), 435–442. doi: 10.1016/j.diii.2015.01.005

Chen, Y., Ai, L., Zhou, Y., Zhao, Y., Huang, J., Tang, W., et al. (2021). Rapid and precise diagnosis of pneumonia coinfected by pneumocystis jirovecii and aspergillus fumigatus assisted by next-generation sequencing in a patient with systemic lupus erythematosus: a case report. *Ann. Clin. Microbiol. Antimicrob.* 20 (1), 47. doi: 10.1186/s12941-021-00448-5

Chen, X., Ding, S., Lei, C., Qin, J., Guo, T., Yang, D., et al. (2020). Blood and bronchoalveolar lavage fluid metagenomic next-generation sequencing in pneumonia. *Can. J. Infect. Dis. Med. Microbiol.* 2020, 1–9. doi: 10.1155/2020/6839103

Denning, D. W. (2021). Diagnosing pulmonary aspergillosis is much easier than it used to be: a new diagnostic landscape. *Int. J. Tuberc Lung Dis.* 25 (7), 525–536. doi: 10.5588/ijtld.21.0053

El-Baba, F., Gao, Y., and Soubani, A. O. (2020). Pulmonary aspergillosis: What the generalist needs to know. *Am. J. Med.* 133 (6), 668–674. doi: 10.1016/j.amjmed.2020.02.025

Hagiwara, D., Takahashi, H., Watanabe, A., Takahashi-Nakaguchi, A., Kawamoto, S., Kamei, K., et al. (2014). Whole-genome comparison of aspergillus fumigatus strains serially isolated from patients with aspergillosis. *J. Clin. Microbiol.* 52 (12), 4202–4209. doi: 10.1128/jcm.01105-14

Hasan, M. R., Rawat, A., Tang, P., Jithesh, P. V., Thomas, E., Tan, R., et al. (2016). Depletion of human DNA in spiked clinical specimens for improvement of sensitivity of pathogen detection by next-generation sequencing. *J. Clin. Microbiol.* 54 (4), 919–927. doi: 10.1128/jcm.03050-15

He, B. C., Liu, L. L., Chen, B. L., Zhang, F., and Su, X. (2019). The application of next-generation sequencing in diagnosing invasive pulmonary aspergillosis: three case reports. *Am. J. Transl. Res.* 11 (4), 2532–2539.

Jenks, J. D., Mehta, S. R., Taplitz, R., Aslam, S., Reed, S. L., and Hoenigl, M. (2019). Point-of-care diagnosis of invasive aspergillosis in non-neutropenic patients: Aspergillus galactomannan lateral flow assay versus aspergillus-specific lateral flow device test in bronchoalveolar lavage. *Mycoses* 62 (3), 230–236. doi: 10.1111/myc.12881

Jiang, J., Bai, L., Yang, W., Peng, W., An, J., Wu, Y., et al. (2021). Metagenomic next-generation sequencing for the diagnosis of pneumocystis jirovecii pneumonia in non-HIV-Infected patients: A retrospective study. *Infect. Dis. Ther.* 10 (3), 1733–1745. doi: 10.1007/s40121-021-00482-y

Jing, C., Chen, H., Liang, Y., Zhong, Y., Wang, Q., Li, L., et al. (2021). Clinical evaluation of an improved metagenomic next-generation sequencing test for the diagnosis of bloodstream infections. *Clin. Chem.* 67 (8), 1133–1143. doi: 10.1093/clinchem/hvab061

Kang, Y., Yu, Y., and Lu, L. (2020). The role of pentraxin 3 in aspergillosis: Reality and prospects. *Mycobiology* 48 (1), 1–8. doi: 10.1080/12298093.2020.1722576

Li, H. (2022). Editorial: mNGS for fungal pulmonary infection diagnostics. *Front. Cell Infect. Microbiol.* 12. doi: 10.3389/fcimb.2022.864163

Liu, L., Yuan, M., Shi, Y., and Su, X. (2021). Clinical performance of BAL metagenomic next-generation sequence and serum (1,3)-β-D-Glucan for differential diagnosis of pneumocystis jirovecii pneumonia and pneumocystis jirovecii colonisation. *Front. Cell Infect. Microbiol.* 11. doi: 10.3389/fcimb.2021.784236

Long, Y., Zhang, Y., Gong, Y., Sun, R., Su, L., Lin, X., et al. (2016). Diagnosis of sepsis with cell-free DNA by next-generation sequencing technology in ICU patients. *Arch. Med. Res.* 47 (5), 365–371. doi: 10.1016/j.arcmed.2016.08.004

Marotz, C. A., Sanders, J. G., Zuniga, C., Zaramela, L. S., Knight, R., and Zengler, K. (2018). Improving saliva shotgun metagenomics by chemical host DNA depletion. *Microbiome* 6 (1), 42. doi: 10.1186/s40168-018-0426-3

Ma, X., Zhang, S., Xing, H., Li, H., Chen, J., Li, H., et al. (2022). Invasive pulmonary aspergillosis diagnosis *via* peripheral blood metagenomic next-generation sequencing. *Front. Med.* 9. doi: 10.3389/fmed.2022.751617

Patterson, K. C., and Strek, M. E. (2014). Diagnosis and treatment of pulmonary aspergillosis syndromes. *Chest* 146 (5), 1358–1368. doi: 10.1378/chest.14-0917

Salter, S. J., Cox, M. J., Turek, E. M., Calus, S. T., Cookson, W. O., Moffatt, M. F., et al. (2014). Reagent and laboratory contamination can critically impact sequence-based microbiome analyses. *BMC Biol.* 12, 87. doi: 10.1186/s12915-014-0087-z

Sugui, J. A., Kwon-Chung, K. J., Juvvadi, P. R., Latgé, J. P., and Steinbach, W. J. (2014). Aspergillus fumigatus and related species. *Cold Spring Harb. Perspect. Med.* 5 (2), a019786. doi: 10.1101/cshperspect.a019786

Thoendel, M. J., Jeraldo, P. R., Greenwood-Quaintance, K. E., Yao, J. Z., Chia, N., Hanssen, A. D., et al. (2018). Identification of prosthetic joint infection pathogens using a shotgun metagenomics approach. *Clin. Infect. Dis.* 67 (9), 1333–1338. doi: 10.1093/cid/ciy303

Tong, T., Shen, J., and Xu, Y. (2018). Serum galactomannan for diagnosing invasive aspergillosis in pediatric patients: A meta-analysis. *Microb. Pathog.* 118, 347–356. doi: 10.1016/j.micpath.2018.03.059

Wilson, M. R., Sample, H. A., Zorn, K. C., Arevalo, S., Yu, G., Neuhaus, J., et al. (2019). Clinical metagenomic sequencing for diagnosis of meningitis and encephalitis. *N Engl. J. Med.* 380 (24), 2327–2340. doi: 10.1056/NEJMoa1803396

Xie, G., Zhao, B., Wang, X., Bao, L., Xu, Y., Ren, X., et al. (2021). Exploring the clinical utility of metagenomic next-generation sequencing in the diagnosis of pulmonary infection. *Infect. Dis. Ther.* 10 (3), 1419–1435. doi: 10.1007/s40121-021-00476-w

Yang, L., Song, J., Wang, Y., and Feng, J. (2021). Metagenomic next-generation sequencing for pulmonary fungal infection diagnosis: Lung biopsy versus bronchoalveolar lavage fluid. *Infect. Drug Resist.* 14, 4333–4359. doi: 10.2147/idr.S333818

Zhang, K., Yu, C., Li, Y., and Wang, Y. (2020). Next-generation sequencing technology for detecting pulmonary fungal infection in bronchoalveolar lavage fluid of a patient with dermatomyositis: a case report and literature review. *BMC Infect. Dis.* 20 (1), 608. doi: 10.1186/s12879-020-05341-8

Zhou, W., Li, H., Zhang, Y., Huang, M., He, Q., Li, P., et al. (2017). Diagnostic value of galactomannan antigen test in serum and bronchoalveolar lavage fluid samples from patients with nonneutropenic invasive pulmonary aspergillosis. *J. Clin. Microbiol.* 55 (7), 2153–2161. doi: 10.1128/jcm.00345-17

frontiers | Frontiers in Cellular and Infection Microbiology

TYPE Original Research
PUBLISHED 17 August 2022
DOI 10.3389/fcimb.2022.961297

OPEN ACCESS

EDITED BY
Jinmin Ma,
Beijing Genomics Institute (BGI), China

REVIEWED BY
Chunling Dong,
Second Affiliated Hospital of Jilin University, China
Lei Rong,
The University of Hong Kong, China

*CORRESPONDENCE
Jing Liu
liujing25@sysu.edu.cn

†These authors have contributed equally to this work

SPECIALTY SECTION
This article was submitted to Clinical Microbiology, a section of the journal Frontiers in Cellular and Infection Microbiology

RECEIVED 04 June 2022
ACCEPTED 29 July 2022
PUBLISHED 17 August 2022

CITATION
Lin M, Wang K, Qiu L, Liang Y, Tu C, Chen M, Wang Z, Wu J, Huang Y, Tan C, Chen Q, Zheng X and Liu J (2022) *Tropheryma whipplei* detection by metagenomic next-generation sequencing in bronchoalveolar lavage fluid: A cross-sectional study. *Front. Cell. Infect. Microbiol.* 12:961297. doi: 10.3389/fcimb.2022.961297

Tropheryma whipplei detection by metagenomic next-generation sequencing in bronchoalveolar lavage fluid: A cross-sectional study

Minmin Lin[1,2†], Kongqiu Wang[1†], Lidi Qiu[3], Yingjian Liang[1], Changli Tu[1], Meizhu Chen[1], Zhenguo Wang[1], Jian Wu[1], Yiying Huang[1], Cuiyan Tan[1], Qijiu Chen[1], Xiaobin Zheng[1] and Jing Liu[1,2*]

[1]Department of Pulmonary and Critical Care Medicine (PCCM), the Fifth Affiliated Hospital of Sun Yat-sen University, Zhuhai, China, [2]Guangdong Provincial Key Laboratory of Biomedical Imaging and Guangdong Provincial Engineering Research Center of Molecular Imaging, The Fifth Affiliated Hospital of Sun Yat-sen University, Zhuhai, China, [3]Department of Infectious Disease Intensive Care Unit, The Fifth Affiliated Hospital of Sun Yat-sen University, Zhuhai, China

Tropheryma whipplei is the bacterium associated with Whipple's disease (WD), a chronic systemic infectious disease primarily involving the gastrointestinal tract. *T. whipplei* can also be detected in different body site of healthy individuals, including saliva and feces. Traditionally, *Tropheryma whipplei* has a higher prevalence in bronchoalveolar lavage fluid (BALF) of immunocompromised individuals. Few studies have explored the significance of the detection of *T. whipplei* in BALF. Herein, we retrospectively reviewed 1725 BALF samples which detected for metagenomic next-generation sequencing (mNGS) from March 2019 to April 2022 in Zhuhai, China. Seventy BALs (70/1725, 4.0%) from 70 patients were positive for *T. whipplei.* Forty-four patients were male with an average age of 50 years. The main symptoms included cough (23/70), expectoration (13/70), weight loss (9/70), and/or dyspnea (8/70), but gastrointestinal symptoms were rare. Chronic liver diseases were the most common comorbidity (n=15, 21.4%), followed by diabetes mellitus (n=13, 18.6%). Only nine patients (12.9%) were immunocompromised. Twenty-four patients (34.3%) were finally diagnosed with reactivation tuberculosis and 15 patients (21.4%) were diagnosed with lung tumors, including 13 primary lung adenocarcinoma and two lung metastases. Fifteen patients (21.4%) had pneumonia. Among the 20 samples, *T. whipplei* was the sole agent, and Mycobacterium tuberculosis complex was the most common detected other pathogens. Among the non-tuberculosis patients, 31 (31/46, 67.4%) had ground glass nodules or solid nodules on chest CT. Our study indicates that *T. whipplei* should be considered as a potential contributing factor in some lung diseases. For non-immunocompromised patients, the detection of *T. whipplei* also needs attention. The mNGS technology improves the detection and attention of rare pathogens. In the

future, the infection, colonization, and prognosis of *T. whipplei* in lung still need to be studied.

KEYWORDS

***Tropheryma whipplei*, metagenomic next-generation sequencing, bronchoalveolar lavage fluid, Mycobacterium tuberculosis complex, pulmonary nodules**

Introduction

Tropheryma whipplei is the bacterium associated with Whipple's disease (WD), described by George H.Whipple in 1907 (GH, 1907). Whipple's disease is a rare, chronic, and systemic illness, which mainly involves the gastrointestinal tract. It can also lead to the involvement of joints, nervous system, and cardiovascular system. The most common symptoms of patients with classic Whipple's disease are arthralgia, diarrhea, weight loss, lymphadenopathy, abdominal pain, and fever (Dolmans et al., 2017). Only a few studies on the prevalence and incidence rate of Whipple's disease were performed. According to a research from the United States, the overall prevalence of Whipple's disease in the US was 9.8 cases per 1 million people (Elchert et al., 2019). Of concern, the classic Whipple's disease is typically found in Caucasian populations, but carriage is common in the native Asian and Africa populations (Keita et al., 2015).

T. whipplei is a rod-shaped, Gram-positive bacterium belonging to *Actinomycetes*. With the development of molecular biology technology, the bacterial 16S ribosomal DNA was first identified in small-bowel biopsy specimens of patients with classic Whipple's disease by nucleotide sequencing and PCR amplification in 1991 (Relman et al., 1992). Subsequently, the *T. whipplei* DNA has been detected in various samples by using PCR, including stool (Schoniger-Hekele et al., 2007), saliva, urine, blood, cerebrospinal fluid, and bronchoalveolar lavage fluid (BALF) (Fenollar et al., 2012). In some studies, *T. whipplei* has been shown to be an etiological pathogen in pneumonia (Bousbia et al., 2010). Moreover, *T. whipplei* was significantly more common in BALF in HIV-positive individuals, which was considered to be a potential contributing factor with lung complications (Lozupone et al., 2013). This further indicates that *T. whipplei* may be involved in the occurrence of some lung diseases.

With the application of metagenomic next-generation sequencing (mNGS) technology with high sensitivity in our country, the detection of *T. whipplei* has increased. However, at present, the epidemiology of *T. whipplei* in BALF in our country is still lacking. Therefore, the BALF samples which detected for mNGS in our hospital were reviewed, and the characteristics of patients with positive *T. whipplei* were analyzed.

Material and methods

Study patients and cases definition

We retrospectively reviewed 1725 BALF samples which detected for metagenomic next-generation sequencing from March 2019 to April 2022 at the Fifth Affiliated Hospital of Sun Yat-sen University in Zhuhai, China. The collection process of BALF was in line with clinical operation standard and followed the principle of sterility. The involved sub-segments were washed with 20 to 50ml normal saline. 3-5ml BALF samples were placed in sterile sputum containers, stored in -20°C, and then sent to BGI (Shenzhen, China) for detection.

The baseline data on patients with positive *Tropheryma whipplei* was collected, including demographic information, laboratory data, clinical symptoms, imaging examination results, diagnosis, pathological results, and treatment history. Immunocompromised status was defined as any of the following: (1) solid organ transplantation; (2) long-term therapy with corticosteroid (≥ 20mg prednisone or equivalent daily for ≥ 14d or a cumulative dose > 600mg of prednisone) or other immunosuppressive drugs; (3) agranulocytosis after cancer chemotherapy; (4) hematological malignancy; (5) inherited or acquired severe immunodeficiency or human immunodeficiency virus infection.

DNA extraction and mNGS sequencing

1.5mL microcentrifuge tube with 0.6mL sample and 250μL 0.5mm glass bead were attached to a horizontal platform on a vortex mixer and agitated vigorously at 2800-3200 rpm for 30 min. Then 7.2μL lysozyme was added for wall-breaking reaction. 0.3mL sample was separated into a new 1.5mL microcentrifuge tube and DNA was extracted using the TIANamp Micro DNA Kit (DP316, TIANGEN BIOTECH) according to the manufacturer's recommendation. DNA libraries were constructed through DNA-fragmentation, end-

repair, adapter-ligation and PCR amplification. Agilent 2100 was used for quality control of the DNA libraries. Quality qualified libraries were pooled, DNA Nanoball (DNB) was made and sequenced by MGISEQ-2000 platform.

Bioinformatic analysis

High-quality sequencing data were generated by removing low-quality reads, followed by computational substraction of human host sequences mapped to the human reference genome (hg19) using Burrows-Wheeler Alignment (Li and Durbin, 2009). The remaining data by removal of low-complexity reads were classified by simultaneously aligning to Pathogens metagenomics Database (PMDB), consisting of bacteria, fungi, viruses and parasites. The classification reference databases were downloaded from NCBI (ftp://ftp.ncbi.nlm.nih.gov/genomes/). RefSeq contains 4,945 whole genome sequence of viral taxa, 6,350 bacteral genomes or scaffolds, 1064 fungi related to human infection, and 234 parasites associated with human diseases. *T. whipplei* was considered positive when at least 3 reads were mapped to the species level.

Statistical analysis

Categorical variables were expressed as percentages. Continuous variables subject to normal distribution were expressed by mean and SD, otherwise, median and IQR. Comparative analysis was conducted by t test, Pearson's test, Fisher's exact test, or Mann-Whitney U test where appropriate. Data analysis was performed with SPSS 20.0 and GraphPad Prism. $P < 0.05$ was considered significant.

Results

Clinical presentation

Seventy BALs (70/1725, 4.0%) from 70 patients were positive for *T. whipplei*. Forty-four patients were male (62.9%). The age of the 70 patients ranged from 25 to 78 years (mean age: 50 years). All patients were hospitalized. Twenty-eight (40%) patients were hospitalized in infectious diseases department, 24 (34.3%) in thoracic surgery, 15 (21.4%) in respiratory department, two in an intensive-care unit and one in endocrine department at the sampling time of BALF. The distribution of sampling time was dispersed. The main clinical symptoms of patients included cough (23/70), expectoration (13/70), weight loss (9/70), and/or dyspnea (8/70) (Table 1). Only nine patients complained about gastrointestinal symptoms such as abdominal pain, diarrhea, vomiting, or poor appetite.

TABLE 1 The characteristics of patients with *T. whipplei* positive in BALF.

Parameters	*T. whipplei* positive (n=70)
Age (mean, SD)	50 (11.18)
Male	44 (62.9%)
Sampling year[a]	
2019	9 (12.9%)
2020	24 (34.3%)
2021	25 (35.7%)
2022	12 (17.1%)
BMI (mean, SD)	23.17 (3.67)
Smoking history	21 (30%)
Immunocompromised	9 (12.9%)
Clinical symptoms	
Cough	23 (32.9%)
Expectoration	13 (18.6%)
Weight loss	9 (12.9%)
Dypnea	8 (11.4%)
Fever	7 (10%)
Chest pain	4 (5.7%)
Abdominal pain	4 (5.7%)
Diarrhea	3 (4.3%)
Vomiting	3 (4.3%)
Hemoptysis	2 (2.9%)
Arthralgia	1 (1.4%)
Neurological	1 (1.4%)
Blood test result	
White blood cell count (×10^9/L) (mean, SD)	6.2 (2.05)
Lymphocyte count (×10^9/L) (mean, SD)	1.58 (0.58)
Haemoglobin (g/L) (mean, SD)	132 (21.4)
Platelet count (×10^12/L) (mean, SD)	219 (72.7)
CRP (mg/L) (median, IQR)	22.54 (1-11.12)
Erythrocyte sedimentation rate (mm/H) (median, IQR)	29.8 (5-47)

[a]The collection of sample began in March 2019, and ended in April 2022.

One patient had joint pain, and one had neurological symptoms. Nearly half of the patients (n=32) had no clinical symptoms.

Comorbidity, immune status, and inflammatory response

Chronic liver diseases were the most common comorbidity (n=15, 21.4%), including hepatitis B, cirrhosis and fatty liver, followed by diabetes mellitus (n=13, 18.6%). Non-immunocompromised patients accounted for the majority. Immunodeficiency in nine patients (12.9%) was due respectively to drug including cyclosporin (n=1) or corticosteroids (n=1), and to medical conditions including HIV infection (n=5) and solid organ transplantation (n=2)

(Figure 1). Four patients had extrapulmonary tumors. Almost all patients were tested for relevant inflammatory indicators after admission and before treatment. The overall inflammatory response was not strong. The average white blood cell count and haemoglobin of all 70 patients was 6.2×10^9/L (IQR 5.06-7.09×10^9/L) and 132 g/L (IQR 120-149 g/L) respectively. The median C-reactive protein was 3.5 mg/L (IQR 1-11.12 mg/L) (Table 1). The overall BMI index was normal (mean: 23.17, SD: 3.67), and patients with tuberculosis had a lower BMI (21.35 vs 24.13, p=0.002).

Histological presentation

Twenty-one patients underwent surgery, three underwent transbronchial lung biopsy and three underwent percutaneous lung biopsy. Therefore, a total of 27 patients had lung histopathological results. The histopathological results of 15 patients were tumors, including primary lung adenocarcinoma (n=13), metastatic intestinal adenocarcinoma (n=1) and metastatic esophageal squamous cell carcinoma (n=1). Two patients showed multinucleated giant cells in histopathology, which were considered to be tuberculosis; One patient's histopathology was positive for PAS and silver hexamine staining, which was considered as cryptococcal infection. The remaining histopathological results included nonspecific inflammatory cell infiltration (n=5), hamartoma (n=2), suspected lung cancer (n=1), and suspected multifocal micronodular alveolar epithelial hyperplasia (MMPH) (n=1).

Whipple's disease often involves the gastrointestinal tract. Therefore, we collected the gastroscopic results. In the lamina propria of the duodenal (as well as the gastric antral region, jejunum, or ileum), foam macrophages containing large amounts of diastase-resistant PAS-positive particles was the typical histological detection. Six patients underwent gastroscopy within three months, which showed various degrees of gastritis. Other gastroscopic findings included gastric antrum ulcer (n=1), duodenal erosion and superficial ulcer (n=1), gastric mucosal intraepithelial neoplasia (n=1), gastric polyp (n=1) and esophageal cancer (n=1). Pathological biopsy of duodenal lesions showed lymphocyte and plasma cell infiltration, but PAS staining was not performed.

mNGS and microbiological association

Among 20 BALF samples, *T. whipplei* was the only pathogen detected. The most common detected bacterial pathogen with *T. whipplei* was Mycobacterium tuberculosis complex, followed by *Streptococcus pneumoniae*, *Haemophilus influenzae*, *Staphylococcus aureus*, *Haemophilus parainfluenzae*, and *Actinomyces*. The most common detected fungi was *Candida albicans*, followed by *Pneumocystis jirovecii*. Human gamma-herpes virus 4 (Epstein-Barr virus, EBV) was the most detected virus (Table 2). The mapped reads number of *T. whipplei* was normalized to reads per million (RPM). The RPM value of *T. whipplei* in immunodeficiency patients outnumbered those in non-immunodeficiency patients, but it did not reach statistical difference. The RPM value of *T. whipplei* sequences was not related to whether it was the sole agent and whether the patients had symptoms (Figure 2). Immunodeficient patients had higher detection rate of fungi and virus, but only virus reached statistical difference (66.7% vs 18.0%, p=0.005) (Supplementary Figure S1). The detection rate of Mycobacterium tuberculosis

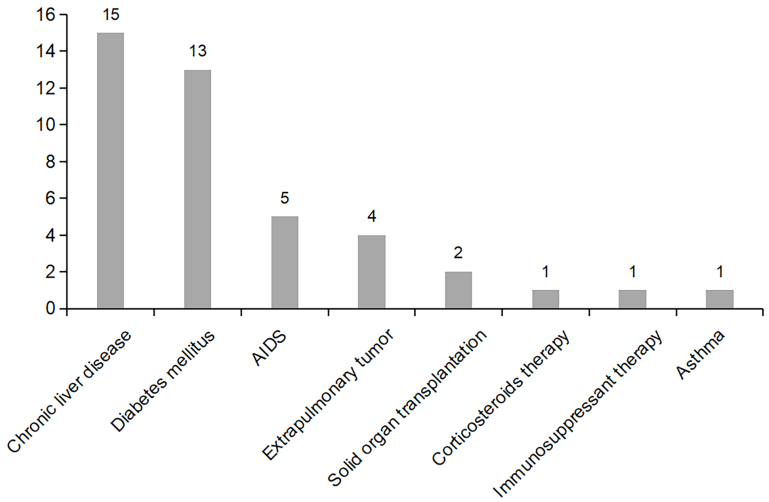

FIGURE 1
Distribution of major comorbidities in patients with positive *T. whipplei* in BALF.

10.3389/fcimb.2022.961297

TABLE 2 Pathogen detected by mNGS.

n=70	
T. whipplei as sole agent	20 (28.6%)
Mycobacterium tuberculosis complex	10 (14.3%)
Streptococcus pneumoniae	7 (10.0%)
Haemophilus influenzae	7 (10.0%)
Staphylococcus aureus	7 (10.0%)
Haemophilus parainfluenzae	5 (7.1%)
Actinomyces	5 (7.1%)
Klebsiella pneumoniae	4 (5.7%)
Moraxella catarrhalis	4 (5.7%)
Non-tuberculosis mycobacteria	3 (4.3%)
Corynebacterium striatum	1 (1.4%)
Enterococcus faecalis	1 (1.4%)
Legionella	1 (1.4%)
Klebsiella variicola	1 (1.4%)
Candida albicans	5 (7.1%)
Pneumocystis jirovecii	4 (5.7%)
Candida parapsilosis	1 (1.4%)
Aspergillus fumigatus	1 (1.4%)
Human gamma-herpes virus 4 (EBV)	9 (12.9%)
Human beta-herpes virus 5 (CMV)	2 (2.9%)

complex in patients with diabetes was significantly higher (38.5% vs 8.8%, p=0.015).

Chest CT findings

According to the classification of diseases, we simply described the chest CT findings. Among the tuberculosis (TB) patients, the most chest CT findings were common reactivation TB changes, including focal or patchy heterogeneous consolidation, poorly defined nodules or linear opacities, cavity (n=6), tuberculoma (n=1), and pleural effusion (n=1). One patient's chest CT showed miliary tuberculosis. Among the non-TB patients, 31 (31/46, 67.4%) had ground glass nodules or solid nodules on chest CT. The remaining CT findings included patchy, mass, pleural effusion (n=6), cystic (n=2), cavity (n=2), and interstitial fibrosis (n=2). Classification of chest CT in non-tuberculosis patients, especially considering the *T. whipplei* as the main pathogen, it could be roughly divided into nodular type, pneumonia type and mixed type, as shown in Figure 3. In general, the chest imaging manifestations were various.

Diagnosis, treatment, and prognosis

Twenty-four patients (34.3%) were finally diagnosed with reactivation tuberculosis and received anti-tuberculosis treatment. Sixteen of them improved after treatment. Fifteen patients (21.4%) were diagnosed with pneumonia, and all received antimicrobial treatment, such as β-lactams/β-lactamase inhibitor, Trimethoprim-sulfamethoxazole, doxycycline or quinolones. Six patients improved radiographically after treatment. More immunocompromised patients were diagnosed with pneumonia (p=0.001). According to histopathology, fifteen patients (21.4%) were diagnosed with lung tumors, including 13 primary lung adenocarcinoma and two lung metastases. Fourteen of them received surgery and one received chemotherapy. The remaining diagnoses include unexplained pulmonary nodules (n=4), benign pulmonary nodules (n=3), pleurisy (n=3), cryptococcal infection (n=1), and suspected lung cancer (n=1) (Figure 4). None of the patients died in hospital.

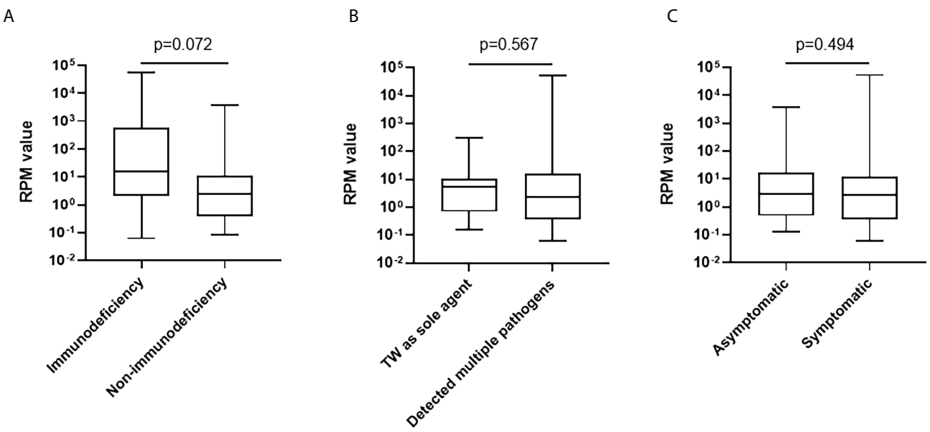

FIGURE 2
Comparisons of the RPM value of *T. whipplei* according to immune deficiency status **(A)**, mixed detection **(B)**, and clinical symptoms **(C)**.

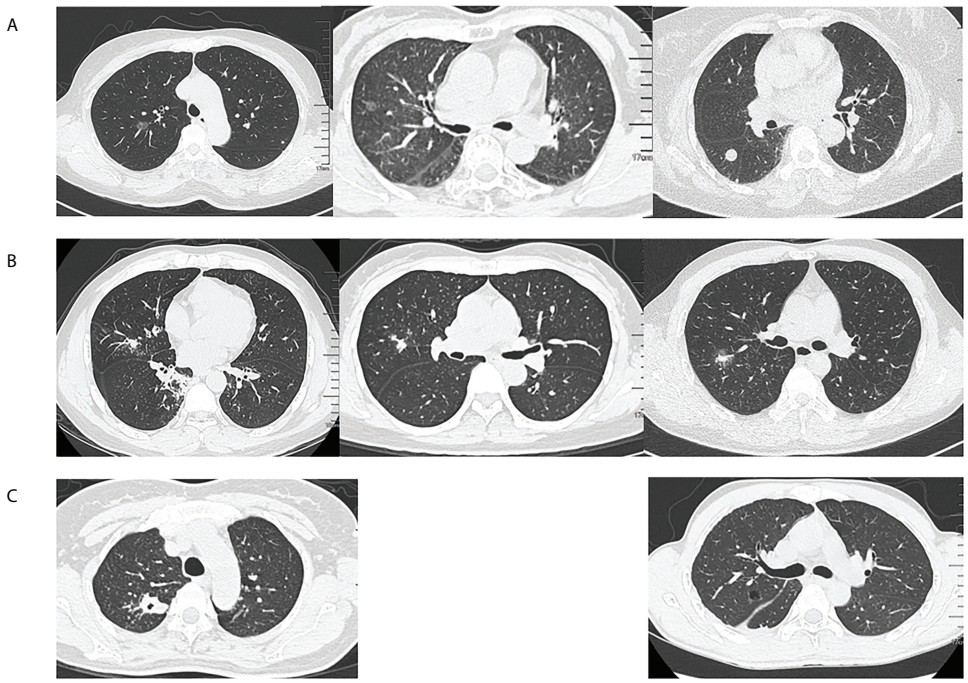

FIGURE 3
Classification of chest computed tomography (CT) in non-tuberculosis patients. **(A)** Nodular type: ground glass nodules or solid nodules, **(B)** Pneumonia type: focal or patchy mixed density shadow, and **(C)** Mixed type: other manifestations such as cavity, cystic or pleural effusion.

Discussion

Although WD was described as early as 1907, *T. whipplei* was only successfully cultured in macrophages until 1997 (Schoedon et al., 1997). Due to the lack of specificity of the clinical manifestations, and the lack of understanding of WD, the disease was often misdiagnosed or undiagnosed in our country. With the development of molecular methods and application of mNGS technology, the number of positive cases detected in BALF increased. Meanwhile, there was an increasing number of cases reported about pulmonary infection caused by *T. whipplei* or pulmonary involvement of WD in recent years. However, the significance of *T. whipplei* detection in BALF still needs to be comprehensively considered. Our study found that

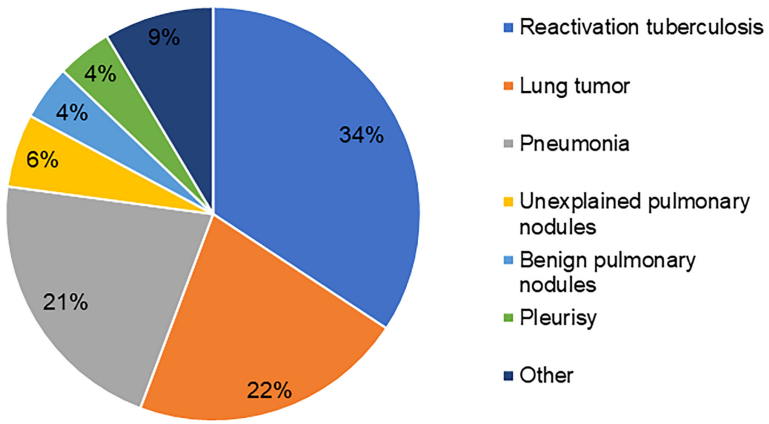

FIGURE 4
Diagnostic distribution of *T. whipplei* positive patients in BALF.

the majority of *T. whipplei* positive patients in BALF were non-immunodeficient, with a large proportion of patients diagnosed with tuberculosis, lung tumors, and pneumonia. Pulmonary nodules were the main manifestation of chest CT. To our knowledge, our study has the largest sample size in the epidemiological study of *T. whipplei* detected in BALF in China.

In this study, mNGS was used to detect *T. whipplei*. In the process of sequencing and bioinformatics analysis, the technology has strictly set up positive and negative controls and carried out quality control. The distribution of departments during the patients sampling was relatively scattered, and the collection time was evenly distributed. Therefore, the possibility of nosocomial infection or outbreak could be ruled out, and the contamination in the collection process or laboratory process could also be basically ruled out. Accordingly, we consider the detected results to be credible.

The prevalence of *T. whipplei* in our study was slightly lower than that reported by Lagier et al. (6.1%, 88/1438) (Lagier et al., 2016), which was close to the 3% (6/210) reported by Boubia et al., (2010). Respiratory symptoms, weight loss and fever were the main clinical manifestations of patients, while gastrointestinal symptoms were rare, which was similar with the previous case reports of pneumonia caused by *T. whipplei* (Urbanski et al., 2012; Guo et al., 2021). However, nearly half of the patients in our study were asymptomatic, and the overall inflammatory response was not strong. This suggests that some patients may be carriers of *T. whipplei* in the lungs. Our results indicated that non-immunodeficient status was predominant in *T. whipplei* positive patients in BALF, which was inconsistent with the previous view that *T. whipplei* was more prevalent among HIV-positive individuals (Lozupone et al., 2013; Garcia-Alvarez et al., 2016). The case-control study of Lagier et al. found that the prevalence of *T. whipplei* may not be related to immune status (Lagier et al., 2016). In addition, our results suggest that patients with diabetes and chronic liver disease may be susceptible to *T. whipplei* in the lungs, which has not been concerned in previous studies. The significance and causes of *T. whipplei* detection in non-immunocompromised patients still need to be further explored.

Our study also confirm that *T. whipplei* is an etiologic pathogen in acute respiratory infections (Lagier et al., 2017). *T. whipplei* could be co-infected with *Pneumocystis jirovecii* and *Candida albicans*, as reported in previous cases (Li et al., 2021; Yan et al., 2021), or leaded to pulmonary infection alone (Guo et al., 2021). Moreover, we also found that immunocompromised patients were more likely to be diagnosed with pneumonia, suggesting that *T. whipplei* should be considered more as a pathogen when detected in BALF in immunocompromised patients with clinical symptoms. Mycobacterium tuberculosis complex and *T. whipplei* co-infection or detection were occasionally reported in other studies (Lagier et al., 2016; Zhu et al., 2021). However, our study found that Mycobacterium tuberculosis complex was the most common pathogenic bacteria detected together, and a considerable number of patients (34.3%) were diagnosed as reactivation pulmonary tuberculosis. The reason may be that the incidence of tuberculosis in China is still high. At the same time, our hospital was a designated hospital for tuberculosis treatment, which leaded to the increase of detection rate. On the other hand, both Mycobacterium tuberculosis complex and *T. whipplei* belong to *Actinobacteria*. Mycobacterium tuberculosis complex is facultative intracellular bacterium, and *T. whipplei* is obligate intracellular bacterium. The infection of both bacteria have been associated with macrophages. In the pathogenesis of classic WD, macrophages in duodenal mucosa can be induced by bacteria to polarize into M2/alternatively activated macrophages (Desnues B, Lepidi et al., 2005). The impaired antigen-presenting function of macrophages and dendritic cells further weakened the response of T cells (Moos et al., 2010). In addition, the increased activity of regulatory T cells in the gut and blood further increases the immunosuppressive environment (Schinnerling et al., 2011). However, due to the lack of research on the pathogenesis of *T. whipplei* in lung infection, we can only speculate that the co-infection or detection of Mycobacterium tuberculosis complex and *T. whipplei* may be related to the impairment of pulmonary macrophage function. The interaction and causality between *T. whipplei* and other pathogens in the lung need to be further studied.

We performed a general classification of chest CT findings in non-pulmonary tuberculosis patients, especially those considering *T. whipplei* as the dominant pathogen. Therefore, our results are representative and convincing. The overall chest CT findings were diverse, with pulmonary nodules as the main manifestation, which had also been mentioned in several previous case reports (Urbanski et al., 2012; Zhang and Xu, 2021). Nevertheless, according to the histopathological results, a considerable number of pulmonary nodules were identified as tumors, most of which were early-stage lung adenocarcinoma. In the long-term follow-up survey of WD patients with a small sample size (35 patients) by Schiepatti et al., 22% (7 patients) had preneoplastic/neoplastic disorders (Schiepatti et al., 2020). At present, the risk factors for the occurrence of pulmonary nodules are not clear. We speculate that there may be a relationship between lung lesions and *T. whipplei*. Whether the presence of *T. whipplei* in the lung microbiome may promote the occurrence of pulmonary nodules or even early-stage lung cancer directly or indirectly by changing the immune microenvironment still needs to be further confirmed by prospective studies with a larger sample size.

In this study, duodenal mucosal biopsy was performed in a small number of patients, and PAS staining was not performed in suspected patients, so WD was not clearly diagnosed. As WD is a multisystem disease, untreated WD is fatal (Marth and Raoult, 2003). Therefore, we believe that duodenal mucosal biopsy, PAS staining, and immunohistochemistry can be considered for patients suspected of *T. whipplei* infection to

further improve the diagnosis. PCR in sterile body fluids, such as blood, cerebrospinal fluid, and joint fluid, can help diagnose WD, but most of them are invasive procedures, which still need to be evaluated according to the condition. This study also had limitations. It was a single-center retrospective descriptive study without longitudinal follow-up, and partial information was not comprehensive. No control group was established, so correlation and causality could not be determined. But we believe our study is informative.

Conclusion

In summary, this study objectively analyzed the clinical characteristics of patients with positive *T. whipplei* detected by mNGS in BALF. Our study adds to the evidence that *T. whipplei* in BALF may be related to some lung diseases. *T. whipplei* should be considered as a potential risk factor for pneumonia when detected in immunocompromised patients. For non-immunocompromised patients, the detection of *T. whipplei* also needs attention because of the relationship between *T. whipplei* and pulmonary nodules. mNGS has improved the detection and attention of rare pathogens. Moreover, the infection, colonization, and prognosis of *T. whipplei* in the lung need further study.

Data availability statement

The raw data supporting the conclusions of this article will be made available by the authors, without undue reservation.

Ethics statement

The studies involving human participants were reviewed and approved by the Ethics Committee of the Fifth Affiliated Hospital of Sun Yat-Sen University (approve number [2022] K82-1). Written informed consent for participation was not required for this study in accordance with the national legislation and the institutional requirements.

Author contributions

ML participated in data collection, analysis, and manuscript drafting. KW participated in drafting the work, acquisition, and analysis. LQ and YL participated in data sorting and input. CTu, MC, ZW, JW, YH, and CTa participated in sample collection. QC and XZ participated in the conception and design of the work. JL conceived of the study, and participated in its design, and helped to draft the manuscript. All authors contributed to the article and approved the submitted version.

Funding

JL was grant from Guangdong Basic and Applied Basic Research Foundation (2020A1515011147). ML was supported by Open project of Key Laboratory of Tropical Disease Control (Sun Yat-sen University), Ministry of Education (2020kfkt04).

Acknowledgement

We are grateful to BGI for their assistance in detection methodology.

Conflict of interest

The authors declare that the research was conducted in the absence of any commercial or financial relationships that could be construed as a potential conflict of interest.

Publisher's note

All claims expressed in this article are solely those of the authors and do not necessarily represent those of their affiliated organizations, or those of the publisher, the editors and the reviewers. Any product that may be evaluated in this article, or claim that may be made by its manufacturer, is not guaranteed or endorsed by the publisher.

Supplementary material

The Supplementary Material for this article can be found online at: https://www.frontiersin.org/articles/10.3389/fcimb.2022.961297/full#supplementary-material

References

Bousbia, S., Papazian, L., Auffray, J. P., Fenollar, F., Martin, C., Li, W., et al. (2010). Tropheryma whipplei in patients with pneumonia. *Emerg. Infect. Dis.* 16 (2), 258–263. doi: 10.3201/eid1602.090610

Desnues B, Lepidi, H., Raoult, D., and Mege, J. L. (2005). Whipple Disease: intestinal infiltrating cells exhibit a transcriptional pattern of M2/alternatively activated macrophages. *J. Infect. Dis.* 192 (9), 1642–1646. doi: 10.1086/491745

Dolmans, R. A., Boel, C. H., Lacle, M. M., and Kusters, J. G. (2017). Clinical manifestations, treatment, and diagnosis of tropheryma whipplei infections. *Clin. Microbiol. Rev.* 30 (2), 529–555. doi: 10.1128/CMR.00033-16

Elchert, J. A., Mansoor, E., Abou-Saleh, M., and Cooper, G. S. (2019). Epidemiology of whipple's disease in the USA between 2012 and 2017: A population-based national study. *Dig Dis. Sci.* 64 (5), 1305–1311. doi: 10.1007/s10620-018-5393-9

Fenollar, F., Ponge, T., La Scola, B., Lagier, J. C., Lefebvre, M., and Raoult, D. (2012). First isolation of tropheryma whipplei from bronchoalveolar fluid and clinical implications. *J. Infect.* 65 (3), 275–278. doi: 10.1016/j.jinf.2011.11.026

Garcia-Alvarez, L., Perez-Matute, P., Blanco, J. R., Ibarra, V., and Oteo, J. A. (2016). High prevalence of asymptomatic carriers of tropheryma whipplei in different populations from the north of Spain. *Enferm Infecc Microbiol. Clin.* 34 (6), 340–345. doi: 10.1016/j.eimc.2015.09.006

GH, W. (1907). A hitherto undescribed disease characterized anatomically by deposits of fat and fatty acids in the intestinal and mesenteric lymphatic tissues. *Bull. Johns Hopkins Hosp* 18, 382–393.

Guo, Y., Li, L., Li, Z., Sun, L., and Wang, H. (2021). Tropheryma whipplei detection by nanopore sequencing in patients with interstitial lung disease. *Front. Microbiol.* 12. doi: 10.3389/fmicb.2021.760696

Keita, A. K., Dubot-Peres A, Phommasone, K., Sibounheuang, B., Vongsouvath, M., Mayxay, M., et al. (2015). High prevalence of tropheryma whipplei in lao kindergarten children. *PLoS Negl. Trop. Dis.* 9 (2), e0003538. doi: 10.1371/journal.pntd.0003538

Lagier, J.-C., Fenollar, F., and Raoult, D. (2017). Acute infections caused by tropheryma whipplei. *Future Microbiol.* 2017 (12), 247–254. doi: 10.2217/fmb-2017-0178

Lagier, J. C., Papazian, L., Fenollar, F., Edouard, S., Melenotte, C., Laroumagne, S., et al. (2016). Tropheryma whipplei DNA in bronchoalveolar lavage samples: A case control study. *Clin. Microbiol. Infect.* 22 (10), 875–879. doi: 10.1016/j.cmi.2016.07.010

Li, H., and Durbin, R. (2009). Fast and accurate short read alignment with burrows-wheeler transform. *Bioinf. (Oxford England)* 25 (14), 1754–1760. doi: 10.1093/bioinformatics/btp324

Li, W., Zhang, Q., Xu, Y., Zhang, X., Huang, Q., and Su, Z. (2021). Severe pneumonia in adults caused by tropheryma whipplei and candida sp. infection: A 2019 case series. *BMC Pulm Med.* 21 (1), 29. doi: 10.1186/s12890-020-01384-4

Lozupone, C., Cota-Gomez, A., Palmer, B. E., Linderman, D. J., Charlson, E. S., Sodergren, E., et al. (2013). Widespread colonization of the lung by tropheryma whipplei in HIV infection. *Am. J. Respir. Crit. Care Med.* 187 (10), 1110–1117. doi: 10.1164/rccm.201211-2145OC

Marth, T., and Raoult, D. (2003). Whipple's disease. *Lancet (London England)* 361 (9353), 239–246. doi: 10.1016/s0140-6736(03)12274-x

Moos, V., Schmidt, C., Geelhaar, A., Kunkel, D., Allers K, Schinnerling, K., et al. (2010). Impaired immune functions of monocytes and macrophages in whipple's disease. *Gastroenterology* 138 (1), 210–220. doi: 10.1053/j.gastro.2009.07.066

Relman, D. A., Schmidt, T. M., MacDermott, R. P., and Falkow, S. (1992). Identification of the uncultured bacillus of whipple's disease. *New Engl. J. Med.* 327 (5), 293–301. doi: 10.1056/nejm199207303270501

Schiepatti, A., Nicolardi, M. L., Marone, P., and Biagi, F. (2020). Long-term morbidity and mortality in whipple's disease a single-center experience over 20 years. *Future Microbiol.* 15), 847–854. doi: 10.2217/fmb-2019-0315

Schinnerling, K., Moos, V., Geelhaar, A., Allers K, Loddenkemper, C., Friebel, J., et al. (2011). Regulatory T cells in patients with whipple's disease. *J. Immunol.* 187 (8), 4061–4067. doi: 10.4049/jimmunol.1101349

Schoedon, G., Goldenberger, D., Forrer, R., Gunz, A., Dutly, F., Höchli, M., et al. (1997). Deactivation of macrophages with interleukin-4 is the key to the isolation of tropheryma whippelii. *J. Infect. Diseases* 176 (3), 672–677. doi: 10.1086/514089

Schoniger-Hekele, M., Petermann, D., Weber, B., and Muller, C. (2007). Tropheryma whipplei in the environment: survey of sewage plant influxes and sewage plant workers. *Appl. Environ. Microbiol.* 73 (6), 2033–2035. doi: 10.1128/AEM.02335-06

Urbanski, G., Rivereau, P., Artru, L., Fenollar, F., Raoult, D., and Puechal, X. (2012). Whipple Disease revealed by lung involvement: A case report and literature review. *Chest* 141 (6), 1595–1598. doi: 10.1378/chest.11-1812

Yan, J., Zhang, B., Zhang, Z., Shi, J., Liu, S., Qi, J., et al. (2021). Case report: Tropheryma whipplei hide in an AIDS patient with pneumocystis pneumonia. *Front. Public Health* 9. doi: 10.3389/fpubh.2021.663093

Zhang, W. M., and Xu, L. (2021). Pulmonary parenchymal involvement caused by tropheryma whipplei. *Open Med. (Wars)* 16 (1), 843–846. doi: 10.1515/med-2021-0297

Zhu, B., Tang, J., Fang, R., Fei, X., Wang, Q., Wang, W., et al. (2021). Pulmonary coinfection of mycobacterium tuberculosis and tropheryma whipplei: a case report. *J. Med. Case Rep.* 15 (1), 359. doi: 10.1186/s13256-021-02899-y

frontiers | Frontiers in Cellular and Infection Microbiology

TYPE Original Research
PUBLISHED 31 August 2022
DOI 10.3389/fcimb.2022.963611

OPEN ACCESS

EDITED BY
Jinmin Ma,
Beijing Genomics Institute (BGI), China

REVIEWED BY
Sathyavathi Sundararaju,
Sidra Medicine, Qatar
Ying Liang,
Peking University Third Hospital, China

*CORRESPONDENCE
Yuanyuan Li
leeround@csu.edu.cn
Yisha Li
liyisha@csu.edu.cn

SPECIALTY SECTION
This article was submitted to Clinical Microbiology, a section of the journal Frontiers in Cellular and Infection Microbiology

RECEIVED 07 June 2022
ACCEPTED 10 August 2022
PUBLISHED 31 August 2022

CITATION
Jiang J, Yang W, Wu Y, Peng W, Zhang W, Pan P, Hu C, Li Y and Li Y (2022) Metagenomic next-generation sequencing for identifying pathogens in patients with rheumatic diseases and diffuse pulmonary lesions: A retrospective diagnostic study. *Front. Cell. Infect. Microbiol.* 12:963611. doi: 10.3389/fcimb.2022.963611

Metagenomic next-generation sequencing for identifying pathogens in patients with rheumatic diseases and diffuse pulmonary lesions: A retrospective diagnostic study

Juan Jiang[1,2,3,4,5], Wei Yang[1,2,3,4,5], Yanhao Wu[1,2,3,4,5], Wenzhong Peng[1,2,3,4,5], Wenjuan Zhang[1,2,3,4,5], Pinhua Pan[1,2,3,4,5], Chengping Hu[1,2,3,4,5], Yisha Li[5,6]* and Yuanyuan Li[1,2,3,4,5]*

[1]Department of Respiratory Medicine, National Key Clinical Specialty, Branch of National Clinical Research Center for Respiratory Disease, Xiangya Hospital, Central South University, Changsha, China, [2]Center of Respiratory Medicine, Xiangya Hospital, Central South University, Changsha, China, [3]Clinical Research Center for Respiratory Diseases in Hunan Province, Changsha, China, [4]Hunan Engineering Research Center for Intelligent Diagnosis and Treatment of Respiratory Disease, Changsha, China, [5]National Clinical Research Center for Geriatric Disorders, Xiangya Hospital, Changsha, China, [6]Department of Rheumatology and Immunology, Xiangya Hospital, Central South University, Changsha, China

Objective: Lung involvement is a major cause of morbidity and mortality in patients with rheumatic diseases. This study aimed to assess the application value of metagenomic next-generation sequencing (mNGS) for identifying pathogens in patients with rheumatic diseases and diffuse pulmonary lesions.

Methods: This retrospective study included patients who were diagnosed with rheumatic diseases and presenting diffuse pulmonary lesions on chest radiography in Xiangya Hospital from July 2018 to May 2022. Clinical characteristics were summarized, including demographics, symptoms, comorbidities, radiological and laboratory findings, and clinical outcomes. Pulmonary infection features of these patients were analyzed. Furthermore, diagnostic performance of mNGS and conventional methods (including smear microscopy, culture, polymerase chain reaction assay, and serum immunological test) in identifying pulmonary infections and causative pathogens were compared.

Results: A total of 98 patients were included, with a median age of 58.0 years old and a female proportion of 59.2%. Of these patients, 71.4% showed the evidence of pulmonary infections. Combining the results of mNGS and conventional methods, 129 infection events were detected, including 45 bacterial, 40 fungal and 44 viral infection events. Pulmonary mixed infections were observed in 38.8% of patients. The detection rates of mNGS for any pathogen (71.4% vs 40.8%, $P < 0.001$) and mixed pathogens (40.8% vs 12.2%, $P < 0.001$) were higher than that of conventional methods. Moreover, mNGS had a

significantly higher sensitivity (97.1% vs. 57.1%, $P < 0.001$) than conventional methods in identifying pulmonary infections, while its specificity (92.9% vs. 96.4%, $P = 0.553$) were comparable to conventional methods. Antimicrobial and antirheumatic treatments were markedly modified based on mNGS results in patients with rheumatic diseases and diffuse pulmonary lesions.

Conclusions: For patients diagnosed with rheumatic diseases and presenting diffuse pulmonary lesions, mNGS is a powerful complement to conventional methods in pathogen identification due to its high efficiency and broad spectrum. Early application of mNGS can provide guidance for precision treatment, and may reduce mortality and avoid antibiotic abuse.

KEYWORDS

metagenomic next-generation sequencing (mNGS), rheumatic diseases, diffuse pulmonary lesions, pulmonary infection, immunosuppressed population

Introduction

Rheumatic diseases are a group of autoimmune and inflammatory diseases that are characterized by the presence of inflammation and destruction of joints, tissues and internal organs (Apel et al., 2018; Hardy et al., 2020). Lung is a common target organ of autoimmune mediated injury in patients with rheumatic diseases. Depending on the underlying rheumatic diseases, lung involvement associated with rheumatic diseases shows a considerable heterogeneity in incidence, severity, and the components of the involved lung structure (Ha et al., 2018). For patients with rheumatic disease, lung involvement is recognized as a major cause of morbidity and mortality (Luppi et al., 2022). Besides, internal immune dysregulation and secondary immunosuppression caused by antirheumatic therapy make these patients vulnerable to pulmonary infections, including opportunistic infections, which can also present diffuse pulmonary lesions on chest radiography (Di Franco et al., 2017; Wan et al., 2022). Due to the broad range of diagnostic and therapeutic aspects with an increased risk of mortality, rheumatic diseases complicated by diffuse pulmonary lesions are an important and challenging field in the clinical routine of both pulmonologists and rheumatologists.

Early and proper treatments are vital to improve the prognosis of such patients. However, it remains very difficult to distinguish pulmonary infections from non-infectious lung diseases secondary to rheumatic diseases and further identify the causative pathogens. While culture of blood and lower respiratory tract specimen is routinely conducted, its sensitivity is fairly low. Polymerase chain reaction (PCR) assay for specific microbes is widely used for its high sensitivity and specificity. But only one microbe can be detected by one test, thus its application value is limited in mixed infections, which are frequently seen in immunosuppressed patients. More importantly, these conventional methods are far from perfect to detect rare atypical or novel pathogens.

In recent years, mNGS has become increasingly popular in clinical diagnosis of infectious diseases. mNGS is a microbiologic diagnostic tool that detects all nucleic acids of microorganisms whose sequencing data are included in the database library, thus allowing for an unbiased approach to identify pathogens (Simner et al., 2018). Fast reporting, high accuracy, and the ability to detect multiple pathogens by one test make mNGS a promising microbial detection technology (Wilson et al., 2019), especially in complex miscellaneous infectious diseases among immunosuppressed patients (Peng et al., 2021; Nie et al., 2022). Its diagnostic performance has been highlighted in a variety of infectious diseases, such as pneumonia (Xie et al., 2019), blood stream infections (Jing et al., 2021), and central nervous system infections (Ramachandran and Wilson, 2020). However, whether mNGS is advantageous in patients with rheumatic diseases and suspected pneumonia remains unclear. Therefore, we conducted a retrospective study to assess the application value of mNGS in patients with underlying rheumatic diseases and presenting diffuse pulmonary lesions.

Methods

Study design and subjects

This retrospective diagnostic study was conducted in Xiangya Hospital, a large-scale tertiary care hospital with more than 3,500 beds. Adults diagnosed with rheumatic diseases and

admitted with diffuse pulmonary lesions to the respiratory intensive care unit from July 1, 2018 to May 31, 2022 were consecutively included. Patients were eligible for enrollment if they met all the following criteria: (1) confirmed diagnosis of any kind of rheumatic diseases (Zeng et al., 2008); (2) diffuse pulmonary lesions that newly emerged on chest computed tomography (CT); (3) mNGS test of bronchoalveolar fluid (BALF) was performed. Patients were excluded if they met any of the following criteria: (1) age < 18 years; (2) patients who did not undergo mNGS test; (3) pregnant women; (4) patients with incomplete medical records. Finally, a total of 98 patients were enrolled in this study. The clinical composite diagnosis of pulmonary lesions and causative pathogens for pulmonary infections were determined by two senior experts (LYY and LYS) after discussion with the healthcare team, based on clinical symptoms, laboratory findings, chest radiology, microbiologic tests (including conventional methods and mNGS) and treatment response. This study was approved by the Institutional Review Board and Ethics Committee of Central South University and conducted according to the Declaration of Helsinki. All research data were de-identified and anonymously analyzed.

Sample processing and DNA extraction for mNGS

BALF samples were processed as described in a previous study of our group (Jiang et al., 2021). Briefly, BALF was mixed with lysozyme and 1 g of 0.5-mm glass beads, and then the mixture was attached to a horizontal platform on a vortex mixer and agitated vigorously at 2800–3200 rpm for 30 min. For nucleic acid extraction, 300 μL of supernatant was transferred to a 1.5-mL centrifuge tube. Subsequently, DNA was extracted using the TIANamp Micro DNA kit (Tiangen Biotech) according to standard procedures.

DNA library preparation and sequencing for mNGS

The DNA library was constructed by DNA fragmentation, end repair and PCR amplification using MGIEasy Cell-free DNA Library Prep Set (MGI Tech). Agilent 2100 (Agilent Technologies) and Qubit 2.0 (Invitrogen) were used as library quality control. The double-stranded DNA library was converted into single-stranded circular DNA using DNA degradation and circularization. The DNA Nanoballs were generated by rolling circle amplification technology. Qualified DNA Nanoballs were loaded on the chip and then performed 20 M 50-bp single-end sequencing on the MGISEQ-2000 sequencing platform (BGI Genomics) (Jeon et al., 2014).

Bioinformatic analysis for mNGS

After removing low-quality, short reads (length < 35 base pairs), the human host sequence mapped to the human reference genome using Burrows-Wheeler alignment and low complexity reads (Li and Durbin, 2010; Schmieder and Edwards, 2011), the rest of high-quality data were simultaneously aligned to four large microbial databases, including bacteria (6350 species), fungi (1064 species), viruses (1798 species) and parasites (234 species). The coverage ratio and depth of each microorganism were calculated using BEDTools (Quinlan and Hall, 2010).

Clinically significant microbes detected by mNGS were defined as previously described (Peng et al., 2021). For bacteria (excluding mycobacteria), fungi (excluding molds), viruses, parasites and other atypical pathogens, a microbe detected by mNGS was considered clinically significant when its relative abundance at the species level was more than 30%, and its pulmonary pathogenicity has been recorded in literature. Molds with literature-proven pulmonary pathogenicity were considered as clinically significant when the stringently mapped read number (SMRN) at the species level was more than 10. Oral commensals were not considered as clinically significant microbes regardless of their abundance. Finally, clinically significant microbes were determined as putative pathogens if patients showed suggestive symptoms, laboratory findings and/or radiologic features.

Clinical data collection

Demographics, symptoms, underlying rheumatic diseases, usage of corticosteroids and immunosuppressants, radiological abnormalities, APACHE II score, laboratory findings, antimicrobial and antirheumatic treatments (Arnold et al., 2021), and clinical outcomes of each patient were obtained through reviewing medical records. Demographics included the age, gender, and smoking history. Laboratory parameters included peripheral white blood cells, neutrophils, lymphocytes, serum procalcitonin, C-reactive protein, serum (1,3)-β-D-glucan, serum galactomannan at admission to the respiratory intensive care unit. A serum (1,3)-β-D-glucan level higher than 95 pg/mL and serum galactomannan S/CO (signal to cut-off ratio) higher than 0.8 were considered as positive according to the manufacturer's instruction. Clinical outcomes included the use of invasive mechanical ventilation and treatment failure. Treatment failure was defined as the presence of any condition: (1) all-cause death during hospitalization; (2) persistent or worsening symptoms, signs and/or pulmonary lesions on chest imaging at the end of hospitalization. Conventional methods for identifying pathogens included smear microscopy of lower respiratory tract specimen, bacterial and fungal culture of lower respiratory tract specimen and blood, polymerase chain

reaction assay of *Epstein-Barr virus* and *Cytomegalovirus*, serum IgM antibody tests for *Mycoplasma pneumoniae*, *Chlamydia pneumoniae*, *Adenovirus*, *Influenza virus*, *Parainfluenza virus*, *Respiratory syncytial virus*, *Coxsackieviruses*, and *Legionella pneumophila*. Mixed infection in lung was defined as two or more kinds of pathogens confirmed in one patient.

Statistical analysis

Statistical analyses were performed using SPSS 25.0 software (IBM Corp., Armonk, NY, USA). Continuous variables are presented as medians and interquartile ranges, and categorical variables are presented as counts and percentages. Proportions of different infection events were compared using the chi-square or Fisher's exact tests. The paired chi-square test was used for comparing the pathogen detection rates of mNGS and conventional methods. Kappa test was used for assessing the consistency of mNGS and conventional methods in pathogen identification. Sensitivity, specificity, positive predictive value and negative predictive value were calculated using the clinical composite diagnosis as the reference standard; the chi-square test was used to compare these proportions between mNGS and conventional methods. Significance was fixed at $P < 0.05$.

Results

Clinical characteristics of patients

A total of 98 patients diagnosed with rheumatic diseases and diffuse pulmonary lesions were included, and their clinical characteristics were shown in Table 1. The median age was 58.0 years. Among these patients, 59.2% were females, and 27.6% were either current or former smokers. The most common clinical manifestations included dyspnea (100%), fever (90.8%), cough (87.8%) and expectoration (71.4%). The top five underlying rheumatic diseases included rheumatoid arthritis (22.4%), polymyositis/dermatomyositis (21.4%), vasculitis (19.4%), systemic lupus erythematosus (14.3%), and Sjögren's syndrome (10.2%). There were 58 patients using corticosteroids and 22 patients using immunosuppressants before this admission.

On chest CT images, ground-glass opacity (73.5%), interstitial pattern (63.3%), and pleural effusion (53.1%) were frequently seen in these patients. The median oxygen index was 128.0 (94.0-171.0), and the median APACHE II score was 12 (9-15) points. As for laboratory findings, these patients showed significantly lower peripheral lymphocyte counting (median, 0.6×10^9/L) and C-reactive protein (median, 87.0 mg/L), while serum procalcitonin level were slightly elevated. Positive rates of serum (1,3)-β-D-glucan and serum galactomannan were 36.1% and 11.4%, respectively. Appropriately half (49.0%) of patients required invasive mechanical ventilation, and 23.5% ended up having treatment failure.

Pulmonary infection features of patients

Of the 98 patients, 71.4% showed the evidence of pulmonary infections, including 42 patients with bacterial infections, 32 with fungal infections and 27 with viral infections (Figure 1A). Overall, the proportion of bacterial infections was significantly higher than that of fungal or viral infections (Figure 1A). Proportions of mixed infections were 38.8%, 22.4%, 24.5%, and 23.5% for total, bacterial, fungal and viral infections, respectively (Figure 1B). In patients infected with fungi or viruses, mixed infection was much more common than single infection (Figure 1B). Combining the results of mNGS and conventional methods, 129 infection events were detected, including 45 bacterial infections, 40 fungal infections, and 44 viral infections (Figure 2).

The whole pathogen spectrum in patients with rheumatic diseases and diffuse pulmonary lesions was presented in Figure 3. *Pseudomonas aeruginosae* was the most commonly detected bacterium (8/98, 8.2%), followed by *Klebsiella pneumonia* (7/98, 7.1%), *Acinetobacter baumannii* (6/98, 6.1%), *Burkholderia cepacia* (6/98, 6.1%), and other bacteria. The most common fungus was *Pneumocystis jirovecii* (17/98, 17.3%), followed by *Aspergillus* (11/98, 11.2%), *Candida albicans* (6/98, 6.1%), and other fungi. *Epstein-Barr virus* (23/98, 23.5%) and *Cytomegalovirus* (18/98, 18.4%) were the most frequently detected viruses. Most of infection events were identified by either mNGS alone or simultaneous mNGS and conventional methods, and only 4 infection events were detected by conventional methods alone.

Performance of mNGS and conventional methods for identifying pathogens

Results of pathogen number detected by mNGS or conventional methods were shown in Table 2. The detection rates of mNGS for identifying any pathogen (71.4% vs 40.8%) and mixed pathogens (40.8% vs 12.2%) were both significantly higher than that of conventional methods, with statistically significant differences ($P < 0.001$). Kappa coefficient (0.344) suggested a mild consistency between mNGS and conventional methods. Diagnostic performance of mNGS and conventional methods in identifying pulmonary infections were further compared. As shown in Table 3, mNGS had a significantly higher sensitivity (97.1% vs. 57.1%, $P < 0.001$) and negative predictive value (92.9% vs. 47.4%, $P < 0.001$) than conventional methods, while its specificity (92.9% vs. 96.4%, $P = 0.553$) and positive predictive value (97.1% vs. 97.6%, $P = 0.896$) were comparable to conventional methods.

TABLE 1 Clinical characteristics of enrolled patients.

Characteristics	Patients (n = 98)
Age (years), median (IQR)	58.0 (49.5-67.0)
Female, n (%)	58 (59.2)
Current or former smoker, n (%)	27 (27.6)
Clinical manifestations	
Fever, n (%)	89 (90.8)
Cough, n (%)	86 (87.8)
Expectoration, n (%)	70 (71.4)
Dyspnea, n (%)	98 (100)
Rheumatic diseases	
Rheumatoid arthritis, n (%)	22 (22.4)
Polymyositis/dermatomyositis, n (%)	21 (21.4)
Vasculitis, n (%)	19 (19.4)
Systemic lupus erythematosus, n (%)	14 (14.3)
Sjögren's syndrome, n (%)	10 (10.2)
Antisynthetase syndrome, n (%)	6 (6.1)
Systemic sclerosis, n (%)	3 (3.1)
IgG4-related disease, n (%)	1 (1.0)
Adult-onset Still's disease, n (%)	1 (1.0)
Overlap syndrome, n (%)	1 (1.0)
Systemic use of corticosteroids before admission, n (%)	58 (59.2)
Use of immunosuppressants before admission, n (%)	22 (22.4)
Radiological features on chest CT	
Ground-glass opacity, n (%)	72 (73.5)
Interstitial pattern, n (%)	62 (63.3)
Consolidation, n (%)	10 (10.2)
Nodules, n (%)	17 (17.3)
Pleural effusion, n (%)	52 (53.1)
Oxygen index, median (IQR)	128.0 (94.0-171.0)
APACHE II score, median (IQR)	12 (9-15)
Peripheral white blood cells ($\times 10^9$/L), median (IQR)	9.0 (5.5-11.4)
Peripheral neutrophils ($\times 10^9$/L), median (IQR)	7.5 (4.4-10.0)
Peripheral lymphocytes ($\times 10^9$/L), median (IQR)	0.6 (0.4-1.1)
Procalcitonin (ng/mL), median (IQR)	0.36 (0.11-1.62)
C-reactive protein (mg/L), median (IQR)	87.0 (25.0-182.0)
Serum BDG +, n (%)	26/72 (36.1)
Serum galactomannan +, n (%)	8/70 (11.4)
Invasive mechanical ventilation, n (%)	48 (49.0)
Treatment failure, n (%)	23 (23.5)

IQR, interquartile range; CT, computed tomography; APACHE II score, Acute Physiology and Chronic Health Evaluation II score; BDG, (1,3)-β-D-glucan.

Impact of mNGS results on clinical treatments

Modifications on clinical treatments based on mNGS results were summarized in Table 4. After the report of mNGS results, 10.2% of patients started systemic use of corticosteroids, 29.6% had increased dosage of corticosteroids, and 8.2% had reduced dosage of corticosteroids. Use of immunosuppressants, therapeutic plasma exchange, and Tocilizumab were initiated in 16.3%, 24.5% and 2.0% of patients, respectively. Antimicrobial treatments were also markedly affected by mNGS results. Among all patients, 62.2% had changed antimicrobial spectrum, 28.6% had narrowed antimicrobial spectrum, and 20.4% had antimicrobial de-escalation. Besides, 28.6% of patients had removed and 13.3% had added at least one antimicrobial agent based on mNGS results.

Discussion

In this study, we summarized the pulmonary infection features and assessed the diagnostic value of mNGS in patients with rheumatic diseases and diffuse pulmonary lesions. The probability of bacterial, fungal or viral infections is high, and mixed infections are common in these patients. mNGS shows a good ability for detecting pathogens and is advantageous to identifying mixed infections in lung.

Lung involvement in patients with rheumatic disease is common and associated with significant morbidity and mortality (Doyle and Dellaripa, 2017). Meanwhile, the estimated rates of infectious complications can be as high as 26–50% among patients with polymyositis/dermatomyositis or systemic lupus erythematosus (Hsu et al., 2019), and lung is the most frequent infection site (Mok et al., 2011). To distinguish between pulmonary infections and non-infectious diseases is the crucial but challenging step for clinical physicians, even with the efforts of multidisciplinary collaboration. On one hand, conventional microbiological methods have a low yield for pathogen detection. On the other hand, pulmonary lesions mixing infectious with non-infectious diseases are often observed in these patients. Therefore, how to improve the identification of pulmonary infections and causative pathogens is of a great clinical significance for the management of these patients. By combining conventional methods and mNGS, we found that pulmonary infections were confirmed in more than 70% of patients. Mixed infections in lung were observed in 38.8% of patients with rheumatic diseases, in line with a previous study (Chen et al., 2021). Besides, our data showed that mixed infections were more common in patients with fungal or viral infections. These results highlight the importance of fast and comprehensive pathogen identification in patients with rheumatic diseases.

Based on high-throughput sequencing methods, mNGS enables identification of a comprehensive spectrum of potential microbes by a single test, and becomes a powerful approach for the diagnosis of infectious disease. While the usefulness of mNGS in immunocompromised patients with suspected pneumonia has been confirmed by previous studies (Jiang et al., 2021; Peng et al., 2021; Sun et al., 2021), its application value in patients specifically with rheumatic diseases has remained unexplored. We found that the sensitivity of mNGS were markedly higher than that of conventional methods, and the specificity of mNGS was comparable to that of conventional methods. Particularly, mNGS had an advantage in identifying mixed infections over

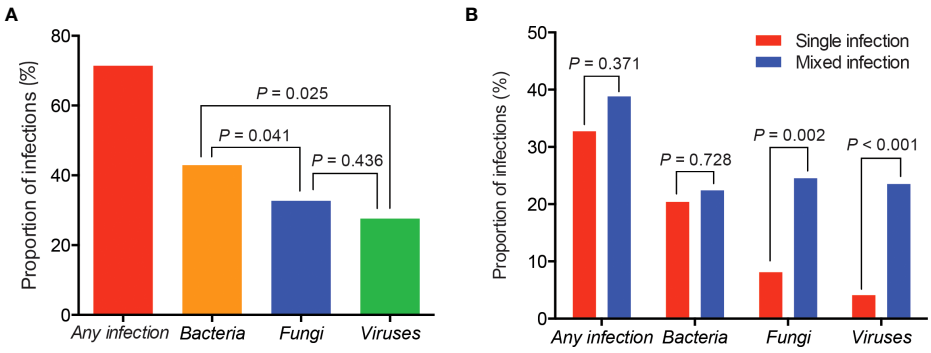

FIGURE 1
Proportions of different types of infections in patients with rheumatic diseases and diffuse pulmonary lesions. **(A)** Proportions of total, bacterial, fungal and viral infection events; **(B)** Proportions of single and mixed infection events.

conventional methods, as demonstrated by a higher detection rate (40.8% vs 12.2%) of co-pathogens. Furthermore, mNGS has a unique utility in detecting unculturable and difficult-to-culture microorganisms, such as *Pneumocystis jirovecii* and *Nocardia* (Saubolle and Sussland, 2003; Liu et al., 2018). While PCR test is commonly used for diagnosis of *Pneumocystis jirovecii* pneumonia, simultaneous PCR test of *Pneumocystis jirovecii* was not performed in these patients, due to its inaccessibility in our hospital. Besides, there were a small number of pathogens detected by conventional methods but not by mNGS, including two infection events of *Aspergillus*, one of *Klebsiella pneumonia*, and one of *Epstein-Barr virus*. Although mNGS is well recognized to have a high sensitivity in detecting various pathogens (Parize et al., 2017; Chen et al., 2020), false negative results of mNGS are not rare. Moreover, diagnostic sensitivity of mNGS in fungal infections such as *Aspergillus* is relatively lower (Peng et al., 2021). Difficulty in disrupt the thick polysaccharide cell wall of *Aspergillus* can be an important reason (Zinter et al., 2019). Therefore, the application value of mNGS should be highlighted as a necessary component of the comprehensive pathogen identification system for the diagnosis of pneumonia in patients with rheumatic diseases.

It is worth noting that mNGS results provide important guidance for clinical treatments of patients in this study. As therapeutic strategies for lung diseases secondary to rheumatic diseases are partially contradictory to pulmonary infections, physicians may be overcautious when making treatment plans for patients with rheumatic diseases and diffuse pulmonary lesions. For example, use of immunosuppressive agents can increase the risk of infections and reduce the efficacy of antimicrobial treatment, leading to a clinical dilemma. Without effective interventions, pulmonary lesions usually progress within a short period of time, and consequently cause a high risk of mortality (Atzeni et al., 2018). In this study, both antimicrobial and antirheumatic treatments are greatly modified based on mNGS results. Initial antimicrobial treatments were modified in 83.7% of patients after the report of mNGS results, which could enhance the precision antimicrobial therapeutics

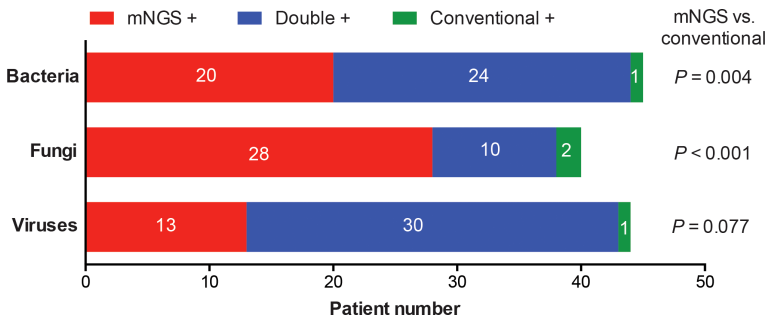

FIGURE 2
Categorization of infection events detected by mNGS and conventional methods alone or simultaneously. Detection rates of bacteria, fungi or viruses were compared between mNGS and conventional methods.

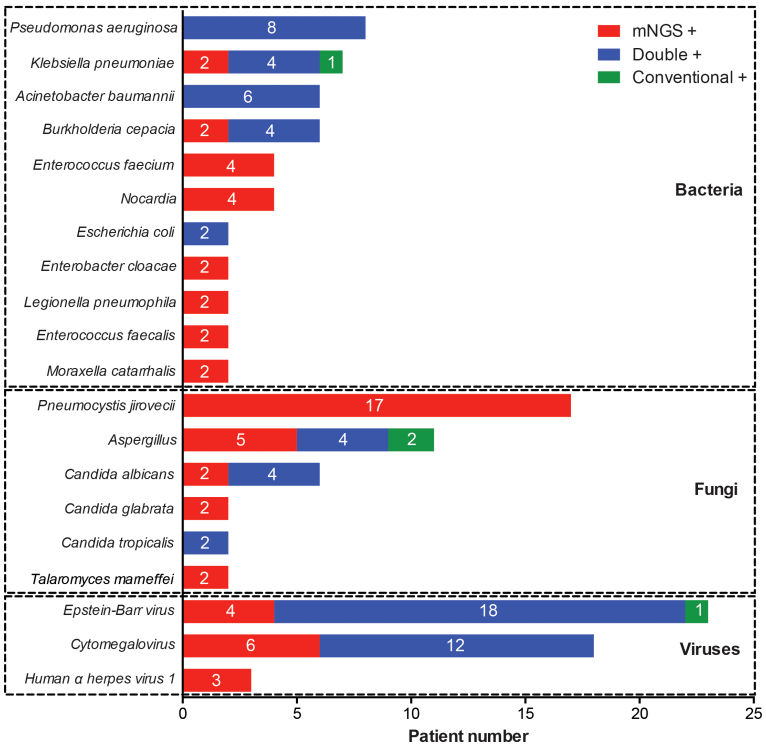

FIGURE 3
Distribution of pathogenic microorganisms detected by mNGS and conventional methods alone or simultaneously.

TABLE 2 Comparison of pathogen species detected by mNGS and conventional methods.

Number of pathogens	mNGS	Conventional methods	*P* value	Kappa coefficient
0	28	58	< 0.001	0.344
1	30	28	0.754	
≥ 2	40	12	< 0.001	

mNGS, metagenomic next-generation sequencing.

TABLE 3 Diagnostic performance of mNGS and conventional methods.

Performance	mNGS	Conventional methods	*P* value
Sensitivity	97.1%	57.1%	<0.001
Specificity	92.9%	96.4%	0.553
Positive predictive value	97.1%	97.6%	0.896
Negative predictive value	92.9%	47.4%	<0.001

mNGS, metagenomic next-generation sequencing.

and reduce antibiotic side effects. Moreover, corticosteroids, immunosuppressants and therapeutic plasma exchange were not started until the report of mNGS results in a considerable number of patients, indicating that except for detecting possible pathogens, mNGS tests may be helpful in excluding infections in patients with rheumatic diseases. These modifications on clinical treatments may be beneficial to patient prognosis, as suggested by a relatively low rate of treatment failure (23.5%) in this study.

TABLE 4 Impact of mNGS results on clinical treatments.

Modifications on clinical treatments	Patient number (%)
Systemic use of corticosteroids	
Any	47 (48.0)
Initiation of corticosteroids	10 (10.2)
Increasing dosage	29 (29.6)
Reducing dosage	8 (8.2)
Initiation of immunosuppressants	
Initiation of Tocilizumab	16 (16.3)
	2 (2.0)
Initiation of TPE	24 (24.5)
Antimicrobial treatments	
Any	82 (83.7)
Changing antimicrobial spectrum	61 (62.2)
Narrowing antimicrobial spectrum	28 (28.6)
Antimicrobial de-escalation	20 (20.4)
Removing ≥ 1 antimicrobial agent	28 (28.6)
Adding ≥ 1 antimicrobial agent	13 (13.1)

mNGS, metagemonic next-generation sequencing; TPE, therapeutic plasma exchange.

However, prospective studies are required to confirm the potential clinical benefits of mNGS in these patients.

Prompt and appropriate clinical management is directly associated with patient prognosis. Thus, it is crucial to early recognize possible pulmonary infections in patients with rheumatic diseases. This study revealed the infection features in patients with rheumatic diseases and diffuse pulmonary lesions. More importantly, application value of mNGS for identifying pathogens in these patients was highlighted. Therefore, this study has significant clinical implications and provides useful information for physicians. Based on our data and clinical experience, we proposed a guiding strategy flow-chart for clinical management of patients with rheumatic diseases and presenting diffuse pulmonary lesions (Figure 4). First of all, we recommend fast and comprehensive microbiological tests including conventional methods and mNGS side-by-side within 24 hours after patient admission. Next, multidisciplinary team discussion should be held to decide the therapeutic strategies of patients. Individual therapeutic strategies must be adopted, avoiding delays in effective treatment and antibiotic abuse.

There are several limitations in the present study. First, this is a single-center retrospective study, thus the intrinsic bias was unavoidable. Second, there is no standard method and widely accepted threshold values for interpreting mNGS results so far, which may affect the objectiveness of mNGS interpretation, especially when distinguishing colonization, infection and contamination. Furthermore, although our data support the diagnostic value of mNGS in patients with rheumatic diseases and diffuse pulmonary lesions, whether its use could improve patient prognosis requires further investigation in large-scale prospective studies.

Conclusions

In summary, pulmonary infections, including mixed infections, are very common among patients with rheumatic

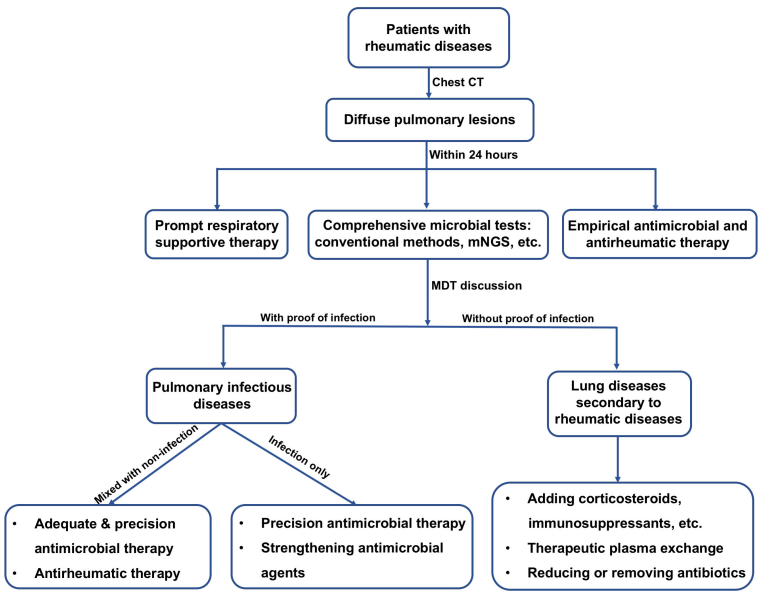

FIGURE 4
Flow-chart for suggested clinical management of patients diagnosed with rheumatic diseases and presenting diffuse pulmonary lesions. CT, computed tomography; mNGS, metagenomic next-generation sequencing; MDT, multidisciplinary team.

diseases and diffuse pulmonary lesions. The application of mNGS should be highlighted as a powerful complement to conventional methods in clinical management of patients with rheumatic diseases and presenting diffuse pulmonary lesions, due to its high efficiency and broad spectrum of pathogen identification.

Data availability statement

The original contributions presented in the study are included in the article/supplementary material, further inquiries can be directed to the corresponding authors.

Ethics statement

The studies involving human participants were reviewed and approved by The Institutional Review Board and Ethics Committee of Central South University. Written informed consent for participation was not required for this study in accordance with the national legislation and the institutional requirements.

Author contributions

Study concept and design: YYL and YSL. Acquisition of data: JJ, WY, YW, WP, WZ, PP and CH. Statistical analysis: JJ. Analysis and interpretation of data: YYL, YSL and JJ. Drafting of the manuscript: JJ. Critical revision of the manuscript: YYL and YSL. All authors contributed to the article and approved the submitted version.

Funding

This work is supported by grants from the National Natural Science Foundation of China (82170041 and 82100099), and the Innovative Research Platform of Hunan Development and Reform Commission (2021-212).

Acknowledgments

We appreciate the professionalism and compassion demonstrated by all the healthcare workers involved in patient care. We also acknowledge all the patients for their involvement in this study.

Conflict of interest

The authors declare that the research was conducted in the absence of any commercial or financial relationships that could be construed as a potential conflict of interest.

Publisher's note

References

Apel, F., Zychlinsky, A., and Kenny, E. F. (2018). The role of neutrophil extracellular traps in rheumatic diseases. *Nat. Rev. Rheumatol.* 14 (8), 467–475. doi: 10.1038/s41584-018-0039-z

Arnold, J., Winthrop, K., and Emery, P. (2021). COVID-19 vaccination and antirheumatic therapy. *Rheumatology* 60 (8), 3496–3502. doi: 10.1093/rheumatology/keab223

Atzeni, F., Gerardi, M. C., Barilaro, G., Masala, I. F., Benucci, M., and Sarzi-Puttini, P. (2018). Interstitial lung disease in systemic autoimmune rheumatic diseases: a comprehensive review. *Expert Rev. Clin. Immunol.* 14 (1), 69–82. doi: 10.1080/1744666X.2018.1411190

Chen, X., Cao, K., Wei, Y., Qian, Y., Liang, J., Dong, D., et al. (2020). Metagenomic next-generation sequencing in the diagnosis of severe pneumonias caused by chlamydia psittaci. *Infection* 48 (4), 535–542. doi: 10.1007/s15010-020-01429-0

Chen, Y., Feng, W., Ye, K., Guo, L., Xia, H., Guan, Y., et al. (2021). Application of metagenomic next-generation sequencing in the diagnosis of pulmonary infectious pathogens from bronchoalveolar lavage samples. *Front. Cell. infection Microbiol.* 11, 168. doi: 10.3389/fcimb.2021.541092

Di Franco, M., Lucchino, B., Spaziante, M., Iannuccelli, C., Valesini, G., and Iaiani, G. (2017). Lung infections in systemic rheumatic disease: focus on opportunistic infections. *Int. J. Mol. Sci.* 18 (2), 293. doi: 10.3390/ijms18020293

Doyle, T. J., and Dellaripa, P. F. (2017). Lung manifestations in the rheumatic diseases. *Chest* 152 (6), 1283–1295. doi: 10.1016/j.chest.2017.05.015

Ha, Y.-J., Lee, Y. J., and Kang, E. H. (2018). Lung involvements in rheumatic diseases: Update on the epidemiology, pathogenesis, clinical features, and treatment. *BioMed. Res. Int.* 2018, 6930297–6930297. doi: 10.1155/2018/6930297

Hardy, R. S., Raza, K., and Cooper, M. S. (2020). Therapeutic glucocorticoids: mechanisms of actions in rheumatic diseases. *Nat. Rev. Rheumatol.* 16 (3), 133–144. doi: 10.1038/s41584-020-0371-y

Hsu, C. Y., Ko, C. H., Wang, J. L., Hsu, T. C., and Lin, C. Y. (2019). Comparing the burdens of opportunistic infections among patients with systemic rheumatic diseases: a nationally representative cohort study. *Arthritis Res. Ther.* 21 (1), 211. doi: 10.1186/s13075-019-1997-5

Jeon, Y. J., Zhou, Y., Li, Y., Guo, Q., Chen, J., Quan, S., et al. (2014). The feasibility study of non-invasive fetal trisomy 18 and 21 detection with semiconductor sequencing platform. *PLoS One* 9 (10), e110240. doi: 10.1371/journal.pone.0110240

Jiang, J., Bai, L., Yang, W., Peng, W., An, J., Wu, Y., et al. (2021). Metagenomic next-generation sequencing for the diagnosis of pneumocystis jirovecii pneumonia in non-HIV-Infected patients: A retrospective study. *Infect. Dis. Ther.* 10 (3), 1733–1745. doi: 10.1007/s40121-021-00482-y

Jing, C., Chen, H., Liang, Y., Zhong, Y., Wang, Q., Li, L., et al. (2021). Clinical evaluation of an improved metagenomic next-generation sequencing test for the diagnosis of bloodstream infections. *Clin. Chem.* 67 (8), 1133–1143. doi: 10.1093/clinchem/hvab061

Li, H., and Durbin, R. (2010). Fast and accurate long-read alignment with burrows-wheeler transform. *Bioinformatics* 26 (5), 589–595. doi: 10.1093/bioinformatics/btp698

Liu, Y., Fahle, G. A., and Kovacs, J. A. (2018). Inability to culture pneumocystis jirovecii. *mBio* 9 (3), e00939–18. doi: 10.1128/mBio.00939-18

Luppi, F., Sebastiani, M., Salvarani, C., Bendstrup, E., and Manfredi, A. (2022). Acute exacerbation of interstitial lung disease associated with rheumatic disease. *Nat. Rev. Rheumatol.* 18 (2), 85–96. doi: 10.1038/s41584-021-00721-z

Mok, C., Kwok, C., Ho, L., Chan, P., and Yip, S. (2011). Life expectancy, standardized mortality ratios, and causes of death in six rheumatic diseases in Hong Kong, China. *Arthritis Rheumatism* 63 (5), 1182–1189. doi: 10.1002/art.30277

Nie, J., Yang, L., Huang, L., Gao, L., Young, K. H., Le Grange, J. M., et al. (2022). Infection complications in febrile chimeric antigen receptor (CAR)-T recipients during the peri-CAR-T cell treatment period examined using metagenomic next-generation sequencing (mNGS). *Cancer Commun.* 42 (5), 476. doi: 10.1002/cac2.12260

Parize, P., Muth, E., Richaud, C., Gratigny, M., Pilmis, B., Lamamy, A., et al. (2017). Untargeted next-generation sequencing-based first-line diagnosis of infection in immunocompromised adults: a multicentre, blinded, prospective study. *Clin. Microbiol. Infect.* 23 (8), 574.e571–574.e576. doi: 10.1016/j.cmi.2017.02.006

Peng, J. M., Du, B., Qin, H. Y., Wang, Q., and Shi, Y. (2021). Metagenomic next-generation sequencing for the diagnosis of suspected pneumonia in immunocompromised patients. *J. Infect.* 82 (4), 22–27. doi: 10.1016/j.jinf.2021.01.029

Quinlan, A. R., and Hall, I. M. (2010). BEDTools: a flexible suite of utilities for comparing genomic features. *Bioinformatics* 26 (6), 841–842. doi: 10.1093/bioinformatics/btq033

Ramachandran, P. S., and Wilson, M. R. (2020). Metagenomics for neurological infections - expanding our imagination. *Nat. Rev. Neurol.* 16 (10), 547–556. doi: 10.1038/s41582-020-0374-y

Saubolle, M. A., and Sussland, D. (2003). Nocardiosis: review of clinical and laboratory experience. *J. Clin. Microbiol.* 41 (10), 4497–4501. doi: 10.1128/jcm.41.10.4497-4501.2003

Schmieder, R., and Edwards, R. (2011). Quality control and preprocessing of metagenomic datasets. *Bioinformatics* 27 (6), 863–864. doi: 10.1093/bioinformatics/btr026

Simner, P. J., Miller, S., and Carroll, K. C. (2018). Understanding the promises and hurdles of metagenomic next-generation sequencing as a diagnostic tool for infectious diseases. *Clin. Infect. Dis.* 66 (5), 778–788. doi: 10.1093/cid/cix881

Sun, T., Wu, X., Cai, Y., Zhai, T., Huang, L., Zhang, Y., et al. (2021). Metagenomic next-generation sequencing for pathogenic diagnosis and antibiotic management of severe community-acquired pneumonia in immunocompromised adults. *Front. Cell. Infection Microbiol.* 11, 475. doi: 10.3389/fcimb.2021.661589

Wan, R., Bai, L., Yan, Y., Li, J., Luo, Q., Huang, H., et al. (2022). A clinically applicable nomogram for predicting the risk of invasive mechanical ventilation in pneumocystis jirovecii pneumonia. *Front. Cell. Infection Microbiol.* 12. doi: 10.3389/fcimb.2022.850741

Wilson, M. R., Sample, H. A., Zorn, K. C., Arevalo, S., Yu, G., Neuhaus, J., et al. (2019). Clinical metagenomic sequencing for diagnosis of meningitis and encephalitis. *New Engl. J. Med.* 380 (24), 2327–2340. doi: 10.1056/NEJMoa1803396

Xie, Y., Du, J., Jin, W., Teng, X., Cheng, R., Huang, P., et al. (2019). Next generation sequencing for diagnosis of severe pneumonia: China 2010-2018. *J. Infect.* 78 (2), 158–169. doi: 10.1016/j.jinf.2018.09.004

Zeng, Q. Y., Chen, R., Darmawan, J., Xiao, Z. Y., Chen, S. B., Wigley, R., et al. (2008). Rheumatic diseases in China. *Arthritis Res. Ther.* 10 (1), 1–11. doi: 10.1186/ar2368

Zinter, M. S., Dvorak, C. C., Mayday, M. Y., Iwanaga, K., Ly, N. P., McGarry, M. E., et al. (2019). Pulmonary metagenomic sequencing suggests missed infections in immunocompromised children. *Clin. Infect. Dis.* 68 (11), 1847–1855. doi: 10.1093/cid/ciy802

frontiers | Frontiers in Cellular and Infection Microbiology

TYPE Original Research
PUBLISHED 08 September 2022
DOI 10.3389/fcimb.2022.987692

OPEN ACCESS

EDITED BY
Gilberto Sabino-Santos,
Tulane University School of Public Health and Tropical Medicine, United States

REVIEWED BY
Giorgia Bucciol,
KU Leuven, Belgium
Wang Ke,
Guangxi Medical University, China

*CORRESPONDENCE
Jia Hou
doctorhoujia@hotmail.com
Xiaochuan Wang
xchwang@shmu.edu.cn

†These authors have contributed equally to this work

SPECIALTY SECTION
This article was submitted to Clinical Microbiology, a section of the journal Frontiers in Cellular and Infection Microbiology

RECEIVED 06 July 2022
ACCEPTED 17 August 2022
PUBLISHED 08 September 2022

CITATION
Liu L, Sun B, Ying W, Liu D, Wang Y, Sun J, Wang W, Yang M, Hui X, Zhou Q, Hou J and Wang X (2022) Rapid Diagnosis of *Talaromyces marneffei* Infection by Metagenomic Next-Generation Sequencing Technology in a Chinese Cohort of Inborn Errors of Immunity. *Front. Cell. Infect. Microbiol.* 12:987692. doi: 10.3389/fcimb.2022.987692

Rapid diagnosis of *Talaromyces marneffei* infection by metagenomic next-generation sequencing technology in a Chinese cohort of inborn errors of immunity

Lipin Liu†, Bijun Sun†, Wenjing Ying, Danru Liu, Ying Wang, Jinqiao Sun, Wenjie Wang, Mi Yang, Xiaoying Hui, Qinhua Zhou, Jia Hou* and Xiaochuan Wang*

Department of Clinical Immunology, Children's Hospital of Fudan University, National Children's Medical Center, Shanghai, China

Talaromyces marneffei (*T. marneffei*) is an opportunistic pathogen. Patients with inborn errors of immunity (IEI) have been increasingly diagnosed with *T. marneffei* in recent years. The disseminated infection of *T. marneffei* can be life-threatening without timely and effective antifungal therapy. Rapid and accurate pathogenic microbiological diagnosis is particularly critical for these patients. A total of 505 patients with IEI were admitted to our hospital between January 2019 and June 2022, among whom *T. marneffei* was detected in 6 patients by metagenomic next-generation sequencing (mNGS), and their clinical and immunological characteristics were summarized. We performed a systematic literature review on *T. marneffei* infections with published immunodeficiency-related gene mutations. All patients in our cohort were confirmed to have genetic mutations in *IL12RB1*, *IFNGR1*, *STAT1*, *STAT3*, and *CD40LG*. *T. marneffei* was detected in both the blood and lymph nodes of P1 with *IL12RB1* mutations, and the clinical manifestations were serious and included recurrent fever, weight loss, severe anemia, splenomegaly and lymphadenopathy, all requiring long-term antifungal therapy. These six patients received antifungal treatment, which relieved symptoms and improved imaging findings. Five patients survived, while one patient died of sepsis after hematopoietic stem cell transplantation. The application of mNGS methods for pathogen detection in IEI patients and comparison with traditional diagnosis methods were investigated. Traditional diagnostic methods and mNGS tests were performed simultaneously in 232 patients with IEI. Compared to the traditional methods, the sensitivity and specificity of mNGS in diagnosing *T. marneffei* infection were 100% and 98.7%, respectively. The reporting time for *T. marneffei* detection was approximately 26 hours by mNGS, 3-14 days by culture, and 6-11 days by histopathology. *T. marneffei* infection was first reported in IEI patients with *IL12RB1* gene mutation, which expanded the IEI lineage susceptible to *T. marneffei*. For IEI patients with *T.*

marneffei infection, we highlight the application of mNGS in pathogenic detection. mNGS is recommended as a front-line diagnostic test for rapidly identifying pathogens in complex and severe infections.

KEYWORDS

***Talaromyces marneffei*, metagenomic next-generation sequencing, inborn errors of immunity, *IL12RB1* mutation, T-cell-mediated immunity, intrinsic and innate immunodeficiencies**

1 Introduction

Talaromyces marneffi (*T. marneffei*), previously known as *Penicillium marneffei*, is an emerging pathogenic fungus causing fatal systemic mycosis in Southeast Asia, especially Thailand, northeastern India, Vietnam, southern China, Hong Kong and Taiwan (DiSalvo et al., 1973; Deng et al., 1988; Hu et al., 2013). The common manifestations of disseminated *T. marneffei* infection include recurrent fever, anemia, weight loss, skin lesions, hepatosplenomegaly, lymphadenopathy, and gastrointestinal and respiratory signs. When *T. marneffei* infection disseminates systemically, it can run a rapidly progressive course and be life-threatening without timely and effective antifungal therapy (You et al., 2021).

The vast majority of *T. marneffei* cases are diagnosed in HIV-positive patients (Supparatpinyo et al., 1994; Kawila et al., 2013), while cases have also been described in other immunocompromised individuals, such as patients with adult-onset acquired immunodeficiency due to autoantibodies against interferon-gamma (IFN-γ) (Guo et al., 2020), various inborn errors of immunity (IEI) (Tangye et al., 2020), hematological malignancies, diabetes mellitus and those taking corticosteroids or immunosuppressive agents (Qiu et al., 2015). In recent years, *T. marneffei* infection in children with IEI has been increasingly diagnosed. Genetic mutations involving *STAT1, STAT3, CD40LG, CARD9* and *IFNGR1* have been reported to be associated with *T. marneffei* infection (Ma et al., 2009; Lee et al., 2012; Du et al., 2019; Lee et al., 2019; Ba et al., 2021; You et al., 2021). However, as more cases are reported, other potential gene mutations may be discovered that predispose the host to *T. marneffei* infection.

Early identification and rapid diagnosis of *T. marneffei* infection are critical to a good prognosis. Traditional diagnostic methods of *T. marneffei* infection rely on culture or microscopy, which are time-consuming and have a lower positive rate. In recent years, the development of metagenomic next-generation sequencing (mNGS) has greatly improved the detection of pathogenic microorganisms (Chiu and Miller, 2019; Li et al., 2020; Qian et al., 2020; Chen et al., 2021; Su et al., 2022). mNGS can simultaneously accomplish the detection of bacteria, fungi, viruses, parasites and other pathogens with high efficiency and high sensitivity (Goldberg et al., 2015; Schlaberg et al., 2017). Currently, mNGS has matured into clinical applications in the diagnosis of complex and severe infections (Wang et al., 2020).

In this study, we reported the clinical and immunological characteristics of six patients with *T. marneffei* infection in a cohort of Chinese patients with IEI and emphasized the application value of mNGS in the diagnosis of *T. marneffei* infection. We aimed to improve the early recognition of *T. marneffei* infection in IEI patients. The immunodeficiency spectrum of *T. marneffei* infection was further broadened.

2 Methods

This study was approved by the Ethics Committee of the Children's Hospital of Fudan University. Written informed consent was obtained from the parents of all patients.

2.1 Study design and patients

Patients with IEI admitted to the Children's Hospital of Fudan University between January 2019 and June 2022 were enrolled consecutively, and patients with *T. marneffei* infection were retrospectively summarized.

Children with IEI were defined as patients previously assigned a diagnosis of IEI or patients admitted for abnormal clinical manifestations, including severe/unusual infections, and then diagnosed with IEI. The clinical manifestations, immune function, genetic testing, and pathogenic microorganisms were evaluated. Routine tests of peripheral blood, urine, stool and blood culture were performed in all patients. The cultures of sputum or bronchoscopic alveolar lavage fluid (BALF) were detected in patients with pulmonary infection. Further mNGS testing was performed in patients considered to have severe or unusual pathogen infection.

Definition of terms: The age at the last follow-up was defined as the age at July 2022 or the age at death. The diagnosis of bacterial infections was based on positive culture results. The (1–3) -β-d-glucan (G) tests were defined as positive when

>100 pg/ml (Lu et al., 2011; Li et al., 2015). The galactomannan (GM) index was defined as positive when > 0.5. The GM test is highly sensitive to Aspergillus infection (Guo et al., 2010). The diagnostic criteria for Bacillus Calmette Guerin (BCG) disease were described in a previous publication (Zhou et al., 2018). Epstein-Bar virus (EBV) and cytomegalovirus (CMV) infections were based on PCR detection of DNA. Disseminated *T. marneffei* infection was defined as infections involving more than two organs or systems.

2.2 Routine immune function evaluation

Routine blood counts and immunological function analyses were performed. We used nephelometry to detect immunoglobulins (Igs), including IgG, IgA, and IgM. Lymphocyte subsets were measured using flow cytometry (Becton Dickinson, Franklin Lakes, NJ, USA). The following validated antibodies were used for flow cytometry: anti-CD3 (UCHT1), anti-CD8 (RPAT8), anti-CD27 (M-T271), anti-CD45RA (HI100), anti-CD4 (RPA-T4), anti-TCRαβ (T10B9.1A-31), anti-TCRγδ (B1), anti-CD19 (HIB19), anti-CD24 (ML5), anti-CD38 (HIT2), and anti-IgD (IA6-2) (all from BD Biosciences) (Ding et al., 2018). Flow cytometry detection of CD119 and CD212 was performed.

2.3 Genetic analysis

Genomic DNA was extracted from the peripheral blood of the patients and their parents using the QIAamp DNA Blood Mini kit (Qiagen, Hilden, Germany). DNA quality was assessed using a NanoDrop ultraviolet spectrophotometer (Thermo Fisher Scientific, USA).

Next-generation sequencing was performed using a panel that included all previously reported immunodeficiency genes. Genomic DNA fragments of patients were ligated with adaptors so that two paired-end DNA libraries with insert sizes of 500 bp were formed for all samples. After enrichment, the DNA libraries were sequenced on the HiSeq 2000 platform in accordance with the manufacturer's instructions (Illumina, San Diego, CA). The variants were annotated in ANNOVAR and VEP software and predicted with SIFT, PolyPhen-2 and MutationTaster.

2.4 Culture and identification of *T. marneffei*

T. marneffei was traditionally identified by culture or histopathology (Cao et al., 2019). In our study, *T. marneffei* was isolated from bacterial or fungal cultures of blood and BALF samples. This microorganism typically took approximately 3 to 14 days (Le et al., 2011; Cao et al., 2019). *T. marneffei* was identified by the following criteria (Segretain, 1959; Liyan et al., 2004; Cao et al., 2019) (1): Colonies of *T. marneffei* were verified by a MALDI-TOF mass spectrometer system (Bruker, Germany) (2). Positive fungal cultures were confirmed by Gram staining of a smear of the blood culture broth, followed by subculture onto Sabouraud dextrose agar (SDA) with incubation at 25 ˚C and 37 ˚C in room air. Yeast conversion was performed to confirm the identification of *T. marneffei*, and typical fungal colonies were observed (yeast phase at 37 ˚C with no red pigment production and mycelia at 25 ˚C with massive red pigment production) (3). Microscopically, the fungus had typical filamentous reproductive structures of the genus Penicillium, including the presence of conidiophore-bearing biverticillate penicilli, with each penicillus being composed of four to five metulae with smooth-walled conidia. *T. marneffei.* can be observed in histopathological sections, and methenamine silver or periodic acid-Schiff (PAS) staining was preferred. The presence of sausage-like cells, 2-3 μm in diameter, or elongated yeast-like organisms with clear central septum was the specific feature of *T. marneffei* (Liyan et al., 2004).

2.5 Metagenomic next-generation sequencing

2.5.1 Nucleic acid extraction

Blood and lymph node biopsy tissue samples were collected according to standard procedures. Plasma was prepared from blood samples, and circulating cell-free DNA (cfDNA) was isolated from plasma with the QIAamp Circulating Nucleic Acid Kit (Qiagen) according to the manufacturer's protocols. Lymph node biopsy tissue was extracted using the QIAamp DNeasy Blood & Tissue Kit (Qiagen) according to the manufacturer's protocols. The quantity and quality of DNA were assessed using Qubit (Thermo Fisher Scientific) and NanoDrop (Thermo Fisher Scientific), respectively.

2.5.2 Library preparation and sequencing

DNA libraries were prepared using the KAPA Hyper Prep kit (KAPA Biosystems) according to the manufacturer's protocols. An Agilent 2100 was used for quality control, and DNA libraries were 75 bp single-end sequenced on an Illumina NextSeq 550Dx (Illumina).

2.5.3 Bioinformatics analysis

Raw sequencing data were split by bcl2fastq2, and high-quality sequencing data were generated using Trimmomatic by removing low-quality reads, adapter contamination, duplicates and shot (length<36 bp) reads. Human host sequences were subtracted by mapping to the human reference genome (hs37d5) using Bowtie2. Reads that could not be mapped to the human genome were retained and aligned with the microorganism genome database for microbial identification by Kraken and for species abundance estimation by Bracken. The microorganism genome database

contained genomes or scaffolds of bacteria, fungi, viruses and parasites (downloaded from GenBank release 238, ftp://ftp.ncbi.nlm.nih.gov/genomes/genbank/).

2.5.4 Interpretation and reporting

We used the following criteria for positive mNGS results: For Mycobacterium, Nocardia and Legionella pneumophila, the result was considered positive if a species detected by mNGS had a species-specific read number ≥1. For bacteria (excluding Mycobacterium, Nocardia and Legionella pneumophila), fungi, viruses and parasites, the result was considered positive if a species detected by mNGS had at least 3 nonoverlapping reads. Pathogens detected in the negative 'no-template' control (NTC) were included only if the detected reads were ≥10-fold greater than those in the NTC.

2.6 Statistical analysis

Data were analyzed using SPSS 26.0 (IBM Corp., Armonk, NY, USA). Categorical variables were displayed as numbers and percentiles. The paired McNemar chi-square test was used to analyze the diagnostic efficiency of mNGS vs. conventional culture methods. Two-sided P values < 0.05 were considered statistically significant.

3 Results

From January 2019 to June 2022, a total of 505 cases of IEI were admitted to our hospital (Table 1). One hundred and three (20.4%) patients were diagnosed with IEI before admission, while 402 (79.6%) patients were definitively diagnosed with IEI after admission. Most of the patients (425/505) were admitted with various infectious manifestations. All patients underwent routine blood cultures. Seventy-three patients underwent histopathology. Nearly half of the patients (232/505) underwent further mNGS testing. Therefore, 232 patients (45.9%) underwent both culture and mNGS detection.

T. marneffei infection was detected in six patients. The frequency of *T. marneffei* infection was 1.2% (6/505) in our cohort. The genetic mutations of *T. marneffei*-infected patients included *IL12RB1, IFNGR1, STAT3, STAT1* and *CD40LG* (Figure 1A). Detailed clinical (Table 2) and immunological (Table 3) information of each patient is described as follows.

3.1 Case description

3.1.1 Patient 1

A 3-year-old girl was admitted to our hospital with the chief complaint of lymphadenopathy and intermittent fever. The girl was vaccinated with BCG after birth, and she developed left subaxillary and cervical lymph node enlargement at the age of 3 months. The local hospital performed lymph node resection and administered anti-tuberculosis treatment for 6 months. Nine months after drug withdrawal, the cervical lymph node enlargement recurred, and anti-tuberculosis therapy was administered again. *IL12RB1* complex heterozygous mutations were detected: exon 14-16 deletion (maternal) and c.875-885 deletion (paternal). The expression of IL12RB1 protein was impaired (Figure 2). At the age of 3, the child developed recurrent fever, severe anemia, hepatosplenomegaly, and lymphadenopathy (Figure 3A), and the blood culture suggested *T. marneffei*. The serum G test (271.89 pg/ml) and GM test (6.682) were significantly increased. *T. marneffei* was detected in the blood (reads, 14) and lymph nodes (reads, 108380) by mNGS (Figure 3B). Therefore, isoniazid, rifampicin and ethambutol were used for antituberculosis, itraconazole for antifungal, and IFN-γ for immune regulation. The erythrocyte sedimentation rate (ESR) (120 mm/H) and G test (112.6 pg/ml) remained high after 2 months of anti-infective therapy, despite negative pathogens in blood by mNGS. Imaging examination revealed that the lymph nodes were still enlarged (Figure 4A2), and the liver and spleen lesions were smaller than before. After nearly 3 months of treatment with itraconazole, the biopsy of cervical lymph nodes suggested granulomatous inflammation (Figure 3C). PAS staining of the cervical lymph node tissues revealed fungal spores (Figure 3D), and *T. marneffei* was still identified by mNGS (reads, 15545702). Antifungal therapy was adjusted to amphotericin B liposomes intravenously for 2 weeks, followed by oral itraconazole. The follow-up CT scans revealed that the lymph nodes were obviously shrunken (Figure 4A3). ESR and G tests were reduced to normal, and then she was discharged.

3.1.2 Patient 2

A 5-month-old boy (P2) was referred for enlarged axillary lymph nodes and ulceration of the BCG vaccination site. From 3 months of age, the child presented with left axillary lymph node enlargement and suppuration at the BCG vaccination site. Lymph node dissection and abscess removal were performed at 4 months of age. Acid fast bacilli were seen on pus smear, and Xpert examination of focal tissue suggested *Mycobacterium tuberculosis*. *Mycobacterium tuberculosis* (reads, 124) and *Escherichia coli* (reads, 952090) were detected in stool by mNGS. The child began to receive anti-tuberculosis treatment with isoniazid, rifampicin and ethambutol. At the age of 5 months, his lung CT indicated pulmonary cavities, and *Mycobacterium tuberculosis* was detected in BALF by mNGS. Levofloxacin was further added. In addition, the two blood GM test results were 0.589 and 1.497, respectively. Two mNGS tests of blood were performed 9 days apart, both of which were positive for *T. marneffei* (reads 29 and 6), and itraconazole was used for antifungal treatment. Whole-exome sequencing

10.3389/fcimb.2022.987692

TABLE 1 Baseline of patients with IEI in our cohort.

		Number of cases
Total patients		505
novelty diagnosed IEI		402
admitted due to infections		425
Culture		505
	blood stream	505
	sputum	260
	BALF	142
	bone marrow	10
	hydrothorax	1
	ascites	0
	blood+BALF	142
	blood+sputum	260
Histopathology		73
	lymph node	39
	colon	46
	liver	11
	bronchial mucosa	4
	skin	12
	bone	4
mNGS		232
	blood	131
	sputum	32
	BALF	131
	bone marrow	1
	hydrothorax/ lung abscess	3
	ascites	0
	biopsy	36
	lymph node	17
	liver	10
	lung	3
	skin	4
	bone	2
	blood+BALF	53
	blood+sputum	21
Culture + mNGS simultaneously		232
	blood	131
	BALF	131
	sputum	32
Histopathology + mNGS simultaneously		33
	lymph node	17
	liver	9
	lung	3
	skin	2
	bone	2

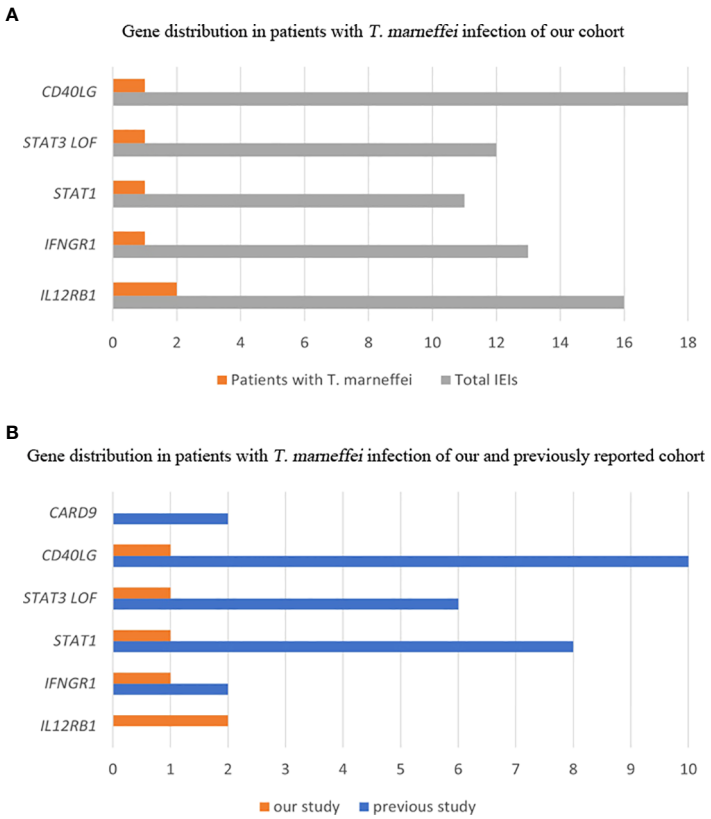

FIGURE 1
Gene distribution of patients with *T. marneffei* infection in IEIs. Gene distribution in our cohort **(A)**. Gene distribution in previously reported cases **(B)**.

revealed a homozygous mutation of the *IL12RB1* gene, c.632G>C, p. R211P, derived from his parents. IL12RB1 protein was not expressed (Figure 2). He received oral itraconazole for 6 months with a good response and has continued anti-tuberculosis treatment to date.

3.1.3 Patient 3

This male child was hospitalized for pneumonia during the neonatal period and was admitted with sepsis and liver dysfunction at the age of 2 months. At 3 months of age, he developed enlarged left axillary lymph nodes, redness, swelling and ulceration at the BCG vaccination site. The PPD test was strongly positive, and lymph node biopsy suggested granulomatous lesions. Isoniazid, rifampicin and ethambutol were used as anti-tuberculosis therapy, and IFN-γ was given as immunotherapy. Further genetic analysis indicated a homozygous mutation in the *IFNGR1* gene: c. 655G>A, p.G219R. IFNGR1 protein was confirmed not expressed (Figure 2). His parents discontinued medication on their own. The child developed leg pain at 24 months old and mandibular swelling 2 months later. Imaging examination suggested multiple bone destruction. The anti-tuberculosis treatment was performed again. He had recurrent fever, and lung CT suggested pneumonia and partial consolidation of the left lung (Figure 4B1). *T. marneffei* (reads, 15) was detected in BALF by mNGS, and then itraconazole was added for antifungal treatment for 9 months. After 3 and 8 months of antifungal treatment, chest CT revealed significant improvement (Figures 4B2, 4B3).

3.1.4 Patient 4

The girl presented with recurrent skin eczema with pruritus from 1 month after birth. At the age of 9 months, the child developed low fever with a peak temperature of 38° C, accompanied by cough and expectoration, and pulmonary CT suggested bronchopneumonia. Routine blood examination revealed eosinophils of 1.58×10^9/L and IgE raised to 548 IU/ml. The BALF was positive for *T. marneffei* by culture and mNGS (reads, 43) and CMV DNA. The GM test of the BALF was not tested at that time. She was treated with amphotericin B for 20 days, followed by voriconazole. Fever and cough recurred, and fibrobronchoscopy was performed again at 14 months. BALF indicated an elevated result of the GM test (1.335), and *Staphylococcus aureus* (reads, 42) and *Streptococcus pneumoniae* (reads, 14) were

TABLE 2 Clinical characteristics of T. marneffei infection in 6 patients with IEI.

	P1	P2	P3	P4	P5	P6
Gender	F	M	M	F	M	M
Province of residence	Hunan	Guangdong	Zhejiang	Jiangxi	Jiangxi	Guangdong
Age at diagnosis of IEI (m)	35m	5m	6m	12m	31m	7m
Age at T.marneffei infection (m)	36m	5m	29m	11m	29m	25m
Method of T. marneffei detection	mNGS of peripheral blood and lymph node biopsy tissue; blood culture; histopathology of lymph node	mNGS of peripheral blood	mNGS of BALF	mNGS and culture of BALF	mNGS of peripheral blood; histopathology of abdominal lymph nodes; blood culture	mNGS of peripheral blood and BALF
Infected site of T.marneffei	Blood, lymph node	Blood	Pulmonary	Pulmonary	Blood, lymph nodes, liver, spleen, pancreas	Blood, pulmonary
Clinical presentations						
Fever	+	-	-	+	+	+
Weight loss	+	-	-	-	NA	+
Anemia	+	-	+	+	+	+
Hepatomegaly	-	-	+	-	Multiple lesions of the liver	-
Splenomegaly	+	-	+	-	Multiple lesions of the spleen	Multiple lesions of the spleen
Lymphadenopathy	+	-	+	-	+	+
Bone destruction	-	-	+	-	-	-
Serous effusion	-	-	Pleural effusion	-	Pleural, peritoneal and pericardial effusion	-
Respiratory symptoms	Cough	-	-	Cough, shortness of breath, laryngeal stridor	Dysponea	_
Gastrointestinal symptoms	-	-	-	-	Recurrent nausea, diarrhea, vomiting, bloating	Diarrhea
Genetic tests	IL12RB1: c.875-885 deletion (paternal); exon 14-16 deletion (maternal)	IL12RB1: c.632G>C, p.R211P, hom	IFNGR1: c.655G>A, p.G219R, hom	STAT3: c.1394C>T, p.S465F, het	STAT1: c.821G>A, p.R274Q, het	CD40LG fragment deletion, hemi
Anti-antifungal Treatment	Itraconazole for 3 month, amphotericin B liposome for 2 weeks, then long-term itraconazole	Itraconazole for 6 months	Itraconazole for 9 months	Amphotericin B for 20 days, then long-term voriconazole	Intravenous voriconazole for 25 days, oral voriconazole for 7 months, then Itraconazole for 22 months	Itraconazole for 2 months
The last follow-up	Alive, 40m	Alive, 21m	Alive, 51m	Alive, 23m; HSCT at 18m	Alive, 68m	HSCT at 27m, died of sepsis at 29m

m, month; M, male; F, female; IEI, inborn error of immunity; BALF, bronchoalveolar lavage fluid; NA, Not Available; HSCT, hematopoietic stem cell transplantation.

detected by mNGS. Voriconazole and linezolid were given for anti-infective therapy, and regular intravenous immunoglobulin (IVIG) was recommended. Gene testing suggested a *STAT3* gene heterozygous mutation: c.1394 C>T, p. S465F. With an NIH score of 39 (Grimbacher et al., 1999; Grimbacher et al., 1999), she was diagnosed with hyper IgE syndrome. Hematopoietic stem cell transplantation was performed at 18 months of age. She was in good condition during the six-month follow-up after transplantation.

3.1.5 Patient 5

The patient developed recurrent nausea at 27 months of age without an obvious cause. Two months later, the symptoms worsened, with lethargy and fever. The G test was elevated at 1817.7 pg/ml, and abdominal CT indicated hepatosplenomegaly and multiple abnormal lesions (Figure 4C1). Routine blood tests suggested anemia and thrombocytopenia, while elevated levels of amylase and lipase suggested pancreatitis. Multiple lymph nodes were enlarged throughout the body, and histopathological

TABLE 3 Hematological and immunological parameters at the time of T. marneffei infection in the six patients.

	P1	P2	P3	P4	P5	P6
WBC (´10^9/L)	10.92	10.02	33↑	27↑	3.9↓	6.9
ANC (´10^9/L)	7.73↑	1.74	24.72↑	13.15↑	1.94↓	4.38
ALC (´10^9/L)	2.09↓	7.06	5.5	10.29↑	1.60↓	1.70↓
PLT (´10^9/L)	188	402↑	680↑	662↑	40↓	353
Hb (g/L)	57↓	114	91↓	101↓	51↓	97↓
CRP (mg/L)	79↑	<8	79.8↑	8.7	20↑	46↑
ESR (mm/h)	125↑	2	120↑	NA	2	68↑
Ferritin (ng/mL)	256.6↑	60.5	51.3	NA	928.4↑	227↑
ALT (U/L)	6.22	17.1	16.2	21	26.1	45.9
AST (U/L)	18.5	42.5	28.6	38	136.9↑	63.1↑
G test (pg/mL)	271.89 ↑	<37.5	17.5	NA	1817.7 ↑	NA
GM test (blood/BALF)	6.682 ↑/NA	1.497 ↑/0.087	NA/0.120	NA/NA	6.192 ↑/NA	7.899↑/0.336
CD19 (cells/ul)	323.1 (18.60%)	1659.7 (27.54%)↑	439.7 (10.35%)↓	1734.9 (20.03%)	1304.6 (52.61%)↑	294.20 (15.95%)
Naive B (%)	84.02	NA	NA	89.62↑	96.30 ↑	97.7 ↑
Memory B (%)	7.89	NA	NA	2.76↓	0.10 ↓	0.2 ↓
Transitional B (%)	0.44↓	NA	NA	2.73↓	10.20	2.5↓
Plasmablasts (%)	0.41↓	NA	NA	0.29↓	0.20 ↓	0.80
CD3 (cells/ul)	1251.8 (72.05%)	4037.6 (66.99%)	3180.0 (74.88%)↑	5693.56 (68.86%)	945.7 (38.13%)↓	1452.3 (78.73%)
CD4 (cells/ul)	935.0 (53.82%)↑	2758.5 (45.77%)↑	2489.6 (58.62%)↑	3919.0 (45.25%)↑	628.4 (25.34%)↓	1034.72 (56.09%)
CD4 Naive (%)	58.87	NA	NA	74.20	51.80	85.30
CD4 CM (%)	34.85	NA	NA	23.40	45.60	14.30
CD4 EM (%)	6.21 ↑	NA	NA	2.25	2.60	0.4↓
CD4 TEMRA (%)	0.07	NA	NA	0.15	0.00	0.00
CD8 (cells/ul)	245.7 (14.14%) ↓	1177.6 (19.54%)↓	618.6 (14.57%)↓	1634.0 (18.87%)	247.92 (10%)↑	280.49 (15.21%)
CD8 Naive (%)	81.64	NA	NA	55.08	50.70	89.70
CD8 CM (%)	16.18	NA	NA	15.29	22.10	9.80
CD8 EM (%)	1.77	NA	NA	3.37	19.90 ↑	0.20
CD8 TEMRA (%)	0.42 ↓	NA	NA	26.26↑	7.20	0.30
DNT (%)	7.61	NA	NA	3.42	6.60	4.70
γδ T (%)	5.87	NA	NA	2.49↓	4.10 ↓	3.8↓
CD16CD56 (cells/ul)	118.7 (6.83%)	242.3 (4.02%)	533.4 (12.56%)	877.41 (10.13%)	199.4 (8.04%)↓	69.44 (3.76%)
IgG (g/L)	53.00↑	9.40↑	21.80↑	13.56↑	19.40 ↑	1.00 ↓
IgM (g/L)	1.89	0.32↓	2.35↑	1.06	0.85	0.58 ↓
IgA (g/L)	0.60	0.09↓	1.21↑	0.70	0.84↑	0.02 ↓
IgE (KU/L)	49.46	16.12	142.11↑	548.00↑	18.14	9.81
The reference of immunoglobulin:						
	1-3m	4-6m	12-36m			
IgG (g/L)	2.75-7.50	3.7-8.3	5.52-11.46			
IgM (g/L)	0.05-0.60	0.14-0.5	0.06-0.74			
IgA (g/L)	0.10-0.70	0.33-1.25	0.6-2.12			
IgE (KU/L)	<100	<100	<100			

WBC, white blood count; ALC, absolute lymphocyte count; ANC, absolute neutrophil count; HB, haemoglobin; CM, central memory; EM, effector memory; TEMRA, terminal effector memory cytotoxic T cells; DNT, TCR αβ+ CD4 and CD8 double-negative T cell; NA, not available.
The percentage and numbers of lymphocyte subsets in the peripheral blood reference to the literature (Ding et al., 2018).
↑: higher than the normal value; ↓: lower than the normal value.

examination of the abdominal lymph node biopsy presented a large number of neutrophil infiltrates and fungal spores in the tissue cells (Figures 3E, F). *T. marneffei* was further detected in blood by culture and mNGS (reads, 1452), and voriconazole was used for antifungal treatment. In addition, recurrent thrush began at the age of 1 year old, and genetic testing was performed, which revealed one *de novo* heterozygous mutation in the *STAT1* gene: c.821G>A, p.R274Q. After voriconazole treatment for 3 months, *T. marneffei* was negative in blood by mNGS. The multiple abnormal lesions in the liver and spleen

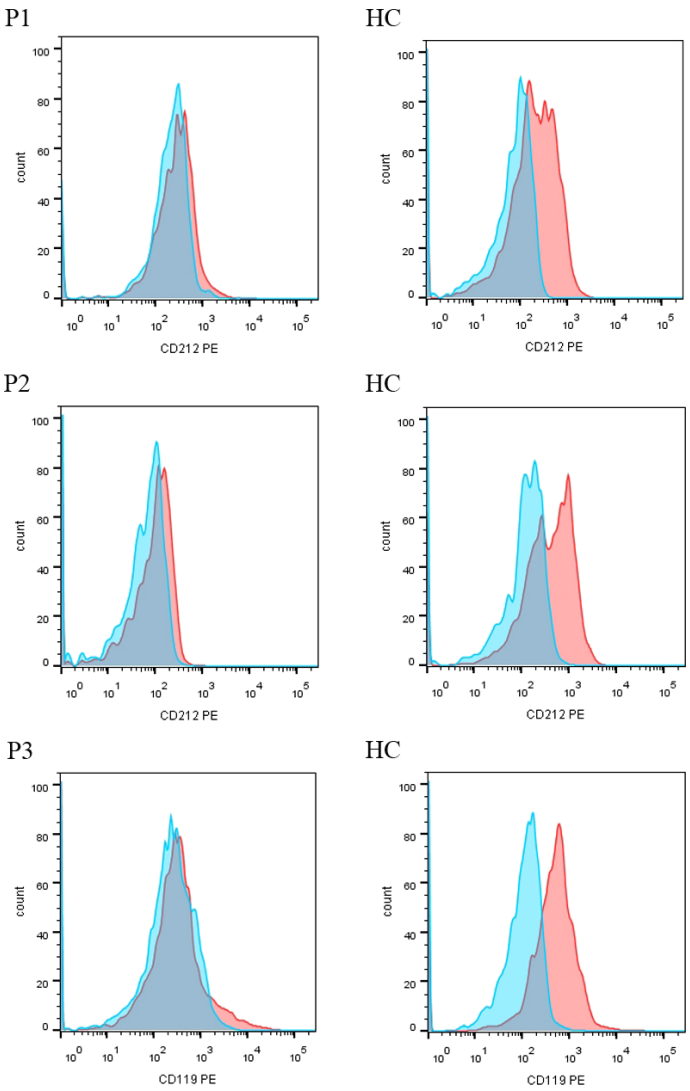

FIGURE 2
The expression of IL12RB1 (CD212) and IFNGR1 (CD119) protein in P1-P3. IL12RB1 protein was not expressed in P1 and P2. IFNGR1 protein was not expressed in P3.

improved (Figure 4C3). Then, he took itraconazole as a preventive antifungal treatment. Now the child has stopped antifungal drugs and is generally being well.

3.1.6 Patient 6

The male patient presented with left axillary lymph node enlargement at 2 months of age, followed by supraclavicular lymph node enlargement. The 4-month-old child developed poor appetite, and *Pneumocystis jiroveci* was further detected in sputum and blood. The G test results significantly increased to 767-2242 pg/ml. Isoniazid and rifampicin were given for anti-tuberculosis treatment, sulfamethoxazole (SMZ) for *Pneumocystis jiroveci*, linezolid for bacteria, and itraconazole for anti-fungal treatment. According to his clinical presentations, he was considered to have an IEI, and his genetic test result was hemizygous *CD40LG* deletion. The child developed recurrent diarrhea and fever at the age of 2 after his parents stopped the medications on their own. Lung CT suggested exudation in both lungs. Abdominal MRI suggested abnormal signals in the spleen and both kidneys, multiple small lymph nodes in the abdominal cavity and ascites. *T. marneffei* (reads, 31) was detected in blood, and *T. marneffei* (reads, 58) and *Pneumocystis jiroveci* (reads, 4) were detected in BALF. Gastroenteroscopy showed ulceration of rectal, colonic, and small intestinal ulcers. Cefoperazone sulbactam, metronidazole, itraconazole, and SMZ were used as anti-infection treatments, and mesalazine was used as an inhibitor of intestinal

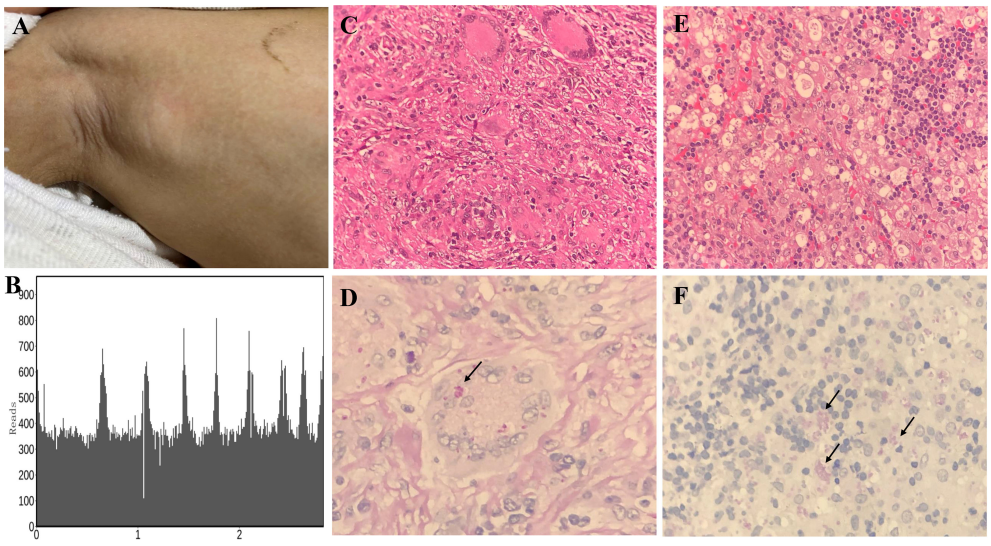

FIGURE 3
Histopathological staining and mNGS results in P1 and P5. Lymph node enlargement of the right axilla was seen in P1 **(A)**. Confirmation of T. marneffei-specific amplification from lymph node tissue by mNGS showed 108,380 unique sequence reads of T. marneffei, accounting for 18.93% of the genome coverage **(B)**. Granulomatous inflammation observed during histopathological examination of the cervical lymph node **(C)**. PAS staining of the cervical lymph node revealed fungal spores (arrows) (magnification × 400) **(D)**. A large number of neutrophil infiltrates were observed in the histopathological examination of abdominal lymph nodes of P5, and a patchy distribution of tissue cells was observed. Fungal spore-like substances were scattered or clustered in some tissue cells (magnification × 400) **(E)**. PAS staining of the abdominal lymph node tissues revealed fungal spores (arrows) (magnification × 400) **(F)**.

inflammation. He died of sepsis after hematopoietic stem cell transplantation.

3.2 Diagnostic methods and sample types

A statistical study was performed in 232 patients who underwent both traditional standard and mNGS tests simultaneously (Table 4). We defined the patient as a positive case if *T. marneffei* was detected, regardless of specimen type. Traditional gold standard tests were culture and histopathology. Both mNGS and traditional methods were positive in 3 patients and negative in 226 patients. *T. marneffei* was detected only by mNGS in 3 patients but was negative by traditional methods. Next, we evaluated the diagnostic accuracy of mNGS in detecting *T. marneffei* infection. The sensitivity, specificity, positive likelihood ratio, and negative likelihood ratio of mNGS in our cohort were 100%, 98.7%, 76.9, and 0, respectively. McNemar chi-square analyses showed that there was no significant difference between the two methods (p=0.25).

The sample detection methods of these 6 patients with *T. marneffei* infection were analyzed in detail. *T. marneffei* was identified in a total of 15 samples from six patients (Figure 5). In our cohort, *T. marneffei* was most commonly detected by mNGS, covering 5 blood samples, 3 BALF samples, and 2 lymph node samples. Only two blood samples and one BALF sample were identified by culture. The histopathological examination of the lymph nodes in two samples indicated the presence of *T. marneffei* infection. Culture and mNGS were performed on 12 samples from these six patients simultaneously. *T. marneffei* was identified in 2 samples by the culture method (16.7%, 2/12) and 8 samples by the mNGS method (66.7%, 8/12). One biopsy sample of a cervical lymph node was tested by histopathological staining and mNGS simultaneously. *T. marneffei* was identified with mNGS (reads, 15545702), and the histopathological PAS staining was also positive.

The time required for diagnosis using different methods for all six patients was further analyzed. The median reporting time for mNGS was 26 hours, with a range of 21.5-30 hours. The cultural identification periods of *T.marneffei* in the three positive samples were 3, 10 and 14 days. Two positive lymph node pathologic results were reported within 6 and 11 days. Therefore, the time consumption of mNGS was much less than that of culture or histopathology.

3.3 Literature review

A systematic literature review was performed in PubMed on human *T. marneffei* infections published between 1950 and 2022 using the key words "*Talaromyces marneffei*" or

TABLE 4 Diagnostic accuracy analysis of mNGS compared to traditional diagnostic methods.

	Tranditonal diagnostic methods +	Tranditonal diagnostic methods -	Total
mNGS +	3	3	6
mNGS -	0	226	226
Total	3	229	232

Sensitivity = 100%, Specificity = 98.7%, LR+ = 76.9, LR - = 0.
LR, likelihood ratio.

"*Penicillium marneffei*" or "*Penicilliosis*" or "*Talaromycosis*". Articles reporting *T. marneffei*-infected patients with immune-related gene mutations were included. HIV-positive cases were excluded. As a result, a total of 28 cases with confirmed IEI from seventeen articles were analyzed. The characteristics of the patients are summarized in Table 5 (Yuen et al., 1986; Kamchaisatian et al., 2006; Ma et al., 2009; Sripa et al., 2010; Lee et al., 2012; Lee et al., 2014; Fan et al., 2018; Li et al., 2018; Du et al., 2019; Lee et al., 2019; Chen et al., 2020; Pan et al., 2020; Zhang et al., 2020; Ba et al., 2021; Chen et al., 2021; Fan et al., 2021; You et al., 2021).

The median age of patients detected with *T. marneffei* reported previously was 3 years, ranging from 5 months to 34 years. Most of them were Chinese (82%, 23/28), and the others were from Thailand. Twenty patients (71%) had disseminated *T. marneffei* disease involving blood or bone marrow, lungs, colon, skin, lymph nodes, and liver. The immunodeficiency genes included *CD40LG* (35%), *STAT1*

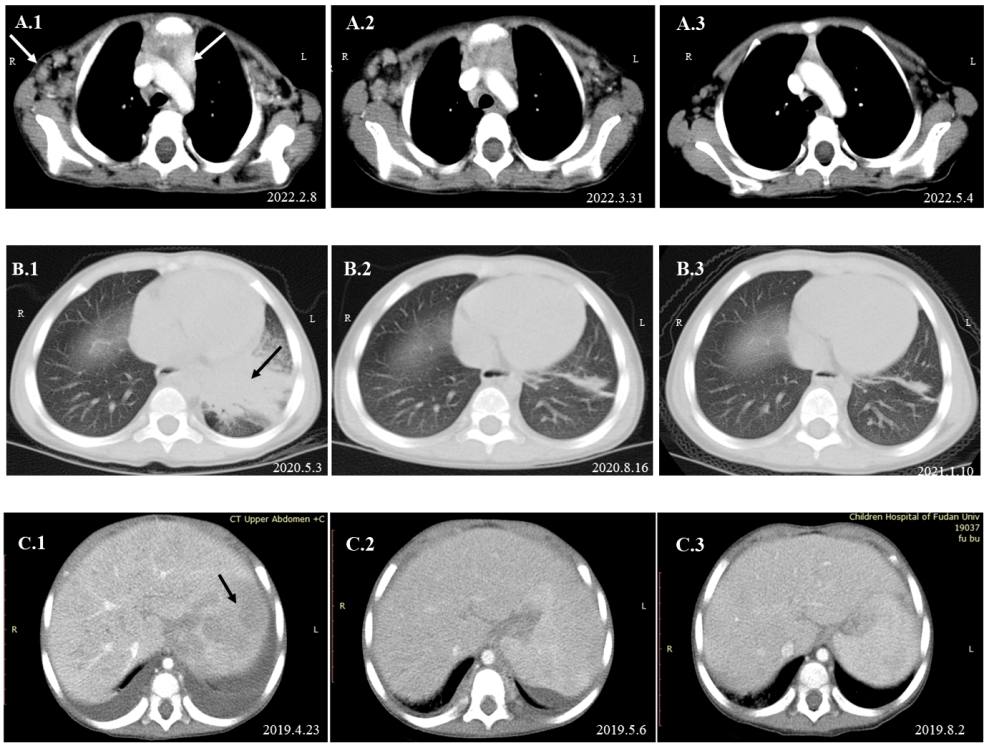

FIGURE 4
Dynamic changes in imaging examinations of patients during follow-up. Imaging examination of P1 revealed that the axillary and mediastinal lymph nodes were enlarged **(A.1)**. After oral itraconazole and anti-tuberculous therapy for nearly 2 months, chest CT re-examination showed that the axillary and mediastinal lymph nodes were still enlarged **(A.2)**. A lymph node biopsy was performed on April 19, 2022, and mNGS indicated high reads of T. marneffei. Antifungal therapy was adjusted to amphotericin B for 2 weeks, followed by oral itraconazole. One month later, the imaging examination suggested that the lymph nodes were smaller than before **(A.3)**. Chest CT of P3 suggested pneumonia and partial consolidation of the left lung with slight pleural effusion in the acute phase **(B.1)**, and the patient received oral itraconazole antifungal combined with anti-tuberculosis therapy. Chest CT re-examination revealed significant improvement in the lungs after 3 months **(B.2)** and 8 months **(B.3)**. Abdominal CT of P5 indicated hepatosplenomegaly and multiple abnormal lesions at the beginning **(C.1)**. He received intravenous voriconazole treatment for 25 days and then oral voriconazole. The multiple abnormal lesions improved after treatment for 2 weeks **(C.2)** and 3.5 months **(C.3)**.

TABLE 5 Primary Immunodeficiencies reported in HIV-negative children with T. marneffei infection.

Patients	Genetic defect	Mutation	Gender	Age	Residence	Detection methods	Extent of T.marneffei infection	Treatment and outcome
p1 (Lee et al., 2012) (Lee et al., 2019) (Lee et al., 2014)	STAT1, GOF	c.800C>T (p.A267V)	M	15y	Hong Kong, China	Fine-needle aspiration of the cervical lymph node for culture yielded T. marneffei	Disseminated	Liposomal amphotericin B for 6 weeks, followed by itraconazole prophylaxis with good clinical response
p2 (Lee et al., 2012) (Lee et al., 2019) (Lee et al., 2014)	STAT1, GOF	c.1074G>T (p.L358F)	F	7y	Hong Kong, China	BALF culture yielded T. marneffei	Disseminated	Lliposomal amphotericin B for 6 weeks, followed by itraconazole prophylaxis with good clinical response
p3 (Lee et al., 2012) (Lee et al., 2019) (Lee et al., 2014)	STAT1, GOF	c.863C>T (p.T288I)	F	7y	Hong Kong, China	Lymph node biopsy yielded T. marneffei	Disseminated	Treated with itraconazole with good response, died of massive pulmonary hemorrhage at 16 years old
p4 (Lee et al., 2019) (Yuen et al., 1986)	STAT1, GOF	c.1170G>A (p.M390I)	M	10y	Hong Kong, China	Tissue from the neck ulcer and axillary lymph node for culture yielded T. marneffei	Disseminated	Intravenous amphotericin B and oral flucytosine for 3 months with good response
p5 (Chen et al., 2020)	STAT1, GOF	c.193G>A (p.D65N)	M	5y11m	China	NA	Lymphadenitis	Amphotericin B and voriconazole, alive
p6 (Chen et al., 2020)	STAT1, GOF	c.1053G>T (p.L351F)	F	9y11m	China	NA	Pulmonary	Itraconazole and amphotericin B, alive
p7 (Fan et al., 2021)	STAT1	NA	M	2y	Hunan, China	Bone marrow culture yielded T. marneffei, Lymph node biopsy (Right inguinal hernia) fungal spore structure, PAS(+)	Disseminated	Intravenous voriconazole for 2 weeks, amphotericin B for 3 weeks, oral itraconazole for 1 year
p8 (Chen et al., 2021)	STAT1, GOF	nt.859T > A (Y287N)	M	20y	China	Blood, bone marrow and sputum cultures yielded T. marneffei	Disseminated	Amphotericin B for 6 months, recovery
p9 (Lee et al., 2012)	STAT3, Hyper-IgE syndrome	c.1121A>G (p.D374G)	F	12m	China	Blood and bone marrow cultures yielded T. marneffei	Disseminated	Treated with itraconazole with good response
p10 (Ma et al., 2009)	STAT3, Hyper-IgE syndrome	NA	M	10y	Hong Kong, China	Sputum and abscess fluid cultures yielded T. marneffei	Pulmonary	Treated with amphotericin B, died of respiratory failure due to rapid disease progression
p11 (Fan et al., 2018)	STAT3, Hyper-IgE syndrome	c.1593A>T (p.K531N)	M	13y	Guangzhou, China	BALF culture yielded T. marneffei	Disseminated	Treated with amphotericin B, voriconazole for 2 weeks and itraconazole orally for 2 months with good response
p12 (Pan et al., 2020)	STAT3, Hyper-IgE syndrome	c.1673G>A (p.G558D)	M	37m	Guangxi, China	The colon biopsy showed a large number of fungal spores, liver tissue revealed numerous intracellular yeast-like or sausage-like cells, bone marrow culture confirmed T.marneffei	Disseminated	Intravenous voriconazole and antibiotics for 10 days and oral voriconazole for 7 months, recovery
p13 (Zhang et al., 2020)	STAT3, Hyper-IgE syndrome	c.92G>A (p.R31Q)	M	34y	Zhejiang, China	mNGS of BALF confirmed T. marneffei (readers 566), cultures of BALF and the endobronchial biopsied tissue mass yielded T. marneffei	Pulmonary	Itraconazole, recovery
p14 (Fan et al., 2021)	STAT3, Hyper-IgE syndrome	NA	F	2y	Hunan, China	Cultures of bone marrow, sputum and BALF yielded T. marneffei	Disseminated	Amphotericin B for 2 days (discontinued due to liver dysfunction), Intravenous voriconazole

(Continued)

TABLE 5 Continued

Patients	Genetic defect	Mutation	Gender	Age	Residence	Detection methods	Extent of T.marneffei infection	Treatment and outcome
								for 4 days, give up and died
p15 (Lee et al., 2019) (Du et al., 2019)	CD40L (TNFSF5)	g.IVS1 +1G>A	M	29m	China	Cervical lymph node and endobronchial biopsy yielded T. marneffei; cultures of blood, nasal secretions, throat swab and sputum yielded T. marneffei	Disseminated	Treated with voriconazole for 4 months and subsequent recurrence treated with voriconazole, with good response
p16 (Kamchaisatian et al., 2006)	CD40L deficiency	Complex mutation in exon 5	M	14m	Northeastern Thailand	Throat swab, sputum, blood and bone marrow cultures grew T. marneffei	Disseminated	Treated with amphotericin B for 21 days, followed by itraconzole for 10–12 weeks
p17 (Kamchaisatian et al., 2006)	CD40L deficiency	NA	M	1y	Northern Thailand	Lymph node tissue culture yielded T. marneffei	Pulmonary disease and lymphadenopathy	Treated with amphotericin B for 21 days, followed by itraconzole for 10–12 weeks
p18 (Sripa et al., 2010)	CD40L deficiency	NA	M	3y	Thailand	T. marneffei infection of the sputum	Pulmonary	Itraconazole, good response
p19 (Du et al., 2019)	CD40L deficiency	g.IVS1-3T>G	M	2y	Hunan,China	Blood culture and hepatic biopsy showed T. marneffei	Disseminated	Treated with amphotericin B, died of multi-organ failure
p20 (Li et al., 2018)	CD40L deficiency	NA	M	14m	Jiangxi,China	Blood culture yielded T. marneffei	Disseminated	Treated with itraconazole for 2 weeks and improved
p21 (Du et al., 2019)	CD40L deficiency	IVS3 + 1G>A	M	2y11m	China	Bone marrow culture yielded T. marneffei	Disseminated	Responded effectively to anti-fungal therapy
p22 (Du et al., 2019)	CD40L deficiency	IVS1-1 G > A	M	2y3m	China	Blood culture yielded T. marneffei	Disseminated	Lost to follow-up
p23 (Du et al., 2019)	CD40L deficiency	IVS4 + 1G>C	M	3y	China	Bone marrow culture yielded T. marneffei	Disseminated	Responded effectively to anti-fungal therapy
p24 (Du et al., 2019)	CD40L deficiency	Large fragment deletion including exon 4 and 5	M	13y7m	China	Blood culture yielded T. marneffei	Disseminated	Responded effectively to anti-fungal therapy
p25 (Lee et al., 2019)	IFNGR1	c.182dupT (p.V61fs69)	F	5m	Northern Thailand	NA	Disseminated	Die
p26 (Lee et al., 2019)	IFNGR1	c.182dupT (p.V61fs69)	M	12m	Northern Thailand	Blood culture yielded T. marneffei	Disseminated	Treated with amphotericin B for 6 weeks with good response, followed by itraconazole prophylaxis
p27 (You et al., 2021)	CARD9, compound heterozygote	c.440T>C (p.L147P), c.586A>G (p.K196E)	M	5y	Chongqing, China	Bone marrow smear identified T. marneffei infection, ascites culture yielded T. marneffei	Disseminated	Treated with amphotericin B and voriconazole, died of multiple organ failure
p28 (Ba et al., 2021)	CARD9, compound heterozygote	c.1118G>C (p.R373P), c.610C>T (p.R204C)	M	7m	Guangzhou, China	Blood culture and mNGS of blood confirmed T. marneffei (readers 248)	Disseminated	Voriconazole, good response

y, year; m, month; BALF, bronchoalveolar lavage fluid; mNGS, metagenomic next-generation sequencing; GOF, gain of function; M, male; F, female; NA, not available.

(29%), *STAT3* (22%), *CARD9* (7%) and *IFNGR1* (7%). Comparisons between our cohort and previously reported gene spectra are shown in Figure 1B.

A total of 46 positive clinical samples from these 28 patients were collected (Figure 5). *T. marneffei* was mainly detected by cultures (78.2%) of blood, bone marrow, sputum, BALF, tissue and so on. Histopathological staining of the biopsy tissue was followed (8.7%), including lymph node, liver, colonic mucosa and bone marrow samples. Only two patients were detected to have *T. marneffei* by mNGS (4.3%), 566 reads in BALF (Zhang et al., 2020) and 248 reads in blood (Ba et al., 2021). The detection method of *T. marneffei* in the remaining four samples (8.7%), including endobronchial biopsy, lymph node biopsy and hepatic biopsy, was not available.

Nearly half of the patients (12/28) were treated with amphotericin B, followed by itraconazole or voriconazole. Other patients were treated with itraconazole (5/28), voriconazole (2/28), or amphotericin B (3/28) alone. Only one patient received intravenous amphotericin B and oral flucytosine. The treatments of five patients were unknown. Except for one patient lost to follow-up, most patients (21/28) had improved symptoms with effective antifungal therapy. Six patients (6/28) died. Two patients died of multiorgan failure, one patient died of respiratory failure due to rapid disease progression, one patient died of massive pulmonary hemorrhage at 16 years old, and the other two patients died of unknown reason.

4 Discussion

T. marneffei is an opportunistic infectious pathogen. Inhalation of conidia is the primary route of infection, which are subsequently phagocytosed by alveolar macrophages, and then *T. marneffei* disseminates to the reticuloendothelial system, causing systemic infection when the host immune response is suppressed (Supparatpinyo et al., 1994). Therefore, patients susceptible to *T. marneffei* are usually immunosuppressed. Fungal infections in children with IEI are a growing concern.

T-cell-mediated immunity plays a central role in the immune defense mechanism against *T. marneffei* infection. Congenital athymic mice developed severe pulmonary and disseminated systemic Penicillium disease (Kudeken et al., 1996; Kudeken et al., 1997). A literature review showed that CD40 ligand deficiency was the most common type of immune deficiency in *T. marneffei* infection. CD40L mediates the interaction between T cells and different cells through ligation with its receptor CD40 (van Kooten and Banchereau, 2000; Erdos et al., 2005; Du et al., 2019). CD40 ligand-deficient patients suffered from opportunistic infections, especially *Pneumocystis jiroveci* and *Cryptosporidium parvum* infections. Recently, Pamela P. Lee discussed endemic mycoses in IEI, in which she highlighted *T. marneffei* infection in CD40 ligand deficiency in Southeast Asia (Lee and Lau, 2017).

Intrinsic and innate immunodeficiencies associated with *T. marneffei* infection have also been reported, such as *STAT1* and *CARD9*. Caspase recruitment domain–containing protein 9

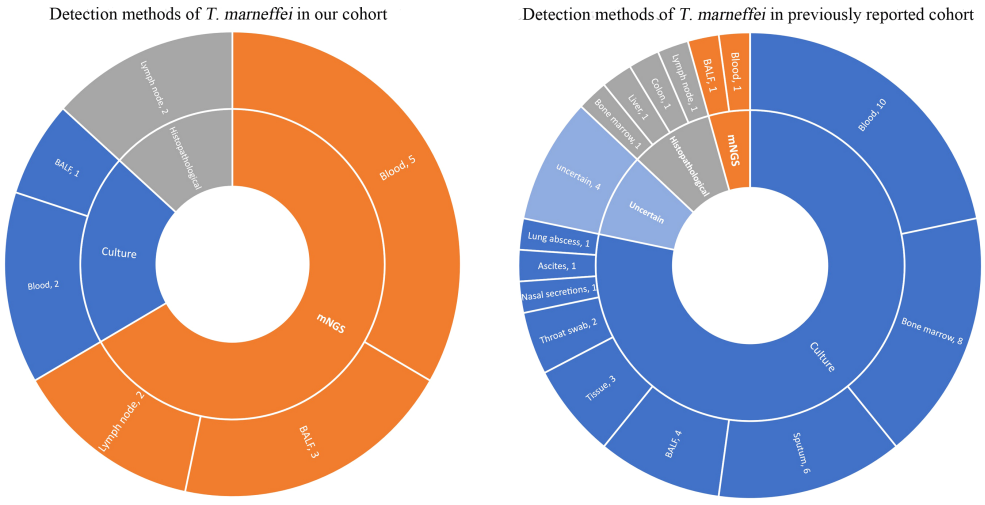

FIGURE 5
Distribution of sample types with T. marneffei positivity. In our cohort, T. marneffei was detected in 15 samples using different methods, including mNGS (n=10), culture (n=3), and histopathological staining (n=2). In the previous cohort, T. marneffei was mainly detected by cultures (n=36) and histopathological staining (n=4), and only two patients were detected by mNGS (n=2).

(CARD9) is an adaptor molecule in the cytosol of myeloid cells required for the induction of T-helper cells producing interleukin-17 (Th17 cells), and it can effectively integrate the recognition signals of various natural immune receptors and plays an important role in antifungal immunity (Drummond et al., 2011; Salazar and Brown, 2018; You et al., 2021). Signal transducer and activator of transcription (STAT) proteins are critical transcription factors for the appropriate regulation of cellular responses to interferons, cytokines, growth factors, and hormones. There is tight regulation of their function *via* several mechanisms, and STAT1 and STAT3 play a central role (Villarino et al., 2015). A consistent immunophenotype in GOF *STAT1* and HIES patients is impaired development of Th17 lymphocytes, which could be the reason for their susceptibility to chronic mucocutaneous candidiasis or invasive fungal infection (Stark and Darnell, 2012; Olbrich and Freeman, 2018; Danion et al., 2020). This could explain the *T. marneffei* infection of P4 with *STAT3* and P5 with *STAT1* mutation.

It is noteworthy that the *IL12RB1* gene was first reported to be associated with *T. marneffei* infection in our cohort. *T. marneffei* infection has previously been reported in children with *IFNGR1* gene mutations. Both the *IL12RB1* and *IFNGR1* genes are involved in Mendelian susceptibility to mycobacterial disease (MSMD). Susceptibility to nontuberculous mycobacteria (NTM) infection, talaromycosis, histoplasmosis, cryptococcosis, melioidosis, and nontyphoidal salmonellosis has been reported in IFN-γ knockout mice or in patients with IFN-γ signaling defects, such as MSMD (Erb et al., 1999; Tang et al., 2010; Lee et al., 2013; Chi et al., 2016). A high prevalence of anti–IFN-γ autoantibodies is the major cause of severe *T. marneffei* infections in HIV-negative adults in China, which suggests that IFN-γ has a role in combating this fungal infection in humans (Guo et al., 2020). Human and mouse macrophages can control *T. marneffei* growth and kill intracellular yeast cells when activated by T-cell-derived cytokines (Cogliati et al., 1997; Sisto et al., 2003). IFN-γ is essential in the control of intracellular pathogens, such as Mycobacterium tuberculosis and fungi (Cooper et al., 1993). The fungicidal activity of *T. marneffei* yeast by macrophages could be enhanced by IFN-γ *via* stimulation of macrophages, which involves the nitric oxide (NO)-mediated killing system (Cogliati et al., 1997; Kudeken et al., 1998). In our study, three children were confirmed to have MSMD, including *IL12RB1* gene deficiency (P1, P2) and *IFNGR1* deficiency (P3). They had Mycobacterium tuberculosis and *T. marneffei* infections simultaneously. The clinical manifestations of P1 were the most serious, with recurrent fever, weight loss, severe anemia, splenomegaly and lymphadenopathy, requiring prolonged intensive antifungal treatment, as well as concomitant anti-Mycobacterium treatment.

Recently, mNGS has been successfully applied in the diagnosis of disseminated *T. marneffei* infection. The traditional standard for infection diagnosis relies on culture, histopathological staining and microscopy. Studies have shown that the combination of quantitative polymerase chain reaction (qPCR) and serum GM detection can be a valuable tool for the diagnosis of *T. marneffei* infection (Li et al., 2020; Wei et al., 2021). Patients with fungemia often have high GM results, such as P1, P2, P5 and P6. The measurement of BALF-GM is likely to be a useful tool for diagnosing invasive aspergillosis (Guo et al., 2010); however, its role in diagnosing *T. marneffei* has not been well established. mNGS is a new diagnostic technology to sequence all biological genomes in various clinical samples (Voelkerding et al., 2009). Compared with culture-based methods, mNGS showed obvious advantages with respect to high detection efficiency and quick speed. The detection accuracy of microorganisms, along with the positive rate, was higher in mNGS (Tsang et al., 2021; Zhou et al., 2021), which provides a faster and more accurate diagnostic method in clinical practice. The diagnostic efficiency analysis revealed that mNGS had a high diagnostic sensitivity of 100% and specificity of 98.7%. The significantly high positive likelihood rate indicated high accuracy of mNGS in determining *T. marneffei*, and the significantly low negative likelihood rate predicted that negative mNGS results could exclude *T. marneffei* infection. However, there was no significant difference between the two methods (p=0.25). Our study was a retrospective study, and there could be a risk of bias, which may originate in the relatively few patients enrolled, data collection and incomplete clinical data.

In clinical practice, the rapid diagnosis of *T. marneffei* infection in patients with IEI is of great importance. Disseminated *T. marneffei* infection may run a rapidly progressive course and be life-threatening without timely and effective antifungal therapy. However, cultures are quite time consuming (Cao et al., 2019), with a relatively limited positive rate due to the difficulty in cultivating slow-growing and fastidious microbes (Mo et al., 2002), which results in delayed diagnosis and increased mortality. A few studies have shown that mNGS has marked advantages over conventional methods for pathogenic diagnosis, particularly opportunistic pathogens and mixed infections in patients with IEI (Parize et al., 2017; Tang et al., 2021). For novel, rare, and treatment-refractory infectious diseases and for patients with immunocompromising disease, mNGS can significantly improve the pathogen detection rate and can be used as the front-line detection method (Cao et al., 2020). Unlike previous studies, mNGS was the main methodology in our cohort. mNGS can detect *T. marneffei* in a variety of samples, while traditional culture methods are often negative. In addition, the detection period of *T. marneffei* by mNGS was approximately 26 hours. Since infection can progress rapidly in children with immunodeficiency disease, pathogens should be identified as soon as possible using mNGS, and treatment can be initiated in time. Immunodeficient children may benefit from rapid detection of pathogens by mNGS.

5 Conclusion

T. marneffei is an opportunistic pathogen, suggesting potential immune impairment in infected individuals. We reported two cases of *IL12RB1* mutation in children infected with *T. marneffei*, extending the immunodeficiency spectrum of *T. marneffei* infection. For IEI patients with *T. marneffei* infection, we highlight the application of mNGS in the clinical diagnosis. mNGS is proposed as an important adjunctive diagnostic approach for rapidly identifying pathogens in complex and severe infections.

Data availability statement

The datasets presented in this study can be found in online repositories. The names of the repository/repositories and accession number(s) can be found below: NCBI repository, the accession number is PRJNA860094.

Ethics statement

The studies involving human participants were reviewed and approved by the ethics committee of Children's Hospital of Fudan University. Written informed consent to participate in this study was provided by the participants' legal guardian/next of kin. Written informed consent was obtained from the minor(s)' legal guardian/next of kin for the publication of any potentially identifiable images or data included in this article.

Author contributions

LL and BS contributed to conceptualizing and designing the study, conducting the investigation, and drafting the manuscript. JH contributed to conceptualizing and designing the study, conducting the investigation, and reviewing and revising the manuscript. XW contributed to conceptualizing the study and reviewing and revising the manuscript. JS contributed to supervising the methodology and reviewing the manuscript. WW, WY, MY, XH, and QZ contributed to collecting clinical data, conducting the investigation, carrying out the initial analyses, and reviewing the manuscript. YW and DL contributed to designing the methodology, conducting the laboratory experiments, and reviewing the manuscript. All authors approved the final manuscript as submitted and agreed to be accountable for all aspects of the work.

Acknowledgments

We gratefully acknowledge Meili Shen from Dinfectome Inc., Nanjing, China, who helped with the bioinformatics analysis.

Conflict of interest

The authors declare that the research was conducted in the absence of any commercial or financial relationships that could be construed as a potential conflict of interest.

Publisher's note

References

Ba, H., Peng, H., Cheng, L., Lin, Y., Li, X., He, X., et al. (2021). Case report: Talaromyces marneffei infection in a Chinese child with a complex heterozygous CARD9 mutation. *Front. Immunol.* 12, 685546. doi: 10.3389/fimmu.2021.685546

Cao, Q., Chen, B., Chen, L., Chen, P., and Bijie, H. (2020). Expert consensus on the clinical application of metagenomics next-generation sequencing technology for detection of infectious pathogens in China. *Chin. J. Infect. Dis.* 38 (11), 681–689. doi: 10.3760/cma.j.cn311365-20200731-00732

Cao, C., Xi, L., and Chaturvedi, V. (2019). Talaromycosis (Penicilliosis) due to talaromyces (Penicillium) marneffei: Insights into the clinical trends of a major fungal disease 60 years after the discovery of the pathogen. *MYCOPATHOL [Journal Article; Review].* 184 (6), 709–720. doi: 10.1007/s11046-019-00410-2

Chen, Z., Cheng, H., Cai, Z., Wei, Q., Li, J., Liang, J., et al. (2021). Identification of microbiome etiology associated with drug resistance in pleural empyema. *Front. Cell Infect. Microbiol. [Journal Article; Res. Support Non-U.S. Gov't].* 11, 637018. doi: 10.3389/fcimb.2021.637018

Chen, K., Tan, J., Qian, S., Wu, S., and Chen, Q. (2021). Case report: Disseminated talaromyces marneffei infection in a patient with chronic mucocutaneous candidiasis and a novel STAT1 gain-of-Function mutation. *Front. Immunol. [Case Reports; Res. Support Non-U.S. Gov't].* 12, 682350. doi: 10.3389/fimmu.2021.682350

Chen, X., Xu, Q., Li, X., Wang, L., Yang, L., Chen, Z., et al. (2020). Molecular and phenotypic characterization of nine patients with STAT1 GOF mutations in China. *J. Clin. Immunol. [Journal Article; Res. Support Non-U.S. Gov't].* 40 (1), 82–95. doi: 10.1007/s10875-019-00688-3

Chi, C. Y., Lin, C. H., Ho, M. W., Ding, J. Y., Huang, W. C., Shih, H. P., et al. (2016). Clinical manifestations, course, and outcome of patients with neutralizing anti-interferon-gamma autoantibodies and disseminated nontuberculous mycobacterial infections. *Med. (Baltimore). [Journal Article].* 95 (25), e3927. doi: 10.1097/MD.0000000000003927

Chiu, C. Y., and Miller, S. A. (2019). Clinical metagenomics. *Nat. Rev. Genet. [Journal Article; Review].* 20 (6), 341–355. doi: 10.1038/s41576-019-0113-7

Cogliati, M., Roverselli, A., Boelaert, J. R., Taramelli, D., Lombardi, L., and Viviani, M. A. (1997). Development of an *in vitro* macrophage system to assess penicillium marneffei growth and susceptibility to nitric oxide. *Infect. Immun.* 65 (1), 279–284. doi: 10.1128/iai.65.1.279-284.1997

Cooper, A. M., Dalton, D. K., Stewart, T. A., Griffin, J. P., Russell, D. G., and Orme, I. M. (1993). Disseminated tuberculosis in interferon gamma gene-disrupted mice. *J. Exp. Med.* 178 (6), 2243–2247. doi: 10.1084/jem.178.6.2243

Danion, F., Aimanianda, V., Bayry, J., Dureault, A., Wong, S., Bougnoux, M. E., et al. (2020). Aspergillus fumigatus infection in humans with STAT3-deficiency is associated with defective interferon-gamma and Th17 responses. *Front. Immunol.* 11, 38. doi: 10.3389/fimmu.2020.00038

Deng, Z., Ribas, J. L., Gibson, D. W., and Connor, D. H. (1988). Infections caused by penicillium marneffei in China and southeast Asia: review of eighteen published cases and report of four more Chinese cases. *Rev. Infect. Dis. [Case Reports; J. Article; Res. Support Non-U.S. Gov't; Review].* 10 (3), 640–652. doi: 10.1093/clinids/10.3.640

Ding, Y., Zhou, L., Xia, Y., Wang, W., Wang, Y., Li, L., et al. (2018). Reference values for peripheral blood lymphocyte subsets of healthy children in China. *J. Allergy Clin. Immunol. [Letter; Res. Support Non-U.S. Gov't].* 142 (3), 970–973. doi: 10.1016/j.jaci.2018.04.022

DiSalvo, A. F., Fickling, A. M., and Ajello, L. (1973). Infection caused by penicillium marneffei: description of first natural infection in man. *Am. J. Clin. Pathol. [Journal Article].* 60 (2), 259–263. doi: 10.1093/ajcp/60.2.259

Drummond, R. A., Saijo, S., Iwakura, Y., and Brown, G. D. (2011). The role of Syk/CARD9 coupled c-type lectins in antifungal immunity. *Eur. J. Immunol.* 41 (2), 276–281. doi: 10.1002/eji.201041252

Du, X., Tang, W., Chen, X., Zeng, T., Wang, Y., Chen, Z., et al. (2019). Clinical, genetic and immunological characteristics of 40 Chinese patients with CD40 ligand deficiency. *Scand. J. Immunol.* 90 (4), e12798. doi: 10.1111/sji.12798

Erb, K. J., Kirman, J., Delahunt, B., Moll, H., and Le Gros, G. (1999). Infection of mice with mycobacterium bovis-BCG induces both Th1 and Th2 immune responses in the absence of interferon-gamma signalling. *Eur. Cytokine Netw.* 10 (2), 147–154.

Erdos, M., Durandy, A., and Marodi, L. (2005). Genetically acquired class-switch recombination defects: the multi-faced hyper-IgM syndrome. *Immunol. Lett.* 97 (1), 1–6. doi: 10.1016/j.imlet.2004.09.021

Fan, H., Huang, L., Yang, D., Lin, Y., Lu, G., Xie, Y., et al. (2018). Pediatric hyperimmunoglobulin e syndrome: A case series of 4 children in China. *Med. (Baltimore). [Case Reports; J. Article].* 97 (14), e215. doi: 10.1097/MD.0000000000010215

Fan, J. H., Luo, H. Y., Yang, L. G., Wang, M. Y., and Xiao, Z. H. (2021). Penicilliosis marneffei in HIV negative children: three case reports. *Ann. Palliat Med. [Case Reports].* 10 (7), 8437–8447. doi: 10.21037/apm-20-2056

Goldberg, B., Sichtig, H., Geyer, C., Ledeboer, N., and Weinstock, G. M. (2015). Making the leap from research laboratory to clinic: Challenges and opportunities for next-generation sequencing in infectious disease diagnostics. *MBIO. [Journal Article; Review].* 6 (6), e1815–e1888. doi: 10.1128/mBio.01888-15

Grimbacher, B., Holland, S. M., Gallin, J. I., Greenberg, F., Hill, S. C., Malech, H. L., et al. (1999). Hyper-IgE syndrome with recurrent infections–an autosomal dominant multisystem disorder. *N Engl. J. Med.* 340 (9), 692–702. doi: 10.1056/NEJM199903043400904

Grimbacher, B., Schaffer, A. A., Holland, S. M., Davis, J., Gallin, J. I., Malech, H. L., et al. (1999). Genetic linkage of hyper-IgE syndrome to chromosome 4. *Am. J. Hum. Genet.* 65 (3), 735–744. doi: 10.1086/302547

Guo, Y. L., Chen, Y. Q., Wang, K., Qin, S. M., Wu, C., and Kong, J. L. (2010). Accuracy of BAL galactomannan in diagnosing invasive aspergillosis: a bivariate metaanalysis and systematic review. *CHEST. [Journal Article; Meta-Analysis; Systematic Review].* 138 (4), 817–824. doi: 10.1378/chest.10-0488

Guo, J., Ning, X., Ding, J., Zheng, Y., Shi, N., Wu, F., et al. (2020) Anti–IFN-γ autoantibodies underlie disseminated talaromyces marneffei infections. *J. Exp. Med* 217(12), e20190502. doi: 10.1084/jem.20190502

Hu, Y., Zhang, J., Li, X., Yang, Y., Zhang, Y., Ma, J., et al. (2013). Penicillium marneffei infection: an emerging disease in mainland china. MYCOPATHOLOGIA. *[Journal Article; Res. Support Non-U.S. Gov't].* 175 (1-2), :57–:67. doi: 10.1007/s11046-012-9577-0

Kamchaisatian, W., Kosalaraksa, P., Benjaponpitak, S., Hongeng, S., Direkwattanachai, C., Lumbiganon, P., et al. (2006). Penicilliois in patients with X-linked hyperimmunoglobulin m syndrome (XHIGM), case reports from Thailand. *J. Allergy Clin. Immunol.* 117 (2), S282. doi: 10.1016/j.jaci.2005.12.1166

Kawila, R., Chaiwarith, R., and Supparatpinyo, K. (2013). Clinical and laboratory characteristics of penicilliosis marneffei among patients with and without HIV infection in northern Thailand: a retrospective study. *BMC Infect. Dis. [Journal Article].* 13, 464. doi: 10.1186/1471-2334-13-464

Kudeken, N., Kawakami, K., Kusano, N., and Saito, A. (1996). Cell-mediated immunity in host resistance against infection caused by penicillium marneffei. *J. Med. Vet. Mycol. [Journal Article].* 34 (6), 371–378. doi: 10.1080/02681219680000671

Kudeken, N., Kawakami, K., and Saito, A. (1997). CD4+ T cell-mediated fatal hyperinflammatory reactions in mice infected with penicillium marneffei. *Clin. Exp. Immunol. [Journal Article].* 107 (3), 468–473. doi: 10.1046/j.1365-2249.1997.d01-945.x

Kudeken, N., Kawakami, K., and Saito, A. (1998). Different susceptibilities of yeasts and conidia of penicillium marneffei to nitric oxide (NO)-mediated fungicidal activity of murine macrophages. *Clin. Exp. Immunol. [Journal Article; Res. Support Non-U.S. Gov't].* 112 (2), 287–293. doi: 10.1046/j.1365-2249.1998.00565.x

Lee, P. P. W., Chan, K., Lee, T., Ho, M. H., Chen, X., Li, C., et al. (2012). Penicilliosis in children without HIV infection–are they immunodeficient? *Clin. Infect. Dis.* 54 (2), e8–19. doi: 10.1093/cid/cir754

Lee, W., Huang, J., Wu, T., Lee, M., Chen, I. J., Yu, K., et al. (2013). Patients with inhibitory and neutralizing auto-antibodies to interferon-γ resemble the sporadic adult-onset phenotype of mendelian susceptibility to mycobacterial disease (MSMD) lacking bacille calmette–guerin (BCG)-induced diseases. *IMMUNOBIOLOGY.* 218 (5), 762–771. doi: 10.1016/j.imbio.2012.08.281

Lee, P. P., Lao-araya, M., Yang, J., Chan, K., Ma, H., Pei, L., et al. (2019). Application of flow cytometry in the diagnostics pipeline of primary immunodeficiencies underlying disseminated talaromyces marneffei infection in HIV-negative children. *Front. Immunol.* 10, 2189. doi: 10.3389/fimmu.2019.02189

Lee, P. P., and Lau, Y. L. (2017). Cellular and molecular defects underlying invasive fungal infections-revelations from endemic mycoses. *Front. Immunol.* 8, 735. doi: 10.3389/fimmu.2017.00735

Lee, P. P., Mao, H., Yang, W., Chan, K. W., Ho, M. H., Lee, T. L., et al. (2014). Penicillium marneffei infection and impaired IFN-gamma immunity in humans with autosomal-dominant gain-of-phosphorylation STAT1 mutations. *J. Allergy Clin. Immunol. [Letter; Res. Support Non-U.S. Gov't].* 133 (3), 894–896. doi: 10.1016/j.jaci.2013.08.051

Le, T., Wolbers, M., Chi, N. H., Quang, V. M., Chinh, N. T., Huong Lan, N. P., et al. (2011). Epidemiology, seasonality, and predictors of outcome of AIDS-associated penicillium marneffei infection in ho chi minh city, Viet nam. *Clin. Infect. Dis.* 52 (7), 945–952. doi: 10.1093/cid/cir028

Li, W. J., Guo, Y. L., Liu, T. J., Wang, K., and Kong, J. L. (2015). Diagnosis of pneumocystis pneumonia using serum (1-3)-beta-D-Glucan: a bivariate meta-analysis and systematic review. *J. Thorac. Dis. [Journal Article].* 7 (12), 2214–2225. doi: 10.3978/j.issn.2072-1439.2015.12.27

Li, L., Li, J., Zheng, R., Zheng, Y., and Wang, W. (2018). Clinical analysis of 3 HIV negative children with penicilliosis. *Jiangxi Med. J.* 53 (09), 986–989. doi: 10.3969/j.issn.1006-2238.2018.9.028

Li, Y., Sun, B., Tang, X., Liu, Y. L., He, H. Y., Li, X. Y., et al. (2020). Application of metagenomic next-generation sequencing for bronchoalveolar lavage diagnostics in critically ill patients. *Eur. J. Clin. Microbiol. Infect. Dis. [Journal Article].* 39 (2), 369–374. doi: 10.1007/s10096-019-03734-5

Liyan, X., Changming, L., Xianyi, Z., Luxia, W., and Suisheng, X. (2004). Fifteen cases of penicilliosis in guangdong, China. *MYCOPATHOLOGIA* 158 (2), 151–155. doi: 10.1023/B:MYCO.0000041842.90633.86

Li, X., Zheng, Y., Wu, F., Mo, D., Liang, G., Yan, R., et al. (2020). Evaluation of quantitative real-time PCR and platelia galactomannan assays for the diagnosis of disseminated talaromyces marneffei infection. *Med. Mycol. [Evaluation Study; J. Article].* 58 (2), 181–186. doi: 10.1093/mmy/myz052

Lu, Y., Chen, Y. Q., Guo, Y. L., Qin, S. M., Wu, C., and Wang, K. (2011). Diagnosis of invasive fungal disease using serum (1–>3)-beta-D-glucan: a bivariate meta-analysis. *Intern. Med. [Journal Article; Meta-Analysis].* 50 (22), 2783–2791. doi: 10.2169/internalmedicine.50.6175

Ma, B. H. M., Ng, C. S. H., Lam, R. K. Y., Wan, S., Wan, I. Y. P., Lee, T. W., et al. (2009). Recurrent hemoptysis with penicillium marneffei and stenotrophomonas maltophilia in job's syndrome. *Can. Respir. J.* 16 (4), e50–e52. doi: 10.1155/2009/586919

Mo, W., Deng, Z., and Li, S. (2002). Clinical blood routine and bone marrow smear manifestations of disseminated penicilliosis marneffei. *Chin. Med. J. (Engl). [Journal Article].* 115 (12), 1892–1894.

Olbrich, P., and Freeman, A. F. (2018). STAT1 and STAT3 mutations: important lessons for clinical immunologists. *Expert Rev. Clin. IMMU.* 14 (12), 1029–1041. doi: 10.1080/1744666X.2018.1531704

Pan, M., Qiu, Y., Zeng, W., Tang, S., Wei, X., and Zhang, J. (2020). Disseminated talaromyces marneffei infection presenting as multiple intestinal perforations and diffuse hepatic granulomatous inflammation in an infant with STAT3 mutation: a case report. *BMC Infect. Dis.* 20 (1):394. doi: 10.1186/s12879-020-05113-4

Parize, P., Muth, E., Richaud, C., Gratigny, M., Pilmis, B., Lamamy, A., et al. (2017). Untargeted next-generation sequencing-based first-line diagnosis of infection in immunocompromised adults: a multicentre, blinded, prospective

study. *Clin. Microbiol. Infect. [Comparative Study; Eval. Study; J. Article; Multicenter Study]*. 23 (8), 571–574. doi: 10.1016/j.cmi.2017.02.006

Qian, Y. Y., Wang, H. Y., Zhou, Y., Zhang, H. C., Zhu, Y. M., Zhou, X., et al. (2020). Improving pulmonary infection diagnosis with metagenomic next generation sequencing. *Front. Cell Infect. Microbiol. [Journal Article; Res. Support Non-U.S. Gov't]*. 10, 567615. doi: 10.3389/fcimb.2020.567615

Qiu, Y., Liao, H., Zhang, J., Zhong, X., Tan, C., and Lu, D. (2015). Differences in clinical characteristics and prognosis of penicilliosis among HIV-negative patients with or without underlying disease in southern China: a retrospective study. *BMC Infect. Dis.* 15 (1):525. doi: 10.1186/s12879-015-1243-y

Salazar, F., and Brown, G. D. (2018). Antifungal innate immunity: A perspective from the last 10 years. *J. INNATE Immun.* 10 (5-6), 373–397. doi: 10.1159/000488539

Schlaberg, R., Chiu, C. Y., Miller, S., Procop, G. W., and Weinstock, G. (2017). Validation of metagenomic next-generation sequencing tests for universal pathogen detection. *Arch. Pathol. Lab. Med. [Journal Article; Validation Study]*. 141 (6), 776–786. doi: 10.5858/arpa.2016-0539-RA

Segretain, G. (1959). [Penicillium marneffei n.sp., agent of a mycosis of the reticuloendothelial system]. *Mycopathol Mycol Appl.* 11, 327–353. doi: 10.1007/BF02089507

Sisto, F., Miluzio, A., Leopardi, O., Mirra, M., Boelaert, J. R., and Taramelli, D. (2003). Differential cytokine pattern in the spleens and livers of BALB/c mice infected with penicillium marneffei: protective role of gamma interferon. *Infect. Immun.* 71 (1), 465–473. doi: 10.1128/IAI.71.1.465-473.2003

Sripa, C., Mitchai, J., Thongsri, W., and Sripa, B. (2010). Diagnostic cytology and morphometry of penicillium marneffei in the sputum of a hypogammaglobulinemia with hyper-IgM patient. *J. Med. Assoc. Thai. [Case Reports; J. Article]*. 93 Suppl 3, S69–S72.

Stark, G. R., and Darnell, J. J. (2012). The JAK-STAT pathway at twenty. *IMMUNITY*. 36 (4), 503–514. doi: 10.1016/j.immuni.2012.03.013

Su, S. S., Chen, X. B., Zhou, L. P., Lin, P. C., Chen, J. J., Chen, C. S., et al. (2022). Diagnostic performance of the metagenomic next-generation sequencing in lung biopsy tissues in patients suspected of having a local pulmonary infection. *BMC PULM Med. [Journal Article]*. 22 (1), 112. doi: 10.1186/s12890-022-01912-4

Supparatpinyo, K., Khamwan, C., Baosoung, V., Nelson, K. E., and Sirisanthana, T. (1994). Disseminated penicillium marneffei infection in southeast Asia. *Lancet [Journal Article]* 344 (8915), 110–113. doi: 10.1016/s0140-6736(94)91287-4

Tang, B. S., Chan, J. F., Chen, M., Tsang, O. T., Mok, M. Y., Lai, R. W., et al. (2010). Disseminated penicilliosis, recurrent bacteremic nontyphoidal salmonellosis, and burkholderiosis associated with acquired immunodeficiency due to autoantibody against gamma interferon. *Clin. Vaccine Immunol.* 17 (7), 1132–1138. doi: 10.1128/CVI.00053-10

Tangye, S. G., Al-Herz, W., Bousfiha, A., Chatila, T., Cunningham-Rundles, C., Etzioni, A., et al. (2020). Human inborn errors of immunity: 2019 update on the classification from the international union of immunological societies expert committee. *J. Clin. Immunol. [Journal Article; Res. Support Non-U.S. Gov't]*. 40 (1), 24–64. doi: 10.1007/s10875-019-00737-x

Tang, W., Zhang, Y., Luo, C., Zhou, L., Zhang, Z., Tang, X., et al. (2021). Clinical application of metagenomic next-generation sequencing for suspected infections in patients with primary immunodeficiency disease. *Front. Immunol. [Comparative Study; J. Article; Res. Support Non-U.S. Gov't]*. 12, 696403. doi: 10.3389/fimmu.2021.696403

Tsang, C. C., Teng, J., Lau, S., and Woo, P. (2021). Rapid genomic diagnosis of fungal infections in the age of next-generation sequencing. *J. Fungi (Basel).* 7 (8), 636. doi: 10.3390/jof7080636

van Kooten, C., and Banchereau, J. (2000). CD40-CD40 ligand. *J. Leukoc. Biol.* 67 (1), 2–17. doi: 10.1002/jlb.67.1.2

Villarino, A. V., Kanno, Y., Ferdinand, J. R., and O'Shea, J. J. (2015). Mechanisms of Jak/STAT signaling in immunity and disease. *J. Immunol.* 194 (1), 21–27. doi: 10.4049/jimmunol.1401867

Voelkerding, K. V., Dames, S. A., and Durtschi, J. D. (2009). Next-generation sequencing: from basic research to diagnostics. *Clin. Chem. [Journal Article; Review]*. 55 (4), 641–658. doi: 10.1373/clinchem.2008.112789

Wang, H., Lu, Z., Bao, Y., Yang, Y., de Groot, R., Dai, W., et al. (2020). Clinical diagnostic application of metagenomic next-generation sequencing in children with severe nonresponding pneumonia. *PloS One [Journal Article; Res. Support Non-U.S. Gov't]*. 15 (6), e232610. doi: 10.1371/journal.pone.0232610

Wei, H. Y., Liang, W. J., Li, B., Wei, L. Y., Jiang, A. Q., Chen, W. D., et al. (2021). Clinical characteristics and risk factors of talaromyces marneffei infection in human immunodeficiency virus-negative patients: A retrospective observational study. *World J. Emerg. Med. [Journal Article]*. 12 (4), 281–286. doi: 10.5847/wjem.j.1920-8642.2021.04.005

You, C., Hu, F., Lu, S., Pi, D., Xu, F., Liu, C., et al. (2021). Talaromyces marneffei infection in an HIV-negative child with a CARD9 mutation in China: A case report and review of the literature. *MYCOPATHOLOGIA*. 186 (4), 553–561. doi: 10.1007/s11046-021-00576-8

Yuen, W. C., Chan, Y. F., Loke, S. L., Seto, W. H., Poon, G. P., and Wong, K. K. (1986). Chronic lymphadenopathy caused by penicillium marneffei: a condition mimicking tuberculous lymphadenopathy. *Br. J. Surg. [Case Reports; J. Article]*. 73 (12), 1007–1008. doi: 10.1002/bjs.1800731224

Zhang, W., Ye, J., Qiu, C., Wang, L., Jin, W., Jiang, C., et al. (2020). Rapid and precise diagnosis of t. marneffei pulmonary infection in a HIV-negative patient with autosomal-dominant STAT3 mutation: a case report. *Ther. Adv. Respir. Dis. [Case Reports]*. 14, 1022303031. doi: 10.1177/1753466620929225

Zhou, Q., Hui, X., Ying, W., Hou, J., Wang, W., Liu, D., et al. (2018). A cohort of 169 chronic granulomatous disease patients exposed to BCG vaccination: a retrospective study from a single center in shanghai, China (2004-2017). *J. Clin. Immunol. [Journal Article; Multicenter Study; Res. Support Non-U.S. Gov't]*. 38 (3), 260–272. doi: 10.1007/s10875-018-0486-y

Zhou, Y., Liu, Y., and Wen, Y. (2021). Gastrointestinal manifestations of talaromyces marneffei infection in an HIV-infected patient rapidly verified by metagenomic next-generation sequencing: a case report. *BMC Infect. Dis. [Case Reports; J. Article]*. 21 (1), 376. doi: 10.1186/s12879-021-06063-1

frontiers | Frontiers in Cellular and Infection Microbiology

TYPE Original Research
PUBLISHED 16 September 2022
DOI 10.3389/fcimb.2022.947486

OPEN ACCESS

EDITED BY
Eda Altan,
University of Turku, Finland

REVIEWED BY
Thomas Jové,
INSERM U1092 Anti-Infectieux supports moléculaires des résistances et innovations thérapeutiques, France
Tsute Chen,
The Forsyth Institute, United States

*CORRESPONDENCE
Huiling Yang
yanghuiling3018@sina.com
Ping Xu
ping-xu@hotmail.com

†These authors have contributed equally to this work

SPECIALTY SECTION
This article was submitted to Clinical Microbiology, a section of the journal Frontiers in Cellular and Infection Microbiology

RECEIVED 18 May 2022
ACCEPTED 22 August 2022
PUBLISHED 16 September 2022

CITATION
Lv Z, Chen Y, Zhou H, Chen Z, Yao Q, Ren J, Liu X, Liu S, Deng X, Pang Y, Chen W, Yang H and Xu P (2022) Genomic characterization of two metagenome-assembled genomes of *Tropheryma whipplei* from China. *Front. Cell. Infect. Microbiol.* 12:947486. doi: 10.3389/fcimb.2022.947486

Genomic characterization of two metagenome-assembled genomes of *Tropheryma whipplei* from China

Zhongdong Lv[1†], Yong Chen[2,3†], Houqing Zhou[4†], Zhonglin Chen[2,3], Qianru Yao[2,3], Jiali Ren[2,3], Xianglu Liu[1], Shuang Liu[1], Xiaomei Deng[5], Yingchen Pang[1], Weijun Chen[2,3], Huiling Yang[6*] and Ping Xu[1*]

[1]Department of Respiration and Critical Care Medicine, Peking University Shenzhen Hospital, Shenzhen, China, [2]Clinical Laboratory of BGI Health, BGI-Shenzhen, Shenzhen, China, [3]BGI PathoGenesis Pharmaceutical Technology Co., Ltd, BGI-Shenzhen, Shenzhen, China, [4]Department of Laboratory Medicine, Fuwai Hospital Chinese Academy of Medical Sciences, Shenzhen, China, [5]Comprehensive Ward, Peking University Shenzhen Hospital, Shenzhen, China, [6]Guangdong Provincial Key Laboratory of Research and Development of Natural Drugs, and School of Pharmacy, Guangdong Medical University, Dongguan, China

Whipple's disease is a rare chronic systemic disease that affects almost any organ system of the body caused by the intracellular bacterium *Tropheryma whipplei*, which is found ubiquitously in the environment. Sequencing of the *T. whipplei genome* has revealed that it has a reduced genome (0.93 Mbp), a characteristic shared with other intracellular bacteria. Until our research started, 19 *T. whipplei* strains had been sequenced from cultures originated in France, Canada, and Germany. The genome of *T. whipplei* bacterium has not been studied in Asia yet. Here, two metagenome-assembled genomes (MAGs) of *T. whipplei* from China were reconstructed through metagenomic next-generation sequencing (mNGS) and genome binning. We also provided genomic insights into the geographical role and genomic features by analyzing the whole genome. The whole-genome phylogenetic tree was constructed based on single-nucleotide polymorphism (SNP) distance calculations and then grouped by distance similarity. The phylogenetic tree shows inconsistencies with geographic origins, thus suggesting that the variations in geographical origins cannot explain the phylogenetic relationships among the 21 *T. whipplei* strains. The two Chinese strains were closely related to each other, and also found to be related to strains from Germany (*T. whipplei* TW08/27) and France (*T. whipplei* Bcu26 and *T. whipplei* Neuro1). Furthermore, the Average Nucleotide Identity (ANI) matrix also showed no association between geographic origins and genomic similarities. The pan-genome analysis revealed that *T. whipplei* has a closed pan-genome composed of big core-genomes and small accessory genomes, like other intracellular bacteria. By examining the genotypes of the sequenced strains, all 21 *T. whipplei* strains were found to be resistant to fluoroquinolones, due to the

genetic mutations in genes *gyrA*, *gyrB*, *parC*, and *parE*. The 21 *T. Whipplei* strains shared the same virulence factors, except for the *alpC* gene, which existed in 7 out of the 21 *T. whipplei* strains. When comparing 21 entire *T. whipplei* pan-genomes from various nations, it was discovered that the bacterium also possessed a closed genome, which was a trait shared by intracellular pathogens.

KEYWORDS

tropheryma whipplei, whole-genome analysis, bronchoalveolar lavage (BAL), immunodeficiency – primary, metagenome-assembled genome (MAGs)

Introduction

The Gram-positive bacterium *Tropheryma whipplei* causes a rare multi-systematic infectious disease known as Whipple's disease, which has clinical manifestations of fever, weight loss, lymphadenopathy, and polyarthritis, as well as cardiac manifestations and central nervous system complications (Ratliff et al., 1984; Durand et al., 1997). The "intestinal lipodystrophy" disease was first reported by George H. Whipple in 1907 and renamed Whipple's disease by Black-Schaffer in 1949 (Black-Schaffer, 1949). A bacterial infection was long believed to be responsible for Whipple's disease until in 1961 when the real origin of the disease was discovered by electron microscopy. Researchers detected bacterial inclusions in macrophages and monocytes, which together constituted the predominant infected cell types of this disease (Yardley and Hendrix, 1961). Researchers discovered that *T. whipplei* is a fastidious bacterium and extremely difficult to culture. The bacterium was first successfully isolated and grown in inactivated human mononuclear phagocytes by Schoedon in 1997, but culture could not be reproduced (Schoedon et al., 1997). In 2000, Raoult isolated the bacterium *T. whipplei* Twist from the aortic valve of a patient with endocarditis and propagated it in a human fibroblast cell line with the doubling time of 18 days; however, it could not be cultivated in the absence of living eukaryotic cells (Raoult et al., 2000). Subsequently, Raoult found a doubling time of 32 to 34 h for *T. whipplei* Twist strain, when propagated in the MRC5 cell culture system (Masselot et al., 2003). However, this doubling time was still longer than the slowly growing bacterium *M. tuberculosis* (14.3 *h* to 24 h) (James et al., 2000). In 2001, the *T. whipplei* strain Twist-Marseille was proposed by La Scola as the type strain of a new species of a new genus. The detailed characterization of the bacterium was described and deposited at the Collection Nationale de Culture de Micro-organisms de l'Institut Pasteur, Paris, France (La Scola et al., 2001).

The cultivation of *T. whipplei* made it possible to reveal the genome. So far, 19 strains of *T. whipplei* had been successfully cultured, and their genomes were sequenced by Bentley et al. (2003); Raoult et al. (2003), and Wetzstein (2017). Similar to other intracellular bacteria with rudimentary metabolic functions, genomic sequencing revealed that *T. whipplei* had a reduced genome (*T. whipplei* Twist, 0.93 Mbp). *T. whipplei* is ubiquitous in the environment, and it can lead to widespread colonization of the lower respiratory tract of healthy children and adults (Dickson et al., 2015). The bacterium could result in endocarditis, gastrointestinal infection, neurological complications and pulmonary infection, but the incident of Whipple's disease is very rare. There were some reports of pulmonary infection caused by *T. whipplei*, which were diagnosed by metagenomic next-generation sequencing (Li et al., 2021; Zhu et al., 2021). *T. whipplei* is a commensal bacterium that only causes Whipple's disease in a small number of individuals. Our understanding of the genome of *T. whipplei* from China is still not clear, due to the harsh cultivation conditions and the lengthy culture period. Metagenomic next-generation sequencing (mNGS) is a high-throughput sequencing technique that sequences all nucleic acids in a sample simultaneously *in situ*, which includes *T. whipplei* DNA if an individual had been infected by Whipple's disease. The possible clinical mNGS applications are tremendous, including diagnosis of infectious diseases, outbreak tracking, infection control surveillance, and new pathogen discovery, among many other purposes. This emerging approach is an unbiased hypothesis-free diagnostic tool. It has been widely applied to guiding infectious disease management and developing treatment strategies. Next-generation sequencing (NGS) makes it possible to analyze genomes precisely and accurately, which aids the detection of single-nucleotide polymorphisms (SNPs) on a large scale. A metagenome-assembled genome *T. whipplei* shenzhen1 was assembly based on binned metagenome data of bronchoalveolar lavage samples from 26 non-immunodeficient patients, and metagenome-assembled genome *T. whipplei* shenzhen2 genome was assembled based on metagenome data of a bronchoalveolar lavage sample from an immunodeficient patient. All bronchoalveolar lavage samples from patients were

collected by Peking University Shenzhen Hospital in China. The purpose of this study is to answer whether there was any difference between *T. whipplei* shenzhen1 and *T. whipplei* shenzhen2 genome, as well as the 19 genomes of *T. whipplei* that had been deposited in the NCBI database, including the two completed genomes of *T. whipplei* Twist and *T. whipplei* TW08/27 (Bentley et al., 2003; Raoult et al., 2003; Wetzstein, 2017).

Materials and methods

Sample collection and DNA extraction

Bronchoalveolar lavage fluid (BALF) samples were collected from one immunodeficient patient and 26 non-immunodeficient patients who had been admitted to Shenzhen Peking University Shenzhen Hospital with pulmonary infection. We subsequently extracted total genomic DNA from each BALF sample. Briefly, 0.6 ml of BALF and 250 µl of 0.5-mm glass beads in a 1.5-ml microcentrifuge tube were attached to a horizontal platform on a vortex mixer and agitated vigorously at 2,800–3,200 rpm for 30 min. Then, 7.2 µl of lysozyme was added for wall-breaking reaction. A 0.3-ml sample was separated into a new 1.5-ml microcentrifuge tube and DNA was extracted using the TIANamp Micro DNA Kit (DP316, TIANGEN BIOTECH) according to the manufacturer's recommendation.

DNA library construction and sequencing

The extracted DNA obtained in the previous step was first fragmented to yield 300-bp fragments using enzymatic digestion (RM0434, BGI Wuhan Biotechnology). To construct the DNA library, fragmented DNA was further end-repaired, ligated to adapters, and amplified using PCR with the PMseq high-throughput gene detection kit for infectious pathogens (combined probe anchored polymerization sequencing method, BGI-Shenzhen, China, RM0438), according to the manufacturer's instruction. Based on the qualified double-strand DNA library, the single-stranded circular DNA library was then generated through DNA denaturation and circularization. Then, DNA nanoballs (DNBs) were formed by rolling circle amplification (RCA) using a universal kit for sequencing reaction (Combinatorial Probe-Anchor Synthesis, BGI-Shenzhen, China, RM0170). DNBs were qualified by the Qubit® ssDNA Assay Kit (Thermo Fisher Scientific) and were further sequenced by the MGISEQ-2000 platform (MGI, China).

Metagenome-assembly genome of *T. whipplei*

A quality control step was conducted on the metagenomic sequencing data by using the fastp tool to filter out low-quality and contaminated reads. By utilizing the Burrows-Wheeler alignment algorithm, the human DNA reads that aligned to human reference genome HG19 were eliminated, and only microbe reads were reserved. The remaining data were mapped and classified by aligning the reads to genomes of bacteria, fungi, viruses, and parasites from the Pathogens Metagenomics Database (PMDB). The classification reference databases were downloaded from NCBI (ftp://ftp.ncbi.nlm.nih.gov/genomes/). *T. whipplei* was found in all 27 BALF samples, according to the mNGS diagnostic results. The *T. whipplei* shenzhen1 genome was assembled by combining metagenomic sequencing data of BALF samples from 26 non-immunodeficient patients with low-quality reads, and host genomes were removed. The *T. whipplei* shenzhen2 genome was assembled using metagenomic sequencing data of BALF sample from one immunodeficient patient. Briefly, the reads were subjected to *de novo* metagenomic assembly through metaSPAdes, and contigs shorter than 1,000 nt were discarded from further processing. Reads were mapped to contigs using Bowtie2, and the mapping output was used for contig binning through MetaBAT2. Lastly, putative genomes were subjected to quality control to generate the final set of reconstructed draft genomes. Two metagenome assembled genomes of *T. whipplei* from China were obtained. Table 1 summarizes the origin and the genome information of *T. whipplei* strains from China in this study and the 19 *T. whipplei* genomes reported by other researchers.

Whole-genome phylogenetic tree analysis

Conducting whole-genome phylogenetic tree for microbial pathogens is a powerful approach that assists scientists to gain a better understanding of how species have evolved while explaining the similarities and differences among species. A wide range of genomic features can be observed across the entire genome derived from mNGS. These characteristics make phylogeny building extremely accurate. To discover the evolution of the 21 *T. whipplei* strains' origin from different countries, the phylogenetic trees were constructed based on SNP datasets.

Characterization of core-genome and pan-genome

To characterize the core- and pan-genomes of the 21 strains of the *T. whipplei* genome, the PEPPAN pipeline, which can construct pan-genomes from thousands of genetically diverse bacterial genomes, was applied (Zhou et al., 2020). Genes presented in all 21 *T. whipplei* genomes were considered to be

TABLE 1 Summary of 21 *T. whipplei* strains studied in this study.

Strain	Genome size (Mb)	GC-content (%)	Level	Accession	Geographical origin
Twist	0.927303	46.3	Chromosome	AE014184.1	Canada
TW08/27	0.925938	46.3	Chromosome	BX072543.1	Germany
SLOW2	0.927621	46.3	Scaffold	HG794425.1	France
NEURO1	0.927567	46.3	Scaffold	NZ_HG421449.1	Germany
DIG7	0.927564	46.3	Scaffold	HG794427.1	France
DIG9	0.880115	46.4	Contig	CAUY000000000	France
DIG10	0.927515	46.4	Scaffold	HG794428.1	Germany
ART1	0.927575	46.3	Scaffold	HG424698.1	France
NEURO14	0.885853	46.4	Contig	CAUR000000000	Germany
DIG15	0.927582	46.3	Scaffold	HG794423.1	Germany
DIGMUSC17	0.884564	46.4	Contig	CAVA000000000	France
NEURO20	0.883582	46.3	Contig	CAUX000000000	Germany
DIGADP25	0.883649	46.3	Contig	CAUW000000000	France
TWBCU26	0.880271	46.4	Contig	CAVB000000000	France
ENDO27	0.927598	46.4	Scaffold	HG794429.1	France
SALI28	0.927465	46.4	Scaffold	HG794430.1	France
ART29	0.927595	46.3	Scaffold	HG794431.1	France
PNEUMO30	0.927553	46.4	Scaffold	HG794432.1	France
ENDO32	0.927567	46.4	Scaffold	HG794424.1	France
shenzhen1	0.883965	46.4	Scaffold	JAMYWJ000000000	China
shenzhen2	0.899012	46.6	Scaffold	JAMYWK000000000	China

Genome size, GC-contents, genome assembly level, accession codes, and geographical origin are depicted as well.

the core-genome, genes presented in more than 95% but not in all strains were defined as the softcore genes, genes presented in 15%–95% of the genomes were considered the shell genes, while genes presented in lower than 15% of the genomes were defined as the cloud genes. The pan-genome analysis of the 21 *T. whipplei* was performed by Anvi`o workflow to display the genome, which is an advanced analysis and visualization platform that offers both automated and/or user-specified characterization of metagenomic assembly genomes. (Eren et al., 2015)

Average nucleotide identity analysis

Average nucleotide identity analysis is a useful approach to compare genetic relatedness among prokaryotic genomes The whole-genome average nucleotide identity (ANI) values for the 21 *T. whipplei* strains belonging to diverse geographic origins (Goris et al., 2007; Jain et al., 2018) were calculated to assess the genome similarities by using the FastANI v.0.1.3 software, which produces accurate ANI estimates and is a more efficient approach than alignment (e.g., BLAST)-based approaches.

Identification of antibiotic-resistant genes and virulence genes

To comprehend the virulence genes of the *T. whipplei* pathogens, 21 *T. whipplei* genomes were annotated with the Prokka annotation pipeline (ProkkaAnnotation v.3.2.1), and we then utilized the BLAST search tool for all known VF-related genes found in the virulence factor database (VFDB) (Chen et al., 2005). At the same time, the virulence factors were compared between *T. whipplei* strains originating from different countries. Reliable virulence genes were confirmed if the sequence identities were greater than 80% and the query coverages were greater than 80%, in which the values are used as benchmarks for virulence factor detection. The aligned amino acid sequences of GyrA, GyrB, ParC, and ParE for 21 *T. whipplei* strains were submitted to ESPript 3 to perform the sequence similarities, respectively (Robert and Gouet, 2014).

For the 21 genomes of *T. whipplei*, antibiotic resistance genes were predicted by aligning the hybrid assembled sequences in the CARD database using RGI v4.2.2 (Resistance Gene Identifier). Subsequently, the genes and the subsequent protein sequence were predicted using Prodigal. During this step,

sequences that had an identity of less than 75% or a length coverage of less than 50% with the resistant genes denoted in the database were removed (Jia et al., 2017). The antibiotic resistance genes of *T. whipplei* were predicted using RAST (Rapid Annotation using Subsystem Technology, https://rast.nmpdr.org/), which is an automated service for annotating bacterial genomes.

Results

The pathogen diagnosis of severe respiratory diseases was carried out using clinical metagenomic next-generation sequencing on 27 BALF samples from one immunodeficient patient and 26 non-immunodeficient patients who were admitted to Shenzhen Peking University Hospital. The metagenome-assembled genome of *T. whipplei* shenzhen1 was constructed based on the binned metagenomes of 26 BALF samples from non-immunodeficient patients, whereas the metagenome-assembled genome *T. whipplei* shenzhen2 genome was built based on one metagenome of a BALF sample from an immunodeficient patient.

Whole-genome phylogenetic tree analysis

The whole-genome phylogenetic tree constructed with 21 strains of the *T. whipplei* genome comprises three major clades, while one clade contains two subclades (Figure 1). The two strains *T. whipplei* shenzhen1 and *T. whipplei* shenzhen2 from China, the two strains *T. whipplei* TW08/27 and *T. whipplei* Meuro1 from Germany, and the one strain *T. whipplei* Bcu26 from France are located within the same subclade in the phylogenetic tree. Furthermore, the clades and subclades in the phylogenetic tree are not correlated with the geographical origins of *T. whipplei*.

Characterization of core-genome and pan-genome

To uncover the view of *T. whipplei* genome contents, the core-genome and pan-genome for 21 *T. whipplei* assembled genomes were calculated. The pan-genome of *T. whipplei* contained 977 genes, which were predicted by using the PEPPAN pipeline. The core-genome contained 809 genes that are common to all 21 strains of *T. whipplei*, and the core-genome accounts for 82.8% of the pan-genome, indicating that *T. whipplei* has a closed pan-genome. An additional 22 genes belong to the softcore genes, 58 genes form the shell genes, and 88 genes belong to the cloud genes. The pan-genome of 21 *T. whipplei* genomes was further analyzed by Anvi`o pan-genomic pipeline to visualize the pan-genome (Figure 2). As Figure 2 shows, the single-copy core genes occupy a major part of the pan-genome. Thirteen singleton gene clusters were found from *T. whipplei* TW08/27, which is the maximum number of singleton gene clusters of *T. whipplei*. We could thus hypothesize that *T. whipplei* is a strictly intracellular living organism that has a reduced genome, and no significant horizontal gene transfer has taken place in the past.

Average nucleotide identity analysis

The whole-genome ANI lay between 99.11% and 99.98%, whereas the median ANI of all sequenced strains is 99.54% when all 21 *T. whipplei* genomes were compared with each other. The

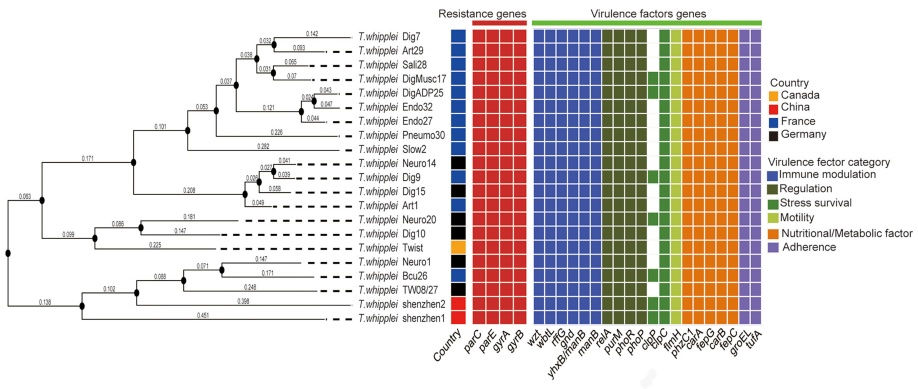

FIGURE 1
Whole-genome phylogenetic tree of 21 *T. whipplei* was constructed by single-nucleotide polymorphism (SNP) distance calculation, and the geographical origin of strains was obtained. The heatmaps represent the predicted resistance genes of chromosomal mutations known to confer resistance (gyrase and topoisomerase mutations conferring fluoroquinolone resistance) and the predicted virulence factors of *T. whipplei*.

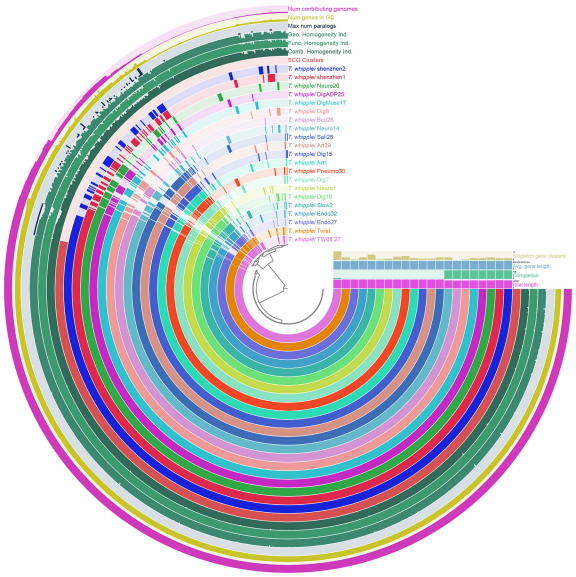

FIGURE 2
Anvi'o representation of the pan-genome of *T. whipplei shenzhen1*, *T. whippleishenzhen2*, and 19 other *T. whipplei* based on the presence/absence of gene clusters. The inner layers represent individual genomes organized by their phylogenetic relationships as indicated by the dendrogram. The first 21 layers represent each genome. Circle bars represent the occurrence of gene clusters in each genome, and the dark colors indicate the existence of the gene cluster. The subsequent seven layers correspond to various statistics related to the analysis, i.e., single-copy core gene clusters, combine homogeneity index, functional homogeneity index, geometric homogeneity index, maximum number of paralogs per gene cluster, number of genes per gene cluster, and the number of contributing genomes per gene cluster.

genomes with maximum and minimum ANI values for *T. whipplei* shenzhen1 are *T. whipplei* Bcu26 (99.74%) and *T. whipplei* strain Endo32 (99.38%) originating from France. The genome with maximum ANI for *T. whipplei* strain shenzhen2 is *T. whipplei* Bcu26. At the same time, the ANI between the two *T. whipplei* strains from China is 99.65%. As Figure 3 illustrates, the average nucleotide identity value calculated between all pairs of strains shows no discernible difference associated with geographical origins.

Identification of antibiotic-resistant genetic determinants and virulence genes

Submitting the 21 strains of *T. whipplei* sequenced genomes to the Resistance Gene Identifier failed to detect any antibiotic resistance genes. However, after utilizing RAST-Annotation, the specific mutation in the genes for DNA gyrase (*gyrA* and *gyrB*) and topoisomerase IV (*parC* and *parE*) leading to the genotypic antibiotic resistance to fluoroquinolones was found in *T. whipplei*. Some reports proved that *gyrA, gyrB, parC*, and *parE* gene mutations induce resistance to fluoroquinolones, due to the altered structures of the target proteins of fluoroquinolones (Gonzalez et al., 1998; Pantel et al., 2012; Johnning et al., 2015; Chien et al., 2016). Alignment of the amino acid sequences of GyrA, GyrB, ParC, and ParE of the 21 *T. whipplei* strains showed that these genes are highly conserved within the species (Figures S1–S4). The *T. whipplei* GyrA and ParC quinolone resistance-determining regions (QRDRs) are shown in Figures S1, S3. According to Didier Raoult's report (Masselot et al., 2003), the *T. whipplei* GyrA QRDR extends from the alanine at position 65 to the glutamine at position 104, and the ParC QRDR extends from the alanine at position 80 to the histidine a position 119. The amino acid sequences of GyrA and ParC QRDR from the 21 *T. whipplei* strains and that of *Escherichia coli* were aligned, and the Ser-to-Ala mutation is indicated in Figure 4. The positions of this mutation are at positions 81 and 96, respectively. Alanines at these positions have previously been associated with increased fluoroquinolone resistance in *T. whipplei, E. coli*, and *Mycobacteria* (Cullen et al., 1989; Yagupsky et al., 1990; Masselot et al., 2003). The *T. whipplei* GyrB and ParE QRDR were identified by aligning with known homologous QRDR sequences of *Mycobacterium fortuitum* H37Rv (Cole et al., 1998). The GyrB QRDR of *T. whipplei* extends from the serine at position 474 to the glutamine at position 512. The ParE QRDR of *T. whipplei* extends from the alanine at position 488 to alanine at position 526. The mutations that likely to cause the fluoroquinolone resistance (e.g., Asp to Asn) were not detected in the GyrB and ParE QRDR regions.

The virulence factors of *T. whipplei* were investigated through the virulence factor database, which harbors information of bacterial virulence factors from various known pathogens. Twenty virulence factors had been predicted to play a role in the pathogenesis of *T. whipplei* (Figure 1). These include six bacterial VF categories: adherence (*groEL* and *ufa*), immune modulation (*wzt*, *wbtL, rffG, gnd, manB*, and *yhxB/manB*), nutritional/metabolic factor (*phzC*1, *carA, fepG, carB*, and *fepC*), regulation (*relA, purM, phoR*, and *phoP*), stress survival (*clpC* and *clpP*), and motility (*flmH*), but further studies need to be done to understand the role of these virulence factors. Among the 21 *T. whipplei* strains, 19 virulence factors are shared among the strains, while the *clpC* gene is found in 7 out of 21 *T. whipplei* strains. It encodes a general stress protein belonging to the HSP-100/Clp family, which promotes intracellular bacteria *Listeria monocytogenes* to escape from the macrophage phagocytosis (Rouquette et al., 1998).

Discussion

T. whipplei is a fastidious bacterium that is difficult to culture, and not until after 2000 could the researchers

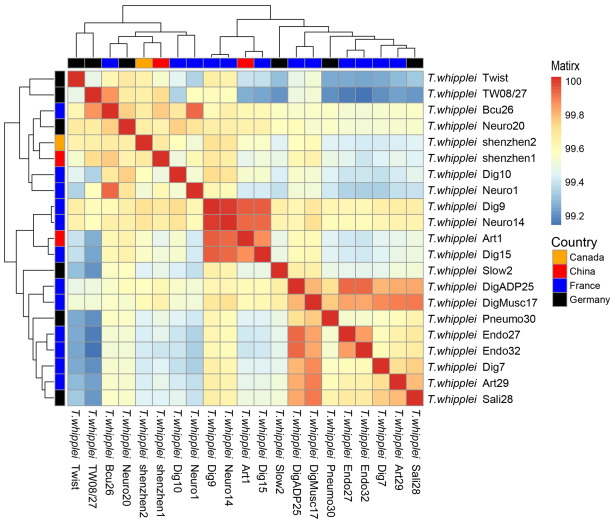

FIGURE 3
Heatmap of Average Nucleotide Identity (ANI) values for 21 whole genomes of *T. whipplei* strains from the different geographical origins (orange, Canada; red, China; blue, France; black, Germany).

successfully culture this bacterium in the human fibroblast cell line in the laboratory (Raoult et al., 2000). There is increasing evidence to suggest that the predominant reservoir of *T. whipplei* is found in humans, as *T. whipplei* is known to be viable in the human respiratory tract, fecal, and saliva samples. It also suggests that *T. whipplei* might be transmitted through both fecal–oral and oral–oral routes (La Scola et al., 2011; Pightling et al., 2018). In previous studies, 19 *T. whipplei* strains were isolated from various specimens, including the aortic valve, small intestine biopsy, mesenterial lymph node, and bronchoalveolar lavage cutaneous biopsy, in which the pathogens were cultured and the genomes were sequenced (Bentley et al., 2003; Raoult et al., 2003; Wetzstein, 2017). The cultivation of *T. whipplei* requires living eukaryotic cells, while the bacterium has a very slow replication with a doubling time of 18 days, which severely impedes routine culture-based diagnostics and genomic analysis. On the other hand, obtaining the bacterial whole genome is significant to understanding the properties of this pathogen, including antibiotic resistance, molecular epidemiology, and pathogenic virulence. Utilizing whole-genome sequence analyses could supplement epidemiological studies and trace back evidence for epidemic regulations (Pightling et al., 2018). Moreover, it could help identify sources of pathogens during disease outbreaks. In this study, we report two genome sequences of *T. whipplei* shenzhen1 and *T. whipplei* shenzhen2, which were assembled using clinical metagenomic sequencing, without the need to conduct long-term bacterial cultivation.

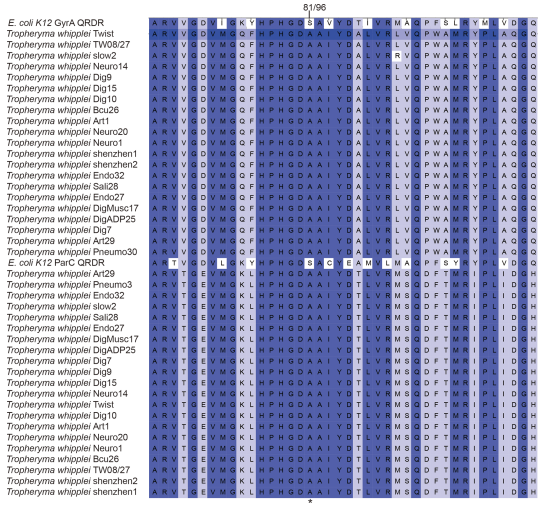

FIGURE 4
Alignment of amino acid sequences of GyrA and ParC QRDRs from the 21 *T. whipplei* strains and *E. coli* K-12. Numbers refer to the amino acid positions in the *T. whipplei* GyrA and ParC sequence.

In comparative genomics, the genetic content of 21 *T. whipplei* was compared to each other. The antibiotic resistance genes and virulence genes were predicted, and the phylogenetic relationships between the strains were determined. Interestingly, even strains of *T. whipplei* that originate from different geographical regions have close relationships, including the isolate *T. whipplei* shenzhen2 from an immunodeficient patient. *T. whipplei* is an intracellular bacterium that has a closed pan-genome, suggested by investigating the core and

pan-genomes of *T. whipplei*. It has a limited capacity to acquire foreign genes likely due to its limited horizontal gene transfer mechanisms. As shown by the whole-genome phylogenetic tree and the ANI matrix, there is no correlation between the strains and their geographical origins. All *T. whipplei* strains exhibit genotypic resistance to fluoroquinolones, due to mutations found in the *gyrA*, *gyrB*, *parC*, and *parE* genes in the RAST annotation. Mutations in the quinolone resistance-determining region (QRDR) of *gyrA*, *gyrB*, *parC*, and *parE* leading to reduce susceptibility to fluoroquinolone have been reported in many bacterial species (Gonzalez et al., 1998; Pantel et al., 2012; Johnning et al., 2015; Chien et al., 2016). All *T. whipplei* strains exhibit genotypic resistance to fluoroquinolones, due to the GyrA and ParC QRDR with an alanine residue at positions 81 and 96 (Masselot et al., 2003). The QRDRs of *T. whipplei* GyrB and ParE were defined as codons 474 to 512 in GyrB, and 488 to 526 in the ParE, but the specific amino acid relative to fluoroquinolone resistance was not discovered. Although the mechanisms of quinolone resistance of GyrB and ParE have not been fully investigated, we still hypothesize that *T. whipplei* has a natural resistance to fluoroquinolones.

In conclusion, we have obtained two metagenome-assembled genomes of *T. whipplei* from China using metagenomic next-generation sequencing (mNGS). The 21 *T. whipplei* strains share highly similar genomic characteristics despite originating from different countries. Aided by the mNGS culture-independent characterization of pathogens, we therefore propose that clinical mNGS could be considered as an approach to obtain and analyze genomic information for difficult or "unculturable" microorganisms.

Data availability statement

The datasets presented in this study can be found in online repositories. The name of the repository and accession number can be found below: NCBI; PRJNA831609.

Ethics statement

The studies involving human participants were reviewed and approved by The Peking University Shenzhen Hospital Ethics Committee. The patients/participants provided their written informed consent to participate in this study.

Author contributions

PX, YH participated in study conception and design. ZL, SL, XLL, XMD enrolled and managed patients, CY, CZ and YQ carried out collection and assembly of data. ZL, CY were involved in data analysis and interpretation. PX, YH, ZL, CY prepared the manuscript and manuscript figures. PX, YH and ZL edited, critically read, and revised the manuscript. All authors contributed to the article and approved the submitted version.

Funding

This study was supported by the National Key Research and Development Program of China (2019YFC1200500 and 2019YFC1200501), the Shenzhen Science and Technology Innovation Commission Foundation (grant no. JCYJ20190809103203711), the Shenzhen Science and Technology Innovation Commission foundation (grant no. JCYJ20210324105411031), the Fund of "Sanming" Project of Medicine in Shenzhen (no. SZSM201811096), the Shenzhen High-level Hospital Construction Fund (LCYJ2021022), and the Shenzhen High-level Hospital Construction Fund Discipline Construction Project of Guangdong Medical University.

Conflict of interest

Authors YC, ZC, QY, JR and WC are employed by BGI.

The remaining authors declare that the research was conducted in the absence of any commercial or financial relationships that could be construed as a potential conflict of interest.

Publisher's note

Supplementary material

The Supplementary Material for this article can be found online at: https://www.frontiersin.org/articles/10.3389/fcimb.2022.947486/full#supplementary-material

References

Bentley, S. D., Maiwald, M., Murphy, L. D., Pallen, M. J., Yeats, C. A., Dover, L. G., et al. (2003). Sequencing and analysis of the genome of the whipple's disease bacterium tropheryma whipplei. *Lancet* 361, 637–644. doi: 10.1016/S0140-6736(03)12597-4

Black-Schaffer, B. (1949). The tinctoral demonstration of a glycoprotein in whipple's disease. *Proc. Soc. Exp. Biol. Med.* 72, 225–227. doi: 10.3181/00379727-72-17388

Chen, L., Yang, J., Yu, J., Yao, Z., Sun, L., Shen, Y., et al. (2005). VFDB: A reference database for bacterial virulence factors. *Nucleic Acids Res.* 33, D325–D328. doi: 10.1093/nar/gki008

Chien, J. Y., Chiu, W. Y., Chien, S. T., Chiang, C. J., Yu, C. J., and Hsueh, P. R. (2016). Mutations in gyrA and gyrB among fluoroquinolone- and multidrug-resistant mycobacterium tuberculosis isolates. *Antimicrob. Agents Chemother.* 60, 2090–2096. doi: 10.1128/AAC.01049-15

Cole, S. T., Brosch, R., Parkhill, J., Garnier, T., Churcher, C., Harris, D., et al. (1998). Deciphering the biology of mycobacterium tuberculosis from the complete genome sequence. *Nature* 393, 537–544. doi: 10.1038/31159

Cullen, M. E., Wyke, A. W., Kuroda, R., and Fisher, L. M. (1989). Cloning and characterization of a DNA gyrase a gene from escherichia coli that confers clinical resistance to 4-quinolones. *Antimicrob. Agents Chemother.* 33, 886–894. doi: 10.1128/AAC.33.6.886

Dickson, R. P., Erb-Downward, J. R., Freeman, C. M., Mccloskey, L., Beck, J. M., Huffnagle, G. B., et al. (2015). Spatial variation in the healthy human lung microbiome and the adapted island model of lung biogeography. *Ann. Am. Thorac. Soc.* 12, 821–830. doi: 10.1513/AnnalsATS.201501-029OC

Durand, D. V., Lecomte, C., Cathebras, P., Rousset, H., and Godeau, P. (1997). Whipple Disease. clinical review of 52 cases. The SNFMI research group on Whipple disease. societe nationale francaise de medecine interne. *Med. (Baltimore)* 76, 170–184. doi: 10.1097/00005792-199705000-00003

Eren, A. M., Esen, O. C., Quince, C., Vineis, J. H., Morrison, H. G., Sogin, M. L., et al. (2015). Anvi'o: An advanced analysis and visualization platform for 'omics data. *PeerJ* 3, e1319. doi: 10.7717/peerj.1319

Gonzalez, I., Georgiou, M., Alcaide, F., Balas, D., Linares, J., and de la Campa, A. G. (1998). Fluoroquinolone resistance mutations in the parC, parE, and gyrA genes of clinical isolates of viridans group streptococci. *Antimicrob. Agents Chemother.* 42, 2792–2798. doi: 10.1128/AAC.42.11.2792

Goris, J., Konstantinidis, K. T., Klappenbach, J. A., Coenye, T., Vandamme, P., and Tiedje, J. M. (2007). DNA-DNA Hybridization values and their relationship to whole-genome sequence similarities. *Int. J. Syst. Evol. Microbiol.* 57, 81–91. doi: 10.1099/ijs.0.64483-0

Jain, C., Rodriguez, R. L., Phillippy, A. M., Konstantinidis, K. T., and Aluru, S. (2018). High throughput ANI analysis of 90K prokaryotic genomes reveals clear species boundaries. *Nat. Commun.* 9:5114. doi: 10.1038/s41467-018-07641-9

James, B. W., Williams, A., and Marsh, P. D. (2000). The physiology and pathogenicity of mycobacterium tuberculosis grown under controlled conditions in a defined medium. *J. Appl. Microbiol.* 88, 669–677. doi: 10.1046/j.1365-2672.2000.01020.x

Jia, B., Raphenya, A.R., Alcock, B., Waglechner, N., Guo, P., Dave, B.M., et al (2017). CARD 2017: Expansion and model-centric curation of the comprehensive antibiotic resistance database. *Nucleic Acids Res* 45, D566–73. doi: 10.1093/nar/gkw1004

Johnning, A., Kristiansson, E., Fick, J., Weijdegard, B., and Larsson, D. G. (2015). Resistance mutations in gyrA and parC are common in escherichia communities of both fluoroquinolone-polluted and uncontaminated aquatic environments. *Front. Microbiol.* 6 1355. doi: 10.3389/fmicb.2015.01355

La Scola, B., Fenollar, F., Fournier, P. E., Altwegg, M., Mallet, M. N., and Raoult, D. (2001). Description of tropheryma whipplei gen. nov., sp. nov., the whipple's disease bacillus. *Int. J. Syst. Evol. Microbiol.* 51, 1471–1479. doi: 10.1099/00207713-51-4-1471

La Scola, B., Fenollar, F., Perreal, C., and Raoult, D. (2011). Epidemiologic implications of the first isolation and cultivation of tropheryma whipplei from a saliva sample. *Ann. Intern. Med.* 154, 443–444. doi: 10.7326/0003-4819-154-6-201103150-00018

Li, W., Zhang, Q., Xu, Y., Zhang, X., Huang, Q., and Su, Z. (2021). Severe pneumonia in adults caused by tropheryma whipplei and candida sp. infection: A 2019 case series. *BMC Pulm Med.* 21, 29. doi: 10.1186/s12890-020-01384-4

Masselot, F., Boulos, A., Maurin, M., Rolain, J. M., and Raoult, D. (2003). Molecular evaluation of antibiotic susceptibility: Tropheryma whipplei paradigm. *Antimicrob. Agents Chemother.* 47, 1658–1664. doi: 10.1128/AAC.47.5.1658-1664.2003

Pantel, A., Petrella, S., Veziris, N., Brossier, F., Bastian, S., Jarlier, V., et al. (2012). Extending the definition of the GyrB quinolone resistance-determining region in mycobacterium tuberculosis DNA gyrase for assessing fluoroquinolone resistance in m. tuberculosis. *Antimicrob. Agents Chemother.* 56, 1990–1996. doi: 10.1128/AAC.06272-11

Pightling, A. W., Pettengill, J. B., Luo, Y., Baugher, J. D., Rand, H., and Strain, E. (2018). Interpreting whole-genome sequence analyses of foodborne bacteria for regulatory applications and outbreak investigations. *Front. Microbiol.* 9 1482. doi: 10.3389/fmicb.2018.01482

Raoult, D., Birg, M. L., La Scola, B., Fournier, P. E., Enea, M., Lepidi, H., et al. (2000). Cultivation of the bacillus of whipple's disease. *N Engl. J. Med.* 342, 620–625. doi: 10.1056/NEJM200003023420903

Raoult, D., Ogata, H., Audic, S., Robert, C., Suhre, K., Drancourt, M., et al. (2003). Tropheryma whipplei twist: A human pathogenic actinobacteria with a reduced genome. *Genome Res.* 13, 1800–1809. doi: 10.1101/gr.1474603

Ratliff, N. B., Mcmahon, J. T., Naab, T. J., and Cosgrove, D. M. (1984). Whipple's disease in the porcine leaflets of a carpentier-edwards prosthetic mitral valve. *N Engl. J. Med.* 311, 902–903. doi: 10.1056/NEJM198410043111407

Robert, X., and Gouet, P. (2014). Deciphering key features in protein structures with the new ENDscript server. *Nucleic Acids Res.* 42, W320–W324. doi: 10.1093/nar/gku316

Rouquette, C., De Chastellier, C., Nair, S., and Berche, P. (1998). The ClpC ATPase of listeria monocytogenes is a general stress protein required for virulence and promoting early bacterial escape from the phagosome of macrophages. *Mol. Microbiol.* 27, 1235–1245. doi: 10.1046/j.1365-2958.1998.00775.x

Schoedon, G., Goldenberger, D., Forrer, R., Gunz, A., Dutly, F., Hochli, M., et al. (1997). Deactivation of macrophages with interleukin-4 is the key to the isolation of tropheryma whippelii. *J. Infect. Dis.* 176, 672–677. doi: 10.1086/514089

Wetzstein, N. (2017). *Genotyping and genomotyping of tropheryma whipplei – the causative agent of whipple's disease.*

Yagupsky, P. V., Kaminski, D. A., Palmer, K. M., and Nolte, F. S. (1990). Cord formation in BACTEC 7H12 medium for rapid, presumptive identification of mycobacterium tuberculosis complex. *J. Clin. Microbiol.* 28, 1451–1453. doi: 10.1128/jcm.28.6.1451-1453.1990

Yardley, J. H., and Hendrix, T. R. (1961). Combined electron and light microscopy in whipple's disease. demonstration of "bacillary bodies" in the intestine. *Bull. Johns Hopkins Hosp* 109, 80–98.

Zhou, Z., Charlesworth, J., and Achtman, M. (2020). Accurate reconstruction of bacterial pan- and core genomes with PEPPAN. *Genome Res.* 30, 1667–1679. doi: 10.1101/gr.260828.120

Zhu, B., Tang, J., Fang, R., Fei, X., Wang, Q., Wang, W., et al. (2021). Pulmonary coinfection of mycobacterium tuberculosis and tropheryma whipplei: A case report. *J. Med. Case Rep.* 15, 359. doi: 10.1186/s13256-021-02899-y

frontiers | Frontiers in Cellular and Infection Microbiology

TYPE Original Research
PUBLISHED 27 September 2022
DOI 10.3389/fcimb.2022.949505

OPEN ACCESS

EDITED BY
Jinmin Ma,
Beijing Genomics Institute (BGI), China

REVIEWED BY
Qiang Wang,
Jiangsu University of Science and Technology, China
Xuesong Fan,
Department of Clinical Laboratory, Capital Medical University, China

*CORRESPONDENCE
Feng Pang
pangfeng_lc.hosp@outlook.com
Qigang Zhao
zqg67680@sina.com

†These authors have contributed equally to this work

SPECIALTY SECTION
This article was submitted to Clinical Microbiology, a section of the journal Frontiers in Cellular and Infection Microbiology

RECEIVED 21 May 2022
ACCEPTED 05 September 2022
PUBLISHED 27 September 2022

CITATION
Wang C, You Z, Fu J, Chen S, Bai D, Zhao H, Song P, Jia X, Yuan X, Xu W, Zhao Q and Pang F (2022) Application of metagenomic next-generation sequencing in the diagnosis of pulmonary invasive fungal disease. *Front. Cell. Infect. Microbiol.* 12:949505. doi: 10.3389/fcimb.2022.949505

Application of metagenomic next-generation sequencing in the diagnosis of pulmonary invasive fungal disease

Chengtan Wang[1†], Zhiqing You[1†], Juanjuan Fu[1†], Shuai Chen[2,3], Di Bai[2], Hui Zhao[1], Pingping Song[1], Xiuqin Jia[4], Xiaoju Yuan[5], Wenbin Xu[1], Qigang Zhao[1*] and Feng Pang[1*]

[1]Department of Clinical Laboratory, Liaocheng People's Hospital, Liaocheng, China, [2]Department of Clinical Laboratory, Liaocheng Third People's Hospital, Liaocheng, China, [3]Department of Virology, School of Public Health, Shandong University, Jinan, China, [4]The Key Laboratory of Molecular Pharmacology, Liaocheng People's Hospital, Liaocheng, China, [5]Department of Gastroenterology, Liaocheng People's Hospital, Liaocheng, China

Background: Metagenomic next-generation sequencing (mNGS) is increasingly being used to detect pathogens directly from clinical specimens. However, the optimal application of mNGS and subsequent result interpretation can be challenging. In addition, studies reporting the use of mNGS for the diagnosis of invasive fungal infections (IFIs) are rare.

Objective: We critically evaluated the performance of mNGS in the diagnosis of pulmonary IFIs, by conducting a multicenter retrospective analysis. The methodological strengths of mNGS were recognized, and diagnostic cutoffs were determined.

Methods: A total of 310 patients with suspected pulmonary IFIs were included in this study. Conventional microbiological tests (CMTs) and mNGS were performed in parallel on the same set of samples. Receiver operating characteristic (ROC) curves were used to evaluate the performance of the logarithm of reads per kilobase per million mapped reads [lg(RPKM)], and read counts were used to predict true-positive pathogens.

Result: The majority of the selected patients (86.5%) were immunocompromised. Twenty species of fungi were detected by mNGS, which was more than was achieved with standard culture methods. Peripheral blood lymphocyte and monocyte counts, as well as serum albumin levels, were significantly negatively correlated with fungal infection. In contrast, C-reactive protein and procalcitonin levels showed a significant positive correlation with fungal infection. ROC curves showed that mNGS [and especially lg(RPKM)] was superior to CMTs in its diagnostic performance. The area under the ROC curve value obtained for lg (RPKM) in the bronchoalveolar lavage fluid of patients with suspected pulmonary IFIs, used to predict true-positive pathogens, was 0.967, and the cutoff value calculated from the Youden index was –5.44.

Conclusions: In this study, we have evaluated the performance of mNGS-specific indicators that can identify pathogens in patients with IFIs more accurately and rapidly than CMTs, which will have important clinical implications.

KEYWORDS

clinical mNGS, invasive fungal infections, immunosuppressed patients, pneumonia, pathogen detection

Introduction

An increasing number of people are living with immunodeficiencies as a result of medical interventions such as aggressive of prolonged cancer treatments, allogeneic organ and hematopoietic cell transplantation, or the use of corticosteroids for the treatment of autoimmune and autoinflammatory diseases (Ferrarese et al., 2020). The immunosuppressed individual is at a higher risk of developing more invasive fungal infections (IFIs) (Pasqualotto et al., 2006; Ben et al., 2008; Kim et al., 2017; Prattes et al., 2021; Suleyman and Alangaden, 2021), which affects two million individuals each year worldwide (D'enfert and Bougnoux, 2014; Suleyman et al., 2022). The clinical manifestations of IFIs are not typical, and thus, diagnosis mainly relies on etiological evidence. A timely and accurate diagnosis is crucial for the prognosis and survival of patients with IFIs (El-Baba et al., 2020). However, existing techniques such as tissue staining, *in vitro* culture, serological testing, and diagnostic imaging are inadequate for the reliable detection of IFI-causing pathogens. Nearly 60% of IFIs still have an unknown etiology, which delays targeted drug treatment and, in turn, affects patient recovery (Donnelly and Maertens, 2013). The gold standard for diagnosing IFIs is the presence of molds or yeasts in a deep tissue biopsy or a culture obtained by a sterile procedure. Unfortunately, histopathological testing is rarely available in a timely manner because of the risks involved in performing biopsies, whereas culture methods are insensitive and time-consuming. Recently, a real-time PCR approach has shown promise in the detection of *Aspergillus*, *Pneumocystis*, and *Candida* spp. (Donnelly and Maertens, 2013; Donnelly et al., 2020). Despite this, PCR is a hypothesis-driven method that is designed to detect specific pathogens and is therefore not capable of detecting rare and emerging infectious agents (Schlaberg et al., 2017).

Advances in genome sequencing technologies and bioinformatics approaches provide powerful alternatives to overcome such clinical diagnostic challenges (Wang et al., 2021). Metagenomic next-generation sequencing (mNGS) is a culture-independent, hypothesis-independent, broad-spectrum sequencing method, which capable of overcoming the limitations of current diagnostic tests. mNGS enables the universal pathogen detection of viruses, bacteria, fungi, and parasites in a single run (Miao et al., 2018). Since its first application in a clinical setting, mNGS has played an increasingly important role in pathogen identification (Palacios et al., 2008). However, there are still many challenges preventing the routine use of mNGS in the clinic. The primary challenge is that there is currently no common standard for interpreting mNGS results. Although numerous studies have reported the clinical application of mNGS, the majority involve summary retrospective analyses of the diagnostic performance of this novel methodology on a heterogeneous group of patients (Qian et al., 2020; Gu et al., 2021; Liu et al., 2022a). mNGS analyses focusing on the diagnosis of IFIs are rare. Furthermore, it has not yet been reported which indicator is most suitable for distinguishing between pathogens and colonizing/contaminant microorganisms that are present in the sample, the reagents, or the laboratory environment.

In this study, we evaluated the performance of an mNGS indicator [lg(RPKM)] to identify pathogenic fungi in patients with suspected pulmonary IFIs and established a cutoff value for the identification of pathogens. Using this cutoff value, we compared the diagnostic value of mNGS with conventional microbiological tests (CMTs). Finally, we analyzed the correlation between eight clinical infection indicators and various forms of fungal infection.

Materials and methods

Study setting and design

We retrospectively reviewed 327 cases of suspected pulmonary IFIs at nine tertiary hospitals in the Shandong Province, China (Liaocheng People's Hospital, Liaocheng Infectious Diseases Hospital, Liaocheng Traditional Chinese Medicine Hospital, Liaocheng Third People's Hospital, Liaocheng Brain Hospital, Liaocheng Dongchangfu District Hospital, Dong'e County People's Hospital, Guan County

Central Hospital, and Guan County Traditional Chinese Medicine Hospital) between August 2020 and February 2022. We followed the revised diagnostic criteria of IFIs outlined by the European Organization for Research and Treatment of Cancer/Invasive Fungal Infections Cooperative Group and the National Institute of Allergy and Infectious Diseases Mycoses Study Group (EORTC/MSG) (De Pauw et al., 2008; Alexander et al., 2021). See supplementary document Table S1 for our diagnostic criteria. Eventually, 310 patients with suspected pulmonary IFIs were enrolled and 17 were excluded (Figure 1A). Clinical data of patients were rigorously evaluated, summarized, and compiled until death or hospital discharge. All the enrolled patients were subjected to mNGS, CMTs, and a serological test (Figure 1A). We divided the 310 subjects into three groups: 1) the fungal infections group, 2) the non-fungal infections group, and 3) the *Candida* group according to the grouping principles outlined in Figure 1C. This study was approved by the Medical Ethics Committee of Liaocheng People's Hospital (No. 2022097). All samples in this study were anonymized, and the experiments were performed in accordance with the Declaration of Helsinki.

Conventional microbiological testing and examination of infection indices

Bronchoalveolar lavage fluid (BALF) samples collected from patients with suspected pulmonary IFIs underwent CMTs and

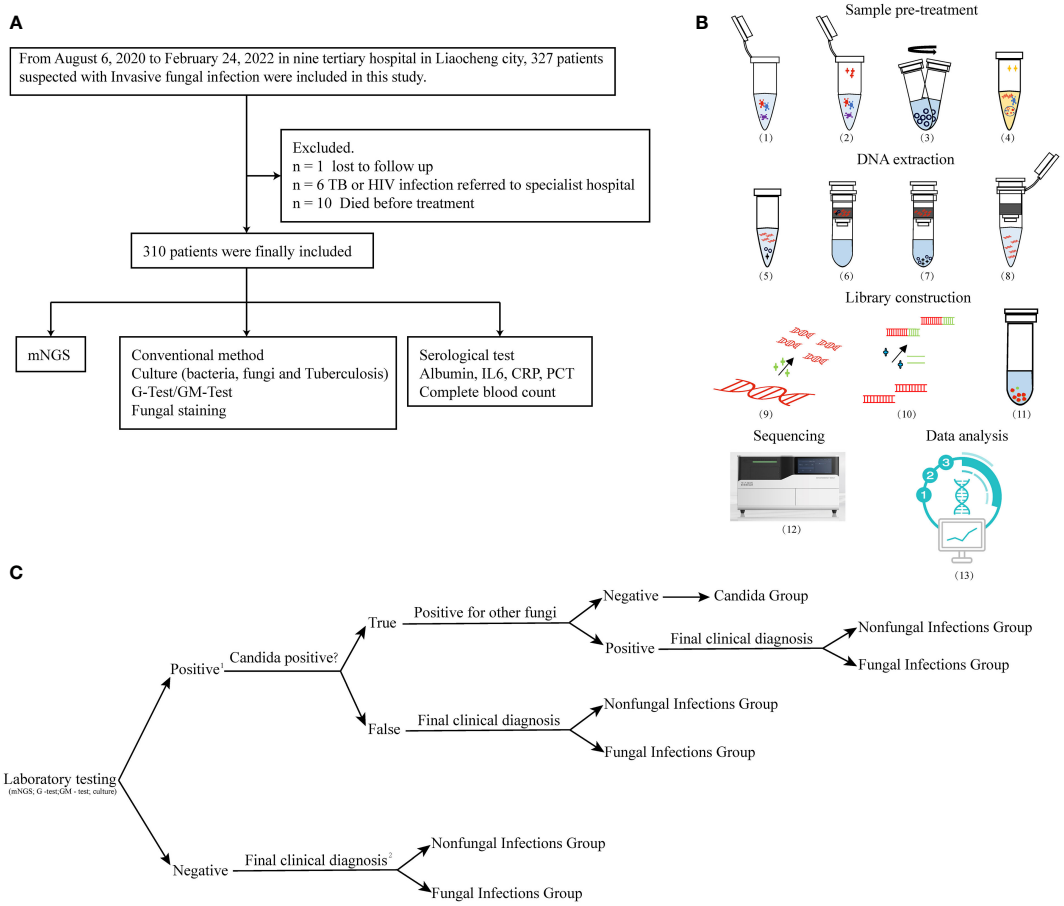

FIGURE 1
Flowchart. **(A)** Flowchart of participant enrollment criteria. **(B)** Workflow of mNGS. Sample pre-treatment includes the following: (1) inactivation: dry bath at 56°C for 30 min; (2) lysozyme treatment at 30°C for 10 min; (3) add micro glass grinding beads to the lysate and vortex the samples at 1,000 x g for 20 min. (4) Lysis: collect supernatants and add proteinase k and lysis solution at 70°C for 15 min. DNA extraction includes (5) application of 100% ethanol concentration to induce nucleic acid precipitation, (6) DNA binding, (7) washing, and (8) elution. Library construction includes (9) nucleic acid fragmentation (10), adapter ligation, (11) DNB library preparation, (12) sequencing in BGI-seq 50, and (13) data analysis. **(C)** Group analysis workflow for the samples included in the study. 1. A positive result was defined as the presence of fungal infection that was detected by any of the following methods: mNGS, G and GM tests, and culture. 2. The final clinical diagnosis of IFIs was made by a decision-making group comprised of clinical experts, laboratory scientists, and bioinformatics experts, and based on the comprehensive evaluation of all available clinical data. Decision was made according to the revised diagnostic criteria of IFIs outlined by the EORTC/MSG.

mNGS in parallel. CMTs were carried out according to the standard procedures (Donnelly et al., 2020). The 1,3-β-D glucan (G) assay (the G test) and galactomannan (GM) assay (the GM test) were performed according to the manufacturer's instructions (Xinuo Biopharmaceutical Co., Ltd., Tianjin, China). The following parameters were subsequently assessed: white blood cell count, neutrophil count, lymphocyte count, monocyte count (Sysmex Co., Ltd., Kobe, Japan), C-reactive protein (CRP) and procalcitonin (PCT) (Shanghai i-Reader Biotech Co., Ltd., Shanghai, China), interleukin-6 (IL-6) [Abbott Diagnostic (Shanghai) Co., Ltd., Shanghai, China], and serum albumin (Beckman Co., Ltd., Brea, America) using the manufacturer's recommendations.

Metagenomic next-generation sequencing

The mNGS uses BGI's high-throughput genetic detection of pathogenic microorganisms (PMseq) process. BALF samples from patients with suspected pulmonary IFIs were collected and stored on dry ice until mNGS. The samples were inactivated at 56°C for 30 min using a dry bath, prior to the addition of wall-lysing enzyme and incubation at 30°C for 10 min. Next, micro glass grinding beads (MGI Tech Co., Ltd., Wuhan, China) were added to the lysate, and the samples were vortexed at 1,000 x g for 20 min. Supernatants were subsequently collected and subjected to DNA extraction using the TIANamp Micro DNA kit (DP316, TIANGEN Biotech, Jiangsu, China). Nucleic acid concentration was determined using the Qubit dsDNA HS Assay kit together with the Qubit 4 Fluorometer (Invitrogen Singapore Pte, Ltd., Singapore, Singapore). Nucleic acid fragmentation (into 250- to 350-bp fragments) was then performed using an enzyme digestion kit (MGI Tech Co., Ltd., Wuhan, China). The digested DNA was purified using commercially available magnetic beads (MGI Tech Co., Ltd., Wuhan, China), and DNA libraries were prepared (after end repair, adapter ligation, and PCR amplification) using the DNA construction kit (MGI Tech Co., Ltd., Wuhan, China). The library was quantified using the Qubit 4 Fluorometer (Invitrogen); the ExKubit dsDNA Assay Kit and Agilent 2100 (Agilent Technologies, Santa Clara, CA) were used to control fragment length. DNA nanoballs (DNBs) were subsequently prepared from the library using rolling circle amplification (BGI Genomics, Wuhan, China). Next, a loading sample was prepared and sequenced on the BGISEQ-50 platform (BGI Genomics, Wuhan, China) using the 50–base read length (SE50) sequencing strategy. Hela cells and *Acinetobacter baumannii* (ATCC 19606) were used as negative and positive controls, respectively, and were consistently included in the analysis of each batch of samples. A specific synthetic sequence tagged onto each specimen was used as an internal standard to monitor the whole process. The quality of the extracted DNA, the sequencing library, DNBs, and final sequence data were all measured to a great degree of accuracy. The workflow of mNGS test was shown in Figure 1B.

For the bioinformatics aspect of mNGS, raw sequencing data were processed, and high-quality data were selected after removing adapter and low-quality sequences. The high-quality data were then mapped to the human genome (hg19; https://www.ncbi.nlm.nih.gov/assembly/GCF_000001405.13/) using the Burrows–Wheeler Alignment (BWA; http://bio-bwa.sourceforge.net/) method and stripped for annotated human genome data (Li and Durbin, 2009). The remaining sequencing data were simultaneously aligned against Pathogenic metagenomics database (PMDB) microbial genome databases, which included the genomes of viruses, bacteria, fungi, and parasites, using BWA, to generate the original mapping list. The PMDB database contained sequence data from 6,039 bacteria, 2,700 DNA viruses, 1,064 fungi, 234 parasites, and 137 mycoplasma/chlamydia (all associated with human disease). Reference genomes in the database were downloaded from the National Center for Biotechnology Information (ftp://ftp.ncbi.nlm.nih.gov/genomes/).

Statistical analysis and data visualization

Bioinformatics analyses and data visualization were performed using the R software. The type of specimen, genome length, sequencing depth, and the throughput rate of the platform will affect the reads number in mNGS. We chose the reads per kilobase of transcript per million mapped reads (RPKM) as the normalization method for mNGS reads, based on the study by Liu et al. (Liu et al., 2022c) and the sequencing characteristics of this study (single-end sequencing). RPKM was calculated using the formula: gene reads/[the total mapped reads (millions) × genome length (KB)].

The Shapiro–Wilk test was used to determine whether the quantitative data conformed to a normal distribution. The Student's t-test and Wilcoxon rank test were used to compare two groups that followed a normal or an abnormal distribution, respectively. The Pearson chi-squared (χ^2) test or the Fisher's exact test was used for the comparison of categorical data frequencies. The correlation between two different indicators was analyzed and expressed as Spearman's r values. A receiver operating characteristic (ROC) curve was drawn for the selection of the best indicator of the true-positive specific pathogen. We applied the Youden index to determine the cutoff values for log (RPKM) and read counts in the ROC curve. The Youden index (*J*) is main summary statistic of the ROC curve used in the interpretation and evaluation of a biomarker, which defines the maximum potential effectiveness of a biomarker (Youden, 1950;

Faraggi, 2000). A *P*-value of < 0.05 was used as a measure of significance.

Results

Clinical characteristics

The 310 participants who enrolled in our study were all hospital inpatients, comprising 96 women (31%) and 214 men (69%), with a median age of 64.5 [interquartile range (IQR), 50–74], range from 0.75 to 93 years. The median duration of hospitalization was 16 days (IQR, 11–23). Of the 310 participants, 152 were admitted to the intensive care unit (ICU), 79 died during therapy (equal to a 25% 30-day mortality rate), 79 received empiric antifungal drug therapy before mNGS, and 268 were immunocompromised. The causes of immunosuppression are classified in Table 1.

TABLE 1 Patient and sample characteristics.

Characteristics	Value
Patient demographics (n = 310)	
Age (years)	
Median (IQR)[1]	64.5 (50–74)
Range	0.75–93
Gender, n (%)	
Female	96 (31)
Male	214 (69)
Hospitalization, n (%)	
Patients, total	310 (100)
In hospital	310 (100)
In intensive care unit	152 (49)
Days hospitalized, median (IQR)	16 (11–23)
30-day mortality, n (%)	79 (25)
Immunocompromised, n (%)	268 (86.5)
On empiric antifungal drugs at time of body fluid collection, n (%)	79 (25)
Causes of Immunodeficiency, n (%)[2,3]	
Diabetes mellitus	21 (7.8)
Hypoproteinemia	45 (16.8)
Cancer	25 (9.3)
Hematologic disease	23 (8.6)
Renal disease	12 (4.5)
Gastrointestinal disease	14 (5.2)
Iatrogenesis[4]	28 (10.4)
Advanced age or organ failure	51 (19)
Surgery and trauma	18 (6.7)
Other[5]	31 (11.6)

[1]IQR, interquartile range. [2]The percentage is based on all immunodeficient patients participating in the study. [3]Because some patients suffer from a variety of diseases that may lead to immunodeficiency, only the primary disease or the disease contributing most to the immunosuppression was counted. [4]Iatrogenic immunodeficiency mainly refers to the application of immunosuppressants such as corticosteroids, radiotherapy, or chemotherapy in patients with cancer (outlined in the "Cancer" category). [5]The "Other" category includes the incomplete development of immune function in infants, immunosuppression induced by severe infection, etc.

Identification of fungi by CTMs and mNGS

Of the 310 study participants, 80 patients were diagnosed with respiratory IFIs, of which 63 cases showed signs of bacterial co-infection. One hundred seventy-nine patients were excluded from further analyses of fungal infection; of these, 162 participants were diagnosed with bacterial infection, and 17 were diagnosed with non-infectious disease (Figure 2A). In addition, *Candida* spp. were detected in the BALF of 51 patients. Because pulmonary *Candida* infection is rarely confirmed by histopathology, the *Candida*-positive patients were placed into the suspected *Candida* colonization group.

In comparison with the non-fungal infection group, the percentage of immunosuppressed patients was higher in fungal infection group (Table 2). CMTs identified 82 fungal strains in 71 samples, of which the most common was *Candida albicans*, accounting for 48.7% of all strains (Figure 2B). Nineteen "true positive samples" were eventually selected, in which 22 strains of five species were detected. *Aspergillus fumigatus* was the most frequently detected species; 14 strains of *A. fumigatus* were detected (Figure 2C). In contrast, mNGS detected suspicious fungal sequences in 290 patients. One hundred forty fungal strains were detected 617 times; *C. albicans* was again the most common, accounting for 9.2% of all strains (Figure 2D). mNGS positively identified 51 patients who were clinically considered to have fungal infection, in which 20 kinds of species were detected 68 times. The most common species was *A. fumigatus*; 27 A. *fumigatus* strains were detected, accounting for 39.7% of all identified strains (Figure 2E).

Evaluation and optimization of mNGS-mediated diagnostic efficacy

The ROC curve was used to evaluate the performance of mNGS, whereas the final clinical diagnosis was used as the gold standard. In mNGS, the number of reads is affected by the type of specimen, genome length, sequencing depth, and the throughput rate of the platform. The use of read numbers for laboratory-based diagnosis may therefore lead to bias. To rule out these effects, the number of sequencing reads was replaced with the logarithm of reads per kilobase per million mapped reads [lg(RPKM)]; RPKM was calculated using the formula: gene reads/[the total mapped reads (millions) × genome length (KB)]. The results showed that read number and lg(RPKM) were significantly higher when infection was classed being "true

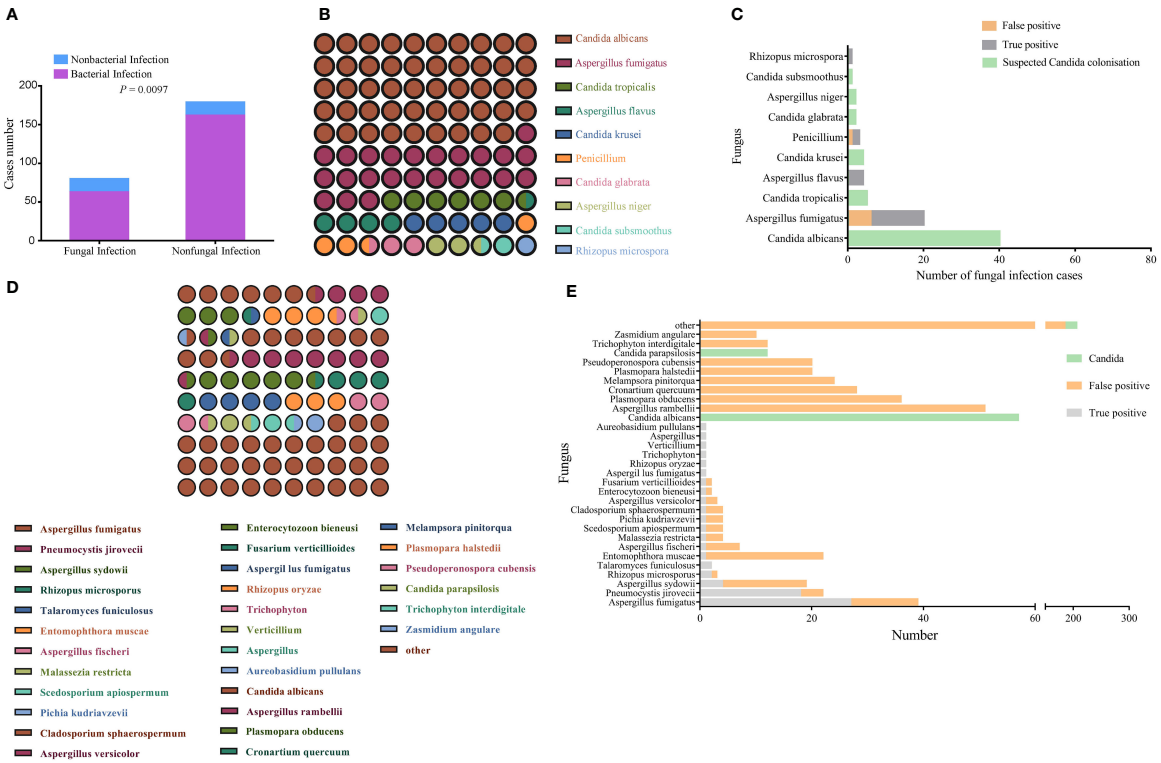

FIGURE 2
Identification of pathogenic fungi by conventional culture methods and mNGS. **(A)** Bacterial infection status of the fungal infection and non-fungal infection groups. The comparison between the two groups was made using the Pearson chi-squared ($\chi 2$) test. $P < 0.05$ indicates a significant difference. **(B)** Matrix of fungal species detected the culture method; the number of points represents species detection frequency. **(C)** Profile of fungal species detected by the culture method that distinguishes between colonization, false positives, and true positives. **(D)** Matrix of fungal species detected by mNGS; the number of points represents detection frequency (species with frequencies <10 were all grouped together). **(E)** Profile of fungal species detected by mNGS that distinguishes between colonization, false positives, and true positives; the number of points represents detection frequency (species with frequencies <10 were grouped other).

positive" (Figures 3A, B). In terms of diagnostic efficacy, both read number and lg(RPKM) can effectively evaluate fungal infection. The area under the ROC curve (AUC) for the read number was 0.939, and the cutoff value calculated according to the Yoden index was greater than 4. Concurrently, we obtained a sensitivity rate of 86.76% and a specificity rate of 86.98% (Figure 3C). We found that the AUC value for lg(RPKM) was 0.967, and the cutoff value calculated according to the Yoden index was greater than −5.44. The sensitivity and specificity rates were 95.59% and 84.6%, respectively (Figure 3D). The DeLong method (DeLong et al., 1988) was used to compare the two ROC curves, showing that lg(RPKM) had significantly higher diagnostic efficiency in relation to fungal detection than the read count method (Table 3).

TABLE 2 Demographic characteristics of study participants with fungal or non-fungal infections of the respiratory tract.

Group	Age (years)	Gender, n (%)		ICU, n (%)		Immunodeficiency, n(%)	
		Female	Male	Yes	No	Yes	No
Fungal infection	59.7 ± 18.6	29 (36.3)	51 (63.7)	42 (51.9)	38 (48.1)	80 (100)	0 (0)
Non-fungal infection	55.7 ± 21.4	53 (29.6)	126 (69.4)	72 (40.6)	107 (59.4)	146 (81.6)	33 (18.4)
P-value	0.062	0.288		0.06		<0.001	

P < 0.05 indicates a significant difference.

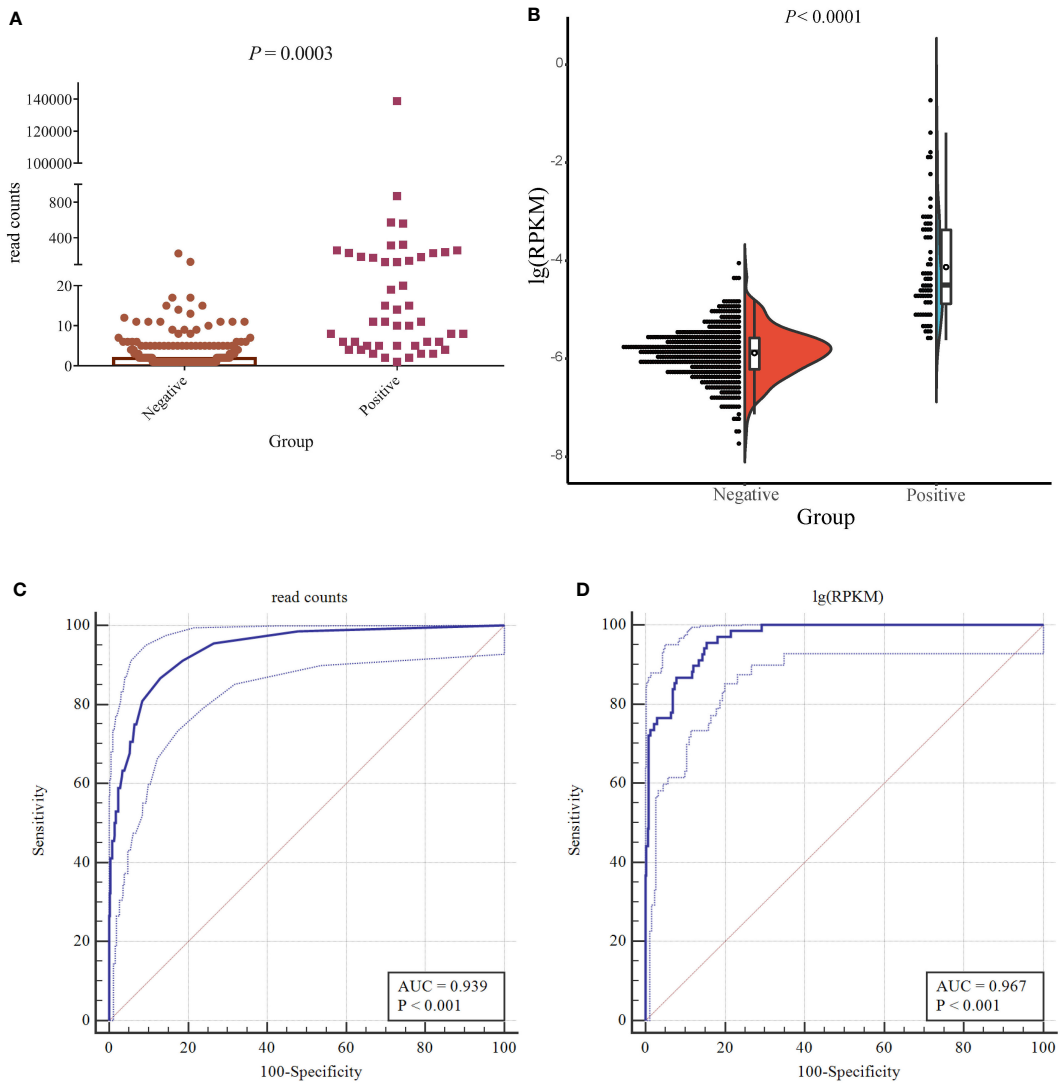

FIGURE 3
Accuracy of mNGS. **(A)** The difference in the number of detected reads between true- and false-positive fungi. **(B)** The half violin diagram shows the difference in lg(RPKM) values between true- and false-positive fungi. **(C, D)** Evaluating the performance of lg(RPKM) **(C)** and read counts **(D)** between the true- and false-positive pathogenic fungal groups using ROC curves.

Comparison of the diagnostic efficiencies of mNGS and CMTs

The total turnaround time (TAT) of mNGS (from nucleic acid extraction to result reporting) is ~24 h, which is higher than that of the G and GM tests. However, the TAT of mNGS was much lower than the average duration of fungal cultures (Figure 4). To clarify the actual diagnostic performance of mNGS in this study, the cutoff value of lg(RPKM) was used to identify the presence of IFI-causing fungi in the study subjects. After taking the final clinical decision as the gold standard, the results showed that the AUC for lg(RPKM) was higher than for the G and fungal culture tests, meaning that lg(RPKM) was superior at identifying fungal infections in patients. Moreover, the positive and negative coincidence rates were also higher than those of the culture method (Figure 5A, C, D). After eliminating the influence of *Candida* infection on the test results, the AUC value of the G test improved from 0.634 to 0.646 (Figures 5A, E). In identifying *Aspergillus* spp. infection, the AUC values of the GM assay and mNGS were 0.727 and 0.874, respectively. The diagnostic performance of mNGS was significantly better than that of GM test (P = 0.0104; Figures 5B, F).

TABLE 3 Pairwise comparison of ROC curves.

Variable	lg(RPKM)	Reads
AUC	0.967	0.939
95% CI	0.948 to 0.981	0.915 to 0.958
Difference between areas		0.0279
Standard error		0.0125
z-statistic		2.234
Significance level		$P = 0.0255$*

*P < 0.05 indicates a significant difference.

Correlation analysis between laboratory indices and fungal infection

Indicators such as white blood cell count, CRP, PCT, IL-6, and albumin may reflect the state of the body after infection to varying degrees. We used the Spearman method to analyze the correlation of eight indicators with the presence of fungal infection. The results showed that the serum albumin levels and lymphocyte counts were significantly lowered, and the CRP levels were significantly raised after fungal infection (Figures 6C, E, H). Leukocyte, neutrophil, monocyte, PCT and IL-6 were not significantly different between the fungal and non-fungal infection groups (Figure 6A, B, D, F, G). In addition, this study found that serum albumin as well as lymphocyte and monocyte counts were significantly negatively correlated with fungal infection, whereas the CRP and PCT values showed a significant positive correlation with fungal infection (Figure 6I; Table 4).

Discussion

IFIs are prevalent in critically ill patients and individuals suffering from pulmonary disease. Furthermore, diagnosing IFIs is challenging because of the non-specific symptoms and a low diagnosis rate (Liu et al., 2022b). The diagnosis of IFIs in immunocompromised patients is even more difficult, as the symptoms are more insidious than those of patients without immunosuppression and the sensitivity of serological tests is lower following the inhibition of the immune response. In immunocompromised patients, the major instigators of fungal pulmonary infection are *Aspergillus* spp. and *Pneumocystis jirovecii* (Fishman and Rubin, 1998; Chong et al., 2006; Brown et al., 2012). Infection with fungi such as *Histoplasma* spp., *Blastomyces* spp., and *Coccidioides* spp. is epidemic in America and Africa but is rare in China, which was in accordance with our results (Azoulay et al., 2020).

In this study, all subjects were suspected of pulmonary IFIs and showed symptoms or radiographic signs of fungal infection, 53% of them were ultimately judged to have a simple bacterial infection. Thus, in the absence of a laboratory diagnosis, bacterial infections can interfere with fungal infections. The occurrence of fungal-bacterial co-infection may be related to the immunocompromised state of the subjects in the fungal group, which was generally immunocompromised and severe. The characteristics of infection in the case of bacterial–fungal co-infection, as well as the specific mechanisms of interaction, need to be further investigated.

Candida spp. are the most frequently detected fungal pathogen in BALF; the top five species are *Candida albicans*, *Candida glabrata*, *Candida tropicalis*, *Candida parapsilosis*, and *Candida krusei* (Williams et al., 2013). Invasive candidiasis usually refers to candidemia and deep-seated infections such as those resulting in intra-abdominal abscesses, peritonitis, or osteomyelitis (Pappas et al., 2018). Despite the ubiquitous existence of *Candida* spp. in respiratory specimens, especially in the critically ill and immunosuppressed patients, true histopathologically confirmed that *Candida* pneumonia is rare (Meersseman et al., 2009; Hamet et al., 2012).

Fungal culture is time-consuming, and the positive rate of growth can be influenced by potential initiation of empirical antibiotics therapy. In contrast, mNGS, which rely on sequencing the DNA already present in clinical samples, can be completed in a short time. In our study, mNGS detected more fungal species than CMTs and with higher degrees of sensitivity and specificity. However, the false-positive rate of mNGS was significantly higher than that of CMTs. Therefore, it is necessary to distinguish between true positives and false positives when interpreting mNGS results. We used lg(RPKM) and read number as indicators for plotting ROC curves and evaluating the performance of mNGS. According to our analysis, lg(RPKM) and read number all showed excellent capacity for IFI diagnostics, and an identification cutoff was also established. Among these prediction parameters, lg(RPKM) exhibited superior performance. To further clarify the actual diagnostic efficacy of the lg(RPKM) threshold in fungal detection, we should apply this threshold to the all cases of suspected fungal infection.

Detection of (1,3)-β-d-glucan (BDG; a cell wall component of all fungi except *Cyrptococcus* and *mucormycetes*) and GM (an *Aspergillus* spp. hyphal cell wall constituent) in the blood or BALF of patients is widely used for the diagnosis of IFIs. The BDG is an adjunct marker of IFIs, but it does not distinguish between *Candida* spp., *Aspergillus* spp., and *P. jirovecii*, which are all associated with a high false-positive rate (Theel and Doern, 2013). In our study, the false-positive rate of BDG in the diagnosis of IFIs was 58.87%, which was lowered to 51.11% on subtraction of the *Candida*-associated bias and infection with

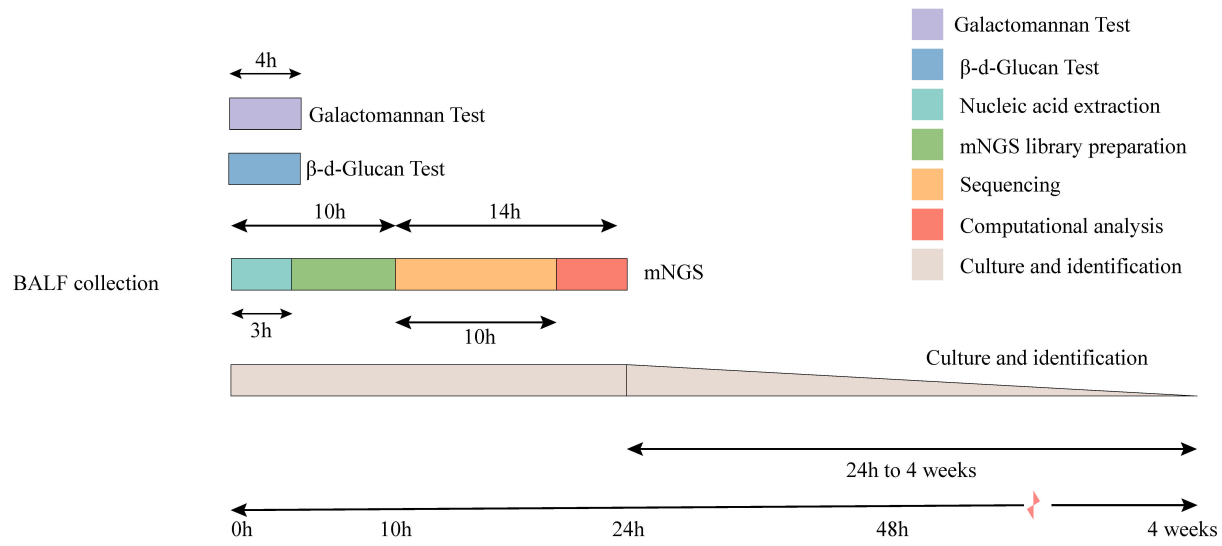

FIGURE 4
Timeline for mNGS and CMTs. Culture-based pathogen identification can take days to weeks. In comparison, mNGS testing using the BGI sequencing platforms has an overall turnaround time of 24 h.

other suspected colonizing fungi. Our study indicates that the combination of mNGS and BDG detection can improve the diagnostic efficiency of IFIs. According to reports, GM specifically identifies aspergillosis (Donnelly et al., 2020), with 21%–86% sensitivity and 80%–92% specificity in serum samples and with 60%–100% sensitivity and 68%–100% specificity in the BALF (Miceli and Kauffman, 2017). In our study, the sensitivity rate of BALF GM in the diagnosis of *Aspergillus* infection was 65.71% and the specificity rate was 78.12%, which was consistent with previous studies (Miceli and Kauffman, 2017; Donnelly et al., 2020). The AUC value for mNGS in the diagnosis of *Aspergillus* infection was 84.7%, which was significantly higher than for GM (72.7%). These findings indicate that mNGS could be especially useful in the diagnosis of *Aspergillus* infection.

We found that the efficiency of *P. jirovecii* detection was much higher for mNGS than that for CMTs. *P. jirovecii* is an important opportunistic fungus that can colonize the respiratory tract and be transmit from person to person *via* the airborne route. Thus, iatrogenically immunocompromised patients are the principal risk group for *P. jirovecii* infection. It was reported that one-third of *Pneumocystis* pneumonia cases occur in HIV-negative immunocompromised patients, possibility of due to an increase in infection when the CD4+ lymphocyte counts drop below 200 cells/μl (Morris et al., 2004; Laura et al., 2016). Immunofluorescence staining and/or PCR of sputum (in a sputum induction test) or BALF samples are feasible methods for the diagnosis of *P. jirovecii* pneumonia (PJP). However, the positive rate of direct immunofluorescent staining is relatively low, and PCR requires prior knowledge of the organisms present in the sample (Alexandre et al., 2016). As a new pathogen detection strategy, mNGS reached a sensitivity rate of 100% in the diagnosis of PJP, according to a study of HIV-negative immunocompromised patients (Jiang et al., 2021). Jiang et al. found that the sensitivity of mNGS was remarkably higher than those of Gomori methenamine silver staining (GMS; 25.0%) or the serum BDG test (67.4%) (Jiang et al., 2021). The specificity of mNGS (96.3%) also significantly surpassed the serum BDG test (81.4%) (Jiang et al., 2021). Similar conclusions were reached by other independent studies, in which mNGS outperformed GMS and BDG detection techniques for *P. jirovecii* infection (Xu et al., 2021; Sun et al., 2022; Duan et al., 2022).

Most of the current studies on the diagnosis of IFD by mNGS are clinical case reports (Chen et al., 2021; Wang et al., 2022; Cui et al., 2022; Hu et al., 2022). Several studies have focused on the diagnosis of pulmonary infections by mNGS, Peng et al. reported on 60 patients with suspected pneumonia in severe immunodeficiency and analyzed the diagnostic efficacy of mNGS versus CMTs for pneumonia (Peng et al., 2021). Peng et al. concluded that mNGS was more effective than CMTs for viral infections in the lung, but the opposite was true for fungal infections. This differs from the conclusion that we reached. In the study by Peng et al., many *Aspergillus*-positive patients tested negative for mNGS because of the

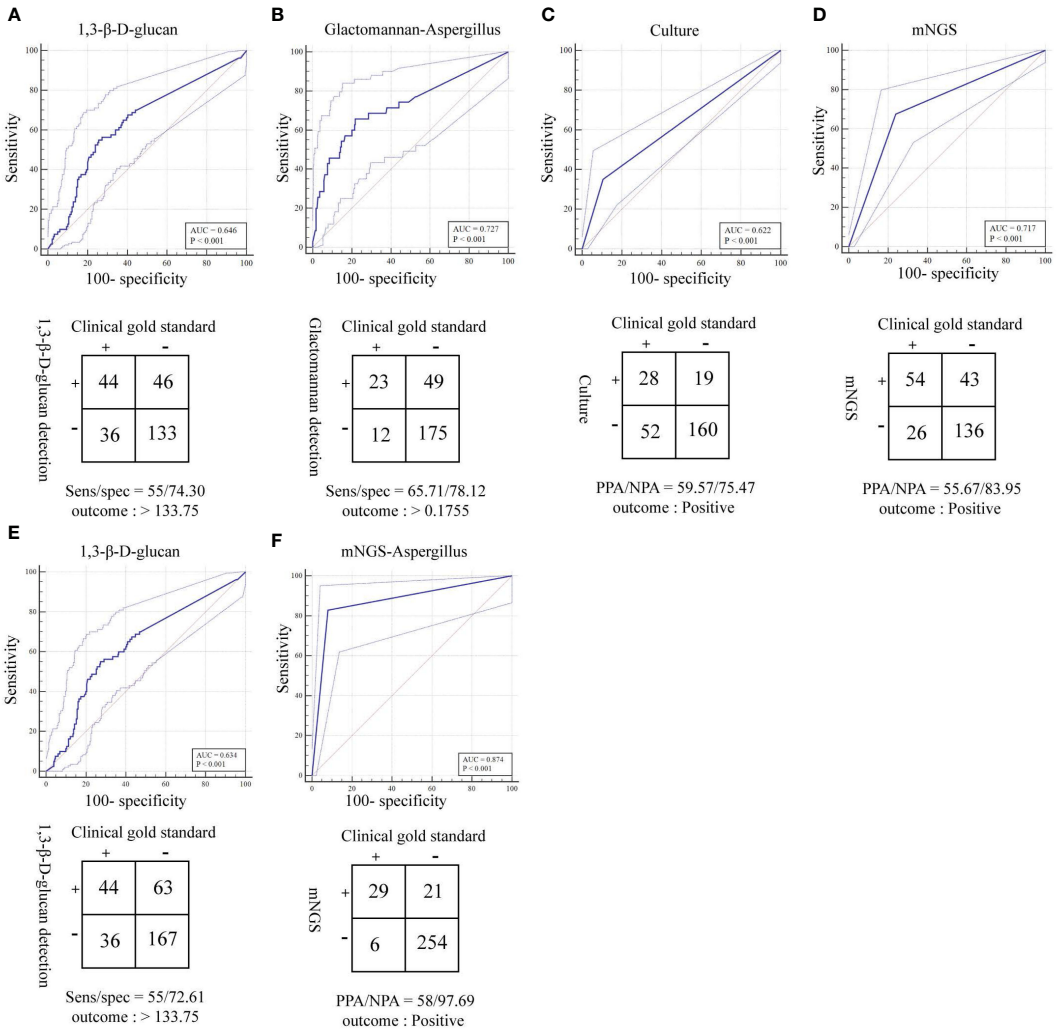

FIGURE 5
ROC curves and 2 × 2 contingency tables showing the respective diagnostic performance for different fungal detection methods; plotted are mNGS test sensitivities and specificities, relative to the clinical gold standard. PPA and NPA are shown in lieu of sensitivity (sens) and specificity (spec), respectively, if a composite standard was used. **(A)** Diagnostic efficacy of the 1,3-β-D glucan test (G test) for fungi (removal of patients with suspected *Candida* infection). **(B)** Diagnostic efficacy of the galactomannan test (GM test) for Aspergillus. **(C)** Diagnostic efficacy of the culture method for fungi. **(D)** Diagnostic efficacy of mNGS for fungi. **(E)** Diagnostic efficacy of the 1,3-β-D glucan test (G test) for fungi. **(F)** Diagnostic efficacy of mNGS for Aspergillus.

thick polysaccharide cell wall of *Aspergillus*, which made DNA extraction difficult. In our study, it has been possible to lyse *Aspergillus* and extract the relevant DNA for amplification detection well, benefiting from the development of pre-treatment techniques for mNGS. A related study by Lin et al., which included 69 immunodeficient patients with suspected pneumonia, concluded in agreement with us that the diagnostic efficacy of mNGS was significantly better than that of CMTs (Lin et al., 2022). Both studies by Peng et al. and Lin et al. compared the sensitivity and specificity of the two methods through simple statistical calculations, without using statistical tools such as ROC curves to comprehensively analyze the difference in diagnostic efficacy between mNGS and CMTs, and did not give diagnostic cutoff values. To the best of our knowledge, the current study is the largest study to evaluate the diagnostic performance of mNGS in immunocompromised patients with invasive fungal disease.

Our study has several limitations. First, the DNA extraction method that we used can be generically applied to viruses, bacteria, fungi, and parasites. Thus, the DNA

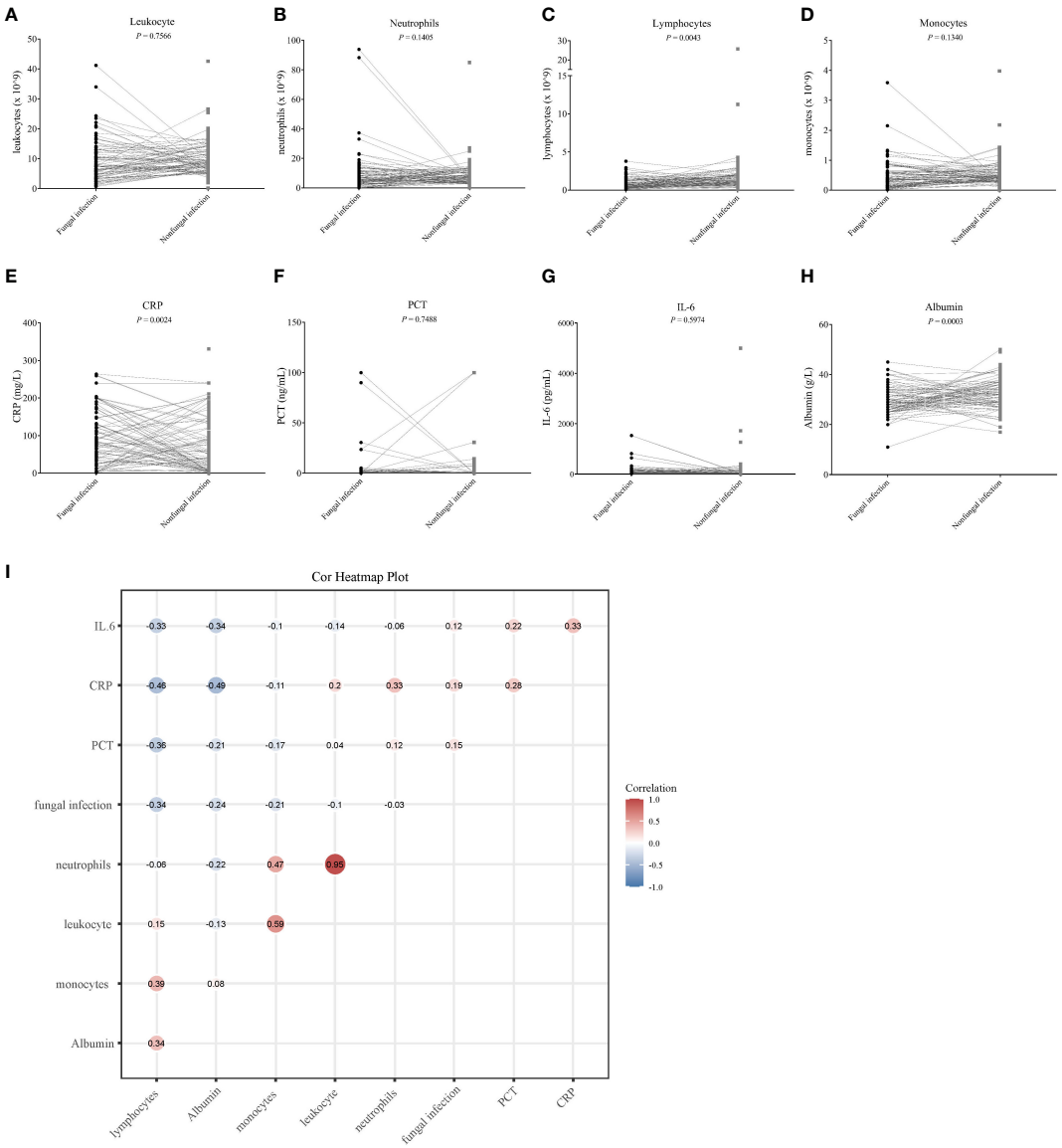

FIGURE 6
The correlation between eight clinical infection indicators and fungal infection. **(A–H)** Differential analysis of eight clinical infection indices in the fungal and non-fungal infection groups. The Student's t-test was used to evaluate the significance of any differences detected, and values with a $P < 0.05$ were considered as significant. **(I)** Heat map corresponding to the correlation analysis between the clinical infection indicators and fungal infection; a correlation coefficient is shown at each spot of the matrix. The Spearman method was used for the correlation analysis.

extraction efficacy for fungi could have been suboptimal due to the thickness of the fungal cell walls, which may require more vigorous DNA extraction methods. Second, we could not definitively distinguish between *Candida* infection and colonization, so this aspect of the data was excluded in certain types of analysis. Finally, the mNGS includes indicators such as read counts, [lg(RPKM)] in addition to genome coverage, and the relative abundance of each organism. Because a single indicator can only reflect part of the characteristics of a test system (Yuan et al., 2019), it is necessary to use multiple indicators to evaluate the test performance of mNGS in combination.

In conclusion, we established mNGS to be a promising diagnostic technique for IFIs. Compared with CMTs, mNGS

TABLE 4 The correlation between conventional indicators and fungal infection was analyzed using the Spearman's method.

Conventionalinfection indicators	Spearman'srank correlation coefficient (rho)	Significance level	95% Confidence interval for rho
Albumin	−0.241	$P = 0.0001$*	−0.352 to −0.122
CRP	0.191	$P = 0.0020$*	0.0709 to 0.306
IL-6	0.119	$P = 0.0558$	−0.00295 to 0.237
Leukocyte count	−0.103	$P = 0.0978$	−0.222 to 0.0190
Lymphocyte count	−0.344	$P < 0.0001$*	−0.447 to −0.232
Monocyte count	−0.209	$P = 0.0007$*	−0.322 to −0.0891
Neutrophil count	−0.0292	$P = 0.6403$	−0.151 to 0.0930
PCT	0.147	$P = 0.0175$*	0.0261 to 0.265

*P < 0.05 indicates a significant correlation.

has multiple advantages in identifying true-positive fungal infections. Although many challenges remain in the clinical application of mNGS, our study had shed new light on the applicability of this novel methodology for the diagnosis of IFIs.

Data availability statement

The datasets presented in this study can be found in online repositories. The name of the repository and accession number can be found below: CNGB Sequence Archive (CNSA) of China National GeneBank DataBase (CNGBdb); accession number CNP0003204.

Ethics statement

The studies involving human participants were reviewed and approved by Medical Ethics Committee of Liaocheng People's Hospital.

Author contributions

CW, ZY, and FP designed and drafted the paper; JF, SC, DB, HZ, PS, and XY collected medical records; CW, WX, and XJ performed statistical analyses; CW analyzed the mNGS data; FP and QZ revised the article. All authors read and approved the final article. All authors contributed to the article and approved the submitted version.

Funding

This research was supported by the Medical Science and Technology Development Foundation of Department of Health of Shandong Province, China (Grant No. 2019WS113).

Conflict of interest

The authors declare that the research was conducted in the absence of any commercial or financial relationships that could be construed as a potential conflict of interest.

Publisher's note

Supplementary material

The Supplementary Material for this article can be found online at: https://www.frontiersin.org/articles/10.3389/fcimb.2022.949505/full#supplementary-material

References

Alexander, B. D., Lamoth, F., Heussel, C. P., Prokop, C. S., Desai, S. R., Morrissey, C. O., et al. (2021). Guidance on imaging for invasive pulmonary aspergillosis and mucormycosis: From the imaging working group for the revision and update of the consensus definitions of fungal disease from the EORTC/MSGERC. *Clin. Infect. Dis.* 72, S79–s88. doi: 10.1093/cid/ciaa1855

Alexandre, A., Hauser, P. M., Lagrou, K., and Melchers, W. J.G. (2016). ECIL guidelines for the diagnosis of Pneumocystis jiroveciipneumonia in patients with haematological malignancies and stem cell transplant recipients. *J. Antimicrob. Chemother.* 71 (9), 2386–2396. doi: 10.1093/jac/dkw156

Azoulay, E., Russell, L., Louw, A., Metaxa, V., and Mirouse, A. (2020). Diagnosis of severe respiratory infections in immunocompromised patients. *Intensive Care Med.* 46 (2), 298–314. doi: 10.1007/s00134-019-05906-5

Ben, D. P., Walsh, T. J., Peter, D. J., Stevens, D. A., Edwards, J. E., Thierry, C., et al. (2008). Revised definitions of invasive fungal disease from the European organization for research and treatment of Cancer/Invasive fungal infections cooperative group and the national institute of allergy and infectious diseases mycoses study group (EORTC/MSG) Co. *Clin. Infect. Dis.* 46 (12), 1813–1821. doi: 10.1086/588660

Brown, G. D., Denning, D. W., Gow, N. A. R., Levitz, S. M., Netea, M. G., and White, T. C. (2012). Hidden killers: Human fungal infections. *Sci. Trans. Med.* 4, 165rv13. doi: 10.1126/scitranslmed.3004404

Chen, L., Su, Y., and Xiong, X. Z. (2021). Rhizopus microsporus lung infection in an immunocompetent patient successfully treated with amphotericin b: A case report. *World J. Clin. cases* 9, 11108–11114. doi: 10.12998/wjcc.v9.i35.11108

Chong, S., Lee, K. S., Yi, C. A., Chung, M. J., Kim, T. S., and Han, J. (2006). Pulmonary fungal infection: imaging findings in immunocompetent and immunocompromised patients. *Eur. J. Radiol.* 59, 371–383. doi: 10.1016/j.ejrad.2006.04.017

Cui, Q., Dai, H., Wu, D., He, J., Xu, Y., Tang, X., et al. (2022). Case report: A case of acute T lymphoblastic leukemia with mixed infection of lethal invasive mucormycosis and multi-drug resistant bacteria. *Front. Med. (Lausanne)* 9, 854338. doi: 10.3389/fmed.2022.854338

DeLong, E. R., Delong, D. M., and Clarke-Pearson, D. L. (1988). Comparing the areas under two or more correlated receiver operating characteristic curves: A nonparametric approach. *Biometrics* 44, 837–845. doi: 10.2307/2531595

D'enfert, C., and Bougnoux, M. E. (2014). "Human fungal infections," in *Encyclopedia of microbiology*, *4th ed.*, vol. 2, 652–664. Elsevier Science 2019. Available at: https://books.google.com.hk/books?id=7fvDDwAAQBAJ

De Pauw, B., Walsh, T. J., Donnelly, J. P., Stevens, D. A., Edwards, J. E., Calandra, T., et al. (2008). Revised definitions of invasive fungal disease from the European organization for research and treatment of Cancer/Invasive fungal infections cooperative group and the national institute of allergy and infectious diseases mycoses study group (EORTC/MSG) consensus group. *Clin. Infect. Dis.* 46, 1813–1821. doi: 10.1086/588660

Donnelly, J. P., Chen, S. C., Kauffman, C. A., Steinbach, W. J., Baddley, J. W., Verweij, P. E., et al. (2020). Revision and update of the consensus definitions of invasive fungal disease from the European organization for research and treatment of cancer and the mycoses study group education and research consortium. *Clin. Infect. Dis.* 71, 1367–1376. doi: 10.1093/cid/ciz1008

Donnelly, J. P., and Maertens, J. (2013). The end of the road for empirical antifungal treatment? *Lancet Infect. Dis.* 13, 470–472. doi: 10.1016/s1473-3099(13)70112-9

Duan, J., Gao, J., Liu, Q., Sun, M., Liu, Y., Tan, Y., et al. (2022). Characteristics and prognostic factors of non-HIV immunocompromised patients with pneumocystis pneumonia diagnosed by metagenomics next-generation sequencing. *Front. Med. (Lausanne)* 9, 812698. doi: 10.3389/fmed.2022.812698

El-Baba, F., Gao, Y., and Soubani, A. O. (2020). Pulmonary aspergillosis: What the generalist needs to know. *Am. J. Med.* 133, 668–674. doi: 10.1016/j.amjmed.2020.02.025

Faraggi, D. (2000). The effect of random measurement error on receiver operating characteristic (ROC) curves. *Stat. Med.* 19, 61–70. doi: 10.1002/(SICI)1097-0258(20000115)19:1<61::AID-SIM297>3.0.CO;2-A

Ferrarese, A., Cattelan, A., Cillo, U., Gringeri, E., Russo, F. P., Germani, G., et al. (2020). Invasive fungal infection before and after liver transplantation. *World J. Gastroenterol.* 26, 7485–7496. doi: 10.3748/wjg.v26.i47.7485

Fishman, J. A., and Rubin, R. H. (1998). Infection in organ-transplant recipients. *New Engl. J. Med.* 339, 773–778. doi: 10.1056/NEJM199806113382407

Gu, W., Deng, X., Lee, M., Sucu, Y. D., Arevalo, S., Stryke, D., et al. (2021). Rapid pathogen detection by metagenomic next-generation sequencing of infected body fluids. *Nat. Med.* 27, 115–124. doi: 10.1038/s41591-020-1105-z

Hamet, M., Pavon, A., Dalle, F., Pechinot, A., Prin, S., Quenot, J. P., et al. (2012). *Candida* spp. airway colonization could promote antibiotic-resistant bacteria selection in patients with suspected ventilator-associated pneumonia. *Intensive Care Med.* 38, 1272–1279. doi: 10.1007/s00134-012-2584-2

Hu, Q., Li, Y., Zhang, Y., Sun, S., Wang, H., Jiang, Z., et al. (2022). Case report: First report of T-cell Large granular lymphocytic leukemia with NPL-DHX9 gene fusion successfully treated with cladribine: Clinical experience and literature review. *Front. Oncol.* 10 (3), 1733–1745, 824393. doi: 10.3389/fonc.2022.824393

Jiang, J., Bai, L., Yang, W., Peng, W., An, J., Wu, Y., et al. (2021). Metagenomic next-generation sequencing for the diagnosis of pneumocystis jirovecii pneumonia in non-HIV-Infected patients: A retrospective study. *Infect. Dis. Ther.*, 10 (3), 1733–1745. doi: 10.1007/s40121-021-00482-y

Kim, S. H., Choi, J. K., Cho, S. Y., Lee, H. J., Park, S. H., Choi, S. M., et al. (2017). Risk factors and clinical outcomes of breakthrough yeast bloodstream infections in patients with hematological malignancies in the era of newer antifungal agents. *Med. Mycol.* 56 (2), 197–206. doi: 10.1093/mmy/myx038

Laura, A., Naylor, S., and Roecker, A. M. (2016). Pneumocystis jirovecii pneumonia in the non-HIV-Infected population. *Ann. Pharmacother.* 50 (8), 673–679. Available at: https://www.ncbi.nlm.nih.gov/pmc/articles/PMC3805843/

Li, H., and Durbin, R. (2009). Fast and accurate short read alignment with burrows-wheeler transform. *Bioinformatics* 25, 1754–1760. doi: 10.1093/bioinformatics/btp324

Lin, P., Chen, Y., Su, S., Nan, W., Zhou, L., Zhou, Y., et al. (2022). Diagnostic value of metagenomic next-generation sequencing of bronchoalveolar lavage fluid for the diagnosis of suspected pneumonia in immunocompromised patients. *BMC Infect. Dis.* 22, 416. doi: 10.1186/s12879-022-07381-8

Liu, H., Zhang, Y., Chen, G., Sun, S., Wang, J., Chen, F., et al. (2022a). Diagnostic significance of metagenomic next-generation sequencing for community-acquired pneumonia in southern China. *Front. Med.* 9. doi: 10.3389/fmed.2022.807174

Liu, H., Zhang, Y., Chen, G., Sun, S., Wang, J., Chen, F., et al. (2022b). Diagnostic significance of metagenomic next-generation sequencing for community-acquired pneumonia in southern China. *Front. Med. (Lausanne)* 9, 807174. doi: 10.3389/fmed.2022.807174

Liu, H., Zhang, Y., Yang, J., Liu, Y., and Chen, J. (2022c). Application of mNGS in the etiological analysis of lower respiratory tract infections and the prediction of drug resistance. *Microbiol. Spectr.* 10, e0250221. doi: 10.1128/spectrum.02502-21

Meersseman, W., Lagrou, K., Spriet, I., Maertens, J., Verbeken, E., Peetermans, W. E., et al. (2009). Significance of the isolation of *candida* species from airway samples in critically ill patients: A prospective, autopsy study. *Intensive Care Med.* 35, 1526–1531. doi: 10.1007/s00134-009-1482-8

Miao, Q., Ma, Y., Wang, Q., Pan, J., Yao, Z., Wenting, J., et al. (2018). Microbiological diagnostic performance of metagenomic next-generation sequencing when applied to clinical practice. *Clin. Infect. Dis* 67 (suppl_2), S231–S240. doi: 10.1093/cid/ciy693

Miceli, M. H., and Kauffman, C. A. (2017). Aspergillus galactomannan for diagnosing invasive aspergillosis. *Jama* 318, 1175–1176. doi: 10.1001/jama.2017.10661

Morris, A., Lundgren, J. D., Masur, H., Walzer, P. D., Hanson, D. L., Frederick, T., et al. (2004). Current epidemiology of pneumocystis pneumonia. *Emerg. Infect. Dis.* 10, 1713–1720. doi: 10.3201/eid1010.030985

Palacios, G., Druce, J., Du, L., Tran, T., Birch, C., Briese, T., et al. (2008). A new arenavirus in a cluster of fatal transplant-associated diseases. *N Engl. J. Med.* 358, 991–998. doi: 10.1056/NEJMoa073785

Pappas, P. G., Lionakis, M. S., Arendrup, M. C., Ostrosky-Zeichner, L., and Kullberg, B. J. (2018). Invasive candidiasis. *Nat. Rev. Dis. Primers* 4, 18026. doi: 10.1038/nrdp.2018.26

Pasqualotto, A. C., Nedel, W. L., Machado, T. S., and Severo, L. C. (2006). Risk factors and outcome for nosocomial breakthrough candidaemia. *J. Infect.* 52, 216–222. doi: 10.1016/j.jinf.2005.04.020

Peng, J. M., Du, B., Qin, H. Y., Wang, Q., and Shi, Y. (2021). Metagenomic next-generation sequencing for the diagnosis of suspected pneumonia in immunocompromised patients. *J. Infect.* 82, 22–27. doi: 10.1016/j.jinf.2021.01.029

Prattes, J., Valentin, T., Hoenigl, M., Talakic, E., Reisinger, A. C., and Eller, P. (2021). Invasive pulmonary aspergillosis complicating COVID-19 in the ICU - a case report. *Med. Mycol. Case Rep.* 31, 2–5. doi: 10.1016/j.mmcr.2020.05.001

Qian, Y. Y., Wang, H. Y., Zhou, Y., Zhang, H. C., Zhu, Y. M., Zhou, X., et al. (2020). Improving pulmonary infection diagnosis with metagenomic next generation sequencing. *Front. Cell Infect. Microbiol.* 10, 567615. doi: 10.3389/fcimb.2020.567615

Schlaberg, R., Chiu, C. Y., Miller, S., Procop, G. W., Weinstock, G.Committee, P. P, et al. (2017). Validation of metagenomic next-generation sequencing tests for universal pathogen detection. *Arch. Pathol. Lab. Med.* 141, 776. doi: 10.5858/arpa.2016-0539-RA

Suleyman, G., and Alangaden, G. J. (2021). Nosocomial fungal infections: Epidemiology, infection control, and prevention. *Infect. Dis. Clin. North Am.* 35, 1027–1053. doi: 10.1016/j.idc.2021.08.002

Suleyman, G., Fadel, R., Brar, I., Kassab, R., Khansa, R., Sturla, N., et al. (2022). Risk factors associated with hospitalization and death in COVID-19 breakthrough infections. *Open Forum Infect. Dis.* 9, ofac116–ofac116. doi: 10.1093/ofid/ofac116

Sun, H., Wang, F., Zhang, M., Xu, X., Li, M., Gao, W., et al. (2022). Diagnostic value of bronchoalveolar lavage fluid metagenomic next-generation sequencing in pneumocystis jirovecii pneumonia in non-HIV immunosuppressed patients. *Front. Cell Infect. Microbiol.* 12, 872813. doi: 10.3389/fcimb.2022.872813

Theel, E. S., and Doern, C. D. (2013). β-d-glucan testing is important for diagnosis of invasive fungal infections. *J. Clin. Microbiol.* 51, 3478–3483. doi: 10.1128/JCM.01737-13

Wang, J., Wang, Y., Han, F., and Chen, J. (2022). Multiple diagnostic methods for mucormycosis: A retrospective case series. *J. Clin. Lab. Anal.* 36, e24588. doi: 10.1002/jcla.24588

Wang, C., Yang, Y., Xu, M., Mao, F., Yang, P., Yuan, S., et al. (2021). Deep sequencing of the rat MCAO cortexes reveals crucial circRNAs involved in early stroke events and their regulatory networks. *Neural Plast.* 2021, 9942537. doi: 10.1155/2021/9942537

Williams, D. W., Jordan, R., Wei, X. Q., Alves, C. T., Wise, M. P., Wilson, M. J., et al. (2013). Interactions of *candida albicans* with host epithelial surfaces. *J. Oral. Microbiol.* 5. doi: 10.3402/jom.v5i0.22434

Xu, J., Yu, Y., Lv, J., Yang, S., Wu, J., Chen, J., et al. (2021). Application of metagenomic next-generation sequencing to diagnose pneumocystis jirovecii pneumonia in kidney transplantation recipients. *Ann. Transplant.* 26, e931059. doi: 10.12659/AOT.931059

Youden, W. J. (1950). Index for rating diagnostic tests. *Cancer* 3, 32–35. doi: 10.1002/1097-0142(1950)3:1<32::AID-CNCR2820030106>3.0.CO;2-3

Yuan, H., Fan, X. S., Jin, Y., He, J. X., Gui, Y., Song, L. Y., et al. (2019). Development of heart failure risk prediction models based on a multi-marker approach using random forest algorithms. *Chin. Med. J. (Engl)* 132, 819–826. doi: 10.1097/CM9.0000000000000149

frontiers | Frontiers in Cellular and Infection Microbiology

TYPE Original Research
PUBLISHED 20 October 2022
DOI 10.3389/fcimb.2022.997256

OPEN ACCESS

EDITED BY
Gilberto Sabino-Santos,
Tulane University School of Public Health and Tropical Medicine, United States

REVIEWED BY
Guoqing Qian,
Ningbo First Hospital, China
Hossein Zarrinfar,
Mashhad University of Medical Sciences, Iran
Kazuhiro Horiba,
Karolinska Institutet (KI), Sweden

*CORRESPONDENCE
Jue Pan
pan.jue@zs-hospital.sh.cn

SPECIALTY SECTION
This article was submitted to Clinical Microbiology, a section of the journal Frontiers in Cellular and Infection Microbiology

RECEIVED 18 July 2022
ACCEPTED 04 October 2022
PUBLISHED 20 October 2022

CITATION
Su Y, Miao Q, Li N, Hu B-j and Pan J (2022) Diagnostic accuracy of metagenomic next-generation sequencing for cryptococcosis in immunocompetent and immunocompromised patients. *Front. Cell. Infect. Microbiol.* 12:997256. doi: 10.3389/fcimb.2022.997256

Diagnostic accuracy of metagenomic next-generation sequencing for cryptococcosis in immunocompetent and immunocompromised patients

Yi Su, Qing Miao, Na Li, Bi-jie Hu and Jue Pan*

Zhongshan Hospital, Fudan University, Shanghai, China

Objective: To compare the diagnostic accuracy of metagenomic next-generation sequencing (mNGS) for cryptococcosis in patients with different immune statuses with that of conventional detection.

Methods: A total of 1442 specimens including 71 specimens from patients with cryptococcosis were analyzed in the study. The chi square test was used to screen the sensitivity and specificity of different detection methods for different specimen types. One-way ANOVA was used to compare the mNGS results with age, CD4, lymphocytes, IFN, IL-6, IL-2 and serum antigen assay.

Results: The sensitivity of mNGS was 44.29% in *Cryptococcus* infection cases. The positive rate of mNGS results for bronchoalveolar lavage fluid (BALF, 87.50%) from immunocompromised patients was higher than that of BALF from immunocompetent patients (40.00%, p=0.04). The sensitivity of the serum *Cryptococcus* capsular antigen assay was 80.00% in immunocompetent patients and 96.42% in immunocompromised patients (p = 0.049). A positive rate of detection of *Cryptococcus* from mNGS was higher when cryptococcal antigen ≥1:160 (p=0.022) in immunocompromised patients. A positive rate of detection of *Cryptococcus* from mNGS was higher when lymphocyte counts were lower in both immunocompetent patients(p=0.017) and in immunocompromised patients(p=0.029).

Conclusions: The sensitivity of mNGS is lower than that of serum cryptococcal antigen assay and histopathology in immunocompetent patients. However, BALF detection is recommend for immunocompromised patients compared with tissue and CSF. The positive mNGS result was correlated with lower lymphocyte counts, higher IL-2 and higher serum antigen assay in immunocompromised patients.

KEYWORDS

cryptococcosis, mNGS, immunocompetent, immunocompromised, diagnosis

Introduction

Cryptococcosis is an invasive fungal infection caused by *Cryptococcusneoformans* or *CryptococcusC. gattii* that has become increasingly prevalent in both immunocompetent and immunocompromised patients. Cryptococcosis is confirmed by positive culture, which can define the types of *Cryptococcus* and their antifungal susceptibility, but this method always takes 3-5 days. Positive results of cryptococcal antigen assays of serum, bronchoalveolar lavage fluid (BALF) or cerebrospinal fluid (CSF) and positive histopathologic results can help to quickly diagnose the infection but may be present false positive and false negative results.

Metagenomic next-generation sequencing (mNGS) is a technique that is increasingly used for the clinical diagnosis of infectious diseases, especially when the pathogen of the infectious disease cannot be cultured or detected normally (Han et al., 2019). Most studies have reported the use of mNGS in the diagnosis of bacterial and viral infections (Miao et al., 2018; Xie et al., 2019). In addition, many cases of rare pathogen infections detected by mNGS have been reported (Salzberg et al., 2016). However, few studies have analyzed the value of mNGS in the diagnosis of fungal infections, especially in patients with cryptococcosis. In our research, we summarized 1442 mNGS results and evaluate their diagnostic accuracy compared with that of conventional diagnosis methods.

Previous studies on cryptococcosis have mainly focused on cryptococcal infections in immunocompromised patients with central nervous system (CNS) infections. As a new detection method, for the first time, mNGS was analyzed and evaluated for its efficacy in both immunocompetent and immunocompromised patients, mainly for pulmonary cryptococcosis.

Materials and methods

Case series

Cases met the inclusion criteria if the patients were admitted to the Department of Infectious Disease from Zhongshan Hospital, Fudan University, from April 1, 2017, to January 31, 2021. This study is part of a research project that aims to detect pathogens from patients with clinically suspected infections using mNGS. The demographic, clinical feature, laboratory result, pathogenic finding, treatment and outcome data were extracted from the Hospital Information System of Zhongshan Hospital. The project was approved by the ethics committee of Zhongshan Hospital. All data were checked by two physicians (QM and YS), and a third researcher (JP) settled any difference in interpretation between the two primary reviewers.

Case definition

Cases with an admitting diagnosis of suspected pulmonary infection or central nervous system infection were included in this retrospective analysis. Cryptococcus detection by mNGS (strict mapping read number (SMRN)≥1 or strict mapping read number genus (SMRNG)≥1) was defined as a positive result. Cryptococcosis includes confirmed cryptococcosis and clinical cryptococcosis.Confirmed cryptococcosis was defined as a positive *Cryptococcus* culture of a specimen from any site. Clinical cryptococcosis was defined byorpositive results on histopathologyor positive cryptococcal antigen assay, together with clinical or radiographic evidence of disease (Baddley et al., 2008). Immunocompromised hosts were considered to have at least one predisposing condition, including AIDS, liver cirrhosis, hematologic malignancy, malignant solid tumor, chronic steroid use and rheumatologic disease (rheumatoid arthritis, lupus, psoriatic arthritis, ankylosing spondylitis (AS), Sjogren's syndrome, and inflammatory myopathy) (Brizendine et al., 2013; Lin et al., 2015).

Laboratory diagnosis

Culture and identification

Cryptococcus was cultured from CSF, sputum, BALF, blood and tissue biopsy on Sabouraud Dextrose GC Agarplates (OXOID, Thermo Scientific, USA). Colonies are observed on solid agar plates after 48 to 72 hours incubation at 30°C to 35°C in aerobic conditions and will appear as opaque, white-to-cream colonies that may turn orange-tan or brown after prolonged incubation. Identifcation of fungal isolates was performed using the MALDI-Biotyper system.

Histopathology

Cryptococcus can be identified by histologic staining of tissues from the lung, skin, and other organs. The organism is observed as a yeast that reproduces by narrow-based budding. The yeast is identified by special stains that label the polysaccharide capsule including periodic acid-Schiff and Gomori methenamine silver. Biobsy was independently analysed by two trained examiners.

Serology

All blood, BALF and CSF samples were analysed using the Latex Cryptococcus Antigen Detection System (IMMY, Norman, USA). The test was performed according to the

manufacturers' instructions. Samples were independently analysed by two trained examiners, and no incongruences occurred. The results were read out in titre levels.

mNGS procedure for specimens

A 0.5-3 mL sputum or BALF or CSFspecimen from the patients was collected according to standard procedures. Sputum was liquefied by addition of 0.1% DTT for 30 min at room temperature, and BALF or CSF was directly submitted to the next operation. Then, 1.5 mL microcentrifuge tubes with 0.5 mL of specimen and 1 g of 0.5 mm glass bead were attached to a horizontal platform on a vortex mixer and agitated vigorously at 2800-3200 RPM for 30 min. Next, 0.3 mL of specimen was separated into a new 1.5 mL microcentrifuge tube, and DNA was extracted using a TIANamp Micro DNA Kit (DP316, TIANGEN BIOTECH) according to the manufacturer's recommendation. DNA could also be extracted directly from 300 μL CSF specimens and tissue specimens using the TIANamp Micro DNA Kit. The extracted DNA was sonicated to obtain 200-300 bp fragments (Bioruptor Pico protocols). Then, DNA libraries were constructed through end repair, adapter ligation and PCR amplification. We used an Agilent 2100 for quality control of the DNA libraries, and quality qualified libraries were sequenced by the BGISEQ-100 platform (Jeon et al., 2014). High-quality sequencing data were generated by removing low-quality and short (length<35 bp) reads, followed by computational subtraction of human host sequences mapped to the human reference genome (hg19) using Burrows–Wheeler alignment (Li and Durbin, 2009). The remaining data were classified by the removal of low-complexity reads and by simultaneous alignment to four microbial genome databases. The reference database for microbial classification was The Pathogens metagenomics Database (PMDB, v6.0), a commercial pathogen alignment database developed by PathoGenesis Pharmaceutical Technology (BGI-Shenzhen, Shenzhen), containing 4,945 whole genome sequence of viral taxa, 6,350 bacteral genomes or scaffolds, 1064 fungi related to human infection, and 234 parasites associated with human diseases. The PMDB contains genomes and genome assembles from NCBI, including Refseq and high quality genome assembles registered with NCBI.

Statistical analysis of the data

Depending on the distribution of the data, categorical variables were described as percentages, and continuous variables were described as the mean and standard deviation. The chi square test was used to screen the sensitivity of mNGS from BALF, tissue and CSF, the specificity of mNGS from sputum, BALF, tissue, CSF and blood, the sensitivity of antigen assay from blood, BALF and CSF, the sensitivity of pathology from tracheoscopic, lung puncture and total and the sensitivity of culture from BALF, CSF and tissue. One-way ANOVA was used to compare the mNGS results withage ,CD4, lymphocytes, IFN, IL-6, IL-2,serum antigen assay. A probability (P) value <.05 implies a statistically significant difference. Statistical analyses were performed using SPSS software (version 23). The figures were constructed using GRAPHPAD PRISM 8.0.

Results

Specimens and patient characteristics

A total of 1442 specimens were included in the analysis, with 71 specimens from cryptococcosis cases and 1371 specimens from non-cryptococcosis cases (Figure 1). 61 (85.92%) specimens from 71 cryptococcosis cases were positive in antigen assay from blood, 20 (28.17%) were positive in culture, and 39 (54.93%) were positive in pathology. Of all 71 specimens from cryptococcosis cases before diagnosis, 19 specimens of cases did not use any antibacterial and antifungal drugs, 32 used antibacterial drugs, 8 used antifungal drugs, and 12 used both antibacterial and antifungal drugs. Of 20 specimens from confirmed *Cryptococcus* patients, 9 were from immunocompetent patients and 11 were from immunocompromised patients. Of 51 specimens from clinical *Cryptococcus* patients, 33 were from immunocompetent patients and 18 were from immunocompromised patients.Of all the specimens, 969 specimens were from immunocompetent patients, among which 530 (54.70%) specimens were from males with an average age of 53.79 ± 16.43 years and 439 (45.30%) specimens were from females with an average age of 54.05 ± 17.15 years. A total of 473 specimens were from immunocompromised patients, among which 251 (53.07%) specimens were from males with an average age of 55.90 ± 14.11 years and 222 (46.93%) specimens were from females with an average age of 59.36 ± 14.90 years. The distribution of different kinds of specimens from patients with different immune states is shown in Figure 2. SMRN of cryptococcosis cases ranged from 1 to 1333873 and the median was 40.5, SMRNG of cryptococcosis cases ranged from 1 to 1506102 and the median was 48.

Sensitivity and specificity of mNGS from different specimens

The sensitivity of mNGS was 44.29% in Cryptococcus infection cases, and the specificity was 99.8%. The positive rate of mNGS of BALF from immunocompromised patients was higher than that of BALF from immunocompetent patients (p=0.04) (Figure 3).

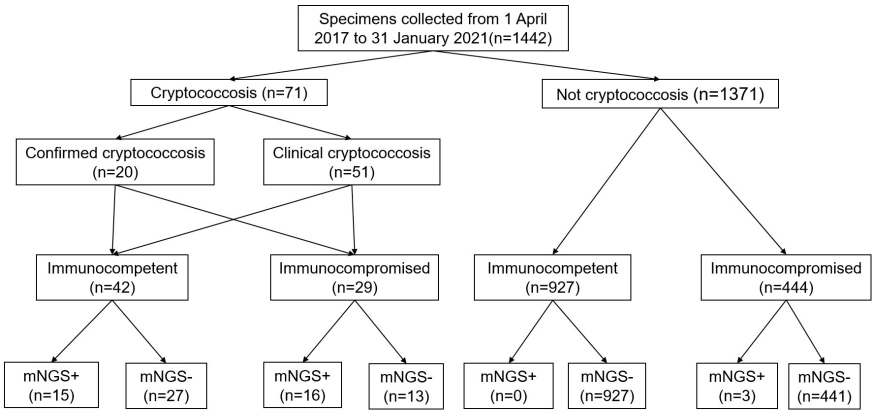

FIGURE 1
Flow chart of sample selection and classification. In total, 1442 specimens were divided into cryptococcosis and NOT cryptococcosis on the retrospective diagnosis of the corresponding patients, mNGS+ refers to strict mapping reads number(SMRN)2 for strict mapping reads number genus(SMRNG)21. mNGS, metagenomic next generation sequencing.

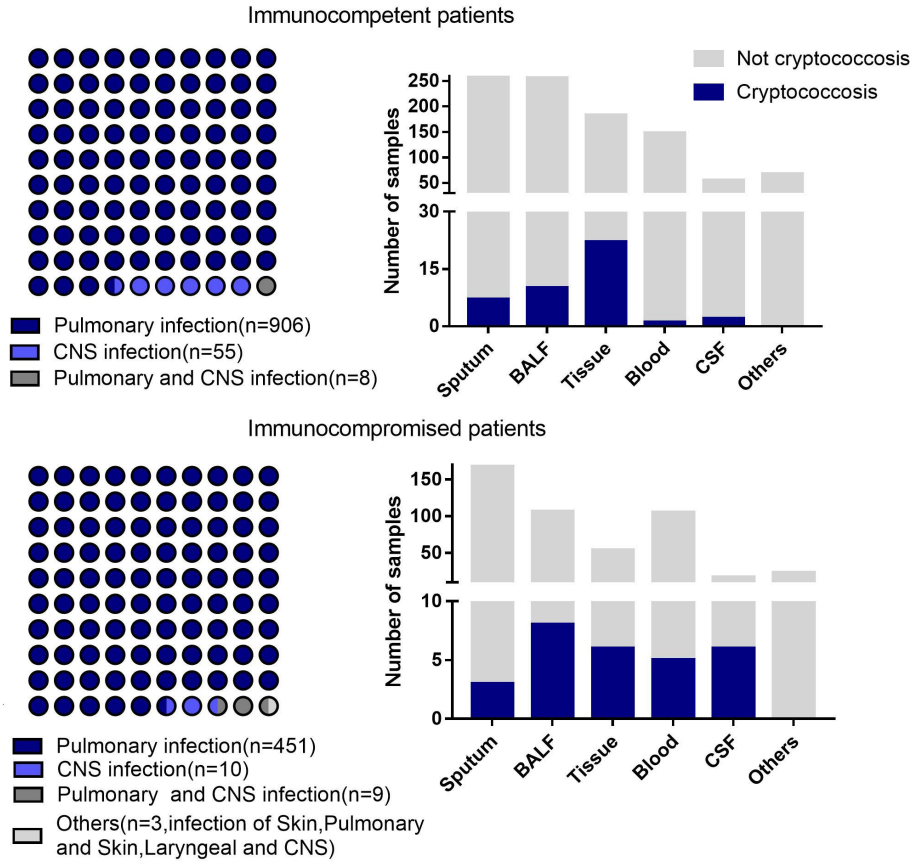

FIGURE 2
Disease distribution and different kinds of samples from the patients with different immune states. Others includes pleural effusion.

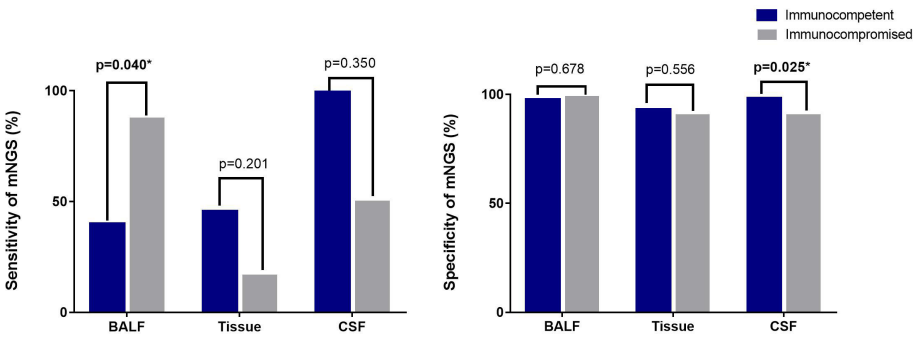

FIGURE 3
Sensitivity and specificity of mNGS from different samples by different immune statuses. The sensitivity of mNGS with sputum from 7 immunocompetent patients was 0%, and the positive rate of 3 sputum samples of immunocompromised patients was 33.33%. Sensitivity of mNGS from blood was not detected in immunocompetent patients. Two immunocompromised patients with disseminated cryptococcal infections were evaluated for mNGS of blood and the positive rate was 50%. The specificity of mNGS for sputum samples was 97.31% in immunocompetent patients and 98.79% in immunocompromised patients. The specificity of blood samples was 99,32% in immunocompetent patients and was 98.01% in immunocompromised patients. *means results has statistically significant.

Sensitivity of different detection methods

The sensitivity of the serum cryptococcal antigen assay in immunocompetent patients was 80%, and that in immunocompromised patients was 96.42% (p = 0.049). Compared with those from immunocompromised patients, there were no significant sensitivity differences in the pathology, culture and tissue from immunocompetent patients (Figure 4).

mNGS results with laboratory indexes

A positive rate of detection of *Cryptococcus* from mNGS was higher when cryptococcal antigen ≥1:160 (p=0.022) in immunocompromised patients. A positive rate of detection of *Cryptococcus* from mNGS was higher when lymphocyte counts were lower in both immunocompetent patients(p=0.017) and immunocompromised patients(p=0.029), as shown in Table 1.

Negative results from conventional detection methods and positive results from mNGS

From 3 patients diagnosed with community-acquired pneumonia, 2 sputum specimens and 1 BALF specimen for which *Cryptococcus* read number were detected were considered false positives. mNGS of 2 BALF specimens from immunocompetent cases detected the read number of *Cryptococcus*, but the serum antigen assay, pathology and culture were all negative. Combined with the patient's clinical manifestations clinical diagnosis of *Cryptococcus* was considered (Table 2).

Discussion

Pulmonary fungal infections are one of the main problems in patients with immune disorders, and one of these infections is

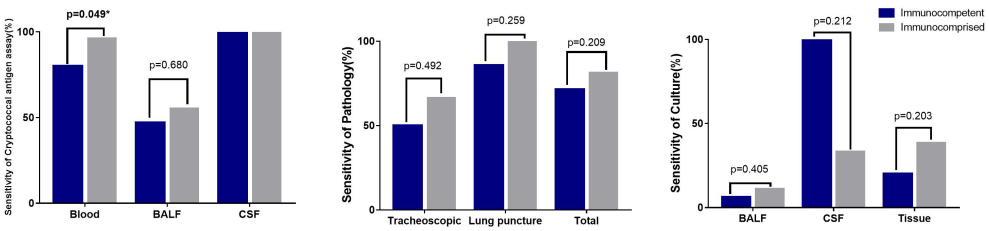

FIGURE 4
Sensitivity of different detection methods in different samples Sensitivity of 2 skin pathology from immunocomprised patients was 100%. The CSF culture in one immunocomptent patients of CNS cryptococcus infection was positive (100%), and 2 samples of CSF culture were positive from 6 samples of immunocomprised patients (33.3%).

TABLE 1 Relationship between positive mNGS results and laboratory indexes in patients with different immune statuses.

	Immunocompetent			Immunocompromised		
	mNGS+(n=15)	mNGS-(n=27)	p	mNGS+(n=16)	mNGS-(n=13)	p
Male/female	4/11	13/14	0.183	2/14	5/8	0.112
Age, years	46.67±14.11	44.52±14.49	0.645	56.06±11.59	54.69±15.95	0.791
CD4 (cells/μL)	518.35±255.66	621.19±282.26	0.265	291.07±257.18	505.85±369.51	0.083
Lymphocytes *10^9/L	1.31±0.81	1.81±0.46	***0.017****	0.77±0.65	1.37±0.73	***0.029****
IFN (8.1 pg/mL)	5.50±3.85	8.88±10.02	0.235	33.02±89.44	8.42±5.25	0.332
IL-6 (pg/mL)	4.36±6.21	7.69±25.51	0.635	4.64±4.34	7.38±5.74	0.162
IL-2>400 U/mL	327.42±286.53	382.92±268.67	0.185	437.28±405.83	648.15±432.12	***0.006****
Serum antigen assay≥1: 160	184.13±355.61	128.15±279.32	0.293	716.00±894.91	253.23±689.05	***0.022****

*means results has statistically significant. Bold values means results has statistically significant.

cryptococcosis, which must be differentiated from other fungal infections using precise laboratory methods (direct examination, culture, histopathology, antigens). As a new accurate diagnostic technique, the diagnostic value from mNGS in cryptococcosis patients with different immune states is worth exploring (Zarrinfar et al., 2012; Zanganeh et al., 2018; Kashefi et al., 2021). In our previous research, the values of mNGS outperformed those of culture, especially for Mycobacterium tuberculosis, viruses, anaerobes and fungi (Miao et al., 2018). This article confirms that the diagnostic value of mNGS in cryptococcosis is superior than that of culture.

The sensitivity of mNGS was only 44.29% in the diagnosis of Cryptococcus infections in our study, which was lower than that of cryptococcal antigen assay tests (>95% sensitivity) (Kabanda et al., 2014) and pathology (88% sensitivity in CT-guided percutaneous needle biopsy). The *Cryptococcus* cell wall is a two-layered structure composed of α-1,3-glucan, β-1,3 and β-1,6-glucan, chitin, chitosan, mannoproteins and other GPI-anchored proteins. The inner layer is mainly composed of β-glucans and chitin arranged as fibers parallel to the plasma membrane, and the outer layer contains α-glucan and β-glucan. The main reason for the low positive rate of *Cryptococcus* is that the nucleic acid cannot be released due to the thick cell wall and incomplete disruption of the *Cryptococcus* cell wall (Wang et al., 2018; Garcia-Rubio et al., 2020). Although mNGS has no advantage in sensitivity and cost, it is a fast method that takes less than 24 hours and reports microbial population identification. As cryptococcal antigen tests can be yield false negative results and biopsy could also fail, positive mNGS findings could remind clinicians of *Cryptococcus* infections and help to prove the diagnosis quickly (Wilson et al., 2011). Appropriate targeted antifungal drugs can be chosen immediately due to the speed of the test, and the microbial population can be identified.

In our research, three mNGS results were positive for *Cryptococcus* but were confirmed to be false positives. Since *Cryptococcus* is not a common contaminant or background fungus, a SMRN≥1 or a SMRNG≥1 should be reported in our rules. False positives may be caused by the operator's misoperation, contamination by the same batch of specimens or other undetected reasons. On the other hand, the results of 2 cases were negative by traditional detection methods, and only mNGS results were positive. Since the clinical manifestation and imaging findings were consistent with cryptococcosis and pulmonary lesions were absorbed after anti-cryptococcal treatment, these positive results were considered true positives. Therefore, positive results in *Cryptococcus* detection from mNGS alone could not independently confirm cryptococcosis, and the clinical manifestations and results of conventional methods should be additionally considered for the diagnosis of cryptococcosis.

Positive mNGS results are quite different for different types of specimens. In our research, the positive rates of *Cryptococcus*

TABLE 2 List of patients with negative traditional detection method and positive mNGS results.

Sample No.	Age	Gender	Diagnosis	Immune status	Sample	SMRN	SMRNG	Treatment	Prognosis
List of "false positive" samples in non-cryptococcus cases									
S53	54	male	CAP	immunocompetent	sputum	0	1	levofloxacin	cure
S279	75	male	CAP	immunocompetent	sputum	9	8	levofloxacin	cure
S637	50	male	CAP		BALF	5	5	SMZ	cure
List of "positive" samples in probable cryptococcus cases									
S45	54	female	pulmonary infection	immunocompetent	BALF	8	8	fluconazole	cure
S372	51	male	pulmonary infection	immunocompetent	BALF	5	5	fluconazole	cure

detection in BALF and CSF specimens were higher than that in lung tissues, while the positive rate in sputum was the lowest. Since few blood specimens were analyzed, the corresponding rate could not be assessed in this research. In a previous study, 90 patients with focal pulmonary infections were analyzed, and the sensitivity of mNGS analysis in the pathological specimen group, transbronchial brushing group and bronchoalveolar lavage group was 90%, 66.7 and 50%, respectively (Chen et al., 2021). The positive rate of mNGS in tissues in radial probe endobronchial ultrasound guided transbronchial lung biopsy (TBLB) (78.7%) was significantly higher than that in the TBLB group (60.6%) (Li et al., 2020). Therefore, obtaining and analyzing appropriate specimens are recommended to improve the sensitivity of the mNGS detection.

Articles about the value of laboratory tests in patients with cryptococcosis with different immune states are relatively rare. The cryptococcal antigen assay is less sensitive in HIV-negative than in HIV-positive patients, and values of 56–83% have been reported in HIV-negative immunocompromised patients with *Cryptococcus* pneumonia (Singh et al., 2008). In our research, including the cryptococcal antigen assay, the sensitivity of the detection methods in different specimens from immunocompromised patients was higher than that from immunocompetent patients. Therefore, etiological detection should be employed more in immunocompromised patients since cryptococcal infections are preferentially observed immunocompromised patients.

Cytokines are key modulators of the immune response and play an essential role in the defense mechanism against fungal infections. Research on immune response patterns in septic shock patients indicated that increases in IFN-γ and IL-6 levels were significantly elevated in septic patients suffering from fungal infection, especially in the early course of the disease (O.Decker et al., 2017). A study of patients with cryptococcal meningitis reported that a CSF proinflammatory response consists of an interplay of Th1 (IFN-γ and IL-6), Th2 (IL-4 and IL-10) and Th17 cytokines (IL-17A) and has been shown to be highly predictive of increased macrophage activation, rapid infection clearance and consequently improved survival (Jarvis et al., 2015). Another study also reported that IFN-γ could improve host immune responses against cryptococcal infection in HIV-infected patients (Jarvis et al., 2012). In our study, specimens with increasing cytokine levels (IL-2>400) yielded more positive mNGS results. Therefore, mNGS-based *Cryptococcus* findings correspond with plasma cytokine levels, which means that in patients with increasing cytokine levels, the mNGS-based approach revealed signs of a *Cryptococcus* infection prior to the culture-based finding, providing the opportunity to initiate targeted antifungal therapy in infected patients.

Conclusion

The sensitivity of mNGS is lower than that of serum cryptococcal antigen assay and histopathology in immunocompetent patients.BALF detection is recommend for immunocompromised patients compared with tissue and CSF. The positive mNGS result was correlated with lower lymphocyte counts, higher IL-2 and higher serum antigen assay in immunocompromised patients

Data availability statement

The datasets presented in this study can be found in online repositories. The names of the repository/repositories and accession number(s) can be found below: EMBL-EBI, PRJEB55094.

Ethics statement

The studies involving human participants were reviewed and approved by Ethics Committee of Zhongshan Hospital Fudan University. The patients/participants provided their written informed consent to participate in this study. Written informed consent was obtained from the individual(s) for the publication of any potentially identifiable images or data included in this article.

Author contributions

YS conceived and designed the work that led to the submission, QM played an important role in interpreting the results, NL acquired data, B-JH revised the manuscript, and JP revised the manuscript. All authors contributed to the article and approved the submitted version.

Funding

This work was supported by grants from the National Key Research and Development Program of China(2021YFC 2300400), the Clinical Research Plan of SHDC (SHDC2020CR2031B) and the Fund of Zhongshan Hospital (2021ZSFZ15).

Conflict of interest

The authors declare that the research was conducted in the absence of any commercial or financial relationships that could be construed as a potential conflict of interest.

Publisher's note

References

Baddley, J. W., Perfect, J. R., Oster, R. A., Larsen, R. A., Pankey, G. A., Henderson, H., et al. (2008). Pulmonary cryptococcosis in patients without HIV infection: factors associated with disseminated disease. *Eur. J. Clin. Microbiol. Infect. Dis.* 27, 937–943. doi: 10.1007/s10096-008-0529-z

Brizendine, K. D., Baddley, J. W., and Pappas, P. G. (2013). Predictors of mortality and differences in clinical features among patients with cryptococcosis according to immune status. *PloS One* 8 (3), e60413. doi: 10.1371/journal.pone.0060431

Chen, Y., Yan, X., Li, N., Zhang, Q., Lv, Y., and Ruan, T. (2021). Metagenomic next-generation sequencing of radial ultrasound bronchoscopy-guided "cocktail" specimens as an efficient method for the diagnosis of focal pulmonary infections: a randomised study. *Ann. Palliat Med.* 10 (2), 2080–2088. doi: 10.21037/apm-20-2578

Garcia-Rubio, R., de Oliveira, H. C., Rivera, J., and Trevijano-Contador, N. (2020). The fungal cell wall: Candida, cryptococcus, and aspergillus species. *Front. Microbiol.* 10. doi: 10.3389/fmicb.2019.02993

Han, D., Li, Z., Li, R., Tan, P., Zhang, R., and Li, J. (2019). mNGS in clinical microbiology laboratories: on the road to maturity. *Crit. Rev. Microbiol.* 45 (5-6), 668–685. doi: 10.1080/1040841X.2019.1681933

Jarvis, J. N., Meintjes, G., Bicanic, T., Buffa, V., Hogan, L., Mo, S., et al. (2015). Cerebrospinal fluid cytokine profiles predict risk of early mortality and immune reconstitution inflammatory syndrome in HIV-associated cryptococcal meningitis. *PloS Pathog.* 11 (4), e1004754. doi: 10.1371/journal

Jarvis, J. N., Meintjes, G., Rebe, K., Williams, G. N., Bicanic, T., Williams, A., et al. (2012). Adjunctive interferon-gamma immunotherapy for the treatment of HIV-associated cryptococcal meningitis: a randomized controlled trial. *AIDS* 26, 1105–1113. doi: 10.1097/QAD.0b013e3283536a93

Jeon, Y. J., Zhou, Y., Li, Y., Guo, Q., Chen, J., Quan, S., et al. (2014). The feasibility study of non-invasive fetal trisomy 18 and 21 detection with semiconductor sequencing platform. *PloS One* 9 (10), e110240. doi: 10.1371/journal.pone.0110240

Kabanda, T., Siedner, M. J., Klausner, J. D., Muzoora, C., and Boulware, D. R. (2014). Point-of-care diagnosis and prognostication of cryptococcal meningitis with the cryptococcal antigen lateral flow assay on cerebrospinal fluid. *Clin. Infect. Dis.* 58 (1), 113–116. doi: 10.1093/cid/cit641

Kashefi, E., Seyedi, S. J., Zarrinfar, H., Fata, A., Mehrad-Majd, H., Najafzadeh, M. J., et al. (2021). Molecular identification of candida species in bronchoalveolar lavage specimens of hospitalized children with pulmonary disorders. *J. Babol Univ Med. Sci.* 23, 331–336. doi: 10.22088/jbums.23.1.331

Li, H., and Durbin, R. (2009). Fast and accurate short read alignment with burrows-wheeler transform. *Bioinformatics* 25 (14), 1754–1760. doi: 10.1093/bioinformatics/btp324

Li, G., Huang, J., Li, Y., and Feng, J. (2020). The value of combined radial endobronchial ultrasound-guided transbronchial lung biopsy and metagenomic next-generation sequencing for peripheral pulmonary infectious lesions. *Can. Respir. J.* 2020, 2367505. doi: 10.1155/2020/2367505

Lin, Y.-Y., Shiau, S., and Fang, C.-T. (2015). Risk factors for invasive cryptococcus neoformans diseases: a case-control study. *PloS One* 10 (3), e0119090. doi: 10.1371/journal.pone.0119090

Miao, Q., Ma, Y., Wang, Q., Pan, J., Yao, Z., Wenting, J., et al. (2018). Microbiological diagnostic performance of metagenomic next-generation sequencing when applied to clinical practice. *Clin. Infect. Dis.* 67, S231–S240. doi: 10.1093/cid/ciy693

O.Decker, S., Sigl, A., Grumaz, C., Stevens, P., Vainshtein, Y., Zimmermann, S., et al. (2017). Immune-response patterns and next generation sequencing diagnostics for the detection of mycoses in patients with septic shock-results of a combined clinical and Experimental.Investigation. *Int.J.Mol.Sci.* 18 (8), 1796. doi: 10.3390/ijms18081796

Salzberg, S. L., Breitwieser, F. P., Kumar, A., Hao, H., Burger, P., Rodriguez, F. J., et al. (2016). Next-generation sequencing in neuropathologic diagnosis of infections of the nervous system. *Neurol. Neuroimmunol Neuroinflamm* 3 (4), e251. doi: 10.1212/NXI.0000000000000251

Singh, N., Alexander, B. D., Lortholary, O., Dromer, F, Gupta, K. L., John, G. T., et al. (2008). Pulmonary cryptococcosis in solid organ transplant recipients: clinical relevance of serum cryptococcal antigen. *Clin. Infect. Dis.* 46, e12–e18. doi: 10.1086/524738

Wang, Z. A., Li, L. X., and Doering, T. L. (2018). Unraveling synthesis of the cryptococcal cell wall and capsule. *Glycobiology* 10, 719–730. doi: 10.1093/glycob/cwy030

Wilson, D. A., Sholtis, M., Parshall, S., S.Hall, G., and Procop, G. W. (2011). False-positive cryptococcal antigen test associated with use of BBL port-A-Cul transport vials. *J. Clin. Microbiol.* 49 (2), 702–703. doi: 10.1128/JCM.01169-10

Xie, Y. A., Du, J. A., Jin, W. A., Teng, X. A., Cheng, R. A., Huang, P. A., et al. (2019). Next generation sequencing for diagnosis of severe pneumonia: China, 2010–2018. *J. Infect.* 78, 158–169. doi: 10.1016/j.jinf.2018.09.004

Zanganeh, E., Zarrinfar, H., Rezaeetalab, F., Fata, A., Tohidi, M., Najafzadeh, M., et al. (2018). Predominance of non-fumigatus aspergillus species among patients suspected to pulmonary aspergillosis in a tropical and subtropical region of the middle East. *Microbial Pathog* 116, 296–300. doi: 10.1016/j.micpath.2018.01.047

Zarrinfar, H., Saber, S., Kordbacheh, P., Makimura, K., Fata, A., Geramishoar, M., et al. (2012). Mycological microscopic and culture examination of 400 bronchoalveolar lavage (BAL) samples. *Iranian J. Publ Health* 41 (7), 70–76.

frontiers | Frontiers in Cellular and Infection Microbiology

TYPE Original Research
PUBLISHED 21 October 2022
DOI 10.3389/fcimb.2022.962441

OPEN ACCESS

EDITED BY
Jinmin Ma,
Beijing Genomics Institute (BGI), China

REVIEWED BY
Ruijin Guo,
Beijing Genomics Institute (BGI), China
Appakkudal R. Anand,
Sankara Nethralaya, India

*CORRESPONDENCE
Weiliang Huang
huangweil66@163.com

SPECIALTY SECTION
This article was submitted to Clinical Microbiology, a section of the journal Frontiers in Cellular and Infection Microbiology

RECEIVED 06 June 2022
ACCEPTED 27 September 2022
PUBLISHED 21 October 2022

CITATION
Mao Y, Shen H, Yang C, Jia Q, Li J, Chen Y, Hu J and Huang W (2022) Clinical performance of metagenomic next-generation sequencing for the rapid diagnosis of talaromycosis in HIV-infected patients.
Front. Cell. Infect. Microbiol. 12:962441.
doi: 10.3389/fcimb.2022.962441

Clinical performance of metagenomic next-generation sequencing for the rapid diagnosis of talaromycosis in HIV-infected patients

Yuhuan Mao[1], Hui Shen[1], Caili Yang[1], Qunying Jia[2], Jianying Li[1], Yong Chen[1], Jinwei Hu[1] and Weiliang Huang[1]*

[1]Department of Laboratory Medicine, The First Hospital of Changsha, Changsha, China, [2]Hunan Key Laboratory of Oncotarget Gene and Clinical Laboratory, Hunan Cancer Hospital and the Affiliated Cancer Hospital of Xiangya School of Medicine, Central South University, Changsha, China

Background: Talaromycosis is an invasive endemic mycosis caused by the dimorphic fungus *Talaromyces marneffei* (*T. marneffei*, TM). It mainly affects immunodeficient patients, especially HIV-infected individuals, which causes significant morbidity and mortality. Culture-based diagnosis takes a long turnaround time with low sensitivity, leading to treatment delay. In this study, we aimed to evaluate the performance of Metagenomic Next-Generation Sequencing (mNGS) for the rapid diagnosis of talaromycosis in HIV-infected patients.

Methods: Retrospectively analysis was conducted in HIV-infected cases at Changsha First Hospital (China) from January 2021 to March 2022. Patients who underwent routine microbiological examination and mNGS testing in parallel were enrolled. The clinical final diagnosis was used as a reference standard, and cases were classified into the TM group (60 cases) and the non-TM group (148 cases). The clinical performances of mNGS were compared with culture and serum Galactomannan (GM). The mixed infections detected by mNGS were analyzed. The impact of mNGS detection on treatment was also investigated.

Results: The sensitivity of mNGS test reached 98.3% (95% CI, 89.8-99.9), which was significantly higher than culture (66.7% [95% CI, 53.2-77.9], $P < 0.001$) and serum GM (83.3% [95% CI, 71.0-91.2], $P < 0.05$). The specificity of 98.6% (95% CI, 94.7-99.7) was similar to culture (100.0% [95% CI, 96.8-100.0], $P = 0.156$), and superior to serum GM (91.9% [95% CI, 85.9-95.5], $P < 0.05$). In bronchoalveolar lavage fluid (BALF) samples, the positive rate of mNGS was 97.6%, which was significantly higher than culture (28.6%, $P < 0.001$). mNGS has excellent performance in the identification of mixed infection in TM group patients. *Cytomegalovirus*, *Epstein-Barr virus* and *Pneumocystis jirovecii* were the most common concurrent pathogens. In summary, 60.0% (36/60) patients were added or adjusted to antimicrobial therapy after mNGS test.

Conclusion: mNGS is a powerful technique with high specificity and sensitivity for the rapid diagnosis of talaromycosis. mNGS of BALF samples may be a good option for early identification of *T. marneffei* in HIV-infected individuals with manifestations of infection. Moreover, mNGS shows excellent performance in mixed infection, which benefits timely treatment and potential mortality reduction.

KEYWORDS

mNGS, talaromycosis, *Talaromyces marneffei*, HIV/AIDS, diagnosis

1 Introduction

Talaromyces marneffei (*Penicillium marneffei*) is a dimorphic pathogenic fungus, which is mainly epidemic in residents, returning travellers, and immigrants with immunocompromised from southern China, Southeast Asia, and northeast India and causes a life-threatening invasive mycosis—— Talaromycosis (Vanittanakom et al., 2006; Samson et al., 2011; Limper et al., 2017). With the increase in immunosuppressive therapy and the prevalence of AIDS, talaromycosis has become more common in clinical practice. Human infection probably occurs through inhalation of fungal spores from the contaminated surroundings (Vanittanakom et al., 2006), causing disseminated disease involving multiple organs/systems such as lungs, blood, bone marrow, lymphatics, and skin (Limper et al., 2017). In HIV-infected patients, *T. marneffei* is a common opportunistic pathogen after *Mycobacterium tuberculosis*, *Pneumocystis jirovecii*, and *Cryptococcus*, with a mortality of up to 30% (Hu et al., 2013; Jiang et al., 2019). Therefore, early and rapid diagnosis is crucial for antifungal treatment, improving the outcomes, and reducing mortality.

Clinical manifestations of talaromycosis in HIV-infected patients are complex, diverse, and non-specific. So, clinical diagnosis is mainly dependent on laboratory assays. Currently, the culture and species identification of clinical specimens is the golden standard for the diagnosis (Ning et al., 2018). However, it takes 10-14 days to yield a positive result, delaying the early diagnosis and timely treatment (Andrianopoulos, 2020; Chen et al., 2022). In addition, the culture results may be negative because of the low fungal loads in the early stage of infection, which will lead to a missed diagnosis. Microscope findings of yeast organizations in smear staining skin can make a presumptive diagnosis not feasible for patients without skin lesions (Limper et al., 2017; Chen et al., 2020). (1,3)-β-D-glucan (BDG) test and Galactomannan (GM) test were rapid and sensitive (Li et al., 2020), but both of them were unspecific and could not be used for definitive diagnosis. In recent years, novel nonculture-based assays like ELISA and PCR have been explored for early and rapid diagnosis. However, their sensitivity was 82% and 84%, respectively, which cannot meet the clinical diagnosis needs (Wang et al., 2011; Hien et al., 2016; Lu et al., 2016; Ning et al., 2018; Pruksaphon et al., 2018; Ly et al., 2020). *T. marneffei* is not a usually suspected infection pathogen in non-HIV-infected patients or immunocompromised patients (Li et al., 2022). Furthermore, the research based on PCR or ELISA is rarely carried out in these patients, limiting the early diagnostic performance of these two detection methods.

Metagenomic Next-Generation Sequencing (mNGS) is the application of Next-generation sequencing (NGS) technology in clinical microbiological testing. Compared with the traditional pathogen detection methods, mNGS was faster and unbiased, which can simultaneously detect various infectious pathogens, including viruses, bacteria, fungi, and parasites (Gu et al., 2019). Currently, mNGS has been applied in many infectious diseases, especially in unconventional pathogens, novel pathogens, and mixed infections (Duan et al., 2021). However, only few case reports have reported the usefulness of mNGS in the diagnosis of talaromycosis (Shi et al., 2021; Zhou et al., 2021). The performance of mNGS for the rapid diagnosis of talaromycosis in HIV patients remained unknown. Consequently, this study aimed to evaluate the diagnostic performance of this technique in HIV/AIDS individuals with *T. marneffei* infection.

2 Methods

2.1 Study design and subjects

This study retrospectively analyzed the HIV-infected patients hospitalized in the Department of Infection and Immunology of Changsha First Hospital (China) from January 2021 to March 2022. Patients who were suspected of opportunistic infection and underwent routine microbiological examination and mNGS in parallel were enrolled. The culture and serum GM results were collected within 7 days of admission.

Patients meeting the following criteria were excluded: (1) The type of sample tested for mNGS was not cultured, (2) Culture and GM testing more than 7 days after admission, and (3) clinical data were incomplete.

Diagnosis of talaromycosis refers to the previous guidelines and expert consensus (AIDS-Associated Opportunistic Infections Research Group of the National Science and Technology Major Project of China During the 13th Five-Year Plan Period, 2020; AIDS and Hepatitis C Professional Group, 2021). The criteria were as follows:(1) with fever or respiratory/gastrointestinal abnormality, papulonecrotic skin lesions, lymphadenopathy, Splenomegaly, Hepatomegaly, anemia; (2) computed tomography suggested fungal infection; (3) exclude other fungal infections; (4) the talaromycosis-related symptoms and index resolved after anti-*T. marneffei* treatment; (5) *T. marneffei* was identified by culture or specific yeast found by microscopic examination from clinical samples. The clinical final diagnosis was made if (1) and (5) above can be met or if (1)-(4) above can be met. Non-talaromycosis refers to cases with etiology-proven other infectious diseases or non-infectious diseases. The clinical final diagnosis was used as a reference standard, and cases were classified into the TM group and the non-TM group.

2.2 Process of mNGS

2.2.1 DNA extraction

BALF, blood, and bone marrow were collected according to standard operating procedures. 450μl of BALF or bone marrow from patients were mixed with 7.2μl lysozyme, holding 30℃ for 10 min. Then the mixture was transferred to a 2-ml microcentrifuge tube with 250μl 0.5-mm glass beads. The fastprep-24^{TM} 5G instrument was used for vibration crushing, and reaction conditions were 45s*2cycles with an interval of 2 min. Then the supernatant was transferred to a 1.5-ml tube. Finally, a volume of 300μl supernatant or serum was extracted using the TIANamp Micro DNA Kit (TIANGEN BIOTECH) according to the operating manual.

2.2.2 Construction of DNA library and sequencing

For DNA Library construction, the extracted DNA above was processed for breaking, end repair, adapter ligation, and PCR amplification using MGIEasy Cell-free DNA Library Prep Set (MGI Tech). DNA library was detected by Qubit 2.0 (Invitrogen) for quality control. The double-stranded liner DNA library was formed into single-stranded circular DNA by undergoing melting transition and circularization. Then, it was generated to DNA Nanoballs (DNB) through rolling circle amplification (RCA) technology. Qualified DNB was loaded on the chip and ran the "SE50+10" program on the MGISEQ-2000 or MGISEQ-50 platform (BGI Genomics) for sequencing.

2.2.3 Bioinformatic analysis and criteria for positive results

High-quality data were obtained by removing low-quality bases, linker sequences, and short sequences (< 35 bp). The process of subtracting the human host sequence and aligning the remaining sequences were described in the previous study (Jin et al., 2020). The remaining data by removal of low-complexity reads were classified by simultaneously aligning to Pathogens metagenomics Database (PMDB). The PMDB contains the pathogen consisting of bacteria, fungi, viruses and parasites. The classification reference databases were downloaded from NCBI (ftp://ftp.ncbi.nlm.nih.gov/genomes/). RefSeq contains 4945 whole genome sequence of viral taxa, 6350 bacteral genomes or scaffolds, 1064 fungi related to human infection, and 234 parasites associated with human diseases. Positive criteria of mNGS results: A. A species-specific strictly mapped reads number (SMRN) per million ratio or SDSMRN of *T. marneffei* was≥1; B. Other pathogens were defined as the same in the previous study (Peng et al., 2021). The strictly mapped reads number means that, on the basis of meeting the conditions for mapped reads, and the proportion of mapped length in the statistical alignment results is greater than or equal to 90%. The base mismatch rate is less than or equal to 4% or the virus base mismatch rate is less than or equal to 8%, the optimal alignment score is greater than or equal to 30, and the sequence mapped frequency is 1.

2.3 Process of PCR

DNA was extracted according to the steps of 2. 2.1. The amplification was performed in 20μl reaction mix containing 10μl of 2 × TaqMan Universal Master Mix (Applied Biosystems, USA), 1μl (5μM) for each primer, 1μl (5μM) of the TaqMan probe, 5μl of template DNA and 2μl of RNase-free water. The conditions used were: 95℃ for 10 min and 45 cycles of 95℃ for 15 sec, 60℃ for 1 min, and annealing and extension at 60℃ for 1 min. PCR was performed using ABI 7500 (Applied Biosystems, USA), and controls and standard curve were performed in each run. The Cq value≤ 40 was determined as positive. More detailed of PCR method refer to the description of Li, etc. (Li et al., 2020).

2.4 Statistical analysis

The numerical variables were expressed as medians and interquartile ranges, and compared by the *Mann-Whitney U* test. The nominal variables were described by counts and percentages, and compared by the *chi-square* test. Sensitivity, specificity, positive predictive value (PPV), and negative predictive value (NPV) with 95% confidence intervals (CI) of mNGS in the diagnosis of talaromycosis were calculated. *Spearman's* test was performed to analyze correlation. *P* values < 0.05 were considered significant.

2.5 Ethics Statement

The study was approved by the Ethics Committee of Changsha First Hospital, and carried out by relevant guidelines. Patients included in the study were informed and signed the consent for mNGS testing.

3 Results

3.1 Clinical characteristics and laboratory findings

A total of 208 patients were enrolled in this study, with 60 cases for the cases group (TM group) and 148 cases for the control group (non-TM group) according to the clinical final diagnosis. The clinical characteristics and laboratory findings were shown in Table 1. The majority of enrolled participants were male, and there was no difference in the sex composition ratio between the two groups (78.3% *VS* 85.5%, P = 0.186). However, the TM group had a younger median age (39 *VS* 51, P<0.001). The most common clinical symptoms in TM patients were fever (90.0%), lymphadenopathy (85.0%), respiratory symptoms (76.7%), and splenomegaly/hepatomegaly (43.3%). Unexpectedly, skin lesions (25.0%) ranked last. In addition to respiratory and gastrointestinal symptoms, the others had a higher incidence than non-TM patients ($P < 0.05$). Chest Computed tomography (CT) abnormalities in two groups shared a similar high frequency (100% *VS* 98.6%, $P = 0.366$).

Significant differences in laboratory test results were observed between TM and non-TM group ($P < 0.05$). In the TM group, the indexes representing bone marrow hematopoietic function, such as hemoglobin, white blood cell, and platelet, were lower than those in the non-TM group. The non-specific inflammatory markers indicating infection, such as procalcitonin, C-reactive protein, adenosine deaminase (ADA), and lactate dehydrogenase (LDH), were significantly increased in the TM group. The median serum BDG test in TM patients was 87.9 pg/ml, remarkably higher than the non-TM patients (42.4 pg/ml). In the TM group, the median $CD4^+$ T cell count was 19 cells/ul, significantly lower than the non-TM group (60 cells/ul). No patients had $CD4^+$ T cell counts over 200 cells/ul, and 86.7% of patients had $CD4^+$ T cell counts less than 50 cells/ul, which was significantly higher than the non-TM group (44.6%, $P < 0.001$).

TABLE 1 Clinical data of TM and non-TM patients.

Characteristic	TM	non-TM	*P*-value
Cases	60	148	
Age (years)	39 (30-49)	51 (39-59)	0
Sex (male)	47 (78.3)	127 (85.5)	0.186
Clinical manifestations			
Fever	54 (90.0)	87 (58.8)	0
Respiratory symptoms	46 (76.7)	116 (78.4)	0.788
Gastrointestinal symptoms	16 (26.7)	25 (16.9)	0.108
Skin lesions	15 (25.0)	20 (13.6)	0.045
Splenomegaly/Hepatomegaly	26 (43.3)	22 (14.9)	0
Lymphadenopathy	51 (85.0)	50 (33.8)	0
Chest CT abnormalities	60 (100.0)	146 (98.6)	0.336
Laboratory test			
white blood cell ($\times10^9$/L)	3.5 (2.2-5.1)	4.5 (3.2-6.7)	0.008
hemoglobin (g/L)	97 (86-106)	112 (96-128)	0
platelet ($\times10^9$/L)	113 (57-184)	185 (134-243)	0
procalcitonin (ng/ml)	0.49 (0.06-2.45)	0.06 (0.05-0.21)	0
C-reactive protein (mg/L)	59.6 (19.0-87.7)	29.4 (9.4-70.3)	0.014
ADA(U/L)	30.2 (19.5-47.0)	18.6 (12.7-28.3)	0
LDH(U/L)	297.4 (220.8-458.4)	242.4 (179.4-361.8)	0.003
Serum BDG (pg/ml)	87.9 (42.8-244.1)	42.4 (42.4-102.0)	0
$CD4^+$ T cell (cells/ul)	19 (12-37)	60 (21-159)	0
≤50 cells/ul	52 (86.7)	66 (44.6)	0
50-200 cells/ul	8 (13.3)	51 (34.5)	–
>200 cells/ul	0 (0)	31 (20.9)	–

TM, talaromycosis; CT, computed tomography; ADA, adenosine deaminase; LDH, lactate dehydrogenase; BDG, (1;3)-β-D-glucan.

3.2 Diagnostic performance and comparison of mNGS, culture, and GM in talaromycosis

In the TM group, mNGS of blood, bone marrow, and BALF were performed in 13 cases, 5 cases, and 42 cases, respectively. 5 bone marrow and 42 BALF samples were cultured in parallel. 4 patients had different type samples for mNGS testing, while it collected not in the same day. So, we just included the earliest collected sample types in this study. In the non-TM group, mNGS test were performed in 22 blood samples, 3 bone marrow samples, and 123 BALF samples, respectively. 3 bone marrow and 123 BALF samples were cultured in parallel. Blood cultures and serum GM were performed in all 208 cases. The test results are shown in Table 2.

In current clinical practice, culture was a routine method for definitive diagnosis of talaromycosis, and serum GM test was widely used in the rapid adjuvant diagnosis of talaromycosis. Our study defined the optical density value of serum GM ≥ 0.5 as positive. And culture positive was defined as confirmed *T. marneffei* in any specimen of blood, bone marrow and BALF. The sensitivity of mNGS test reached 98.3% (95% CI,89.8-99.9), which was significantly higher than culture (66.7% [95% CI,53.2-77.9], $P < 0.001$) and serum GM (83.3% [95% CI,71.0-91.2], $P < 0.05$). The specificity of mNGS (98.6% [95% CI,94.7-99.7]) was superior to serum GM (91.9% [95% CI,85.9-95.5], $P < 0.05$), and similar to culture (100.0% [95% CI,96.8-100.0], $P = 0.156$). Meanwhile, mNGS also had excellent positive predict value (PPV) and negative predict value (NPV) of 96.7% (95% CI,87.6-99.4) and 99.3% (95% CI,95.7-99.9), respectively, and both significantly exceed serum GM test ($P < 0.05$). More detailed diagnostic performance indices were listed in Table 2.

The SDSMRN of *T. marneffei* detected by mNGS in the culture-positive patients was significantly higher than in the culture-negative patients ($P < 0.05$) (Figure 1A). Moreover, *Spearman's* analysis shows a positive correlation between the SDSMRN of *T. marneffei* and serum GM levels in TM patients (R = 0.330, $P = 0.010$) (Figure 1B).

3.3 PCR validation of *T. marnefei* detected by mNGS

Among the 208 cases, *T. marnefei* were detected by mNGS in 61 cases, including 59 in the TM group and 2 in the non-TM group. 39 out of 59 had been confirmed by culture. The remaining 22 cases were verified by real-time polymerase chain reaction (PCR) (Li et al., 2020). 2 cases in the non-TM group were negative. In the TM group, 3 cases (1 BALF, 1 blood and 1 bone marrow) were negative. 16 BALF samples and 1 blood sample detected *T. marnefei* by the specific PCR.

TABLE 2 Diagnostic performance of mNGS, culture and Serum GM in TM and non-TM patients.

Test	Samples	TM		non-TM		Sensitivity (95%CI)	Specificity (95%CI)	PPV (95%CI)	NPV (95%CI)
		+	−	+	−				
mNGS	Blood	13	0	0	22	100% (71.7-100.0)	100% (81.5-100.0)	100% (71.7-100.0)	100% (81.5-100)
	BALF	41	1	2	121	97.6% (85.9-99.9)	98.4% (93.7-99.7)	95.3% (82.9-99.2)	99.2% (94.9-100.0)
	Bone marrow	5	0	0	3	100% (46.3-100)	100% (31.0-100)	100% (46.3-100)	100% (31.0-100)
	Total	**59**	**1**	**2**	**146**	98.3% (89.8-99.9)	98.6% (94.7-99.7)	96.7% (87.6-99.4)	99.3% (95.7-99.9)
Culture	Blood	32	28	0	148	53.3% (40.1-66.1)	100% (96.8-100.0)	100% (86.7-100.0)	84.1% (77.7-89.0)
	BALF	12	30	0	123	28.6% (16.2-44.8)	100% (96.2-100.0)	100% (69.9-100.0)	80.4% (73.0-86.2)
	Bone marrow	4	1	0	3	80.0% (30.0-98.9)	100% (31.0-100.0)	100% (39.6-100.0)	75.0% (21.9-98.7)
	Total[#]	**40**	**20**	**0**	**148**	66.7%[##] (53.2-77.9)	100% (96.8-100.0)	100% (89.0-100.0)	88.0%[##] (81.9-92.4)
Serum GM	**Total***	**50**	**10**	**12**	**136**	83.3%** (71.0-91.2)	91.9%** (85.9-95.5)	80.6%** (68.3-89.2)	93.1%** (87.4-96.5)

GM, galactomannan; CI, confidence intervals; PPV, positive predictive value; NPV, negative predictive value. [#] culture positive was defined as confirmed T. marneffei in any specimen of blood, bone marrow and BALF, * Serum GM ≥0.5 was defined as positive, [##] P<0.001 when comparing mNGS total with culture total, ** P<0.05 when comparing mNGS total with Serum GM total.

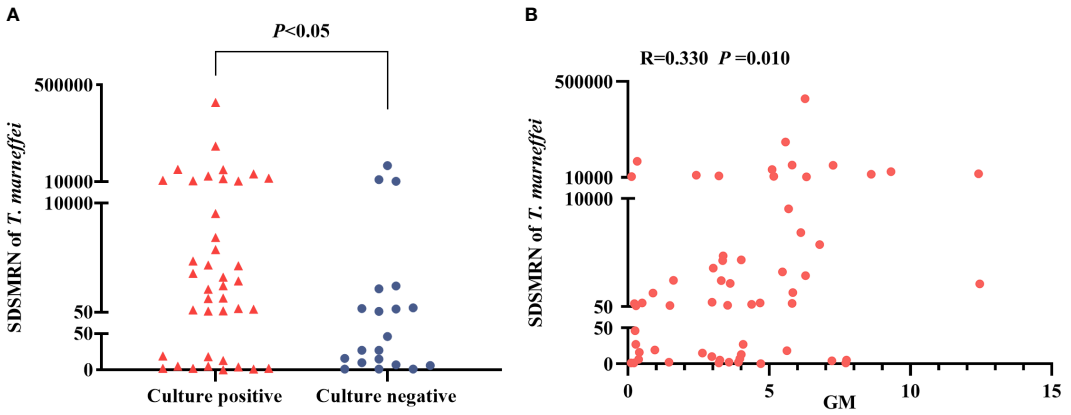

FIGURE 1
Analysis of the strictly mapped reads number per million ratio (SDSMRN) of *T. marneffei* detected by metagenomic Next-Generation Sequencing (mNGS). **(A)** Comparison of the SDSMRN of *T. marneffei* between culture positive and culture negative cases (*Mann-Whitney U* test). **(B)** Correlation analysis between the SDSMRN of *T. marneffei* and serum galactomannan (GM) levels (*Spearman's* test). *P<0.05* statistic difference.

3.4 Positive rates of mNGS in different types of samples

In the TM group, 12 of the 13 blood samples were both positive for mNGS and culture assay, while one sample was positive for mNGS only. The positive rates of mNGS and culture in blood samples were 100.0% and 84.6%, respectively, with no difference ($P > 0.05$). 1 of 5 bone marrow samples tested positive for mNGS only, the remaining samples were positive for the two assays, and the positive rates were 100.0% and 80.0%, respectively. However, for all 42 BALF samples, only 12 were positive for both methods, 1 was negative for mNGS, and as many as 29 were positive for mNGS only. The positive rates of these two methods in BALF samples were significantly different, and mNGS was significantly higher than culture (97.6% VS 28.6%, $P < 0.001$) (Figure 2).

3.5 Analysis of concurrent pathogens detected by mNGS

In the TM group, 58 cases (96.7%) of putative co-infections were identified based on mNGS. It should be noted that, due to the limitation of the DNA detection procedure, only DNA viruses were detected in this study. The types of co-infection pathogens identified by mNGS in different kinds of specimens were different. Among 18 blood or bone marrow samples, *T. marneffei*-virus was the most common mixed infection (72.2%) (Figure 3A). While, in 42 BALF samples, *T. marneffei*-virus-fungi-bacteria mixed

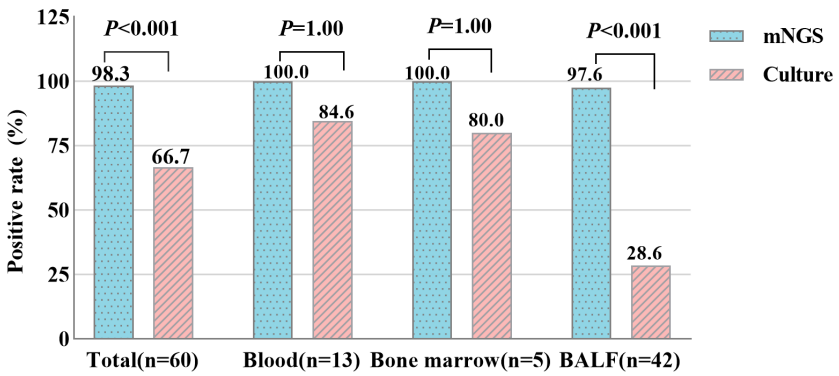

FIGURE 2
Positive rate comparison of metagenomic Next-Generation Sequencing (mNGS) and culture in blood, bone marrow and bronchoalveolar lavage fluid (BALF) samples (*chi-square* test). *P<0.05* statistic difference.

infection accounted for the majority (54.7%) (Figure 3B). *Cytomegalovirus* and *Epstein-Barr virus* were the top two common concurrent pathogens (Figures 3C, D). Particularly, in BALF samples, mNGS detected 28 cases of *Pneumocystis jirovecii*, a common opportunistic infection pathogen in HIV-infected patients (Figure 3D). In addition, mNGS also detected one case of *Cryptococcus neoformans*, *Mycobacterium tuberculosis*, and *Mycobacterium avium*.

3.6 Adjustments of antimicrobial therapy after mNGS

By searching electronic medical records, we collected the adjustments of antimicrobial treatment after mNGS testing in 60 TM patients. A total of 36 cases (60.0%) were adjusted for antimicrobial therapy based on mNGS results. 24 cases (40.0%) were added with amphotericin B(AMB), and 3 (5.0%) cases were added with itraconazole and started anti-*T. marneffei* treatment, respectively. 3 (5.0%) cases were added with trimethoprim-sulfamethoxazole (TMP-SMZ), and 8(13.3%) cases were added with antiviral drugs. All the adjustments were shown in Table 3. BALF (28/42, 66.7%) sample was principal for adjustments of antimicrobial therapy. We mainly observed and recorded the effect of adding AMB and Itraconazole for anti- *T. marneffei* treatment, and we found that the patient's clinical symptoms improved, blood culture turned negative 1-2 weeks later, and chest CT improved 2 weeks later.

4 Discussions

This study retrospectively analyzed the results of using the mNGS method to detect *T. marneffei* in different samples of HIV patients and found that mNGS showed high sensitivity and specificity of 98.3% and 98.6%, respectively. Moreover, we found that mNGS demonstrated apparent advantages in detecting BALF samples and mixed infection.

At present, the culture of clinic samples was the golden standard to identify *T. marneffei* infection. The statistical results of this study showed that the median turnaround time (TAT) of positive culture was 7 (6-9) days, with a sensitivity of 66.7%. Time-consuming and insensitive lead to the missed and delayed diagnosis of clinical application, which was associated with high mortality (Hu et al., 2013; Qiu et al., 2019). Serum GM detection has been applied to detecting Aspergillus and *T. marneffei*, which cannot identify a specific genus. The sensitivity of the serum GM assay in this experiment was 83.3%, which was similar to that of

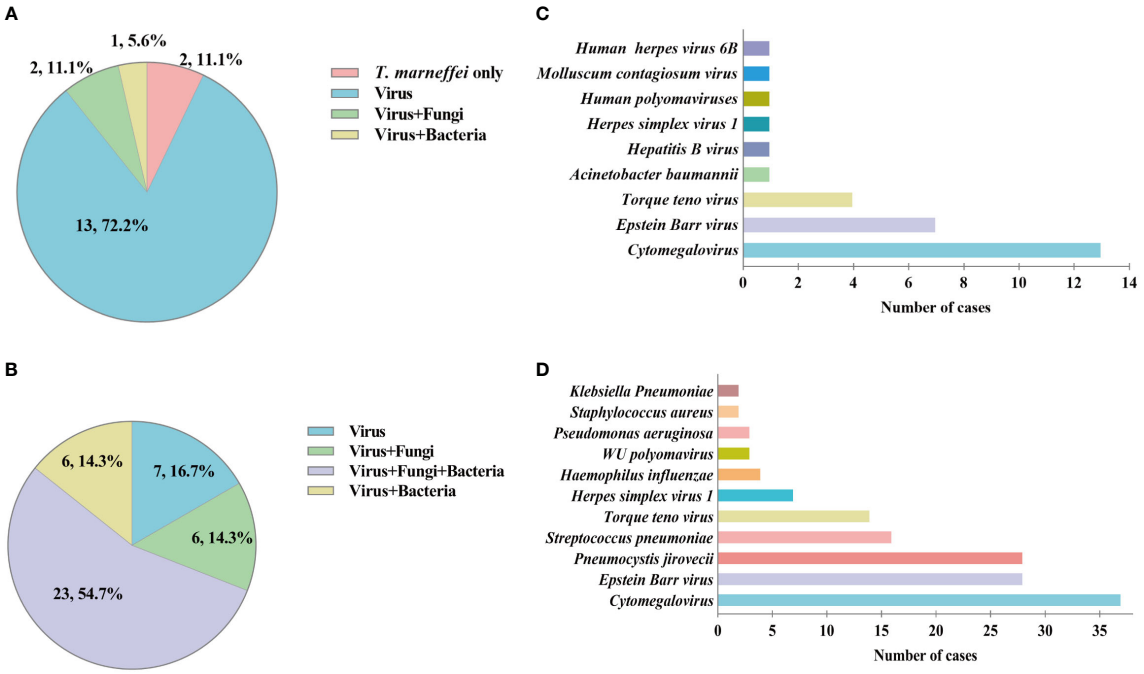

FIGURE 3
Mixed infection and concurrent pathogens detected by metagenomic Next-Generation Sequencing (mNGS) in talaromycosis (TM) patients. **(A)** Proportion of different types of mixed infection in blood and bone marrow samples. **(B)** Proportion of different types of mixed infection in bronchoalveolar lavage fluid (BALF) samples. **(C)** Numbers of various concurrent pathogens in blood and bone marrow samples. **(D)** Numbers of various concurrent pathogens in BALF samples.

TABLE 3 Adjustments of antimicrobial therapy after mNGS on TM patients.

Adjustments	Cases (n [%])
Total adjustments	36 (60.0%)
Add AMB	24 (40.0)
Add Itraconazole	3 (5.0%)
Add TMP-SMZ	3 (5.0%)
Add antiviral drugs	8 (13.3%)
Add antibacterial drugs	1 (1.6%)

AMB, amphotericin B; TMP-SMZ, trimethoprim-sulfamethoxazole.

Li et al. (Li et al., 2020), but was lower than that of Zheng et al (Zheng et al., 2015). This may be caused by the latter using 1.0 as an optical density cutoff value.

mNGS is an emerging molecular biology-based pathogen detection method with the advantages of rapidity, sensitivity and specificity. In our experiment, the median TAT of mNGS was 1 (1-2) days, which was shorter than culture. Comparing the three detection methods, we found that the sensitivity of mNGS was significantly higher than culture (98.3% vs 66.7%, P<0.001) and serum GM (98.3% vs 83.3%, P<0.05), and the specificity of mNGS was similar to culture. The detection assay based on PCR has not been widely used in the clinic, and a commercial PCR kit for detecting *T. marneffei* is not available in China at present. In our study, we used the PCR method established by Li et al. to verify 22 mNGS positive specimens (Li et al., 2020). 3 cases of clinically confirmed talaromycosis were not detected by PCR, which may be related to the sensitivity or long-term preservation of samples. Because we only performed PCR on a small number of samples, we did not compare the diagnostic performance of PCR and mNGS in talaromycosis. Recent studies show that the PCR-based method has a sensitivity of 70.4-91.0% (Hien et al., 2016; Lu et al., 2016; Li et al., 2020), which is lower than mNGS in this study. We speculate that the loss of nucleic acid during extraction may have more impacts on the detecting of specific fragments in PCR. The specificity of PCR-based detection methods varies greatly, ranging from 63.0 to 100.0% (Hien et al., 2016; Lu et al., 2016; Li et al., 2020). *MP1P* antigen of *T. marneffei* was developed for rapid detection and showed a sensitivity of only 86.3% (n=372) and 72.0% (n=93), respectively, in two studies of relatively large sample size (Thu et al., 2021; Chen et al., 2022). Compared with the detection methods mentioned above, mNGS demonstrates better sensitivity and specificity in the rapid diagnosis of talaromycosis in HIV patients.

Talaromycosis is a systemic fungal infection that can spread along the reticuloendothelial system. So, selecting appropriate samples is critical to improving the positive rate and rapid diagnosis. Microscopic examination of scraping pieces of specific skin lesions in the central depression is the most rapid and straightforward method for a preliminary diagnosis. However, in this study, 75% of patients in the TM group had no skin lesions, which could not be identified by this method. Cultures of blood and bone marrow samples have been recommended and well-studied, but positive only during late-stage infections, and 30-50% of infected individuals are missed (Thu et al., 2021). There was no significant difference in the positive rate of mNGS and culture in blood and bone marrow samples in our study, demonstrates that mNGS was not advantageous with blood and bone marrow.The lung is the primary entry portal and also has the highest burden of talaromycosis (Narayanasamy et al., 2021). However, BALF appears to be a less studied sample type. A retrospective analysis of a large sampling showed that the positive rate of BALF cultures was only 28.1% (n = 427) (Ying et al., 2020), which was similar to the results of our study. Surprisingly, the positive rate of mNGS in BALF reachs 97.6%, significantly higher than in culture (97.6% VS 28.6%, P < 0.001). Moreover, our study also found that the SDSMRN of *T. marneffei* in culture-negative patients was significantly lower than in culture-positive patients. Given this, we speculate that this is due to the sensitivity limitation, and the early low fungal load infection in the pulmonary cannot be detected by culture in BALF samples. Furthermore, the isolation culture of *T. marneffei* from BALF samples in advanced HIV/AIDS patients is challenging due to mixed pulmonary infection with multiple pathogens. As a result, pulmonary talaromycosis may have been neglected and underestimated in current practice and reports. These results demonstrate the apparent advantages of mNGS in BALF samples, which may greatly facilitate the early detection of *T. marneffei* in HIV-infected individuals with manifestations infection.

The pathogen spectrum of mNGS is broad, and it has significant advantages in identifying mixed infections. In advanced HIV/AIDS patients with $CD4^+$T cell counts of less than 200 cells/ul, the risk of infection with *T. marneffei* was significantly increased, the same as other pathogens (such as *Mycobacterium tuberculosis*, *Cryptococcus*, and *Pneumocystis jirovecii*) (Jiang et al., 2019; Qin et al., 2020), and the risk of mixed infections was also increased. The application of mNGS in this population may give full play to its cost, which is confirmed by our research. Based on the routine microbiological examination, 42.4% talaromycosis patients were identified with other opportunistic infections (Ying et al., 2020), but it was up to 96.7% by mNGS, which is significantly higher. Aside from bacteria, multiple types of pathogens were detected by mNGS, especially for viruses (such as *Cytomegalovirus* and *Epstein-Barr virus*) and fungi. Advanced HIV/AIDS patients with a high risk of opportunistic infections can significantly benefit from mNGS testing. Most notably, in BALF samples, we observed another common unculturable opportunistic infection pathogen, *Pneumocystis jirovecii*, with several cases ranking third, implying that BALF samples could be a good option for effectively identifying the mixed infections of *T. marneffei* and *Pneumocystis jirovecii*. In our observation, 60.0% of cases had an adjusted antimicrobial regimen, and 45% of cases started anti-*T. marneffei* based on mNGS results. It suggested that

the powerful technology may guide the safe and effective use of antimicrobial drugs in the future.

Despite the significant advantages of mNGS, there are still some challenges in clinical application. How to scientifically interpret mNGS results remains problem which cannot be ignored. In agreement with previous study, *T. marneffei* was considered as an exogenous pathogenic fungus, not colonized in the pulmonary (Limper et al., 2017; Chen et al., 2021). So, the SDSMRN of *T. marneffei* ≥1 was considered positive in our study. However, the microbes and nucleic acid contamination from the process of sample collection and experiments may also be detected with low mNGS reads. Therefore, the mNGS result must be carefully analyzed based on a comprehensive analysis of clinical manifestations and other laboratory tests. Presently, few studies have reported the distinction of pathogens detected by mNGS among contamination, colonization and infection. Authoritative normative guideline was urgently needed. In addition, the high cost of mNGS limits widespread promotion, so the type of patients who can benefit more from this technology should be carefully considered by clinicians.

Our study has some limitations. Firstly, this is a single-centre retrospective analysis. Secondly, this study uses clinical final diagnosis as the classification standard, which is prone to classification bias. Thirdly, this study did not analyze the effect of prophylactic or therapeutic antifungals on mNGS outcomes. In future practice, we should pay more attention to pulmonary talaromycosis. Non-HIV individuals should be included to assess the diagnostic performance of mNGS in talaromycosis, and multicenter prospective studies are also necessary.

In conclusion, mNGS is a powerful technique with high specificity and sensitivity for the rapid diagnosis of talaromycosis. mNGS of BALF samples may be a good option for early identification of *T. marneffei* in HIV-infected individuals with manifestations of infection. Moreover, mNGS shows excellent performance in mixed infection, which benefits timely treatment and potential mortality reduction in HIV-infected patients.

Data availability statement

The datasets presented in this study are deposited in online repositories. The names of the repository/repositories and accession number(s) can be found below: http://db.cngb.org/, CNP0003573.

Ethics statement

The study was performed following with the Ethics Committee of Changsha First Hospital, the Helsinki Declaration of 1964 and its later amendments. Patients included in this study were informed and signed the consent for mNGS testing.

Author contributions

YM, HS, YC, JH and WH designed the study. YM, CY and JL collected and sorted out the original data. YM and WH analyzed the data. QJ participated in the production of figures and tables. YM drafted the manuscript of the paper. WH revised the manuscript. All authors contributed to the article and approved the submitted version.

Acknowledgments

We acknowledge the contributions of authors and patients who participated in this study. We are particularly grateful to the professor of CunWei Cao (Department of Dermatology and Venereology, the First Affiliated Hospital of Guangxi Medical University, Nanning, China) for providing PCR technical support and Yali Wang for English language editing.

Conflict of interest

The authors declare that the research was conducted in the absence of any commercial or financial relationships that could be construed as a potential conflict of interest.

Publisher's note

References

AIDS and Hepatitis C Professional Group, S.o.I.D., Chinese Medical Association, Chinese Center for Disease Control and Prevention (2021). Chinese Guidelines for diagnosis and treatment of HIV/AIDS, (2021 edition). *Zhonghua. Nei. Ke. Za. Zhi.* 60 (12), 1106–1128. doi: 10.3760/cma.j.cn112138-20211006-00676

AIDS-Associated Opportunistic Infections Research Group of the National Science and Technology Major Project of China During the 13th Five-Year Plan Period (2020). Expert consensus on the diagnosis and treatment of talaromycosis in AIDS patients in China. *J. Southwest. University(Natural. Science).* 42 (07), 61–75. doi: 10.13718/j.cnki.xdzk.2020.07.005

Andrianopoulos, A. (2020). Laboratory maintenance and growth of talaromyces marneffei. *Curr. Protoc. Microbiol.* 56 (1), e97. doi: 10.1186/s12879-020-05526-1

Chen, D., Chang, C., Chen, M., Zhang, Y., Zhao, X., Zhang, T., et al. (2020). Unusual disseminated talaromyces marneffei infection mimicking lymphoma in a non-immunosuppressed patient in East China: a case report and review of the literature. *BMC Infect. Dis.* 20 (1), 800. doi: 10.1186/s12879-020-05526-1

Chen, X., Ou, X., Wang, H., Li, L., Guo, P., Chen, X., et al. (2022). Talaromyces marneffei Mp1p antigen detection may play an important role in the early diagnosis of talaromycosis in patients with acquired immunodeficiency syndrome. *Mycopathologia.* 187(2–3), 205–215. doi: 10.1007/s11046-022-00618-9

Chen, Q., Qiu, Y., Zeng, W., Wei, X., and Zhang, J. (2021). Metagenomic next-generation sequencing for the early diagnosis of talaromycosis in HIV-uninfected patients: five cases report. *BMC Infect. Dis.* 21 (1), 865. doi: 10.1186/s12879-021-06551-4

Duan, H., Li, X., Mei, A., Li, P., Liu, Y., Li, X., et al. (2021). The diagnostic value of metagenomic next rectanglegeneration sequencing in infectious diseases. *BMC Infect. Dis.* 21 (1), 62. doi: 10.1186/s12879-020-05746-5

Gu, W., Miller, S., and Chiu, C. Y. (2019). Clinical metagenomic next-generation sequencing for pathogen detection. *Annu. Rev. Pathol.* 14, 319–338. doi: 10.1146/annurev-pathmechdis-012418-012751

Hien, H. T. A., Thanh, T. T., Thu, N. T. M., Nguyen, A., Thanh, N. T., Lan, N. P. H., et al. (2016). Development and evaluation of a real-time polymerase chain reaction assay for the rapid detection of talaromyces marneffei MP1 gene in human plasma. *Mycoses* 59 (12), 773–780. doi: 10.1111/myc.12530

Hu, Y., Zhang, J., Li, X., Yang, Y., Zhang, Y., Ma, J., et al. (2013). Penicillium marneffei infection: an emerging disease in mainland China. *Mycopathologia* 175 (1-2), 57–67. doi: 10.1007/s11046-012-9577-0

Jiang, J., Meng, S., Huang, S., Ruan, Y., Lu, X., Li, J. Z., et al. (2019). Effects of talaromyces marneffei infection on mortality of HIV/AIDS patients in southern China: a retrospective cohort study. *Clin. Microbiol. Infect.* 25 (2), 233–241. doi: 10.1016/j.cmi.2018.04.018

Jin, W., Pan, J., Miao, Q., Ma, Y., Zhang, Y., Huang, Y., et al. (2020). Diagnostic accuracy of metagenomic next-generation sequencing for active tuberculosis in clinical practice at a tertiary general hospital. *Ann. Transl. Med.* 8 (17), 1065. doi: 10.21037/atm-20-2274

Li, D., Liang, H., Zhu, Y., Chang, Q., Pan, P., and Zhang, Y. (2022). Clinical characteristics, laboratory findings, and prognosis in patients with talaromyces marneffei infection across various immune statuses. *Front. Med. (Lausanne).* 9. doi: 10.3389/fmed.2022.841674

Limper, A. H., Adenis, A., Le, T., and Harrison, T. S. (2017). Fungal infections in HIV/AIDS. *Lancet Infect. Dis.* 17 (11), e334–e343. doi: 10.1016/s1473-3099(17)30303-1

Li, X., Zheng, Y., Wu, F., Mo, D., Liang, G., Yan, R., et al. (2020). Evaluation of quantitative real-time PCR and platelia galactomannan assays for the diagnosis of disseminated talaromyces marneffei infection. *Med. Mycol.* 58 (2), 181–186. doi: 10.1093/mmy/myz052

Lu, S., Li, X., Calderone, R., Zhang, J., Ma, J., Cai, W., et al. (2016). Whole blood nested PCR and real-time PCR amplification of talaromyces marneffei specific DNA for diagnosis. *Med. Mycol.* 54 (2), 162–168. doi: 10.1093/mmy/myv068

Ly, V. T., Thanh, N. T., Thu, N. T. M., Chan, J., Day, J. N., Perfect, J., et al. (2020). Occult talaromyces marneffei infection unveiled by the novel Mp1p antigen detection assay. *Open Forum Infect. Dis.* 7 (11), ofaa502. doi: 10.1093/ofid/ofaa502

Narayanasamy, S., Dougherty, J., van Doorn, H. R., and Le, T. (2021). Pulmonary talaromycosis: A window into the immunopathogenesis of an endemic mycosis. *Mycopathologia* 186 (5), 707–715. doi: 10.1007/s11046-021-00570-0

Ning, C., Lai, J., Wei, W., Zhou, B., Huang, J., Jiang, J., et al. (2018). Accuracy of rapid diagnosis of talaromyces marneffei: A systematic review and meta-analysis. *PloS One* 13 (4), e0195569. doi: 10.1371/journal.pone.0195569

Peng, J. M., Du, B., Qin, H. Y., Wang, Q., and Shi, Y. (2021). Metagenomic next-generation sequencing for the diagnosis of suspected pneumonia in immunocompromised patients. *J. Infect.* 82 (4), 22–27. doi: 10.1016/j.jinf.2021.01.029

Pruksaphon, K., Intaramat, A., Ratanabanangkoon, K., Nosanchuk, J. D., Vanittanakom, N., and Youngchim, S. (2018). Development and characterization of an immunochromatographic test for the rapid diagnosis of talaromyces (Penicillium) marneffei. *PloS One* 13 (4), e0195596. doi: 10.1371/journal.pone.0195596

Qin, Y., Huang, X., Chen, H., Liu, X., Li, Y., Hou, J., et al. (2020). Burden of talaromyces marneffei infection in people living with HIV/AIDS in Asia during ART era: a systematic review and meta-analysis. *BMC Infect. Dis.* 20 (1), 551. doi: 10.1186/s12879-020-05260-8

Qiu, Y., Zhang, J. Q., Pan, M. L., Zeng, W., Tang, S. D., and Tan, C. M. (2019). Determinants of prognosis in talaromyces marneffei infections with respiratory system lesions. *Chin. Med. J. (Engl).* 132 (16), 1909–1918. doi: 10.1097/CM9.0000000000000345

Samson, R. A., Yilmaz, N., Houbraken, J., Spierenburg, H., Seifert, K. A., Peterson, S. W., et al. (2011). Phylogeny and nomenclature of the genus talaromyces and taxa accommodated in penicillium subgenus biverticillium. *Stud. Mycol.* 70 (1), 159–183. doi: 10.3114/sim.2011.70.04

Shi, J., Yang, N., and Qian, G. (2021). Case report: Metagenomic next-generation sequencing in diagnosis of talaromycosis of an immunocompetent patient. *Front. Med. (Lausanne).* 8. doi: 10.3389/fmed.2021.656194

Thu, N. T. M., Chan, J. F. W., Ly, V. T., Ngo, H. T., Hien, H. T. A., Lan, N. P. H., et al. (2021). Superiority of a novel Mp1p antigen detection enzyme immunoassay compared to standard BACTEC blood culture in the diagnosis of talaromycosis. *Clin. Infect. Dis.* 73 (2), e330–e336. doi: 10.1093/cid/ciaa826

Vanittanakom, N., Cooper, C. R.Jr., Fisher, M. C., and Sirisanthana, T. (2006). Penicillium marneffei infection and recent advances in the epidemiology and molecular biology aspects. *Clin. Microbiol. Rev.* 19 (1), 95–110. doi: 10.1128/CMR.19.1.95-110.2006

Wang, Y. F., Cai, J. P., Wang, Y. D., Dong, H., Hao, W., Jiang, L. X., et al. (2011). Immunoassays based on penicillium marneffei Mp1p derived from pichia pastoris expression system for diagnosis of penicilliosis. *PloS One* 6 (12), e28796. doi: 10.1371/journal.pone.0028796

Ying, R. S., Le, T., Cai, W. P., Li, Y. R., Luo, C. B., Cao, Y., et al. (2020). Clinical epidemiology and outcome of HIV-associated talaromycosis in guangdong, China, during 2011-2017. *HIV Med.* 21 (11), 729–738. doi: 10.1111/hiv.13024

Zheng, J., Gui, X., Cao, Q., Yang, R., Yan, Y., Deng, L., et al. (2015). A clinical study of acquired immunodeficiency syndrome associated penicillium marneffei infection from a non-endemic area in China. *PloS One* 10 (6), e0130376. doi: 10.1371/journal.pone.0130376

Zhou, Y., Liu, Y., and Wen, Y. (2021). Gastrointestinal manifestations of talaromyces marneffei infection in an HIV-infected patient rapidly verified by metagenomic next-generation sequencing: a case report. *BMC Infect. Dis.* 21 (1), 376. doi: 10.1186/s12879-021-06063-1

frontiers | Frontiers in Cellular and Infection Microbiology

TYPE Brief Research Report
PUBLISHED 02 December 2022
DOI 10.3389/fcimb.2022.985373

OPEN ACCESS

EDITED BY
Jinmin Ma,
Beijing Genomics Institute (BGI), China

REVIEWED BY
Qian-Qiu Wang,
Chinese Academy of Medical Sciences and Peking Union Medical College, China
Bo Chen,
First Affiliated Hospital of Anhui Medical University, China

*CORRESPONDENCE
Li Jiang
u0341992@yahoo.com
Jie Zhang
zhangjiespph@163.com

†These authors have contributed equally to this work

SPECIALTY SECTION
This article was submitted to Clinical Microbiology, a section of the journal Frontiers in Cellular and Infection Microbiology

RECEIVED 03 July 2022
ACCEPTED 10 October 2022
PUBLISHED 02 December 2022

CITATION
Zhou X, Peng S, Song T, Tie D, Tao X, Jiang L and Zhang J (2022) Neurosyphilis with ocular involvement and normal magnetic resonance imaging results affirmed by metagenomic next-generation sequencing. *Front. Cell. Infect. Microbiol.* 12:985373. doi: 10.3389/fcimb.2022.985373

Neurosyphilis with ocular involvement and normal magnetic resonance imaging results affirmed by metagenomic next-generation sequencing

Xiaoli Zhou[1,2†], Shengkun Peng[2,3†], Tiange Song[1,2], Dandan Tie[1,2], Xiaoyan Tao[1,2], Li Jiang[1,2*] and Jie Zhang[1,2*]

[1]Department of Laboratory Medicine, Sichuan Provincial People's Hospital, University of Electronic Science and Technology of China, Chengdu, China, [2]Sichuan Translational Medicine Research Hospital, Chinese Academy of Sciences, Chengdu, China, [3]Department of Radiology, Sichuan Provincial People's Hospital, University of Electronic Science and Technology of China, Chengdu, China

The rapid and accurate identification of pathogenic agents is the key to guide clinicians on diagnosis and medication, especially for intractable diseases, such as neurosyphilis. It is extremely challenging for clinicians to diagnose neurosyphilis with no highly sensitive and specific test available. It is well known that the early transmission and immune evasion ability of *Treponema pallidum* have earned it the title of "stealth pathogen." Neurosyphilis has complex clinical manifestations, including ocular involvement, which is infrequent and often overlooked, but its neuroimaging results may be normal. Therefore, it is important to find a new test that can detect the presence or absence of *Treponema pallidum* immediately for the diagnosis of neurosyphilis. We reviewed all the patients admitted to the Sichuan Provincial People's Hospital between 2021 and 2022 who had ocular involvement and whose clinical samples were examined *via* metagenomic next-generation sequencing (mNGS), and we found 10 candidates for further analysis. The results of magnetic resonance imaging (MRI) were normal for four patients, and three of them met the diagnostic criteria for neurosyphilis confirmed by mNGS. In addition, the results of mNGS from the three patients were further validated using polymerase chain reaction (PCR). Five of the 10 patients had diplopia manifestations; two (20%) experienced abducens nerve palsies, two (20%) had eyelid drooping, and one (10%) had decreased vision. One of the 10 patients (10%) who was HIV positive and five patients had abnormal MRI results. To our knowledge, *Treponema pallidum* was detected by mNGS in

patients with ocular involvement and normal MRI results for the first time. Given this situation, we recommend mNGS as a potential and supplementary tool for the diagnosis and differential diagnosis of neurosyphilis.

KEYWORDS

metagenomic next-generation sequencing (mNGS), *Treponema pallidum*, neurosyphilis, cerebrospinal fluid, normal magnetic resonance imaging, ocular involvement

Introduction

Syphilis has afflicted humans for more than 500 years, and this infection can progress to neurosyphilis, which is bothersome and serious. (Smibert et al., 2018). In a previous study, 40% of patients with syphilis developed neurosyphilis after *Treponema pallidum* invaded the central nervous system (CNS) (Ghanem et al., 2020), which is defined as neurosyphilis. In patients with neurosyphilis, the suppression of systemic immune responses may promote disease progression toward a neurological involvement, whereas CNS damage may be due to uncontrolled local host immune responses (Drago et al., 2016). Hence, neurosyphilis remains a relatively common complication that can occur at any stage of syphilis. Neurosyphilis can be easily treated with appropriate antibiotics, but it is difficult to diagnose because most patients are asymptomatic or have nonspecific symptoms. Neurosyphilis, if left untreated, can lead to syphilitic meningitis, meningovascular syphilis, general paralysis, tabes dorsalis, and ocular forms (Conde-Sendín et al., 2004). Neurosyphilis, which is caused by the infection of the nervous system by *Treponema pallidum*, is often overlooked because of its rarity. In addition, neurosyphilis with ocular involvement is also known as the "great masquerader" due to the multiple clinical features associated with this infection (Desideri et al., 2022).

Treponema pallidum, a helical to sinusoidal bacterium with outer and cytoplasmic membranes, is a species of spirochete in the Treponemataceae family. *Treponema pallidum* is a human obligate parasite, the genome of which is a circular chromosome of 1,138,006 base pairs (bp) containing 1,041 predicted coding sequences (open reading frames) (Fraser et al., 1998). *Treponema pallidum* can invade the central nervous system at the very early stage of infection. Moreover, *Treponema pallidum* establishes persistent infection by promoting the Treg response in the early stage of syphilis (Li et al., 2013). However, there are limitations to culture *Treponema pallidum* directly from the lesion exudate or tissue. Furthermore, diagnosing neurosyphilis is difficult because there is no highly specific and sensitive test yet available.

The clinical symptoms and imaging manifestations of neurosyphilis are diverse and lack specificity (Ropper and Longo, 2019). Its clinical manifestations include asymptomatic neurosyphilis, meningeal neurosyphilis, meningeal vascular neurosyphilis, paralytic dementia, tabes dorsalis, gumma swelling, ear syphilis, and syphilis-related eye diseases. Syphilis-related eye diseases can be seen at all stages of syphilis infection and can affect all structures of the eye; both eyes are often involved, which can be an isolated manifestation of neurosyphilis or a manifestation of tabes dorsalis or paralytic dementia, manifested as eyelid drooping, eye movement restriction, diplopia, decreased vision, blindness, conjunctival hyperemia, visual field defect, etc. Overall, neurosyphilis with ocular involvement needs to be distinguished among iridocyclitis, uveitis, conjunctivitis, scleritis, chorioretinitis, optic neuritis, optic nerve periarthritis, optic nerve retinitis, optic atrophy, oculomotor nerve palsy, abducens nerve palsy, pupil abnormalities, etc. Strikingly, patients with neurosyphilis may have no specific neuroimaging findings. Magnetic resonance imaging (MRI) examination remains an essential procedure for the detection of neurosyphilis although the results for two thirds of patients have been normal or nonspecific mild-to-moderate cerebral atrophy.

Currently, the diagnosis of neurosyphilis relies on the interpretation of serum and cerebrospinal fluid (CSF) serological tests as well as CSF characteristics, the patient's exposure and treatment history, current symptoms, and neurological examination. Serological testing is the detection of antibodies and has been the main method for laboratory diagnosis of syphilis. Presumptive diagnosis of syphilis requires the use of two laboratory serological tests: non-treponemal (TRUST, VDRL, etc.) and treponemal testing (TPHA, TPPA, EIA, etc.) (Gonzalez et al., 2019). Non-treponemal tests detect a mixture of heterophile IgG and IgM although IgM does not help to stage syphilis accurately and should not be relied upon to determine the length of treatment. Above all, these tests require

Abbreviations: CSF, cerebrospinal fluid; mNGS, metagenomic next-generation sequencing; CNS, central nervous system; MRI, magnetic resonance imaging; CT, computed tomography; PCR, polymerase chain reaction; VDRL, venereal disease research laboratory; TPHA, *Treponema pallidum* hemagglutination assay; and TRUST, toluidine red unheated serum test.

further optimizations and subsequent evaluations. The two types of serological tests (non-treponemal and treponemal) should be used together to reduce false-negative and false-positive rates (Workowski et al., 2021). Serological tests such as the newer automated treponemal tests (EIA, CIA, etc.) for syphilis are very sensitive in the early stages of infection (Janier et al., 2021). However, in the case of neurosyphilis, it is impossible to make a diagnosis by serological testing for syphilis alone, and the sensitivity and specificity of PCR are low, and as such, is not a recommended test (Marks et al., 2018). Additionally, the CSF test is imperfect and has no benchmark. In summary, the diagnosis of neurosyphilis is based on clinical evidence, abnormal results of treponemal and non-treponemal serologic assays, and CSF tests, which are time-consuming. In conclusion, direct detection of the pathogen *Treponema pallidum* from clinical specimens is of great importance for the early diagnosis of NS infection.

With the continuous updating and development of sequencing technology, next-generation sequencing (NGS) has gradually become an indispensable research method in the diagnosis of tumors, drug resistance, and infectious diseases (Zhang et al., 2020). Next-generation sequencing technologies include whole genome sequencing (WGS), transcriptome sequencing (RNAseq), whole exon sequencing (WES), metagenomic next-generation sequencing (mNGS), and etc. Since the first use of NGS to identify pathogens of infectious diseases in 2008, the widespread application of NGS in clinically difficult-to-diagnose diseases has kicked off (Chiu and Miller, 2019). Metagenomic next-generation sequencing (mNGS) has wide coverage and strong timeliness and is widely used in the accurate diagnosis of clinical infectious diseases. Furthermore, metagenomic next-generation sequencing (mNGS) technology can directly perform non-targeted, rapid, and accurate auxiliary diagnosis of pathogens in various diseases, such as respiratory system infections (Wilson et al., 2014), blood system infections (Li et al., 2018), and central nervous system infections (Yi et al., 2020). Overall, mNGS, as an emerging technology, can help in finding pathogens and providing evidence for diagnosis and treatment as soon as possible, which is not only beneficial in improving the prognosis of patients but also in the diagnosis and early treatment by clinicians.

Methods

Study design

This is an original study including a retrospective observational study and experimental validation of inpatients diagnosed with ocular involvement at our hospital between September 2021 and June 2022. Eligible patients were selected from the hospital information system, and their medical history, neurological examinations, peripheral blood and CSF laboratory testing, and neuroimaging examinations were recorded and evaluated. This research was approved by the Medical Professional Committee of the Sichuan Provincial People's Hospital (Permit Number: 2022172) with a waiver for informed consent from the participants because of its retrospective nature.

Study patients

We retrospectively reviewed the CT scans and MRI films of 10 inpatients with ocular involvement and whose clinical samples were examined by metagenomic next-generation sequencing during the period from September 2021 to June 2022. Clinical information and laboratory data were also retrieved from the files. The CT scans or MRI films were reexamined by one radiologist who was unaware of the patients' clinical data, and these were retrospectively reviewed and interpreted for possible lesion.

Clinical data

The data extraction included age, sex, symptoms, medical history, MRI results, CSF testing results, and blood testing results. The diagnostic criteria for NS were based on the 2021 sexually transmitted infections treatment guidelines of the U.S. Centers for Disease Control and Prevention and the 2020 European guideline on the management of syphilis. The details were as follows: (1) positive results for the treponemal (TPPA, EIA, TPHA, etc.) and nontreponemal tests (VDRL, RPR, TRUST, etc.); (2) white blood cell (WBC) counts of CSF > 5 cells/mm^3; and (3) protein levels of CSF > 45 mg/dl.

Sample collection

A lumbar puncture was performed to obtain cerebrospinal fluid according to standard procedures, and blood samples were obtained from the 10 patients with ocular involvement without clear origin in the Sichuan Provincial People's Hospital from September 2021 to June 2022. White blood cell count, protein level, metagenomic next-generation sequencing (mNGS), and PCR validation were conducted on every CSF sample.

Serologic tests

The syphilitic serologic tests for blood and CSF samples were performed using TRUST (WanTai, Beijing, China) and TPHA tests (Abbott, Chicago, USA) according to the manufacturer's instructions. In general, TRUST tests were performed when TPHA tests were positive.

Biochemical tests

Approximately 2 ml of CSF samples were collected in sterile tubes and analyzed within 1 h to determine the protein level by an Abbott ci16200 automatic clinical chemistry analyzer (Abbott, USA) and the white blood cell (WBC) count using an automatic blood cell BC-7500 analyzer (Mindray, Shenzhen, China).

Cerebrospinal fluid sample processing and DNA extraction

CSF samples (600 µl each) from the patients were collected according to standard protocol. Lysozyme (7.2 µl) was added to the 600 µl of CSF sample in a 1.5-ml centrifuge tube and incubated in a metal bath at 30°C for the wall-breaking reaction. The mixture was then transferred to a new 2-ml centrifuge tube with 250-µl of 0.5-mm glass beads on a wall breaker and homogenized under the following conditions: 6 m/s, 45 s, two cycles, and an interval of 2 min. Then, 0.3 ml of the above mixture was transferred into a new 1.5-ml centrifuge tube for DNA extraction using the TIANamp Micro DNA Kit (DP316, TIANGEN BIOTECH, Beijing, China) according to the manufacturer's protocol. The extracted DNA specimens were used for the construction of DNA libraries (Long et al., 2016).

Construction of DNA libraries and sequencing

DNA libraries were constructed through DNA fragmentation, end repair, adapter ligation, and PCR amplification. Agilent 2100 (BGI Genomics Co.,Ltd., Shenzhen, China) was used for quality control of the DNA libraries. Qualified libraries were pooled, DNA nanoball (DNB) was made, and samples were sequenced by MGISEQ-2000 (BGI Genomics Co.,Ltd., Shenzhen, China) platform (Jeon et al., 2014).

Bioinformatic analysis

The software fastp was used to trim and map the reads (Chen et al., 2018). High-quality sequencing data were generated by removing low-quality reads, followed by computational subtraction of human host sequences mapped to the human reference genome (hg19) using the Burrows–Wheeler Alignment (Li and Durbin, 2009), and removing low-complexity reads. The remaining data after the removal of low-complexity reads were classified by simultaneously aligning to the Pathogens Metagenomics Database (PMDB), consisting of bacteria, fungi, viruses, and parasites. The classification reference databases were downloaded from NCBI (ftp://ftp.ncbi.nlm.nih.gov/genomes/) containing 4,945 whole genome sequences of viral taxa, 6,350 bacterial genomes or scaffolds, 1,064 fungi related to human infection, and 234 parasites associated with human diseases.

PCR of *Treponema pallidum* 47-kDa protein gene (TpN47)

PCR validation was performed with the primers referred by Orle et al. (1996) to amplify a fragment of the *T. pallidum* 47-kDa protein gene. The primers were as follows: KO3A 5′-GAAGTTTGTCCCAGTTGCGGTT-3′ and KO4 5′-CAGAGCCATCAGCCCTTTTCA-3′. DNA amplification was performed in a 20-µl of the reaction mixture containing primers, Rapid Taq Master Mix (Vazyme, Nanjing, China), and 4 µl of the DNA sample extracted from the clinical specimens (CSF and blood). PCR was performed in a thermal cycler (Thermo Fisher Scientific, Waltham, MA, USA) with the following parameters: 95°C for 5 min, followed by 40 cycles of denaturation (94°C), annealing (60°C), and extension (72°C) for 20 s at each step, and final extension at 72°C for 5 min. Amplified samples were stored at 4°C until analysis. The amplification products were analyzed by electrophoresis using 1.5% of agarose gel.

Results

Clinical data of the 10 patients with ocular involvement

Ten patients had ocular involvement including diplopia, abducens nerve palsies, eyelid drooping, and decreased vision (Table 1). One of the 10 patients had decreased vision manifestation, two (20%) experienced abducens nerve palsies, two (20%) had eyelid drooping, and five (50%) had diplopia. One of the 10 patients (10%) had a history of painless ulcers on the genitals, two had a history of syphilis and they said they had been cured, and their MRI results were all normal (Figure 1). Finally, the diagnosis of neurosyphilis was confirmed by mNGS for three patients with normal MRI results, which was also consistent with the serological and CSF results given in Table 1.

Laboratory findings

As shown in Table 1, seven patients had negative serological results, which can rule out the diagnosis of syphilis. The remaining three patients (30%, 3/10) had positive serum and CSF TPHA. In addition, the three patients also had positive serum TRUST (1 sero-TRUST titers ≤1:16 and 2 sero-TRUST titers ≥1:32). Two CSF samples (20%, 2/10) were TRUST-reactive with titers ≤1:16. Of the three patients, all had CSF

TABLE 1 Clinical characteristics and laboratory tests of the 10 patients with ocular involvement.

P	Age	Sex	Symptom	Syphilis history	Syphilis treatment status	MRI	Final diagnosis	Serological results			Cerebrospinal fluid results					
								TPHA	TRUST	PCR	TPHA	TRUST	White cells (/mm^3)	Proteins (mg/dl)	mNGS	PCR
1	36	M	Diplopia	No	No	Normal	Neurosyphilis	+	1:32	Undetected	+	1:4	137 ↑	42	*Treponema pallidum*	Undetected
2	35	M	Diplopia	Yes, 5 years	cured	Normal	Neurosyphilis	+	1:128	Undetected	+	1:8	138 ↑	60 ↑	*Treponema pallidum*	Yes
3	32	M	Diplopia	Yes, 8 years	cured	Normal	Neurosyphilis	+	1:4	Undetected	+	–	13 ↑	18	*Treponema pallidum*	Undetected
4	68	M	Eyelid drooping	No	No	ND	Intracranial infection	–	ND	ND	ND	ND	740 ↑	1295 ↑	*Listeria ivanovii*	No
5	20	M	Decreased vision	No	No	Normal	Intracranial venous thrombosis	–	ND	ND	ND	ND	23 ↑	31	No	No
6	55	F	Abducens nerve palsies	No	No	Left abducens nerve tortuous vascular shadow	Infected cavernous sinus thrombosis	–	ND	ND	ND	ND	43 ↑	88 ↑	*Streptococcus constellatus*	No
7	56	F	Diplopia	No	No	Right otitis media	Cerebral ischemia	–	ND	ND	ND	ND	140 ↑	266 ↑	*Human gammaherpesvirus 4*	No
8	37	M	Diplopia	No	No	Left brainstem patch, streak shadow	Brainstem inflammation	–	ND	ND	ND	ND	51 ↑	27	*Human gammaherpesvirus 4*	No
9	56	F	Abducens nerve palsies	No	No	Bilateral basal ganglia, paraventricular ischemia	Skull basilar deformity	–	ND	ND	ND	ND	3	40	No	No
10	83	M	Eyelid drooping	No	No	Atrophy, right frontal infarction	Viral meningitis	–	ND	ND	ND	ND	109 ↑	145 ↑	No	No

↑ refers to the white blood cell (WBC) count of CSF >5 cells/mm^3 or protein level of CSF >45 mg/dl. ND refers to 'not done'.

10.3389/fcimb.2022.985373

pleocytosis; strikingly, only one had elevated CSF protein levels, which illustrated that CSF WBC count or protein level is also not the gold standard for the diagnosis of neurosyphilis.

Next-generation sequencing confirms the diagnosis of neurosyphilis

To draw a definitive pathogenic diagnosis and rule out infection by other pathogens, next-generation sequencing of CSF from the 10 patients with ocular involvement was also performed, and three of them were diagnosed with *Treponema pallidum* infection (Figure 2). *Treponema pallidum* DNA was detected in the CSF samples from the three patients whose MRI and CT results were negative. The number of unique reads of the identified *Treponema pallidum* gene ranged from 1 to 5 (0.03%–2.70%). Mapping of the detected reads to the reference *Treponema pallidum* genome resulted in coverage ranging from 0.0189% to 0.1131% with a depth of 1 and read lengths of 50, respectively. The number of unique reads, percentage, and coverage of the identified *Treponema pallidum* DNA sequences are shown in Figure 2. Interestingly, even though *Treponema*

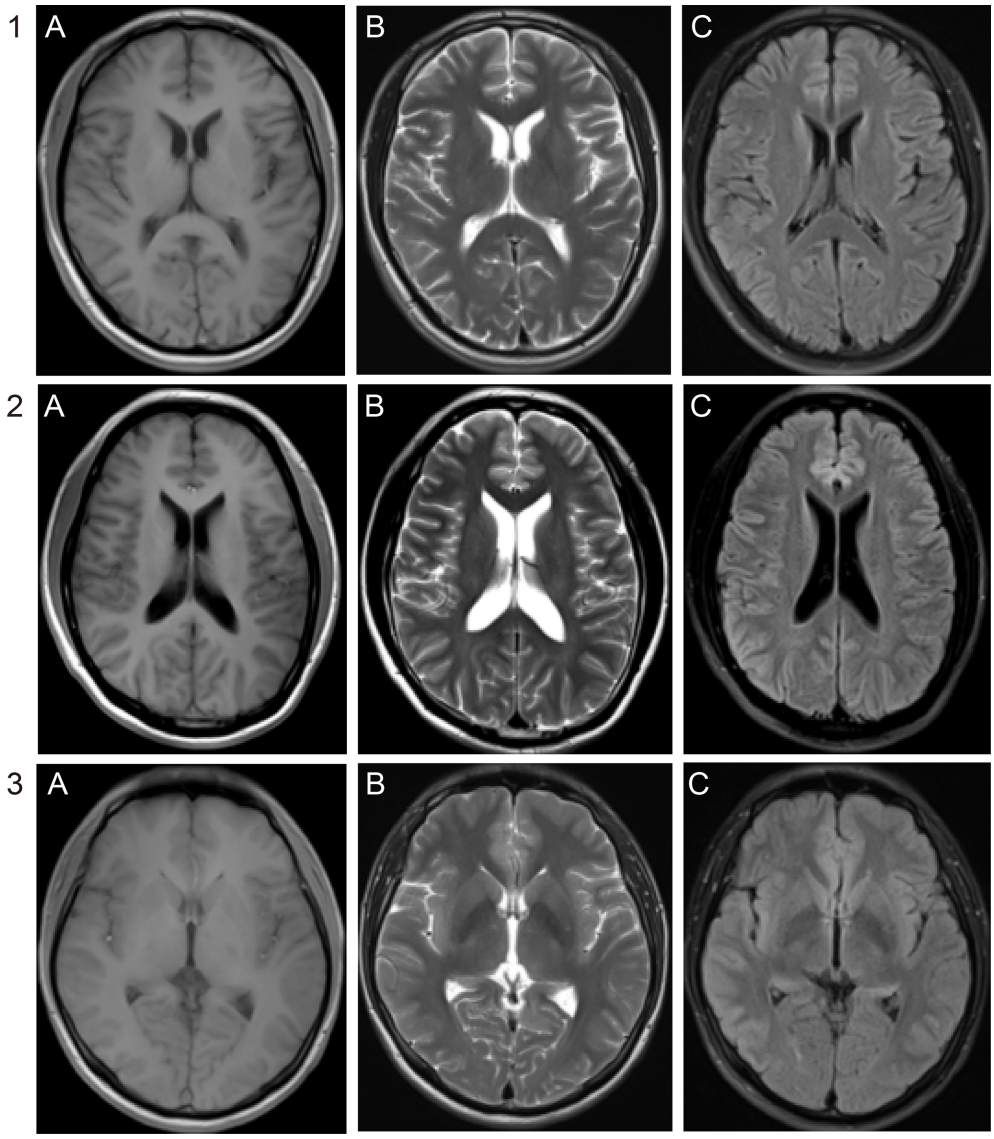

FIGURE 1
Brain MRI of the three patients. No abnormal signals were demonstrated on **(A)** T1WI, **(B)** T2WI, and **(C)** fluid-attenuated inversion recovery (FLAIR) of patients 1, 2, and 3.

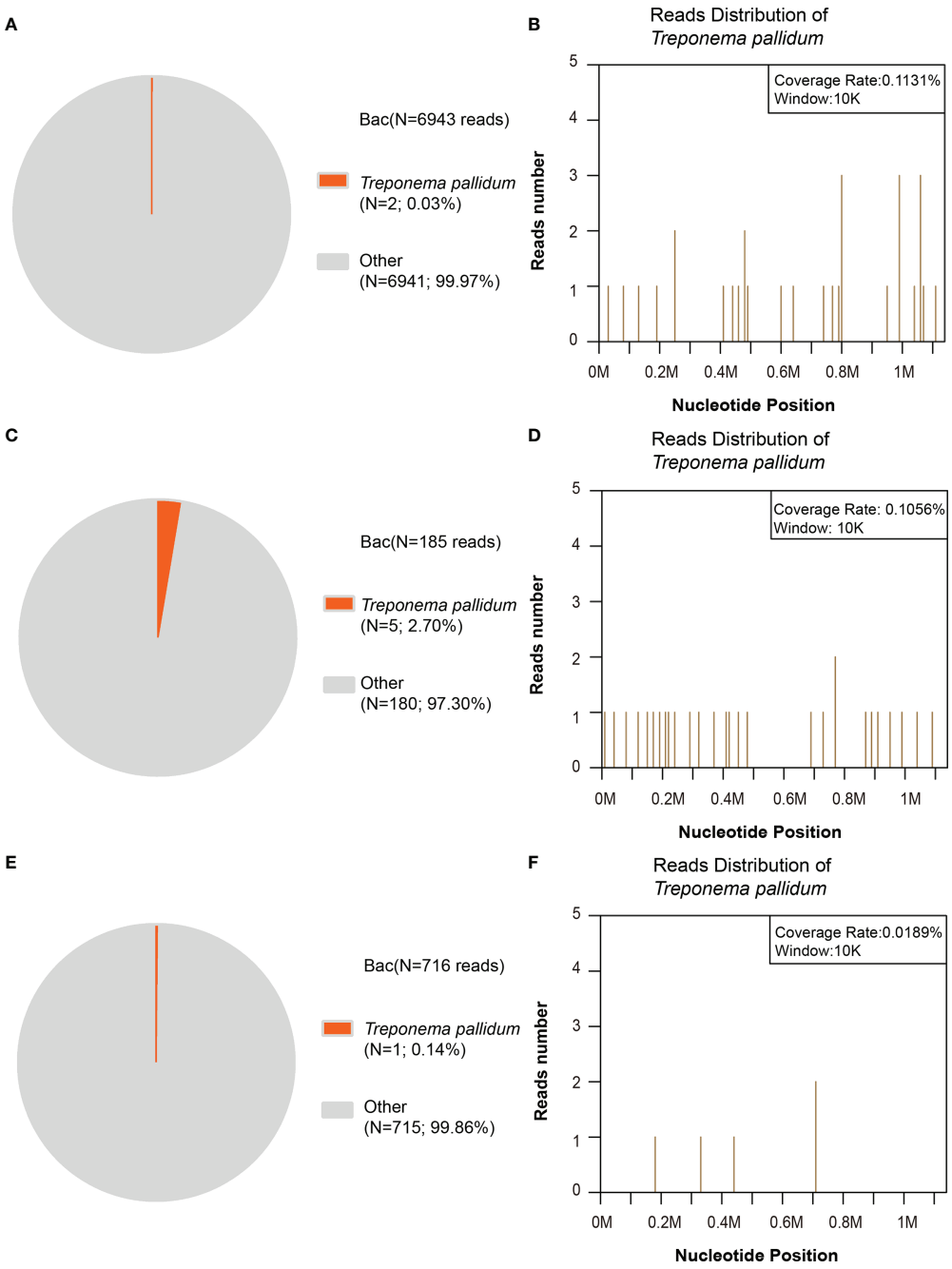

FIGURE 2
Next-generation sequencing (NGS) of the bacterial reads in the patients' cerebrospinal fluid (CSF). **(A, B)** In patient no. 1, the distribution of bacterial reads (two of 6,943 reads; 0.03%) corresponded to *Treponema pallidum* with a coverage of 0.1131%. **(C, D)** In patient no. 2, the distribution of bacterial reads (five of 185 reads; 2.70%) corresponded to *Treponema pallidum* with a coverage of 0.1056%. **(E, F)** In patient no. 3, the distribution of bacterial reads (one of 716 reads; 0.14%) corresponded to *Treponema pallidum* with a coverage of 0.0189%. The others are commonly regarded as contaminating bacterial DNA from the environment and agents.

pallidum was at a relatively low pathogen level and the patients' neuroimaging results were negative, the small number of pathogen reads was still detectable due to the massive sequencing data of mNGS to confirm the diagnosis.

PCR validation

We validated the NGS results using PCR analysis and Sanger sequencing. Specific primers for *T. pallidum* 47-kDa protein

gene (260 bp) were designed (Palmer et al., 2003), and PCR was carried out for the 10 patients. To our surprise, only the second patient's CSF PCR result was positive. The PCR results of the other two diagnosed patients were negative, possibly because the number of reads was small. The results showed that the amplification products (with DNA fragments of 250 bp) were consistent with our expectation, and the reads from Sanger sequencing matched the *Treponema pallidum* genome through NCBI Blast (Figure 3).

Discussion

Neurosyphilis is highly treatable with appropriate antibiotics. Therefore, early recognition and management are essential. However, rapid diagnosis of neurosyphilis is challenging. Especially in immunocompetent individuals, neurosyphilis is more insidious with nonspecific symptoms, and diagnosis is difficult (Timmermans and Carr, 2004). Neurosyphilis with ocular involvement is infrequent, but the incidence of ocular pathology is high in patients coinfected with AIDS and syphilis, which might manifest as multiple fundus changes (Chen et al., 2021). All in all, on the one hand, the clinical manifestations of the disease are complex, and both MRI and CT results can be negative; on the other hand, *Treponema pallidum*, the pathogen of syphilis, is difficult to culture. Serological testing is the most common diagnostic method currently (Harris et al., 2022), and a negative serologic test can rule out neurosyphilis. However, no single test can be used to establish a diagnosis of neurosyphilis, an infection that can be easily missed or misdiagnosed (Du et al., 2021); a single specific deterministic testing remains lacking.

Neurosyphilis is caused by the pathogen *Treponema pallidum*, which can enter the CNS. With syphilis, there is a fierce battle between the host's humoral and cellular immune responses, aimed at eliminating the infection, while *Treponema pallidum* manages to evade eradication and leads to chronic infection. Most patients can have an immune response to clear CNS invasion, and in a minority of patients who are immunocompromised or have immunodeficiency, syphilis may progress to asymptomatic or symptomatic NS. Neurosyphilis can be divided into early and late stages. The clinical manifestations in the early stage (e.g., meningitis, meningovascular syphilis, stroke, and acute altered mental status) usually appear within the first few months or years of infection. The presentation of the late stage (e.g., tabes dorsalis and general paresis) occurs 10 to >30 years after infection. Ocular or otic syphilis can occur at any stage with or without additional CNS involvement (Workowski et al., 2021).

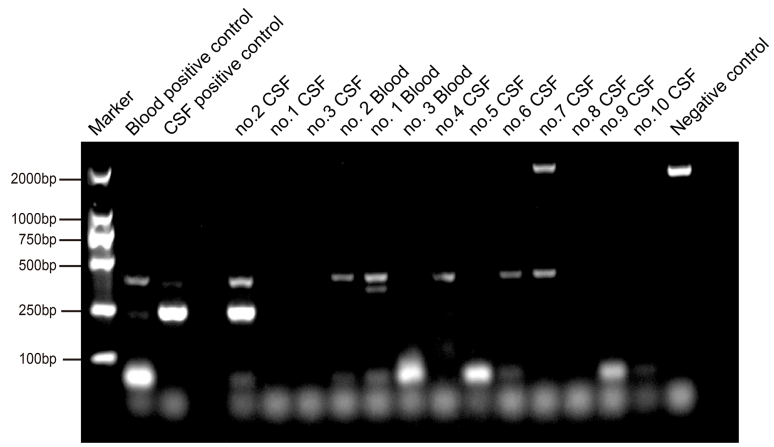

Sample no.	Sequence
no. 2 CSF	CAATACGGGATTGCAAGGAGAAGTTTCACTTCGTGGAAGACTCCCGCGTTACGGAGAATAC CAACGGCCTTAAGACAATGCTCACTGAGGATAGTTTTTCTGCACGTAAGGTAAGCAGCATGG AGAGCCCGCACGACCTTGTGGTAGACACGGTGGGTACCGGTTACCACAGCCGTTTTGGTT CGGACGCAGAGGCTTCTGTGATGCTGAAAAGGCTGGA

FIGURE 3
PCR and sequencing amplification of *Treponema pallidum* by TpN47 were followed by agarose gel electrophoresis to confirm *Treponema pallidum* sequences for three positive blood and 10 cerebrospinal fluid (CSF) samples. The blood positive control was from one patient's blood sample (toluidine red unheated serum test [TRUST] titer was 1:256); the CSF positive control was from one patient's CSF sample (positive serologic assays and metagenomic next-generation sequencing (mNGS); and the negative control was blank without sample.

The diagnosis of symptomatic neurosyphilis requires obtaining clinical features, conducting serological tests, and meeting the CSF criteria, whereas the diagnosis of asymptomatic neurosyphilis relies solely on the latter two (Workowski et al., 2021). However, serological tests for syphilis are relatively insensitive at the early stage of infection. Antibodies are undetectable by both non-treponemal and treponemal tests until infection progresses 1 to 3 weeks after chancroid formation (Larsen et al., 1995; Larsen et al., 1999). Therefrom, direct detection of *Treponema pallidum* from clinical samples has become a significant method for the early diagnosis of *Treponema pallidum* infection.

Moreover, neurosyphilis is classified into five types by imaging: asymptomatic neurosyphilis, meningeal syphilis (meningeal or scleromeningitis), syphilitic vasculitis, parenchymal syphilis (paralytic dementia), and gumma syphilis. The neuroimaging findings of neurosyphilis are usually cerebral infarction, leptomeningeal enhancement, or nonspecific white matter lesions (Tiwana and Ahmed, 2018). Neurosyphilis lacks specific imaging changes, which can also show similar imaging characteristics at different stages of the disease (Czarnowska-Cubała, 2015; Shang et al., 2020). In this study, the imaging findings of some patients were negative. Although the clinical examination was located in the nervous system, the imaging examination may not have meaningful findings.

Metagenomic next-generation sequencing (mNGS) enables non-targeted detection of nucleic acids from a range of potential pathogens, such as bacteria (Wilson et al., 2014), fungi (Christopeit et al., 2016), viruses (Piantadosi et al., 2018), and parasites (Li et al., 2021) present in clinical specimens. In the pathogenic diagnosis of CNS infectious diseases, cerebrospinal fluid mNGS technology has been gradually applied in clinical practice (Guan et al., 2016). Recently, Liu et al. (2022) reported that neurosyphilis with a high signal intensity on fluid-attenuated inversion recovery (FLAIR) was detected with 2,288 reads of *Treponema pallidum* by mNGS. In their study, they emphasize that more evidence from a large number of patients is needed to confirm mNGS as a supplementary method for the diagnosis and differential diagnosis of neurosyphilis. In this study, we were able to detect *Treponema pallidum* at a low pathogen level by mNGS, suggesting the sensitivity of the method. To our knowledge, this is the first time that *Treponema pallidum* was detected with a small number of reads by mNGS, in patients with ocular involvement and normal neuroimaging.

In this study, we retrospectively reviewed the CT scans and MRI films of 10 inpatients with ocular involvement and whose clinical samples were examined *via* metagenomic next-generation sequencing during the period from September 2021 to June 2022. Three out of the 10 patients had normal imaging results and were diagnosed with *Treponema pallidum* infection by mNGS. One read of *Treponema pallidum*, indicating the high sensitivity of mNGS, was also detected in patients with TRUST- or PCR-negative results, as we expected. Given this situation, we recommend NGS as a potential and supplementary tool for the diagnosis and differential diagnosis of neurosyphilis.

Conclusions

Neurosyphilis is a complication of syphilis with potentially serious sequelae. *Treponema pallidum* invades the CNS, often occurring in the early stage of infection. Neurosyphilis with ocular involvement is uncommon in clinical practice and is often confused with eye disease. Moreover, the MRI and CT results may be normal. Therefore, early diagnosis of neurosyphilis with ocular involvement has important implications for patient prognosis. For the first time, we highlight the role of mNGS in diagnosing neurosyphilis with ocular involvement and normal MRI results even at a low pathogen level. This study confirms the significance of CSF mNGS as a diagnostic tool for CNS pathogen infections. Although not yet widely used, its use in CSF screening may provide the most reliable and timely clinical diagnosis of infectious diseases in the CNS in the near future.

Data availability statement

The data analyzed in this study is subject to the following licenses/restrictions: All data supporting this study are reasonably available from the corresponding author. Requests to access these datasets should be directed to Jie Zhang, zhangjiespph@163.com.

Ethics statement

The studies involving human participants were reviewed and approved by Medical Professional Committee of the Sichuan Provincial People's Hospital (Permit Number: 2022172) with a waiver for informed consent from participants because of its retrospective nature.

Author contributions

XZ, LJ, and JZ contributed to the conception and design of the study. XZ, TS, DT, and XT extracted the DNA and performed the NGS. XZ and JZ analyzed the data. JZ and SP helped to collect the clinical data and MRI images. XZ executed the PCR validation. XZ drafted the manuscript. JZ and LJ

revised the manuscript. All authors contributed to the manuscript revision, and read and approved the final version of the manuscript.

Funding

This work was supported by the National Natural Science Foundation of China (No. 81670893, No. 81702064).

Acknowledgments

We sincerely thank the patients for participating in this original study.

Conflict of interest

The authors declare that the research was conducted in the absence of any commercial or financial relationships that could be construed as a potential conflict of interest.

Publisher's note

All claims expressed in this article are solely those of the authors and do not necessarily represent those of their affiliated organizations, or those of the publisher, the editors and the reviewers. Any product that may be evaluated in this article, or claim that may be made by its manufacturer, is not guaranteed or endorsed by the publisher.

References

Chen, C., Du, K.-F., Xie, L.-Y., Jiang, T.-Y., Kong, W.-J., Dong, H.-W., et al. (2021). Clinical features of ocular pathology in patients with acquired immunodeficiency syndrome and syphilis. *Adv. Ther.* 38 (6), 3362–3372. doi: 10.1007/s12325-021-01755-1

Chen, S., Zhou, Y., Chen, Y., and Gu, J. (2018). Fastp: An ultra-fast all-in-one FASTQ preprocessor. *Bioinformatics* 34 (17), i884–i890. doi: 10.1093/bioinformatics/bty560

Chiu, C. Y., and Miller, S. A. (2019). Clinical metagenomics. *Nat. Rev. Genet.* 20 (6), 341–355. doi: 10.1038/s41576-019-0113-7

Christopeit, M., Grundhoff, A., Rohde, H., Belmar-Campos, C., Grzyska, U., Fiehler, J., et al. (2016). Suspected encephalitis with candida tropicalis and fusarium detected by unbiased RNA sequencing. *Ann. Hematol.* 95 (11), 1919–1921. doi: 10.1007/s00277-016-2770-3

Conde-Sendín, M.Á., Amela-Peris, R., Aladro-Benito, Y., and Maroto, A. A.-M. (2004). Current clinical spectrum of neurosyphilis in immunocompetent patients. *Eur. Neurol.* 52 (1), 29–35. doi: 10.1159/000079391

Czarnowska-Cubała, M. (2015). Neurosyphilis and brain magnetic resonance imaging. *Int. J. Dermatol.* 54 (7), 863–863. doi: 10.1111/ijd.12865

Desideri, L. F., Rosa, R., Musetti, D., Vagge, A., Vena, A., Bassetti, M., et al. (2022). The multifaceted presentation of syphilitic chorioretinitis examined by multimodal imaging: A case series. *Am. J. Ophthalmol. Case Rep.* 26, 101434. doi: 10.1016/j.ajoc.2022.101434

Drago, F., Merlo, G., Ciccarese, G., Agnoletti, A., Cozzani, E., Rebora, A., et al. (2016). Changes in neurosyphilis presentation: A survey on 286 patients. *J. Eur. Acad. Dermatol. Venereol.* 30 (11), 1886–1900. doi: 10.1111/jdv.13753

Du, F.-Z., Wang, Q.-Q., Zheng, Z.-J., Zhang, X., Liang, G.-J., Chen, X.-S., et al. (2021). The challenge of diagnosis and treatment of neurosyphilis in China: Results from a nationwide survey. *Sexual Health* 18 (4), 333. doi: 10.1071/sh21023

Fraser, C. M., Norris, S. J., Weinstock, G. M., White, O., Sutton, G. G., Dodson, R., et al. (1998). Complete genome sequence of treponema pallidum, the syphilis spirochete. *Science* 281 (5375), 375–388. doi: 10.1126/science.281.5375.375

Ghanem, K. G., Ram, S., and Rice, P. A. (2020). The modern epidemic of syphilis. *New Engl. J. Med.* 382 (9), 845–854. doi: 10.1056/NEJMra1901593

Gonzalez, H., Koralnik, I. J., and Marra, C. M. (2019). Neurosyphilis. *Semin. Neurol.* 39 (04), 448–455. doi: 10.1055/s-0039-1688942

Guan, H., Shen, A., Lv, X., Yang, X., Ren, H., Zhao, Y., et al. (2016). Detection of virus in CSF from the cases with meningoencephalitis by next-generation sequencing. *J. neurovirol.* 22 (2), 240–245. doi: 10.1007/s13365-015-0390-7

Harris, J. P., Ciaranello, A. L., and Tabb, E. S. (2022). Case 4-2022: A 55-Year-Old man with bilateral hearing loss and eye redness. *New Engl. J. Med.* 386 (6), 583–590. doi: 10.1056/NEJMcpc2107349

Janier, M., Unemo, M., Dupin, N., Tiplica, G., Potočnik, M., and Patel, R. (2021). 2020 European guideline on the management of syphilis. *J. Eur. Acad. Dermatol. Venereol.* 35 (3), 574–588. doi: 10.1111/jdv.16946

Jeon, Y. J., Zhou, Y., Li, Y., Guo, Q., Chen, J., Quan, S., et al. (2014). The feasibility study of non-invasive fetal trisomy 18 and 21 detection with semiconductor sequencing platform. *PloS One* 9 (10), e110240. doi: 10.1371/journal.pone.0110240

Larsen, S., Norris, S., and Pope, V. (1999). Treponema and other host-associated spirochetes. *Manual Clin. Microbiol. ASM Press Washington DC* 759-776.

Larsen, S. A., Steiner, B. M., and Rudolph, A. H. (1995). Laboratory diagnosis and interpretation of tests for syphilis. *Clin. Microbiol. Rev.* 8 (1), 1–21. doi: 10.1128/CMR.8.1.1

Li, H., and Durbin, R. (2009). Fast and accurate short read alignment with burrows–wheeler transform. *bioinformatics* 25 (14), 1754–1760. doi: 10.1093/bioinformatics/btp324

Li, H., Gao, H., Meng, H., Wang, Q., Li, S., Chen, H., et al. (2018). Detection of pulmonary infectious pathogens from lung biopsy tissues by metagenomic next-generation sequencing. *Front. Cell. infect. Microbiol.* 8, 205. doi: 10.3389/fcimb.2018.00205

Li, K., Ma, Y., Ban, R., and Shi, Q. (2021). Case report: Diagnosis of human alveolar echinococcosis *via* next-generation sequencing analysis. *Front. Genet.* 12. 1228 doi: 10.3389/fgene.2021.666225

Liu, C., Zhang, Y., Li, Y., Bu, H., Liu, R., Ji, Y., et al. (2022). Neurosyphilis with a rare magnetic resonance imaging pattern confirmed by metagenomic next-generation sequencing: A case report. *Eur. J. Med. Res.* 27 (1), 1–5. doi: 10.1186/s40001-022-00676-1

Li, K., Wang, C., Lu, H., Gu, X., Guan, Z., and Zhou, P. (2013). Regulatory T cells in peripheral blood and cerebrospinal fluid of syphilis patients with and without neurological involvement. *PloS Negl. Trop. Dis.* 7 (11), e2528. doi: 10.1371/journal.pntd.0002528

Long, Y., Zhang, Y., Gong, Y., Sun, R., Su, L., Lin, X., et al. (2016). Diagnosis of sepsis with cell-free DNA by next-generation sequencing technology in ICU patients. *Arch. Med. Res.* 47 (5), 365–371. doi: 10.1016/j.arcmed.2016.08.004

Marks, M., Lawrence, D., Kositz, C., and Mabey, D. (2018). Diagnostic performance of PCR assays for the diagnosis of neurosyphilis: A systematic review. *Sexually transmitted infect.* 94 (8), 585–588. doi: 10.1136/sextrans-2018-053666

Orle, K. A., Gates, C. A., Martin, D. H., Body, B. A., and Weiss, J. B. (1996). Simultaneous PCR detection of haemophilus ducreyi, treponema pallidum, and herpes simplex virus types 1 and 2 from genital ulcers. *J. Clin. Microbiol.* 34 (1), 49–54. doi: 10.1128/jcm.34.1.49-54.1996

Palmer, H., Higgins, S., Herring, A., and Kingston, M. (2003). Use of PCR in the diagnosis of early syphilis in the united kingdom. *Sexually transmitted infect.* 79 (6), 479–483. doi: 10.1136/sti.79.6.479

Piantadosi, A., Kanjilal, S., Ganesh, V., Khanna, A., Hyle, E. P., Rosand, J., et al. (2018). Rapid detection of powassan virus in a patient with encephalitis by metagenomic sequencing. *Clin. Infect. Dis.* 66 (5), 789–792. doi: 10.1093/cid/cix792

Ropper, A. H., and Longo, D. L. (2019). Neurosyphilis. *New Engl. J. Med.* 381 (14), 1358–1363. doi: 10.1056/NEJMra1906228

Shang, X.-J., He, C.-F., Tang, B., Chang, X.-L., Ci, C., and Sang, H. (2020). Neuroimaging features, follow-up analyses, and comparisons between asymptomatic and symptomatic neurosyphilis. *Dermatol. Ther.* 10 (2), 273–283. doi: 10.1007/s13555-020-00361-3

Smibert, O. C., Jenney, A. W. J., and Spelman, D. W. (2018). Management of neurosyphilis: Time for a new approach? *Internal Med. J.* 48 (2), 204–206. doi: 10.1111/imj.13703

Timmermans, M., and Carr, J. (2004). Neurosyphilis in the modern era. *J. Neurol. Neurosurg. Psychiatry* 75 (12), 1727–1730. doi: 10.1136/jnnp.2004.031922

Tiwana, H., and Ahmed, A. (2018). Neurosyphilis: Mighty imitator forays with benign presentation and unique neuroimaging findings. *Sexual Health* 15 (4), 358–360. doi: 10.1071/SH17088

Wilson, M. R., Naccache, S. N., Samayoa, E., Biagtan, M., Bashir, H., Yu, G., et al. (2014). Actionable diagnosis of neuroleptospirosis by next-generation sequencing. *New Engl. J. Med.* 370 (25), 2408–2417. doi: 10.1056/NEJMoa1401268

Workowski, K. A., Bachmann, L. H., Chan, P. A., Johnston, C. M., Muzny, C. A., Park, I., et al. (2021). Sexually transmitted infections treatment guidelines 2021. *MMWR Recommend. Rep.* 70 (4), 1. doi: 10.15585/mmwr.rr7004a1

Yi, H., Fang, J., Huang, J., Liu, B., Qu, J., and Zhou, M. (2020). Legionella pneumophila as cause of severe community-acquired pneumonia, China. *Emerg. Infect. Dis.* 26 (1), 160. doi: 10.3201/eid2601.190655

Zhang, H. H., Hu, W. Q., Li, J. Y., Liu, T. N., Zhou, J. Y., Opriessnig, T., et al. (2020). Novel circovirus species identified in farmed pigs designated as porcine circovirus 4, hunan province, China. *Transbound. emerg. Dis.* 67 (3), 1057–1061. doi: 10.1111/tbed.13446

frontiers | Frontiers in Cellular and Infection Microbiology

TYPE Original Research
PUBLISHED 09 December 2022
DOI 10.3389/fcimb.2022.1016728

OPEN ACCESS

EDITED BY
Gilberto Sabino-Santos,
Tulane University, United States

REVIEWED BY
Vincenzo Di Stefano,
University of Palermo, Italy
Vitalie Lisnic,
Nicolae Testemițanu State University of Medicine and Pharmacy, Moldova

*CORRESPONDENCE
Sushan Luo
luosushan@fudan.edu.cn
Jianming Zheng
zhengjianming@fudan.edu.cn

†These authors share first authorship

SPECIALTY SECTION
This article was submitted to Clinical Microbiology, a section of the journal Frontiers in Cellular and Infection Microbiology

RECEIVED 11 August 2022
ACCEPTED 18 November 2022
PUBLISHED 09 December 2022

CITATION
Su M, Jin S, Jiao K, Yan C, Song J, Xi J, Zhao C, Zhou Z, Zheng J and Luo S (2022) Pneumonia in myasthenia gravis: Microbial etiology and clinical management.
Front. Cell. Infect. Microbiol.
12:1016728.
doi: 10.3389/fcimb.2022.1016728

Pneumonia in myasthenia gravis: Microbial etiology and clinical management

Manqiqige Su[1,2†], Shan Jin[3†], Kexin Jiao[1,2†], Chong Yan[1,2], Jie Song[1,2], Jianying Xi[1,2], Chongbo Zhao[1,2], Zhirui Zhou[4], Jianming Zheng[5,6*] and Sushan Luo[1,2*]

[1]Huashan Rare Disease Center and Department of Neurology, Huashan Hospital, Fudan University, Shanghai, China, [2]National Center for Neurological Disorders, Huashan Hospital, Fudan Univeristy, Shanghai, China, [3]Department of Neurology, The First Affiliated Hospital of Anhui University of Chinese Medicine, Anhui, China, [4]Radiation Oncology Center, Huashan Hospital, Fudan University, Shanghai, China, [5]Department of Infectious Diseases, Huashan Hospital, Fudan University, Shanghai, China, [6]National Medical Center for Infectious Diseases, Huashan Hospital, Fudan Univeristy, Shanghai, China

Introduction: Patients with myasthenia gravis (MG) are prone to the development of pneumonia due to the long-term immunotherapies they receive and a tendency for aspiration. Pneumonia remains a risk factor for MG worsening and is the most prevalent cause of mortality in MG patients. Classification of the pathogens involved and exploration of the risk factors for mechanical ventilation (MV) could aid in improving clinical outcomes.

Methods: Between January 2013 and October 2022, we performed an inpatient database review for MG patients with pneumonia concurrence in a tertiary research center specializing in neuromuscular disorders. The clinical and microbiological characteristics of 116 MG patients with pneumonia were retrospectively analyzed.

Results: In our cohort, 90.32% (112/124) of organisms were bacteria and 42.86% (48/112) of pathogenic bacteria were carbapenem-resistant. A high abundance of Epstein–Barr virus (EBV) was detected using next-generation sequencing (NGS) in 12 patients, while cytomegalovirus (CMV) was detected in 8 patients. Non-fermentative Gram-negative bacilli were the most prevalent microorganisms, in which ampicillin, sulfamethoxazole-trimethoprim (SMZ-TMP), piperacillin, cefoperazone, ceftazidime, and cefepime may have an anti-infectious effect. Moreover, peripheral lymphocyte percentage [odds ratio (OR) 0.88, 95% CI 0.75–0.96, p = 0.02] and serum globulin (OR 1.16, 95% CI 1.02–1.35, p = 0.03) were significantly associated with the risk of MV demand.

Discussion: Our identification of the microbial etiology of pneumonia in MG patients may provide future perspectives on accurate antibiotic options and enable early interventions when risk factors are present.

KEYWORDS

myasthenia gravis, pneumonia, mechanical ventilation, microbial etiology, antibiotic susceptibility

Introduction

Myasthenia gravis (MG) is an autoimmune neuromuscular disorder associated with autoantibodies affecting neuromuscular junctions (NMJs) that leads to fluctuating weakness in extraocular, limb, bulbar, and even respiratory muscles (Punga et al., 2022). Approximately 85% of MG patients have autoantibodies against the acetylcholine receptor (AChR), and a small proportion of patients have antibodies against muscle-specific tyrosine kinase (MuSK) (Lazaridis and Tzartos, 2020). Anti-low-density lipoprotein receptor-related protein 4 (LRP4) antibodies were detected in approximately 2%–46% of MG patients who were negative for both AChR and MuSK antibodies (Higuchi et al., 2011). In triple-seronegative MG patients, 13.4% were titin antibody positive (Stergiou et al., 2016). Among all causes of MG mortality, pneumonia is the most prevalent cause, ranging from 4% to 21.7% across different ethnicities (Owe et al., 2006; Chen et al., 2020; Westerberg and Punga, 2020). In addition, pneumonia is a well-recognized risk factor for MG worsening and is associated with an increase in intensive care unit (ICU) admission rates, length of hospital stays, mortality, and poor outcomes (Thomas et al., 1997; Bershad et al., 2008; Tiamkao et al., 2014; Gummi et al., 2019). Many studies have been published regarding the effects of COVID-19 and relevant vaccines on MG in recent years (Jakubikova et al., 2021; Lupica et al., 2022).

Pneumonia is most common in all concurrences of infection among MG patients, ranging from 16% to 41.18% (Prior et al., 2018; Sipila et al., 2019; Kassardjian et al., 2020). The high susceptibility of pneumonia in MG patients is mainly related to fluctuated muscle weakness. About 70% of generalized MG (GMG) patients have bulbar muscle weakness and swallowing dysfunction that is significantly associated with aspiration (Hehir and Silvestri, 2018; Kumai et al., 2019). Also, the proportion of respiratory muscle involvement increases from 1% to 80% if the disease progresses into a more advanced stage (Engel, 1994). Longitudinal studies revealed a significant decrease in maximum voluntary ventilation capacity to 35% to 62% of the expected value (Heliopoulos et al., 2003). Moreover, MG worsening impairs the oropharyngeal tract movement and reduces airway clearance (Galassi and Marchioni, 2021). Approximately 15%–20% of GMG patients develop a life-threatening condition with respiratory failure, named myasthenic crisis (MC), and require invasive or non-invasive mechanical ventilation (MV) (Thomas et al., 1997). Of these, MC patients with endotracheal intubation may develop ventilator-associated pneumonia (VAP), which approximately accounts for 50% of hospital-acquired (nosocomial) pneumonia (HAP) (Zaragoza et al., 2020).

In addition to the above risk factors, an immunocompromised status also contributes to a high incidence of pneumonia in MG cohorts. The mainstay in current standard-of-care therapies for MG includes corticosteroids and immunosuppressants (Verschuuren et al., 2022). Consequently, long-term immunotherapies increase the probability of infection and can have potentially worse outcomes.

Although predisposition to pneumonia, clinical features and the prognostic factors of pneumonia in MG patients have not yet been well described. There was a lack of information about the microbiology of causative pathogens and antibiotics treatments supported by etiological evidence. Aiming to optimize the initial antibiotic therapies and improve the outcome of MG patients with pneumonia, this study retrospectively reviewed the causative pathogens for pneumonia and the drug resistance results, and explored the predictors for the unfavorable outcome of MV.

Methods

Study population

This is a retrospective cohort study conducted at a tertiary MG diagnostic center. We retrieved information on MG patients with the concurrence of pneumonia from the inpatient database at Huashan Hospital, Fudan University from January 2013 through October 2022. The diagnosis of MG was based on the criteria after excluding other MG mimicking diseases (Narayanaswami et al., 2021). Patients with a short hospital stay (<3 days) were excluded from our analysis due to incomplete records. Late-onset MG (LOMG) was defined as the disease onset after the age of 50 years and had no concurrence of a thymoma.

Pneumonia was diagnosed according to the American Thoracic Society/Infectious Diseases Society of America (ATS/IDSA) guidelines (Mandell et al., 2007; Metlay and Waterer, 2020). Community-acquired pneumonia (CAP) was defined as an acute infection of pulmonary parenchyma acquired in the community and VAP was defined as pneumonia that arose more than 48 h after patients have been intubated. Hospital-acquired pneumonia (HAP) indicated that pneumonia not associated with MV, which occurs at least 48 h after admission, and that it was not incubating at the time of admission (Kalil et al., 2016). There was no COVID-19 patient in this cohort.

Clinical and laboratory variable collection

Clinical and laboratory data of MG patients were retrospectively reviewed. Baseline laboratory results included in the analysis were limited to those sampled within 24 h after admission. The CURB-65 score and SIPF were used to assess the severity of pneumonia.

Outcome measures

The primary outcome was defined as the MV demand during hospitalization in MG patients with pneumonia. To explore the

risk factors for MV dependence, the clinical variables underwent further analysis including MG post-intervention status (PIS) before admission and laboratory results.

Next-generation sequencing

The sputum or bronchoalveolar lavage fluid (BALF) cultures were collected and sent for next-generation sequencing (NGS) (BGI). Sputum/BALF (1.5–3 ml) and other samples from patients were collected according to standard procedures. Saponin was added to a 0.45-ml sample at a final concentration of 0.025%. Then, the sample was fully vortexed for 15 s and incubated for 5 min at 25°C; 75 µl was added for the dehosting process. The sample was fully vortexed for 15 s and incubated at 37°C for 10 min. Then, the sample was centrifuged at 18,000 *g* for 5 min and ~70–80 µl remained at the bottom after the removal of 450 µl of supernatant. PBS (800 µl) was added to the tube and fully vortexed. After centrifugation at 18,000 *g* for 5 min, 800 µl of supernatant was discarded and ~70–80 µl remained at the bottom. TE buffer (370 µl) was added to the tube, followed by shaking. Then, 7.2 µl of lysozyme was added for wall-breaking reaction. Two hundred fifty microliters of 0.5-mm glass beads were attached to a horizontal platform on a vortex mixer and agitated vigorously at 2,800–3,200 rpm for 30 min. The sample (0.3 ml) was separated into a new 1.5-ml microcentrifuge tube, and DNA was extracted using the TIANamp Micro DNA Kit (DP316, TIANGEN BIOTECH) according to the manufacturer's recommendation.

Then, DNA libraries were constructed through DNA fragmentation, end repair, adapter ligation, and PCR amplification. Agilent 2100 was used for quality control of the DNA libraries. Quality qualified libraries were pooled, and DNA Nanoball (DNB) was made and sequenced by the BGISEQ-50/MGISEQ-2000 platform. High-quality sequencing data were generated by removing low-quality reads, followed by computational subtraction of human host sequences mapped to the human reference genome (hg19) using Burrows–Wheeler Alignment. The remaining data after the removal of low-complexity reads were classified by simultaneously aligning them to the Pathogens Metagenomics Database (PMDB), consisting of bacteria, fungi, viruses, and parasites. The classification reference databases were downloaded from NCBI (ftp://ftp.ncbi.nlm.nih.gov/genomes/).

The raw NGS data were submitted and the accession to these SRA data is PRJNA901187.

Statistical analysis

The missing data of each parameter account for less than 5% and multiple interpolations were performed for missing values. Categorical variables were summarized as proportions and the differences between rates were tested by χ^2 or Fisher's exact test, if appropriate. The Shapiro–Wilk normality test was applied for all continuous parameters to test normality. If the test values were below the level of significance ($p = 0.05$), the median and interquartile (IQR) range were used for the descriptive characteristics; otherwise, the mean and standard deviation (SD) were used to describe the data. To assess the continuous parameters between the two groups, the Mann–Whitney *U* test was used when the assumptions of the Student's *t*-test were not met. The one-way ANOVA or the Kruskal–Wallis test compared three categorical groups, and the Bonferroni test was performed on each pair of groups.

The heatmap was performed by R according to the relative abundance of pathogens in the results of the PM-seq DNA test by the BGI group, and a *Z*-score normalization was performed on the normalized read counts across samples for each gene.

To identify the risk factors for an unfavorable outcome, univariate (statistical significance, $\alpha = 0.2$) and multivariate (statistical significance, $\alpha = 0.05$) logistic regression analysis with an odds ratio (OR) was performed. The assumption of linearity in the logit for the continuous variable was assessed by the Box–Tidwell test. Variance inflation factor (VIF) measured the degree of multicollinearity in a set of independent variables, and a VIF value that exceeded 5 indicated a problematic amount of multicollinearity. Variables showing statistical significance ($p < 0.2$) of univariate analysis were further included in multivariate logistic regression analysis (Mickey and Greenland, 1989; Lemeshow et al., 2013). Variables that did not reach the levels of statistical significance ($p = 0.05$) were eliminated and a new multivariate model was set. All data analysis and chart making were performed using R (v. 4.1.1).

Results

Clinical and laboratory features of MG patients with pneumonia during hospitalization

We recruited a total of 461 patients who met the diagnostic criteria of MG in the inpatient database, including 146 patients with MC and 315 patients with non-MC. Among 146 patients with MC, 86 patients required MV without pneumonia. A total of 116 patients had pneumonia (116/461, 25.16%), among which 85.34% (99/116) had CAP and presented dyspnea before or shortly after admission. Ten patients had two episodes of pneumonia within 1 year before hospitalization, while others did not; 14.66% (17/116) met the diagnosis of VAP in our cohort. A total of 76 patients required MV treatment during hospitalization (Figure 1).

Three patients who demanded MV support eventually died with an average hospital length of 12.83 days. The in-hospital mortality is 2.59% (3/116); 76.72% (89/116) of enrolled patients had pneumonia-associated hospitalization for the first time, and the general length of hospital stay was 30.54 days. Furthermore, the

average age at admission was 52.91 ± 15.04 years, and 54.31% (63/116) of patients were female, 15.51% (18/116) had the comorbidity of hypertension, and 7.76% (9/116) had diabetes upon admission.

Among 83 patients who had antibody testing, 81.93% (68/83) had autoantibodies against AChR, 8.43% (7/83) against MuSK, 26.51% (22/83) against titin, and 0 against LRP-4, and 9.64% (8/83) were seronegative. The age at onset was 48.68 ± 15.4 years and the average duration was 4.26 years. LOMG comprised 50% (58/116) of participants; 58.62% of patients (68/116) had thymoma concurrence, and 52.59% (61/116) received thymectomy with a mean duration of 3.7 years. At admission, 62.07% (72/116) were on corticosteroids and 31.9% (37/116) were on oral immunosuppressant therapies. Tacrolimus was the most prevalent immunosuppressant, which accounted for 21.55% (25/116). Prednisone was widely used as an oral corticosteroid, and the average dose was 29.21 ± 14.6 mg.

To assess the physiological state related to pneumonia when hospitalized, some pneumonia scores and laboratory results relevant to the pneumonia were retrospectively reviewed. CURB-65 was 0.55 on average, ranging from 0 to 3, and the mean SIPF score was 0.95. The white blood cell counts [(10.73 ± 5.1) $\times 10^9$ cells/L] slightly increased. The proportion and the absolute number of neutrophils rose to 80.49% and 10.09$\times 10^9$ cells/L, respectively, while the average proportion of lymphocytes declined to 12.09%. The level of albumin/globulin ratio (A/G ratio, 1.11 ± 0.52) and hematocrit (HCT, 38.07%) decreased relatively. Arterial blood gas analysis revealed acidosis in 16 patients, alkalosis in 30 patients, and hypoxemia in 8 patients with PaO_2 less than 8 kPa.

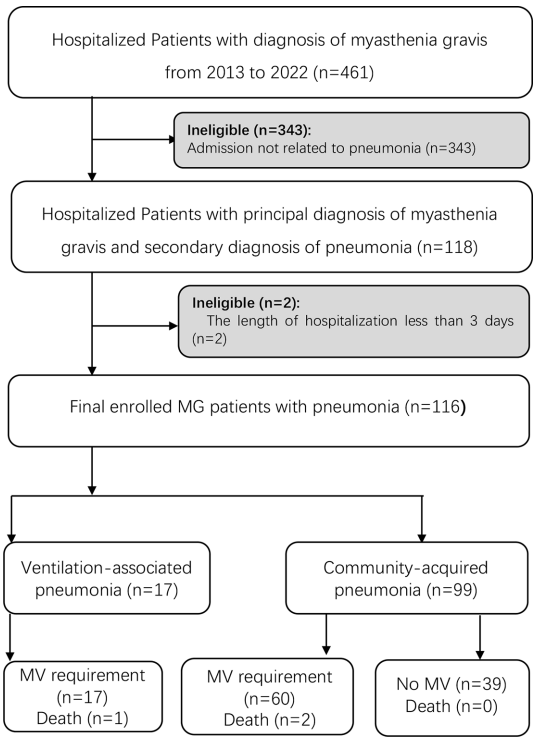

FIGURE 1
Flow diagram of patients included in the study. A total of 88 MG patients diagnosed with pneumonia were enrolled in the study. MG, myasthenia gravis; MV, mechanical ventilation.

Microbial etiology and antibiotic resistance associated with pneumonia

In the sputum or BALF cultures, 72 patients' cultures were positive with a total number of 124 detected organisms. Among these patients, 48.61% (35/72) had mixed infections. Non-fermentative Gram-negative bacilli were the most common bacteria and accounted for 54.46% (61/112), including *Pseudomonas aeruginosa* (28.57%, 32/112), *Acinetobacter baumannii* (16.96%, 19/112), and *Stenotrophomonas maltophilia* (8.93%, 10/112). Given that different immunosuppressive treatments before hospitalization may have an impact on the microbiology of pneumonia, the prevalence of *Klebsiella pneumoniae* was 4.17 times higher in patients with corticosteroid treatment than those who did not (OR 4.17, 95% CI 1.22–19.55, $p = 0.038$).

For 12 patients whose sputum/BALF samples were analyzed by the NGS technique, we identified a total of 29 pathogens from 11 patients. In particular, Epstein–Barr virus (EBV) and cytomegalovirus (CMV) were frequently identified by NGS (Figure 2). The diagnostic yield of NGS was 91.67%, which was higher than that of traditional culture (7/12, 58.33%). There was a significant statistical difference in the detection sensitivity between NGS and traditional methods ($p < 0.001$).

About 90.32% (112/124) of organisms were bacteria, among which 42.86% (48/112) of pathogenic bacteria were carbapenem-resistant (Figure 3). According to the drug sensitivity and resistance profile of 112 bacteria, carbapenem drugs, such as imipenem (54/112, 48.21%) and meropenem (46/112, 41.07%), had the highest resistance rate in the drug resistance tests. The antimicrobial susceptibility test highlighted amikacin, to which the microorganisms were most susceptible (84/112, 75%) (Figure 4). A total of 35 strains of bacteria were identified as MDRO. In particular, 10 strains were carbapenem-resistant *K. pneumoniae* (CRKP), among which 8 strains were in the MV group. In addition, 13 strains were carbapenem-resistant *P. aeruginosa* (CRPA), 9 strains were carbapenem-resistant *A. baumannii* (CRAB), and 3 strains were methicillin-resistant *Staphylococcus aureus* (MRSA).

Clinical management for pneumonia in the MG cohort

Cefoperazone sodium/sulbactam sodium is the common initial antibiotic for our patients (62.07%, 72/116), and piperacillin tazobactam was used in 11.21% (13/116) of patients as the initial

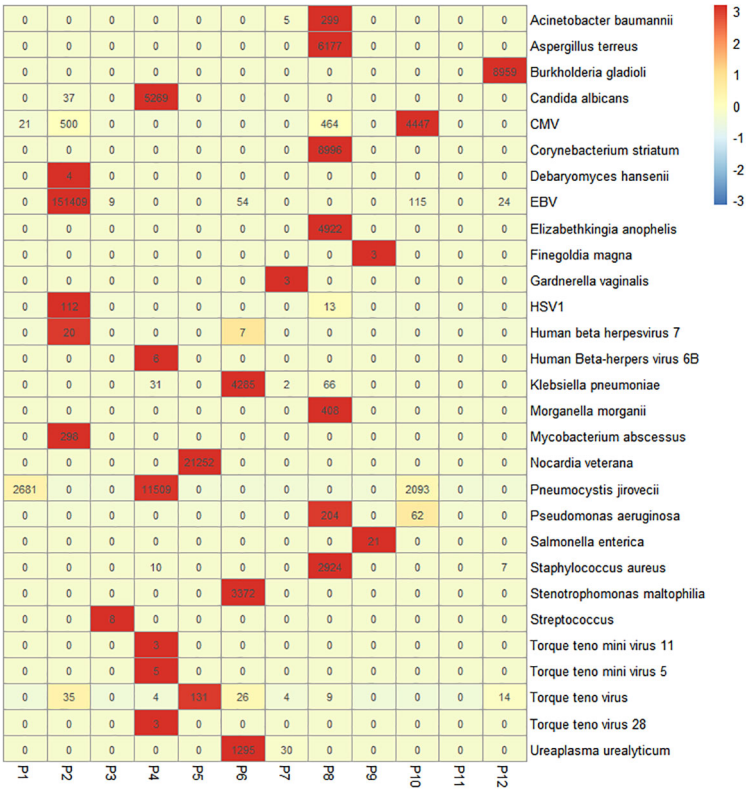

FIGURE 2
Heatmap of the pathogenic microorganism DNA/RNA high-throughput genetic sequencing (PMseq) results in 12 patients. A total of 29 pathogens were identified from 11 patients (91.67%, 11/12) including 15 bacteria, 4 fungi, and 9 viruses with different abundance. CMV, cytomegalovirus; EBV, Epstein–Barr virus; HSV1, herpes simplex virus 1.

antibiotic therapy. In all antimicrobial regimens during hospitalization, β-lactam antibiotics were the most common drugs, which accounted for 82.76% (96/116), and it was highly used as monotherapy (70.83%, 68/96). Combination antibiotic therapies were used to treat 27 patients with the most common combination of β-lactam plus sulfonamides. Compared with the non-MDRO group, there was a significantly higher proportion of combined antibiotics in the MDRO group ($p < 0.01$).

As for ventilatory support, 65.51% of patients (76/116) were MV-dependent due to respiratory failure, namely, 41 invasive

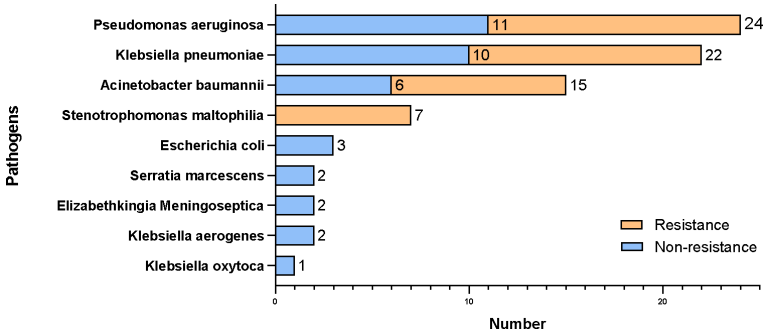

FIGURE 3
Results of microorganism culture and carbapenem resistance profile.

10.3389/fcimb.2022.1016728

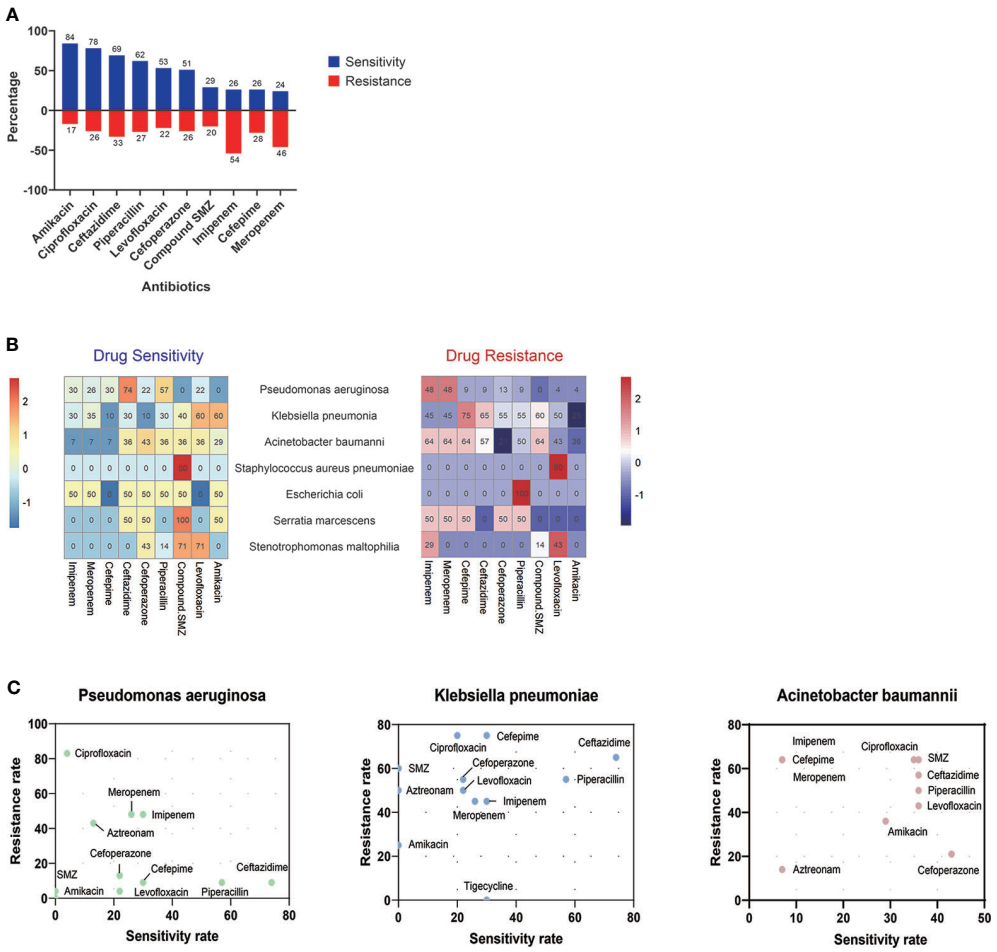

FIGURE 4
Drug resistance and sensitivity results of 112 bacteria. Amikacin (84/116, 72.41%) and ciprofloxacin (78/116, 67.24%) had high-sensitivity rates among 10 antibiotics, while bacteria detected were highly resistant to imipenem (54/116, 48.27%) and meropenem (46/116, 39.66%) **(A)**. The results of antibiotic resistance and sensitivity in different drugs **(B)** and three main pathogens **(C)** are presented. SMZ, sulfamethoxazole.

and 35 non-invasive MV. The average duration of MV during hospitalization was 25.39 (1–133) days. Of these, the length of MV demand in the invasive cohort was significantly longer than that in the non-invasive cohort (33.23 vs. 17.12 days, $p < 0.01$).

Predictive factors for an unfavorable outcome in MG patients with pneumonia

MV demand was defined as an unfavorable in-hospital outcome. Patients were divided into three groups: VAP, CAP with MV, and CAP without MV. Isolated microorganisms of pneumonia in the three groups were not different except the *K. pneumoniae*, which was more prevalent in the CAP patients with MV ($p < 0.05$). The difference between subgroups was statistically significant in nine parameters (Table 1). Larger proportion of patients with a treatment history of oral immunosuppressant within one year before admission ($p<0.01$). The average level of lymphocyte percentage, SO_2, albumin, and A/G ratio was significantly higher in the non-MV group, which hinted a better clinical status ($p < 0.05$).

To explore the risk factors that led to MV demand in the CAP group, we conducted a univariable logistic regression analysis and identified six variables with significance. The result of the Box–Tidwell and VIF test denied the presence of non-linearity between these variables and the logit and interactions between variables. Based on statistical as well as practical considerations, we fitted the multivariable model containing six independent covariates (Table 2). After the elimination of variables above the level of statistical significance in the first fit of a multivariate model, the second analysis finally revealed two important variables: lymphocyte percentage (OR 0.88, 95% CI 0.75–0.96, $p = 0.02$) and globulin (OR 1.16, 95% CI 1.02–1.35, $p = 0.03$).

TABLE 1 Comparisons of clinical and laboratory characteristics in three subgroups.

Variable	VAP (n = 17)	CAP with MV (n = 60)	CAP without MV (n = 39)	p-value
Clinical features at admission				
Length of hospitalization stay (days), median (IQR)	27 (26)	27.25 (25)	13.5 (11.5)	**0.004**
Age at admission (years old), mean ± SD	53.53 ± 18.02	54.65 ± 13.64	49.95 ± 15.65	0.31
Disease duration of MG (years), median (IQR)	1 (5.33)	2 (4.93)	2 (5)	0.7
Thymectomy, *n* (%)	9 (52.94)	30 (50)	16 (41.03)	0.67
LOMG, *n* (%)	9 (52.94)	32 (53.3)	17 (43.59)	0.62
IS within 1 year before hospitalization, *n* (%)	3 (17.65)	13 (21.67)	16 (41.03)	0.08
CS within 1 year before hospitalization, *n* (%)	11 (64.71)	45 (75)	31 (79.49)	0.51
MGFA classification, *n* (%)				
IIa	2 (11.76)	7 (11.67)	7 (17.95)	0.76
IIb	1 (5.88)	5 (8.33)	7 (17.95)	0.34
IIIa	0	2 (3.33)	2 (5.13)	0.81
IIIb	0	12 (20)	11 (28.21)	**0.04**
IVa	0	0	1	0.53
IVb	2 (11.76)	34 (56.67)	11 (28.21)	**<0.001**
V	12 (70.59)	0	0	**<0.001**
Baseline pneumonia score and laboratory test within 24 h				
CURB-65, median (IQR)	0.5 (1)	0 (1)	0 (1)	0.66
SIPF, median (IQR)	1 (1)	1 (1)	1 (1)	0.14
WBC count ($\times10^9$/L), median (IQR)	10.61 (4.45)	9.8 (5.74)	8.13 (6.75)	0.22
Lymphocyte (%), median (IQR)	12.2 (11.3)	7.1 (7)	11.7 (17.85)	**<0.001**
Absolute count of lymphocyte (/μl), median (IQR)	1 (1.01)	0.66 (0.73)	1.19 (1.05)	0.26
Neutrophil (%), median (IQR)	79.5 (16.8)	86.05 (12.95)	79.2 (19.05)	**0.047**
Absolute count of neutrophil (/μl), median (IQR)	6.79 (4.92)	8.57 (5.12)	6.39 (8.15)	0.48
HCT (%), median (IQR)	34.6 (8.4)	36.7 (5.48)	37.8 (10.7)	0.28
SO_2 (%), median (IQR)	98.9 (1.8)	96.9 (3.7)	97.75 (3.33)	**0.02**
$PaCO_2$ (kPa), median (IQR)	6 (1.14)	5.665 (1.44)	5.75 (1.04)	0.9
PaO_2 (kPa), median (IQR)	16.44 (8.73)	13.92 (7.7)	11.9 (5.77)	0.51
BE (mmol/L), median (IQR)	2.3 (4.1)	2.5 (5.68)	2.3 (3.55)	0.38
Albumin (g/L), mean ± SD	33.88 ± 5.85	33.68 ± 5.43	37 ± 4.63	**0.008**
Globulin (g/L), mean ± SD	37.24 ± 12.22	37.99 ± 10.66	32.52 ± 10.76	0.05
A/G ratio, median (IQR)	0.79 (0.42)	0.86 (0.4)	1.2 (0.53)	**0.03**

IQR, interquartile range; LOMG, late-onset myasthenia gravis; HCT, hematocrit; WBC, white blood cell; SO_2, oxygen saturation; PaO_2, partial pressure of oxygen; $PaCO_2$, carbon dioxide; BE, base excess; NLR, neutrophil-to-lymphocyte ratio.
P values less than 0.05 were highlighted in bold type.

Discussion

To the best of our knowledge, this is the first study to comprehensively analyze the microbial spectrum and drug resistance of pneumonia in MG patients, as well as the risk factors for MV demand in this cohort. With the identification of non-fermentative Gram-negative bacilli as the most prevalent organism and multiple organisms that were responsible for the majority of this cohort, we attempt to provide future perspectives for empirical antibiotic therapies.

In comparison to another autoimmune disorder, systemic lupus erythematosus (SLE) (Garcia-Guevara et al., 2018), the etiology spectrum in MG for concurrent pneumonia was different, as evidenced by the prevalent pathogen profile. *P. aeruginosa*, *K. pneumoniae*, and *A. baumannii* were commonly identified in MG patients, while *S. aureus*, *Pneumocystis* pneumonia, and *Aspergillus* were identified in SLE patients from Mexico. The NGS technique exhibited a higher detection sensitivity compared with the traditional cultures, especially for the detection of potential virus infection.

Pathogen spectrums in our cohort largely overlapped with HAP rather than CAP, which indicated the colonization transformation of the oropharynx with virulent organisms in MG patients under long-term immune-compromised treatments. It is worth noting that there is a significant increment of *K. pneumoniae* in CAP patients with MV (p = 0.03), whereas the drug resistance rate of *K. pneumoniae* also increased. The prevalence of *K. pneumoniae* was 4.17 times

TABLE 2 Univariate and multivariate logistic regression models for the severe course in the hospitalized MG patients with pneumonia.

Variables		Univariate analysis *			Multivariate analysis †		
		OR	95% CI	*p*-value	OR	95% CI	*p*-value
Thymectomy	Yes	1.43	0.64–3.28	0.38			
	No						
IS within 1 year before admission	Yes	0.39	0.16–0.96	**0.04**	0.59	0.2–1.71	0.33
	No						
CS within 1 year before admission	Yes	0.85	0.31–2.23	0.74			
	No						
Duration of MG		0.85	0.31–2.23	0.74			
WBC count		1.07	0.99–1.18	**0.11**	1.01	0.91–1.12	0.92
Lymphocyte (%)		0.91	0.86–0.95	**<0.001**	0.88	0.75–0.96	**0.02**
Absolute number of lymphocytes		0.85	0.55–1.14	0.34			
Neutrophil (%)		1.03	1.00–1.07	**0.04**	0.98	0.87–1.03	0.63
Absolute number of neutrophils		0.99	0.95–1.03	0.64			
HCT		0.98	0.94–1.01	0.34			
SO_2		1.03	0.91–1.17	0.58			
$PaCO_2$		0.93	0.7–1.24	0.62			
PaO_2		0.1	0.96–1.04	0.82			
BE		1.04	0.97–1.14	0.38			
Albumin		0.88	0.8–0.96	**0.003**	0.87	0.75–0.13	0.05
Globulin		1.05	1.01–1.09	**0.02**	1.16	1.02–1.35	**0.03**
A/G ratio		0.27	0.1–0.66	**0.006**	14.15	0.56–444.21	0.11

OR, odds ratio; CI, confidence interval; CS, corticosteroid; IS, immunosuppressant; HCT, hematocrit; WBC, white blood cell; SO_2, oxygen saturation; PaO_2, partial pressure of oxygen; $PaCO_2$, carbon dioxide; BE, base excess; NLR, neutrophil-to-lymphocyte ratio.
P values less than 0.2 in univariate analysis and less than 0.05 in multivariate analysis were highlighted in bold type.

higher in patients who underwent corticosteroid treatment than those who did not undergo immunosuppressive therapies (OR 4.17, 95% CI 1.22–19.55, $p = 0.038$).

The clinical decision in selecting an appropriate antibiotic is essential for improving the clinical outcome. In our analysis, carbapenem drugs, including imipenem and meropenem, had the highest resistance rate in the drug resistance tests, while amikacin, ciprofloxacin, ceftazidime, and piperacillin had a higher rate of susceptibility. However, as macrolides and aminoglycosides impair neuromuscular transmission and may aggravate MG (Jones et al., 2011; Van Berkel et al., 2016), amikacin should be avoided in MG patients if there is another alternative. Moreover, fluoroquinolones may impair neuromuscular transmission, which should be cautiously used in MG patients (Sheikh et al., 2021). If there is no alternative therapeutic option, adverse drug reactions should be closely monitored. Given the insufficient adverse reaction reports of cephalosporins, sulfonamides, clindamycin, tetracyclines, polymyxin B, and nitrofurantoin, these drugs can be safely administered to MG patients. Briefly, according to the drug sensitivity test results of our study, ampicillin, sulfamethoxazole-trimethoprim (SMZ-TMP), piperacillin, cefoperazone, ceftazidime, and cefepime may have an excellent anti-infectious effect.

Antimicrobial agents that are active against MDRO, especially carbapenem-resistant Gram-negative bacteria, remain limited. Initial empirical anti-infection treatment should cover a variety of possible pathogens. According to the drug sensitivity results, enzyme inhibitors, tigecycline, ceftazidime-avibactam, polymyxin, and other drugs can be chosen.

To reduce the incidence of MV and intervene in the early stage, we also analyzed the relationship between clinical factors and the risk of MV demand. With OR less than 1, a higher lymphocyte percentage is associated with lower odds of MV demand, which may help identify patients with higher intendancy of MV at the beginning of hospitalization. This result indicates the importance of preadmission therapy status for MG patients. Regular measurements of immune systems including levels of immune system cells and immunoglobulin are necessary under the long-term immunosuppressive treatments, which helps early prevention of infections in MG patients. In addition, globulin is also a valuable predictor of disease severity and prognosis. However, as a higher level of globulin may be associated with pre-admission intravenous immunoglobulin use, whether the high levels of serum globulin are predictive of MV dependence requires further research in future prospective cohort studies.

The retrospective nature mainly limited the power of the study. The inherent shortage of conventional microbiological methods was also a limitation. Due to the time-consuming procedure for natural amplification and false detection of some culture-

unfriendly microorganisms, the identification of pathogens always falls behind the early anti-infectious treatments. To satisfy the need for fast and precise infection diagnosis, new techniques with high efficiency and short turnaround time, such as NGS, should be applied more widely in future practice. We provided a precise diagnosis of disseminated *Talaromyces marneffei* infection assisted by NGS of multifarious specimens in an HIV-negative patient (Zhu et al., 2018). We used NGS to monitor disease progression and therapeutic efficacy in central nervous system infection (Ai et al., 2018). The NGS can even detect whether there is a carbapenem resistance gene in samples, enabling us to know the drug resistance of pathogens earlier. Thus, we used high-throughput sequencing technologies to track carbapenem-producing *K. pneumoniae* outbreak in an intensive care unit (Chen et al., 2019). Nanopore sequencing is another sequencing method, which is not used in the current study. However, we performed the first explorative study with nanopore sequencing in infectious endocarditis previously (Ai et al., 2020). In addition, we developed a rapid CRISPR-based assay for tuberculosis detection in various forms of direct clinical samples, which is also one of the pathogens causing pneumonia in MG patients (Ai et al., 2019). High-throughput sequencing technologies, including NGS, help overcome some limitations of the traditional culture, which includes a longer period of time for some special pathogens to report positive and non-comprehensive coverage of all the microorganisms. The application of high-throughput sequencing, which assists with rapid and accurate microbiological diagnosis, provides a new perspective on the clinical approach.

Conclusion

In conclusion, we characterized the etiological spectrum and clinical management of pneumonia in MG patients. Subsequently, we analyzed the detective yield in the microbial spectrum between NGS and traditional cultures. Lower lymphocyte percentage and a higher level of globulin at admission were identified as risk factors for MV demand, which may lead to unfavorable clinical outcomes. Accurate antibiotic options and early identification of the risk factors are of paramount importance to improve the clinical outcome.

Data availability statement

The raw data supporting the conclusions of this article will be made available by the authors, without undue reservation.

Ethics statement

The studies involving human participants were reviewed and approved by Fudan University Huashan hospital. The ethics committee waived the requirement of written informed consent for participation.

Author contributions

JZ and SL conceived the presented idea. MS, SJ, and KJ performed the computations and manuscript writing. CY, JS, and JX were involved in the interpretation of data. CZ and ZZ revised the manuscript. All authors contributed to the article and approved the submitted version.

Funding

This work was supported by financial grants from the National Natural Science Foundation of China (81870988, 82001335, and 82071410), the Key Laboratory Project of Shanghai Science and Technology Commission (20dz2260100), Shanghai Municipal Science and Technology Major Project (2018SHZDZX01), and ZJLab.

Acknowledgments

We want to thank the patients and the Neuromuscular Research Group at Huashan Hospital, Fudan University.

Conflict of interest

The authors declare that the research was conducted in the absence of any commercial or financial relationships that could be construed as a potential conflict of interest.

Publisher's note

Supplementary material

The Supplementary Material for this article can be found online at: https://www.frontiersin.org/articles/10.3389/fcimb.2022.1016728/full#supplementary-material

References

Ai, J. W., Liu, H., Li, H. X., Ling, Q. X., Ai, Y. Q., Sun, S. J., et al. (2020). Precise diagnosis of neisseria macacae infective endocarditis assisted by nanopore sequencing. *Emerg. Microbes Infect.* 9 (1), 1864–1868. doi: 10.1080/22221751.2020.1807411

Ai, J. W., Zhang, H. C., Cui, P., Xu, B., Gao, Y., Cheng, Q., et al. (2018). Dynamic and direct pathogen load surveillance to monitor disease progression and therapeutic efficacy in central nervous system infection using a novel semi-quantitive sequencing platform. *J. Infect.* 76 (3), 307–310. doi: 10.1016/j.jinf.2017.11.002

Ai, J. W., Zhou, X., Xu, T., Yang, M., Chen, Y., He, G. Q., et al. (2019). CRISPR-based rapid and ultra-sensitive diagnostic test for mycobacterium tuberculosis. *Emerg. Microbes Infect.* 8 (1), 1361–1369. doi: 10.1080/22221751.2019.1664939

Bershad, E. M., Feen, E. S., and Suarez, J. I. (2008). Myasthenia gravis crisis. *South Med. J.* 101 (1), 63–69. doi: 10.1097/SMJ.0b013e31815d4398

Chen, J., Tian, D. C., Zhang, C., Li, Z., Zhai, Y., Xiu, Y., et al. (2020). Incidence, mortality, and economic burden of myasthenia gravis in China: A nationwide population-based study. *Lancet Reg. Health West Pac.* 5, 100063. doi: 10.1016/j.lanwpc.2020.100063

Chen, C., Zhang, Y., Yu, S. L., Zhou, Y., Yang, S. Y., Jin, J. L., et al. (2019). Tracking carbapenem-producing klebsiella pneumoniae outbreak in an intensive care unit by whole genome sequencing. *Front. Cell Infect. Microbiol.* 9. doi: 10.3389/fcimb.2019.00281

Engel, A. G. (1994). *Accquired autoimmune myasthenia gravis* (New York: McGraw-Hill).

Galassi, G., and Marchioni, A. (2021). Myasthenia gravis at the crossroad of COVID-19: focus on immunological and respiratory interplay. *Acta Neurol. Belg* 121 (3), 633–642. doi: 10.1007/s13760-021-01612-6

Garcia-Guevara, G., Rios-Corzo, R., Diaz-Mora, A., Lopez-Lopez, M., Hernandez-Flores, J., Fragoso-Loyo, H., et al. (2018). Pneumonia in patients with systemic lupus erythematosus: Epidemiology, microbiology and outcomes. *Lupus* 27 (12), 1953–1959. doi: 10.1177/0961203318799207

Gummi, R. R., Kukulka, N. A., Deroche, C. B., and Govindarajan, R. (2019). Factors associated with acute exacerbations of myasthenia gravis. *Muscle Nerve* 60 (6), 693–699. doi: 10.1002/mus.26689

Hehir, M. K., and Silvestri, N. J. (2018). Generalized myasthenia gravis: Classification, clinical presentation, natural history, and epidemiology. *Neurol. Clin.* 36 (2), 253–260. doi: 10.1016/j.ncl.2018.01.002

Heliopoulos, I., Patlakas, G., Vadikolias, K., Artemis, N., Kleopa, K. A., Maltezos, E., et al. (2003). Maximal voluntary ventilation in myasthenia gravis. *Muscle Nerve* 27 (6), 715–719. doi: 10.1002/mus.10378

Higuchi, O., Hamuro, J., Motomura, M., and Yamanashi, Y. (2011). Autoantibodies to low-density lipoprotein receptor-related protein 4 in myasthenia gravis. *Ann. Neurol.* 69 (2), 418–422. doi: 10.1002/ana.22312

Jakubikova, M., Tyblova, M., Tesar, A., Horakova, M., Vlazna, D., Rysankova, I., et al. (2021). Predictive factors for a severe course of COVID-19 infection in myasthenia gravis patients with an overall impact on myasthenic outcome status and survival. *Eur. J. Neurol.* 28 (10), 3418–3425. doi: 10.1111/ene.14951

Jones, S. C., Sorbello, A., and Boucher, R. M. (2011). Fluoroquinolone-associated myasthenia gravis exacerbation: evaluation of postmarketing reports from the US FDA adverse event reporting system and a literature review. *Drug Saf.* 34 (10), 839–847. doi: 10.2165/11593110-000000000-00000

Kalil, A. C., Metersky, M. L., Klompas, M., Muscedere, J., Sweeney, D. A., Palmer, L. B., et al. (2016). Management of adults with hospital-acquired and ventilator-associated pneumonia: 2016 clinical practice guidelines by the infectious diseases society of America and the American thoracic society. *Clin. Infect. Dis.* 63 (5), e61–e111. doi: 10.1093/cid/ciw353

Kassardjian, C. D., Widdifield, J., Paterson, J. M., Kopp, A., Nagamuthu, C., Barnett, C., et al. (2020). Serious infections in patients with myasthenia gravis: population-based cohort study. *Eur. J. Neurol.* 27 (4), 702–708. doi: 10.1111/ene.14153

Kumai, Y., Miyamoto, T., Matsubara, K., Samejima, Y., Yamashita, S., Ando, Y., et al. (2019). Assessment of oropharyngeal swallowing dysfunction in myasthenia gravis patients presenting with difficulty in swallowing. *Auris Nasus Larynx* 46 (3), 390–396. doi: 10.1016/j.anl.2018.10.004

Lazaridis, K., and Tzartos, S. J. (2020). Autoantibody specificities in myasthenia gravis; implications for improved diagnostics and therapeutics. *Front. Immunol.* 11. doi: 10.3389/fimmu.2020.00212

Lemeshow, S., Hosmer, D. W.Jr., and Sturdivant, R. X. (2013). *Applied logistic regression. 3rd ed.* (Hoboken, New Jersey: Wiley).

Lupica, A., Di Stefano, V., Iacono, S., Pignolo, A., Quartana, M., Gagliardo, A., et al. (2022). Impact of COVID-19 in AChR myasthenia gravis and the safety of vaccines: Data from an Italian cohort. *Neurol. Int.* 14 (2), 406–416. doi: 10.3390/neurolint14020033

Mandell, L. A., Wunderink, R. G., Anzueto, A., Bartlett, J. G., Campbell, G. D., Dean, N. C., et al. (2007). Infectious diseases society of America/American thoracic society consensus guidelines on the management of community-acquired pneumonia in adults. *Clin. Infect. Dis.* 44 Suppl 2, S27–S72. doi: 10.1086/511159

Metlay, J. P., and Waterer, G. W. (2020). Update in adult community-acquired pneumonia: Key points from the new American thoracic Society/Infectious diseases society of America 2019 guideline. *Curr. Opin. Pulm Med.* 26 (3), 203–207. doi: 10.1097/MCP.0000000000000671

Mickey, R. M., and Greenland, S. (1989). The impact of confounder selection criteria on effect estimation. *Am. J. Epidemiol.* 129 (1), 125–137. doi: 10.1093/oxfordjournals.aje.a115101

Narayanaswami, P., Sanders, D. B., Wolfe, G., Benatar, M., Cea, G., Evoli, A., et al. (2021). International consensus guidance for management of myasthenia gravis: 2020 update. *Neurology* 96 (3), 114–122. doi: 10.1212/WNL.0000000000011124

Owe, J. F., Daltveit, A. K., and Gilhus, N. E. (2006). Causes of death among patients with myasthenia gravis in Norway between 1951 and 2001. *J. Neurol. Neurosurg. Psychiatry* 77 (2), 203–207. doi: 10.1136/jnnp.2005.072355

Prior, D. E., Nurre, E., Roller, S. L., Kline, D., Panara, R., Stino, A. M., et al. (2018). Infections and the relationship to treatment in neuromuscular autoimmunity. *Muscle Nerve* 57 (6), 927–931. doi: 10.1002/mus.26032

Punga, A. R., Maddison, P., Heckmann, J. M., Guptill, J. T., and Evoli, A. (2022). Epidemiology, diagnostics, and biomarkers of autoimmune neuromuscular junction disorders. *Lancet Neurol.* 21 (2), 176–188. doi: 10.1016/S1474-4422(21)00297-0

Sheikh, S., Alvi, U., Soliven, B., and Rezania, K. (2021). Drugs that induce or cause deterioration of myasthenia gravis: An update. *J. Clin. Med.* 10 (7), 1537. doi: 10.3390/jcm10071537

Sipila, J. O. T., Soilu-Hanninen, M., Rautava, P., and Kyto, V. (2019). Hospital admission and prevalence trends of adult myasthenia gravis in Finland in 2004-2014: A retrospective national registry study. *J. Neurol. Sci.* 407, 116520. doi: 10.1016/j.jns.2019.116520

Stergiou, C., Lazaridis, K., Zouvelou, V., Tzartos, J., Mantegazza, R., Antozzi, C., et al. (2016). Titin antibodies in "seronegative" myasthenia gravis–a new role for an old antigen. *J. Neuroimmunol.* 292, 108–115. doi: 10.1016/j.jneuroim.2016.01.018

Thomas, C. E., Mayer, S. A., Gungor, Y., Swarup, R., Webster, E. A., Chang, I., et al. (1997). Myasthenic Crisis: clinical features, mortality, complications, and risk factors for prolonged intubation. *Neurology* 48 (5), 1253–1260. doi: 10.1212/wnl.48.5.1253

Tiamkao, S., Pranboon, S., Thepsuthammarat, K., and Sawanyawisuth, K. (2014). Prevalence of factors associated with poor outcomes of hospitalized myasthenia gravis patients in Thailand. *Neurosci. (Riyadh)* 19 (4), 286–290.

Van Berkel, M. A., Twilla, J. D., and England, B. S. (2016). Emergency department management of a myasthenia gravis patient with community-acquired pneumonia: Does initial antibiotic choice lead to cure or crisis? *J. Emerg. Med.* 50 (2), 281–285. doi: 10.1016/j.jemermed.2015.04.019

Verschuuren, J. J., Palace, J., Murai, H., Tannemaat, M. R., Kaminski, H. J., and Bril, V. (2022). Advances and ongoing research in the treatment of autoimmune neuromuscular junction disorders. *Lancet Neurol.* 21 (2), 189–202. doi: 10.1016/S1474-4422(21)00463-4

Westerberg, E., and Punga, A. R. (2020). Mortality rates and causes of death in Swedish myasthenia gravis patients. *Neuromuscul. Disord.* 30 (10), 815–824. doi: 10.1016/j.nmd.2020.08.355

Zaragoza, R., Vidal-Cortes, P., Aguilar, G., Borges, M., Diaz, E., Ferrer, R., et al. (2020). Update of the treatment of nosocomial pneumonia in the ICU. *Crit. Care* 24 (1), 383. doi: 10.1186/s13054-020-03091-2

Zhu, Y. M., Ai, J. W., Xu, B., Cui, P., Cheng, Q., Wu, H., et al. (2018). Rapid and precise diagnosis of disseminated T.marneffei infection assisted by high-throughput sequencing of multifarious specimens in a HIV-negative patient: A case report. *BMC Infect. Dis.* 18 (1), 379. doi: 10.1186/s12879-018-3276-5

Frontiers in
Cellular and Infection Microbiology

Investigates how microorganisms interact with their hosts

Explores bacteria, fungi, parasites, viruses, endosymbionts, prions and all microbial pathogens as well as the microbiota and its effect on health and disease in various hosts.

Discover the latest Research Topics

See more →

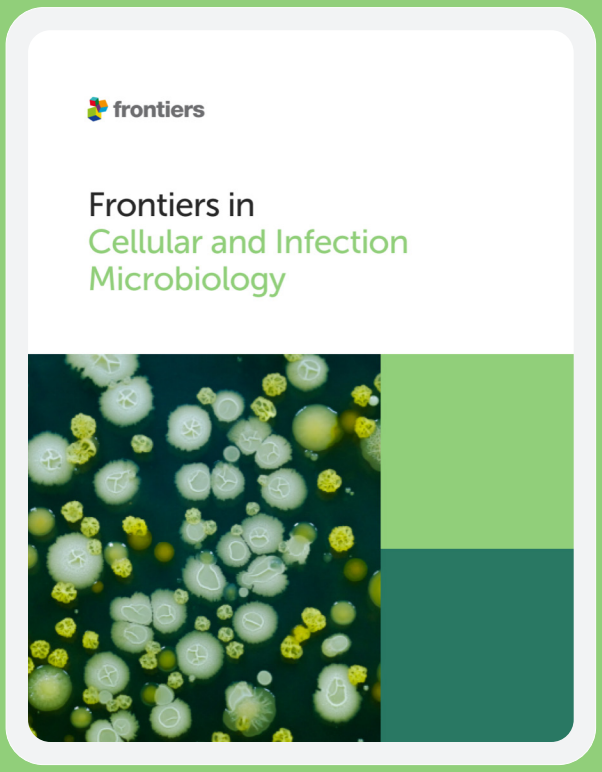

Frontiers

Avenue du Tribunal-Fédéral 34
1005 Lausanne, Switzerland
frontiersin.org

Contact us

+41 (0)21 510 17 00
frontiersin.org/about/contact